

**The Expedition ARKTIS-XX/1 and XX/2  
of the Research Vessel "Polarstern" in 2004**

---

**Edited by  
Gereon Budéus and Peter Lemke  
with contributions of the participants**



## CONTENTS

---

<b>ARK-XX/1:</b>	BREMERHAVEN - LONGYEARBYEN G. BUDEUS	pages 5 - 62
<b>ARK-XX/2:</b>	LONGYEARBYEN - TROMSØ P. LEMKE	pages 63 - 242



**ARK-XX/1**

**16.06.2004 - 16.07.2004  
Bremerhaven - Longyearbyen**

**Fahrtleiter / Chief Scientist**

**Gereon Budéus**

**Koordinator / Coordinator**

**Eberhard Fahrbach**

---

## CONTENTS ARK-XX/1

1.	<b>Zusammenfassung und Fahrtverlauf</b>	<b>7</b>
2.	<b>Overview and Itinerary</b>	<b>9</b>
3.	<b>Meteorology</b>	<b>10</b>
4.	<b>Long term variability of the hydrographic structure, convection and transports the Greenland Sea</b>	<b>12</b>
5.	<b>Interdisciplinary research at a deep-sea long-term station in the Arctic Ocean</b>	<b>17</b>
	5.1    Biological oceanography and sedimentation	18
	5.2    Microbiological and molecular biological investigations of bacterial deep-sea communities	19
	5.3    Benthic studies at the Hausgarten long-term stations	21
	5.4    Ecology of eelpout from the AWI-Hausgarten and the Håkon Mosby Mud Volcano	23
	5.5    Visual observations at the AWI-Hausgarten	24
	5.6    Benthic foraminiferal communities and stable isotopic composition	25
6.	<b>Chemical measurement programme</b>	<b>28</b>
	6.1    Mercury and the VOC/DOC connection	28
	6.2    Persistent organic pollutants (POPs)	30
7.	<b>Sediment acoustics: Atlas Parasound system upgrade DS-1 to DS-2</b>	<b>39</b>
	<b>Appendix</b>	<b>40</b>
A.1	<b>Participants</b>	<b>41</b>
A.2	<b>Participating Institutes</b>	<b>43</b>
A.3	<b>Schiffsbesatzung / Ship's Crew</b>	<b>45</b>
A.4	<b>Station List</b>	<b>46</b>

---

# 1. ZUSAMMENFASSUNG UND FAHRTVERLAUF

Gereon Budéus  
Alfred Wegener Institute, Bremerhaven

Der erste Fahrtabschnitt der 20. FS *Polarstern*-Expedition in die Arktis begann am 16.6.2004 in Bremerhaven. Die ersten Aktivitäten galten der Inbetriebnahme neuer oder modifizierter Geräte: Parasound Anlage sowie ADCP erfuhren in der Wertzeit umfassende Erneuerungen. Der Weg führte zunächst über die Nordsee und weiter an Norwegen vorbei zum untermeerischen Håkon Mosby Schlammvulkan, wo im Rahmen beständigeren Forschungsengagements während dieser Expedition benthische Foraminiferen untersucht wurden. Bereits der Weg dorthin wurde für eine Vielzahl luftchemischer Untersuchungen genutzt. Hier galt das Hauptinteresse der Verbreitung von Quecksilber und persistenten organischen Schadstoffen. Die Fahrtroute von Bremerhaven aus in die arktischen Gewässer bot eine seltene Gelegenheit zu Messungen, die räumlich von den Quellengebieten bis in industrieferne Regionen reichen.

Es schloß sich an ein zonaler hydrographischer Schnitt auf 75°N, der sich von der Bäreninsel bis auf das Grönländische Schelf erstreckt. Dieser Schnitt wird seit einigen Jahren jährlich wiederholt, da man erkannt hat, dass auch die arktischen Gewässer durch hohe Dynamik gekennzeichnet sind und die komplexen Veränderungen nur mit Hilfe langer Zeitreihen konsistenter Qualität richtig erklärt werden können. Zu den Messparametern gehörten neben den physikalischen auch verschiedene Tracer- und Nährstoffkonzentrationen. Die Suche und Erfassung eines langlebigen kleinskaligen Wirbels mit besonderer Relevanz für die tiefe Konvektion war ein weiteres Ziel, welches mit Hilfe von XBT-Abwürfen aus dem Helikopter zeitökonomisch erreicht werden konnte. Auch die Auswechslung von autonom profilierenden Verankerungen fanden auf diesem Weg von Ost nach West statt. Zwei weitere Verankerungen mit akustischen Empfängern werden die Konvektionsvorgänge mit der innovativen 'shadowgraph' Technik untersuchen.

Auch im biologischen Bereich hat sich die Erkenntnis durchgesetzt, dass einmalige Erhebungen zur Erfassung nichtstatischer Systeme unzureichend sind. Die Einrichtung des *Hausgartens* in der Framstraße vor Spitzbergen, der nach den Arbeiten auf dem Zonalschnitt aufgesucht wurde, ist ein Versuch, durch gezielte Ausbringungen und Beprobungen über mehrere Jahre die Dynamik von tiefseespezifischen ökologischen Abläufen und ihr Wechselwirkungsnetz zu erfassen. 1999 wurde die erste Langzeitstation in einer polaren Tiefseeregion eingerichtet, und seitdem wird auch ein Schnitt über einen Tiefengradient zwischen 1000 m und 5500 m Tiefe wiederholend beprobt, was bei unserer Fahrt wegen der geringen Eisbedeckung keinerlei Probleme bereitete. Hier kam eine Vielzahl von Geräten zum Einsatz, von Landern über Sedimentprobennahmegeräte bis zu abbildenden oder messenden optischen Verfahren.

Die bereits erwähnten luftchemischen Untersuchungen fanden auf der gesamten Fahrtstrecke statt. Eine spezifisch polare Erscheinung, der besonderes Interesse

galt, ist der 'atmosphärische Quecksilberrückgang'. Es wird nämlich beobachtet, dass die Quecksilberkonzentrationen in der Atmosphäre deutlich unter die Hintergrundwerte sinken. Hier ist ein Ziel, zu ermitteln, inwieweit die Polarregionen der Erde als endgültige Senken angesehen werden müssen.

Nach dem Ende der Arbeiten im *Hausgarten* fand das Einlaufen von FS *Polarstern* am 16.7.2004 in Longyearbyen statt.

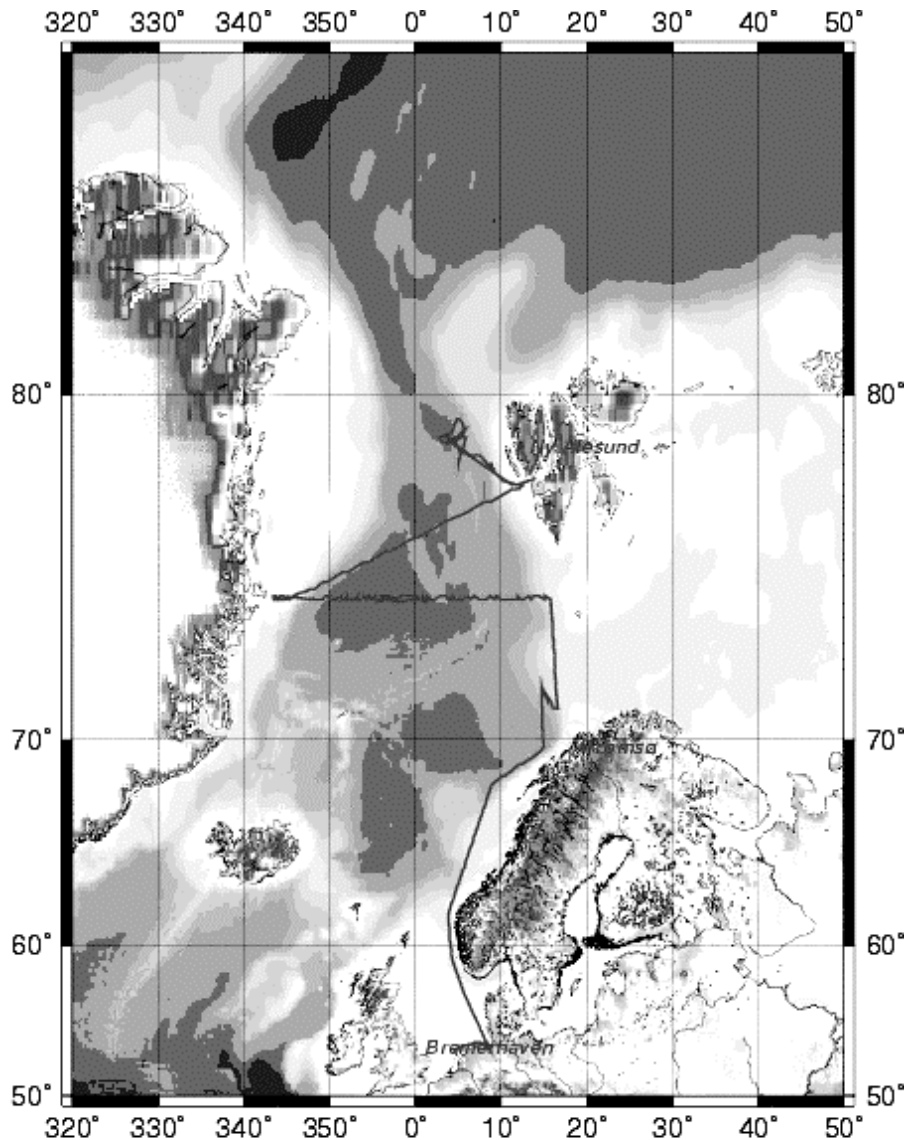


Abb. 1: Fahrtroute ARK-XX/1  
 Fig. 1: Cruise track during ARK-XX/1

---

## 2. OVERVIEW AND ITINERARY

The start of the first leg of the 20th RV *Polarstern* expedition to the Arctic took place on 16 June 2004. First activities were related to the operational start up of new or modified equipment: Parasound and ADCP systems had undergone major modifications during the time in the shipyard. The ship's itinerary did first cross the North Sea, pass by the Norwegian coast and aim at the underwater Håkon Mosby Mud Volcano. At this site, benthic Foraminifera were investigated in the frame of a more perseverative research engagement. The steaming path from Bremerhaven to the Håkon Mosby Mud Volcano was already utilized for extensive investigations in air chemistry. The main interest concerned the spreading of mercury and Persistent Organic Pollutants (POPs). The overall ship's track from the North Sea into remote Arctic waters revealed a rare opportunity to scan the environment from the source regions to the polar areas far off from industrial plants.

A zonal transect was performed along 75°N with predominantly hydrographic measurements. The transect extended from Bear Island to the Greenland coast and is repeated annually since a number of years because it has been recognised that the Arctic Waters experience highly dynamic changes and that the complex modifications due to convection in winter can be correctly explained only with the aid of quality-consistent long term time series. On this way from east to west there were additional activities. One was the exchange of autonomously profiling moorings and a new deployment of innovative acoustic moorings using the shadowgraph technique for convection research. Another aim was the search and investigation of a submesoscale vortex which is of particular importance to deep convection. The vortex could be found very time economic by XBT throws from a helicopter.

In marine biology, too, it has been realised that nonrecurring investigations describe non static systems inadequately. The installation of the *Hausgarten* in Fram Strait off Svalbard is an attempt to comprehend the dynamics of deep sea specific ecological processes and their interactions by systematic deployments and sampling. The first long term station in an arctic deep sea regions was established in 1999, and since then a transect is sampled repeatedly which follows a depth gradient between 1000 m and 5500 m. Owing to low ice concentrations this posed no difficulty during ARK-XX/1. A multitude of instruments was used here, as landers, sediment corers or optical devices.

The already mentioned research in air chemistry was continuously performed on the entire cruise track. A specific polar feature, which was investigated with special emphasis, is the 'Atmospheric Mercury Depletion Event', during which mercury concentrations decrease to values below the background. With respect to this phenomenon it is the aim to assess to what extent the polar regions must be regarded as final sinks.

After having finished the work in the *Hausgarten*, RV *Polarstern*'s arrival at Longyearbyen was on 16 July 2004.

---

### 3. METEOROLOGY

Rüdiger Hartig, Klaus Buldt  
Deutscher Wetterdienst

RV *Polarstern* left Bremerhaven on 16 June steaming along the Norwegian coast heading for the first research area, the Håkon Mosby Mud Volcano. The passage was dominated by northerly winds around force 5 Bft, which resulted from the pressure gradient between a depression over Scandinavia and an anticyclone over Greenland. Off Cape Svinøy winds reached force 8 Bft for a short period, presumably to orographic forcing. First Helicopter flights bound for Tromsø, took place on 20 June at fair weather. A few towering "CB's" along the coastline didn't cause any problems.

The work in the volcano area was accompanied by very uniform weather conditions. Northeasterly winds around force 5 Bft, swell between 1 and 2 m, heavy cloud cover, scattered rain and air temperatures near 7° C describe the typical situation.

Due to bad visibility and low ceiling, on 22 June another flight to Tromsø had to be cancelled. Visibility increased in the ship's vicinity early next morning. To get an idea about the conditions at the destination we received METARs and TAFs of Tromsø and Bardufoss airport from our home office in Hamburg. With the aid of an additional radio sounding and satellite pictures a small frontal zone was observed enroute, which was expected to be flightable. Unfortunately another frontal System visible in the satellite pictures approached from northeast. Taking all the information into consideration a 6 hours timeslot with sufficient weather conditions was forecasted. Thus pilots, master, chief scientist und meteorologist agreed in an immediate attempt to reach Tromsø. After takeoff both helicopters experienced heavy weather at the first 50 miles but better conditions at the second leg of approx. 100 miles. To minimize the risk RV *Polarstern* headed approximately 50 miles to Tromsø shortening the distance for the return flight. Around noon both helicopters returned safely ending this action successfully.

Between 24 June and 3 July research was done on an east-west transect along latitude 75° north. This period was governed by moderate wind-speed, low sea-swell und positive temperatures, giving fair conditions for scientific activities. Though air traffic was partly obstructed by low ceiling and patches of fog, all planed flights were carried out. On Friday, 2 June RV *Polarstern* entered the ice off the Greenland coast. Final works had been done at an ice coverage of 70 % to 80 % first year and multiyear ice. After finishing these works, next stop of the cruise was Longyearbyen, Svalbard.

RV *Polarstern* stopped off the 12 miles zone, while two people were flown by helicopter to Longyearbyen Airport. The flight forecast was done with the aid of Longyearbyen METAR and TAF information (gained via Internet transmission). Flight conditions at takeoff were given by an overcast sky with 300 ft ceiling and 4 to 6 km visibility. Conditions deteriorated due to fog formation along the coastal area, making

the return flight impossible. As there was no significant change in the weather situation predicted, RV *Polarstern* steamed up the “Isfjord” for 3 hours heading for an area free of fog where the helicopter returned safely.

After this RV *Polarstern* set course to the *AWI Hausgarten* research area, where scientific work was continued on 6 July. For the first 5 days weak to moderate southerly winds (Force 2-5 Bft) and wave heights between 0.5 and 2.0 m were observed. Low-pressure influence caused a cloudy to overcast sky, frequent fog and isolated rain, while the temperature ranged between 2° and 5° C. A high-pressure ridge, extending from a Siberian high over the pole to the Greenland Sea dominated the weather situation at the final days. Weak northerly winds and a sea swell below 1 m were observed mainly. At temperatures between 3° and 6° C we experienced some sunny days and for some periods an excellent long-range visibility of 160 km as well as some cloudy and foggy days. With the exception of the air-chemistry group, who liked to have stronger winds, there were no restrictions to scientific work, due to weather conditions.

Abbreviations:

Bft	Beaufort
CB	Cumulonimbus
METAR	Meteorological Aerodrome Report
TAF	Terminal Aerodrome Forecast

---

## 4. LONG TERM VARIABILITY OF THE HYDROGRAPHIC STRUCTURE, CONVECTION AND TRANSPORTS THE GREENLAND SEA

Gereon Budéus<sup>1)</sup>, Stefanie Ronski<sup>1)</sup>,  
Rainer Plugge<sup>1)</sup>, Linda Gerull<sup>1)</sup>, Juliane  
Otto<sup>1)</sup>, Kati Partzsch<sup>1)</sup>, Lisa Kattner<sup>1)</sup>,  
Barbara Cembella<sup>2)</sup>, Arthur Kaletzký<sup>3)</sup>

<sup>1)</sup>Alfred Wegener Institute,  
Bremerhaven

<sup>2)</sup>Optimare, Bremerhaven

<sup>3)</sup>University of Cambridge,  
Cambridge

Bottom water renewal in the Greenland Sea by deep convection in interplay with ice coverage and atmospheric forcing is a major element of the water mass modification in the Arctic Mediterranean. Effects influence both the central Arctic Ocean and the overflow waters into the Atlantic. Since the hydrographic observations became more frequent in the late 1980s, no bottom water renewal by winter convection took place, however. Under these conditions, the deep water properties change towards higher temperatures and salinities. Furthermore, the doming structure in the Greenland Gyre, as it was observed in the mid-80s, was superseded by an essentially 2-layered water mass arrangement with a marked density step separating the two layers presently at about 1800 m. The specific objectives of the project are to investigate the relative importance of atmospheric forcing parameters for winter convection, to clarify whether ice coverage inhibits or facilitates deep convection, to build a long term observational basis about deep water changes in the Greenland Gyre, and to contribute to the decision which deep water exchange mechanisms are at work under the absence of deep winter convection. A special focus is put on the observations of a particularly long lived submesoscale coherent vortex (SCV) within an international cooperation. Within this eddy, winter convection penetrates usually to considerably greater depths (about 2600 m) than in the surrounding waters. The eddy possesses a diameter of only 20 km, and as it shows no surface signal it is difficult to detect.

### Work at sea

In the central Greenland Sea, a long-term zonal CTD transect at 75° N has been performed with a regular station spacing of 10 nautical miles. This distance has not been reduced at frontal zones in order to gain time for a couple of stations dedicated to the search and investigation of the SCV. CTD and water sampler (SBE 911+ with duplicate sensors, SBE Carousel 24 bottles of 12 L each) worked faultlessly. Additional sensors were attached for Oxygen concentrations, transmission, Chlorophyll fluorescence, and Gelbstoff fluorescence.

It is not possible to describe the full details of calibration and data procedures here. A few hints may suffice to give an idea about the general procedure. We use the same sensors already for a number of years and checked for their performance with

respect to unwanted cross dependencies. According to this, one of the temperature sensors shows a pressure sensitivity of roughly 1.5 mK/4000 dbar while no unspecified pressure or temperature dependence of the conductivity sensors could be found. To identify the latter is close to impossible in the field (within the polar oceans) because of the high gradients in the upper water column where suitable temperature differences occur. The locations of *in-situ* comparisons for temperature and salinity have been chosen carefully by checking for each data point whether a comparison is allowed or inhibited. Time alignment has been optimized for each flow path separately and will be applied together with final post cruise calibration. The difference between pre-cruise and post-cruise calibration is normally in the range of a few mK and a few 1/1000 in salinity. Bottle sample salinities were determined immediately on board. Salinities have been corrected by 0.004. Oxygen samples were taken regularly. Occasionally, also several other tracers like technetium and barium were taken.

For the first time, the search for the eddy (SCV) was performed from an helicopter in order to save ship time. A triangle grid formed by equidistant station points was constructed, where the distance between each station pair was 7 nautical miles. This is the largest distance allowed when looking for a feature of 20 km diameter and proved to be a very successful search strategy during last year's cruise.

As instruments we used deep cast XBTs which have a nominal range of 1850 m (T5, Sippican). Frequently they provided data to 2,000 m. During the cast duration of about 5 minutes, the helicopter has to hover at a fixed position, which was not too difficult due to reasonable weather conditions. Data acquisition software has been used which was specially modified for the actual task of our eddy search. It contains an optional one degree Celsius temperature range with a free choice of the lower temperature scale value, so that the vertical structure with the surface warm layer (or its lack) and the mid-depth temperature maximum (and its depth) could easily be recognized. The search was successful within one day and an eddy was identified on 26 June. A following ship bound CTD survey with full depth stations showed that the eddy core was located at about 74° 54' N, 01°E on 27 June 2004.

This was not the eddy observed in the previous year, which was relocated later by a French cruise, but an additional one.

The in-house developed EP/CC (externally powered/compressibility compensated) Jojo-mooring has been exchanged and the time series was thus successfully extended. A shallow water jojo (APV), which had been attached to the top buoyancy of one mooring was lost. This type of instrument will not be used in the future, and a different approach has to be tested in order to monitor the uppermost 100 m of the water column. On one mooring, a sound source was deployed, and two additional moorings were deployed which host hydrophones to apply the shadowgraph technique newly developed by DAMTP, University of Cambridge.

## First results

The most outstanding single feature of the survey in the Greenland Sea (Fig. 4.1 and 4.2) was certainly the additional convective eddy (Fig. 4.3 and 4.4), showing that two of these eddies can coexist at the same time in the central Greenland Gyre. This is remarkable, as a full region survey, performed a few weeks before our cruise, revealed no eddy in the Greenland Sea (presumably due to its coarser station spacing). These features represent the deepest convection level observed in recent years. The eddy structure we observed was broader than expected and the eddy core extended to only 2,300 m, compared to 2,700 m observed in the eddy the previous year. The eddy core was not vertically homogeneous but showed a vertical structure around 1,500 m probably marking the convection depth of the preceding winter.

The general situation was characterized by summer conditions with a low salinity surface layer. The subsurface layer was only marginally influenced by Atlantic Water as the salinities hardly exceed 34.9. At about 70 m depth cold temperatures (below  $-1^{\circ}\text{C}$ ) are encountered around  $3^{\circ}\text{E}$ , while the majority of the profiles shows temperatures warmer than  $-0.75^{\circ}\text{C}$  at that depth due to summer heating. It is difficult to determine the exact depth to which winter convection has proceeded, and this has to be analyzed later. At first sight, convection seems to have affected only the upper 1,000 m. The temperature maximum at intermediate depth descended by about 100 m again, which contrasts the previous winter but is in accord with the long-term development. The bottom water temperature increase continued, and amounts again to about 10 mK between spring 2003 and summer 2004. This temperature increase is observed throughout the whole layer below the temperature maximum.

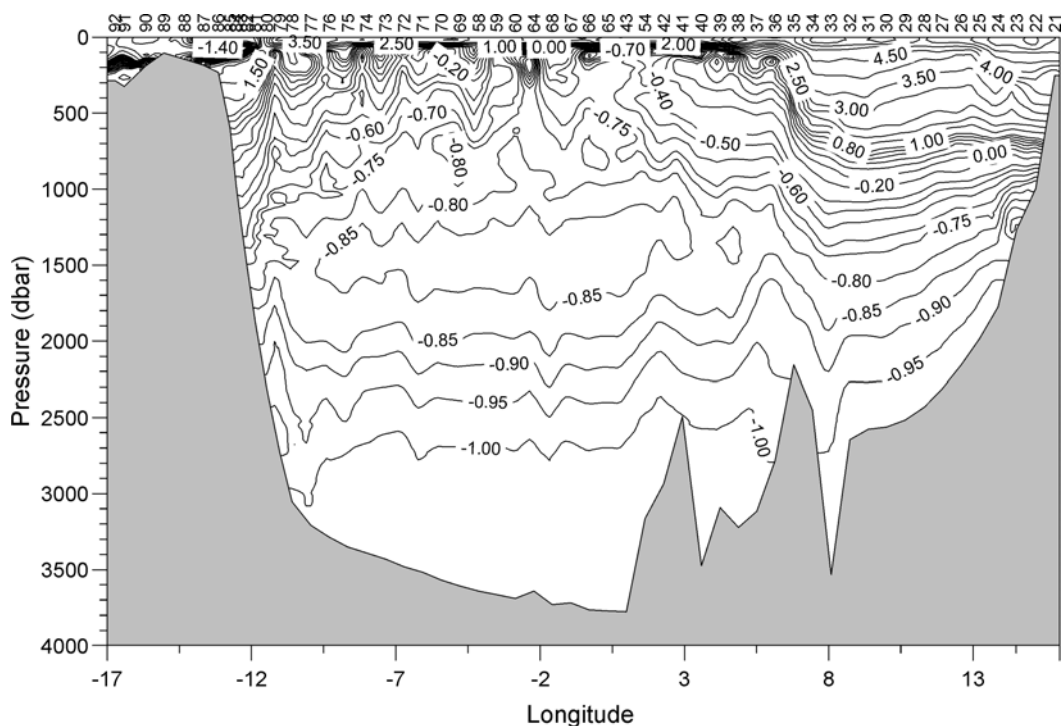


Fig. 4.1: Temperature along the zonal transect at  $75^{\circ}\text{N}$

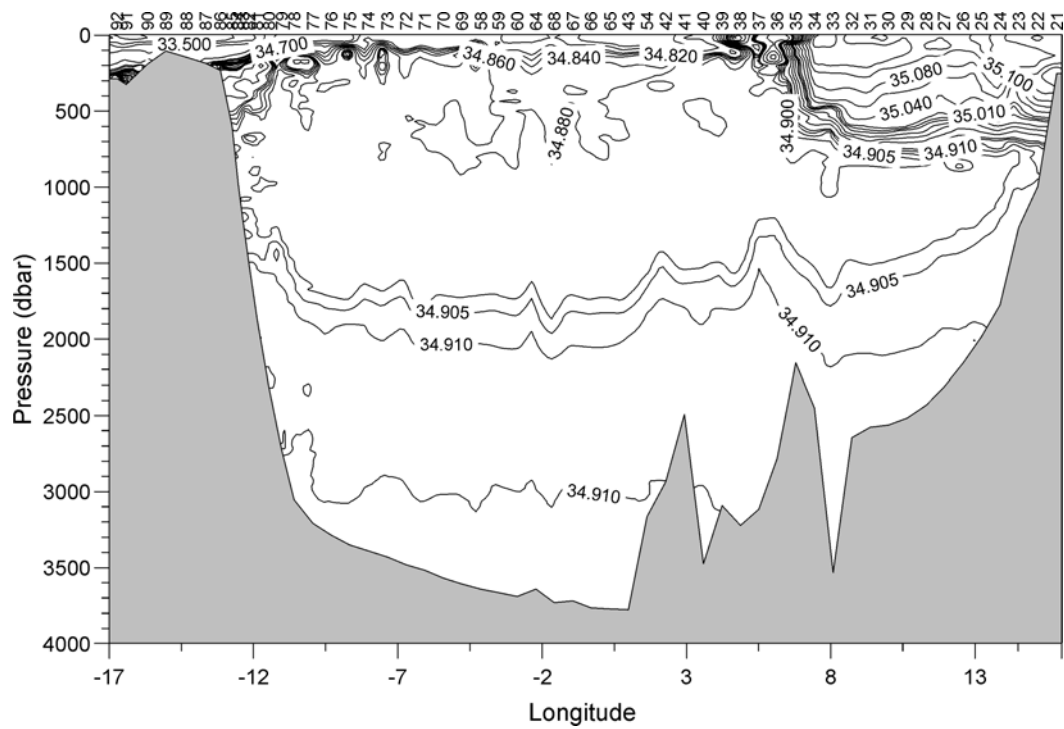


Fig. 4.2: Salinity along the zonal transect at 75° N

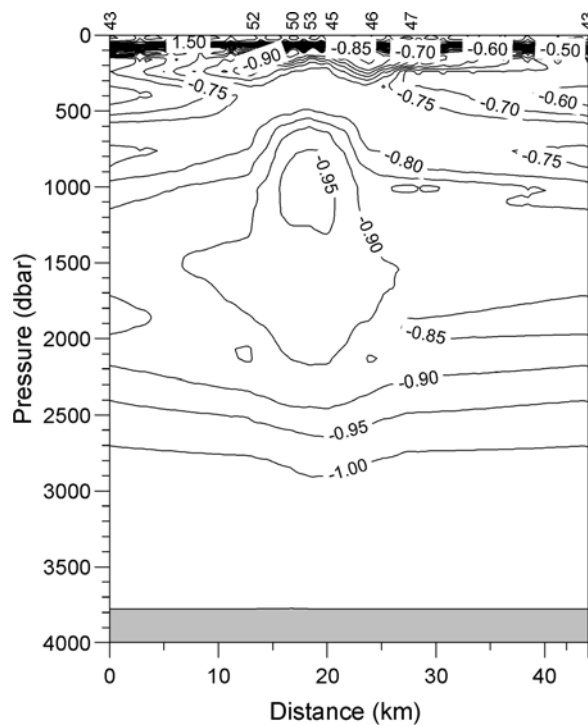


Fig. 4.3: Temperature along a transect across the coherent eddy

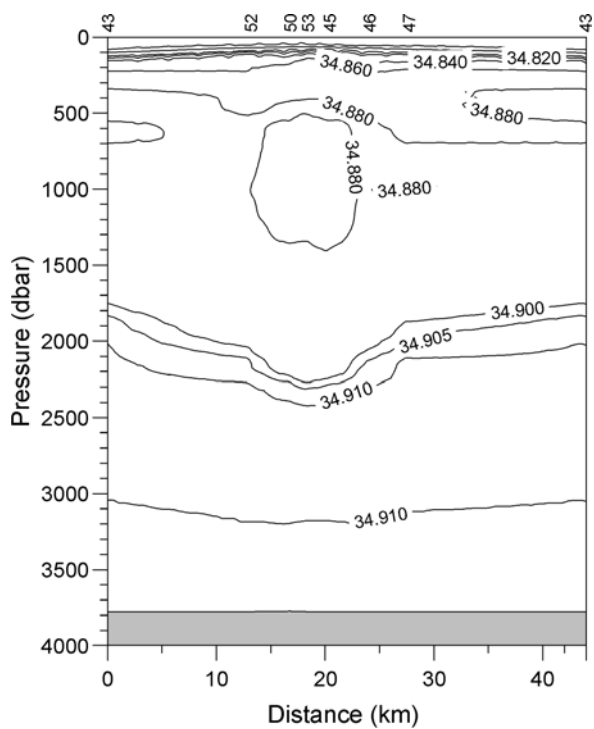


Fig. 4.4: Salinity along a transect across the coherent eddy

---

## 5. INTERDISCIPLINARY RESEARCH AT A DEEP-SEA LONG-TERM STATION IN THE ARCTIC OCEAN

Thomas Soltwedel, Eduard  
Bauerfeind, Melanie Bergmann,  
Janett Feickert, Ingrid Kolar,  
Corinna Kanzog

Alfred Wegener Institute,  
Bremerhaven

Due to its enormous dimensions and inaccessibility, the deep-sea realm remains the world's least known habitat. Until a few years ago, deep-sea research simply meant the assessment of the present status in a distinct, unexplored region of the world's oceans. Single sampling campaigns or measurements, however, generate only snap shots, not allowing extrapolation on temporal variabilities. Consequently, ecological assessments are largely confined. Only long-term investigations at selected sites offer the opportunity to identify environmental settings determining the structure, complexity and the development of deep-sea communities. There is strong evidence that ongoing industrialisation also affects the marine environment, including the deep sea. Hence, basic data are urgently needed to assess anthropogenic impacts on the deep-sea ecosystem. Long-term investigations at selected sites provide the information necessary to assess the present status, and to describe changes due to anthropogenic impacts. The opportunity to measure processes on sufficiently long time scales will finally help to differentiate spatial and temporal variability from (natural) long-term trends.

Following a pre-site study using the French Remotely Operated Vehicle (ROV) "VICTOR 6000" in summer 1999, the AWI Deep-Sea Research Group established the first long-term station in polar deep-sea regions in the eastern Fram Strait off Spitsbergen, the *Hausgarten* (Fig. 5.1). Beside a central experimental area at 2500 m water depth, we defined 9 stations along a depth transect between 1000 - 5500 m, and additional 6 stations along a latitudinal transect crossing the central Hausgarten station, which will be revisited yearly to analyse seasonal and interannual variations in biological, geochemical and sedimentological parameters.

Organic matter produced in the upper water layers or introduced from land is the main food source for deep-sea organisms. To characterise and quantify organic matter fluxes to the seafloor, we use moorings carrying sediment traps. The exchange of solutes between the sediments and the overlaying waters as well as the bottom currents is studied to investigate major processes at the sediment-water-interface. Virtually undisturbed sediment samples are taken using a multiple corer. Various biogenic compounds from the sediments are analysed to estimate activities (e.g. bacterial exoenzymatic activity) and total biomass of the smallest sediment-inhabiting organisms. Results help to describe the eco-status of the benthic system. The quantification of benthic organisms from bacteria to megafauna is a major goal in biological investigations.

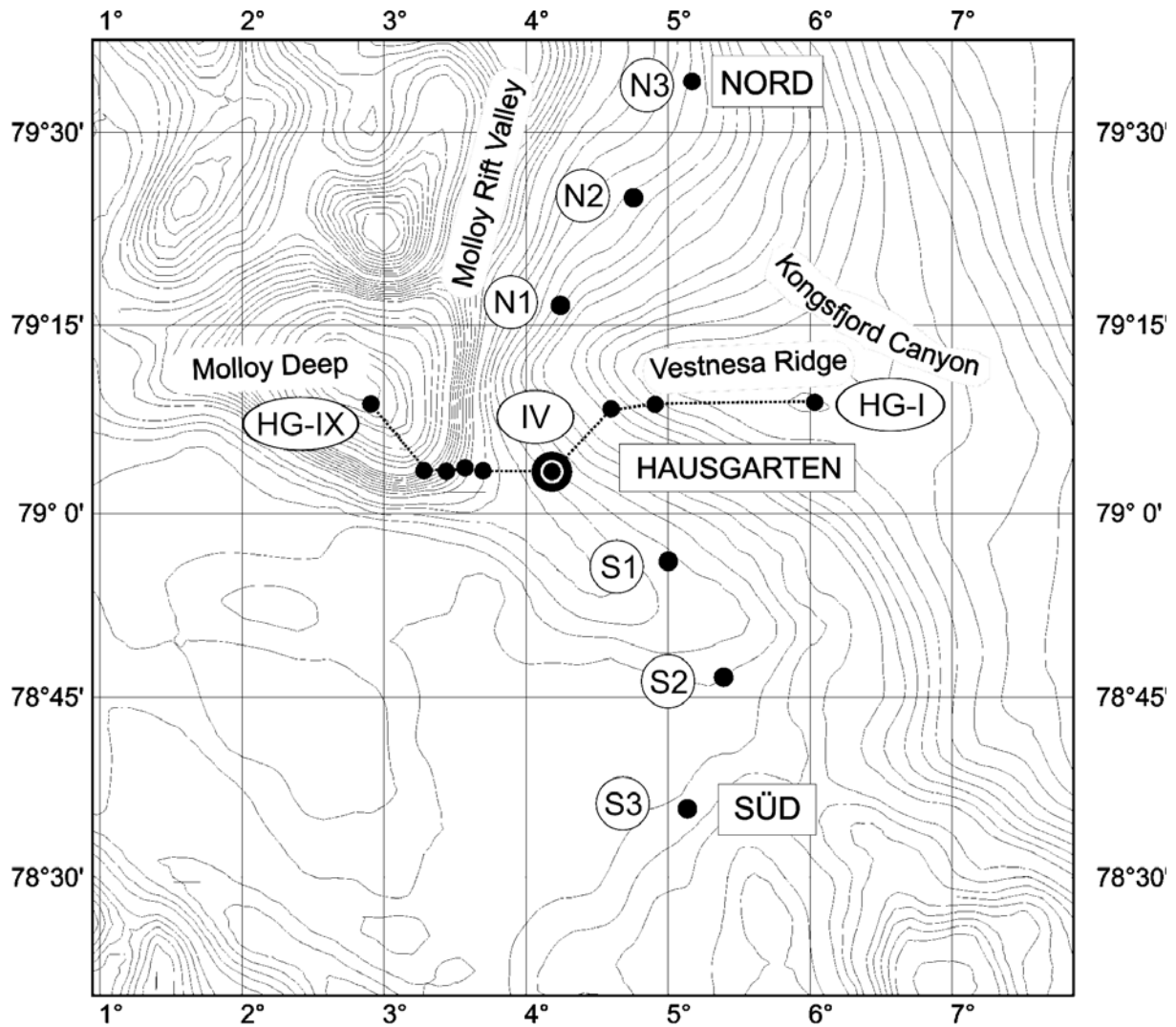


Fig. 5.1: Deep-sea long-term station AWI Hausgarten

## 5.1 Biological oceanography and sedimentation

Eduard Bauerfeind, Burkhard Sablotny  
 Alfred Wegener Institute, Bremerhaven

During the cruise ARK-XX/1 the chance was taken to study the distribution of plankton and its changes along a transect at 75°N in the Norwegian/Greenland Seas. Samples were taken in a distance of 30 nm from the regions dominated by Atlantic waters in the east all across the Greenland Sea to the Greenland continental shelf, where waters of polar origin prevail. Water samples were taken from the CTD-Rosette-Sampler at 6 depths from the surface to 150 m water depth. Subsamples

were filtered for the analysis of the organic carbon and nitrogen content, Chl. *a*, plankton composition, and the amount of particulate silica. In cooperation with E. Falck from the Physical Oceanography Group, samples were also taken for the analysis of inorganic dissolved nutrients. All these samples were stored until further analysis at the land-based laboratory. In the *AWI Hausgarten* area, filtration was done for the same parameters, and additionally for the analysis of particulate <sup>15</sup>N content of the suspended matter. Here samples were taken at the central station (HG IV) and at the northern-most (N3) and southern-most (S3) positions (see Fig. 5.1). In these areas samples were taken from the surface to the seafloor at 12 different water depths.

At the position HG IV a mooring equipped with 3 sediment traps that was installed during the cruise ARK IX/3c in 2003 was successfully recovered. However, due to a technical failure of the control units of the sediment traps almost no samples were obtained. This failure could be repaired on board and three new moorings equipped with sediment traps (7 altogether) and current meters were laid out at the positions HG IV, S3 and N3. The intention of this studies are to get better insights in the seasonal, regional and interannual fluctuations of particle formation, modification and sedimentation in relation to benthic response and possible impacts of climatic changes.

## 5.2 Microbiological and molecular biological investigations of bacterial deep-sea communities

Corinna Kanzog  
Alfred Wegener Institute, Bremerhaven

Large food falls (such as fish carrion) or phytodetritus aggregates sunken to the deep seafloor constitute sudden and rich sources of food for benthic assemblages. This sporadic input of nutrients may affect the diversity and activity of bacterial deep-sea communities. Results from *in situ* experiments started during ARK-XIX/1b will help us to understand how and to what extent the smallest benthic organisms react to such events. In spring 2003, the AWI Deep-Sea Research Group deployed two free-falling Colonization Trays, which contained different types of artificial sediments and organic matter (i.e. fish carrion, detritus, and yeast cultures). These trays were recovered and subsampled during ARK-XIX/3c in summer 2003. Following the addition of fresh sediments, the trays were re-deployed for another year for sampling during ARK-XX/1 summer 2004.

Since it is produced by many marine organisms, including zooplankton and several phytoplankton species, chitin is a common biopolymer in nature and possibly the most common one to occur in marine environments (Gooday, 1990). One Colonization Tray with different concentrations of chitin and different types of artificial sediments was deployed for one week at the central Hausgarten station (HG IV, 2500 m) to assess the effect of different chitin concentrations on the composition of sediment-inhabiting bacterial communities at different times after deployment. Chitinase activity was examined by using the fluorogenic substrate Methylumbelliferone- $\beta$ -N-Acetyl-glucosamine. The fluorescence intensity of the

samples was determined at an excitation wavelength of 356 nm and an emission wave length of 445 nm.

To investigate turn-over rates and the composition of bacterial communities we also sampled deep-sea sediments with a multi-corer (Tab. 5.2.1). In the laboratory, these sediments will be used for long-term incubation experiments to analyse the bacterial break-down of chitin.

**Tab. 5.2.1:** Samples for long-term incubation experiments.

Station number	Water depth (m)	Number of samples
PS 66 / 105-1	2500	4 x 400 ml Sediment (0-3 cm)
PS 66 / 119	2500	4 x 400 ml Sediment (0-3 cm)
PS 66 / 127-3	2500	4 x 400 ml Sediment (0-3 cm)

In addition, we sampled each long-term station of the AWI-Hausgarten (Tab. 5.2.2) to determine bacterial numbers and biomasses, and to identify bacterial communities with molecular methods.

**Tab. 5.2.2:** Samples for bacterial numbers and biomasses.

Station number	Water depth (m)
PS 66 / 100-2	2000
PS 66 / 101-2	1500
PS 66 / 104	1200
PS 66 / 108	2500
PS 66 / 112-2	2500
PS 66 / 113-2	2500
PS 66 114-2	3000
PS 66 / 117	2500
PS 66 / 121-2	3500
PS 66 / 122-2	4000
PS 66 / 124-2	5500
PS 66 / 125-2	2500
PS 66 / 126-2	2500
PS 66 / 127-2	2500

Bacterial biomass was determined from 1 ml sediment samples diluted with 9 ml of a sterile filtered 4 % formaldehyde-seawater solution and stored refrigerated. Subsamples for molecular biological techniques (fluorescent *in situ* hybridization, FISH) were prepared according to the method of Amann et al. (1997).

**Literature:**

- Amann, R., Glöckner, F.O., Neef, A. (1997). Modern methods in subsurface microbiology - *in situ* identification of microorganisms with nucleic acid probes. FEMS Microbiol. Rev., 20: 191-200.
- Gooday, G.W. (1990). The ecology of chitin degradation. Adv. Microb. Ecol., 11: 387-430.

**5.3 Benthic studies at the *Hausgarten* long-term stations**

Ingo Schewe, Janett Feickert, Ingrid Kolar  
Alfred Wegener Institute, Bremerhaven

The standard long-term investigations in the AWI-*Hausgarten* area are dedicated to large-scale ecological investigations on the benthic community. The stations for these investigations are spread over a wide range in water depth and in latitudinal space (Fig. 5.1), so they cover a wide variety of different habitats. Sampling of virtually undisturbed sediments was done with a multiple corer.

During ARK-XX/1, special focus was put on the investigation of variations in environmental parameters at smallest scales (from centimetres to millimetres) and their relevance for the distribution and diversity of benthic organisms. To follow this question we carried out an extremely careful sediment sampling using a giant box corer, to get both, an almost undisturbed sediment-water-interface and a large (0,25 m<sup>2</sup>) coherent surface of the deep seafloor. The sediment surface was divided by a metal frame into sixteen (4 x 4) segments. Each segment was then sampled with a set of 12 syringes with cut of anterior ends to analyse subsamples for a variety of parameters commonly used in ecological studies (Fig. 5.3.1). This sampling strategy will allow a complex combination of parameters coming from sedimentological, biochemical and taxonomical analyses. Thus it will be possible to refer community related parameters with environmental parameters also in smallest scales.

Fig.5.3.1: Subsampling of the box-corer to assess small-scale variabilities



During the cruise we also recovered so-called Colonisation Trays (Fig.5.3.2), which are moored frames equipped with different kinds of artificial and natural soft sediments. These sediments were enriched with different types of food and deployed for one year. The aim of this experimental setting was to investigate preferences of the smallest organisms (from bacteria to meiofauna) in colonising different

kinds of habitat. Each type of sediment-food-combination was sampled for the same set of analyses also carried out for the *Hausgarten* long-term stations. Analyses will enable us to retrieve information about the activity, abundance and biomass as well as the diversity of colonising organisms. In addition, we will also analyse the food sources, which were either sedimented over the year on the experimental settings or which are left from the original application of food.



Fig. 5.3.2: Colonisation Trays during subsampling

#### 5.4 Ecology of eelpout from the *AWI-Hausgarten* and the Håkon Mosby Mud Volcano

Melanie Bergmann  
Alfred Wegener Institute, Bremerhaven

Despite their abundance, little is known about the ecology and habitat preferences of demersal deep-sea fishes, especially of those from polar regions. Footage from the French ROV VICTOR (ARK-XIX/3b and /3c) showed that fish such as zoarcid eelpout (Fig. 5.4.1 a) represent one of the dominant megafaunal organisms present in continental slope environments. Being top predators they may play important role in such ecosystems. Following previous results, we sampled the demersal fish fauna at the *AWI-Hausgarten* and close to the Håkon Mosby Mud Volcano (HMMV) to study their ecology and for ground-truthing of our video imagery. Both, an Agassiz trawl (Fig. 5.4.1 b) and fish traps were used to sample the fish fauna. Four trawls in total were carried out at stations of different depths and baited fish traps that were attached to a benthic lander (Fig. 5.4.1 c) were deployed twice (for 50-85 h) on the seabed at HG IV (Tab. 5.4.1). In addition to fish, the trap also caught high numbers of scavenging amphipods (*Eurythenes gryllus*) that were preserved.



Fig. 5.4.1 a,b,c: Zoarcid eelpout (top), Agassiz trawl (bottom left), and benthic lander carrying two fish traps (bottom right)

All fish were measured, weighed and preserved and will be subject to stomach contents and radio stable isotope analysis to determine the trophic level. The data will be compared with previously collected data on megafaunal abundance to estimate prey selectivity. Furthermore, the gonads and livers will be analysed and the otoliths read to age the fish and to determine growth and production. Different species of eelpout were caught at different stations. Megafaunal samples were also taken at each station for ground-truthing purposes and radio stable isotope analysis.

**Tab. 5.4.1:** Summary of sampling effort (\* sampled by Agassiz trawl; \*\* subsample taken)

	Outside HMMV*	<i>Hausgarten</i> I*	Kongsfjord Canyon*	<i>Hausgarten</i> IV*	<i>Hausgarten</i> IV (Trap 1)	<i>Hausgarten</i> IV (Trap 2)
Water depth (m)	1300	1336	1730	2422	2486	2491
No. of fish	7	68	2	18	9	8
Mean fish condition	0.34±0.23	0.36±0.07	0.27	0.48±0.07	0.59±0.08	0.62± 0.07
No. of species	2	4+	1	2	1	1
Mega-fauna**	x	x	x	x	x	x

## Acknowledgements

I would like to thank Boris Klein (AWI) for providing the fish traps and bait. I am also indebted to Juliane Otto, Linda Gerull, Lisa Kattner, Kati Partzsch and Ulrike Poppe for their assistance in sorting the trawl and trap catches.

## 5.5 Visual observations at the AWI-*Hausgarten*

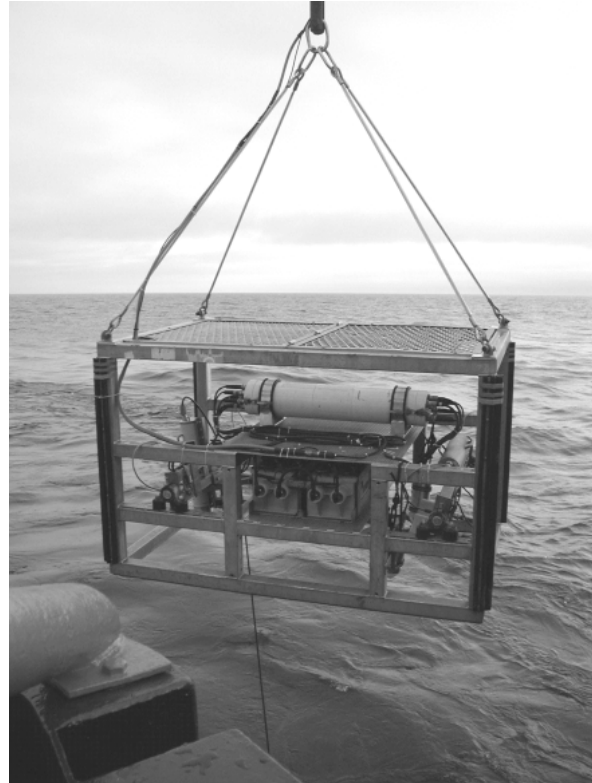
Thomas Soltwedel<sup>1)</sup>  
Friedhelm Kulescha<sup>2)</sup>

<sup>1)</sup> Alfred Wegener Institute, Bremerhaven  
<sup>2)</sup> Oktopus GmbH, Kiel

Large-scale distribution patterns of epifauna organisms were assessed using the so-called "OFOS" (Ocean Floor Observation System, Fig. 5.5.1) carrying a video and a still camera was towed at 1.5 m above ground at a total of 6 stations: at the central *Hausgarten* station (2500 m), thereby repeating a transect already assessed in 1999 and in 2002, at the northern-most and southern-most station (2300 and 2650 m, respectively), and along a transect crossing the Kongsfjord Canyon (1750 m). Additional two OFOS deployments were carried out at a bowl-shape geological structure of approx. 7.5 km in diameter at about 2000 m water depth along the *Hausgarten* depth transect. One OFOS transect was heading from the deepest area

of the depression straight to the North towards shallower regions. The second one was heading to the East, thereby crossing a reef-like structure at the eastern flank of the depression. There is a difference of about 400 m between the base of the depression and the top of the reef.

*Fig. 5.5.1: Ocean Floor Observation System, OFOS*



OFOS deployments generally covered approx. 2 nm at the seafloor thereby producing about 24 hours of video recordings and approx. 4800 colour slides.

## **5.6 Benthic foraminiferal communities and stable isotopic composition**

Laetitia Licari  
Alfred Wegener Institute, Bremerhaven

Benthic foraminifera are widely used as a tool to reconstruct paleoproductivity and past deep-sea ventilation patterns. For paleoceanographers, the most relevant aspect concerns the sensitivity of these organisms to changes in environmental conditions at the seafloor, indirectly recorded by particular faunal compositions specifically adapted to environmental parameters, and directly in the elemental and stable isotopic composition of their calcareous tests (Fig. 5.6.1). The accurate and reliable interpretation of the ecological information conveyed by fossil benthic foraminifera depends, in turn, on the detailed knowledge of the true behaviour of

modern species with regard to given environmental variables, and on how these factors affect the chemical composition of foraminiferal tests.

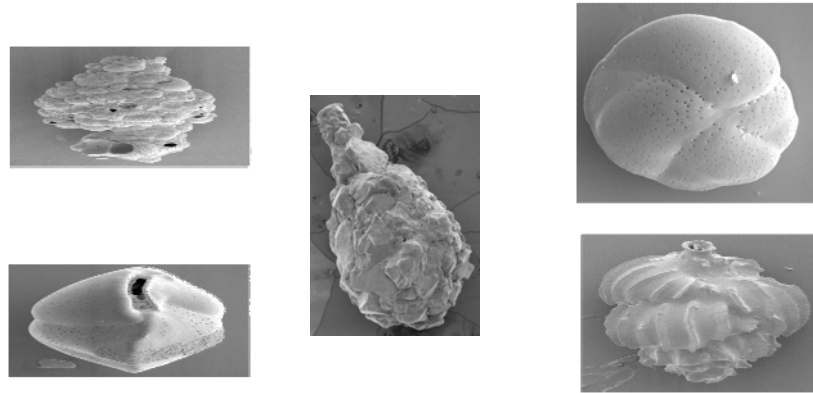


Fig .5.6.1: SEM pictures of some benthic foraminiferal species

During leg ARK-XX/1, sediment samples were recovered with a multicorer (MUC) at the Håkon Mosby Mud Volcano (HMMV) and in the *AWI Hausgarten* area (Fig. 5.1) to investigate benthic foraminiferal assemblages and the stable carbon and oxygen isotopic composition ( $\delta^{13}\text{C}$  and  $\delta^{18}\text{O}$ , respectively) of their tests. At each station, an additional subcore was sampled for sedimentological analyses. In addition, water samples were simultaneously collected at most stations with a rosette sampler to determine the stable carbon and oxygen isotopic composition of the water column.

### ***AWI Hausgarten***

For faunal and isotopic analyses, sediment samples were recovered at eighteen stations in the *Hausgarten* area (Fig. 5.1). At all stations, two subcores were collected and sub-sampled in 1 cm thick slices down to a subbottom depth of 15 cm. Subsamples corresponding to the same depth in the sediment were put together, fixed with a mixture of ethanol and Rose Bengal ( $1 \text{ gl}^{-1}$ ) and kept cool at  $4^\circ \text{C}$ . In addition to these two subcores, a supplementary subcore was separately sampled at stations PS66/101, 104, and 140 following the same procedure. Further treatments and analyses (TEM, fauna, stable isotopy) of samples will be performed in Bremerhaven at the Alfred Wegener Institute for Polar and Marine Research (working group of Prof. A. Mackensen).

### **Håkon Mosby Mud Volcano: the influence of methane on benthic foraminifera**

A major aim of our studies is to determine how methane release affects the ( $\delta^{13}\text{C}$  signature of benthic foraminiferal carbonate and benthic foraminiferal faunas. In that purpose, sediment samples were recovered at five stations located at various habitats of HMMV. Immediately after recovering, two subcores (representing  $78 \text{ cm}^2$

of sediment surface each) were separately sub-sampled in 1 cm slices down to a subbottom depth of 15 cm, and stored at 4° C in a mixture of ethanol and Rose Bengal (1 gl<sup>-1</sup>) until further treatment onshore. In addition, the uppermost centimetre of two subcores was separately sub-sampled in 0.5 cm slices for ultrastructural analyses on benthic foraminifera by Transmission Electron Microscopy. Samples were immediately fixed in a solution of glutaraldehyd (3 %) buffered with sodium cacodylate (0.1 M, in seawater filtered on 2 µm) and mixed with Rose Bengal. Subsequently, samples were sieved over a 63 µm mesh screen and stored at 4° C in buffer solution. Furthermore, an additional subcore was deep-frozen at four stations.

---

## 6. CHEMICAL MEASUREMENT PROGRAMME

Christian Temme<sup>1)</sup>, Jana Baukau<sup>1)</sup>,  
Gerd Blöcker<sup>1)</sup>, Armando Caba<sup>1)</sup>,  
Christina Caliebe<sup>1)</sup>, Wolfgang  
Gerwinski<sup>2)</sup>, Rosalinda Gioia<sup>3)</sup>,  
Edward Hudson<sup>4)</sup>, Annika Jahnke<sup>1)</sup>,  
Zhiyong Xie<sup>1)</sup>

<sup>1)</sup>Institut für Küstenforschung GKSS,  
Geesthacht

<sup>2)</sup>Bundesamt für Seeschifffahrt und  
Hydrographie, Hamburg

<sup>3)</sup>University of Lancaster, Department of  
Environmental Science, Lancaster

<sup>4)</sup>McGill University, Montreal

### Reactions mechanisms of mercury and selected persistent organic pollutants (POPs) in air, water, and snow

Several international leading groups of Environmental Chemistry were joining the RV *Polarstern* on ARK-XX/1 2004. Their common interest was the detection of trace organic contaminants and mercury species in remote environments of the Northern Hemisphere, to investigate the environmental cycling and fate of key global pollutants. The RV *Polarstern* has been found to be well suited to act as a 'clean ship' for the sampling of these trace compounds.

The chemical research programme during ARK-XX/1 was focused on two major topics:

1. Determination of mercury and related volatile organic compounds (VOCs) and dissolved organic carbon (DOC) in different compartments and the calculation of the air/sea-exchange during Arctic summer
2. Determination of selected POPs in air, water, and snow

#### 6.1 Mercury and the VOC/DOC connection

Mercury (Hg) is outstanding among the global environmental pollutants of continuing concern. The element and many of its compounds behave exceptionally in the environment due to their volatility and capability for methylation, in contrast with most of the other heavy metals. Long-range atmospheric transport of mercury, its transformation to more toxic methylmercury compounds, and their bioaccumulation in the aquatic food chain have motivated intensive research on mercury as a pollutant of global concern.

The international process study on board of RV *Polarstern* with the transect from Germany to the North Atlantic helped to examine the temporal end of Atmospheric

Mercury Depletions Events (AMDEs) during Arctic summer and the spatial distribution of the relevant areas in the north Atlantic Ocean. The fate of mercury during polar summer in the Arctic was investigated with several different methods for the detection of mercury species in air, water, snow, and ice.

Two Tekran gas-phase mercury vapour analysers (Model 2537A) were installed on RV *Polarstern* for the determination of Gaseous Elemental Mercury (GEM) and Reactive Gaseous Mercury (RGM) species in the Arctic. RGM was measured with a Tekran 1130 mercury speciation unit which gave one Tekran 2537A mercury vapour analyser the ability to concurrently monitor both elemental (GEM) and reactive gaseous mercury (RGM) species in ambient air at the  $\text{pg m}^{-3}$  level. The sample inlet was located on the upper deck of RV *Polarstern* in front of the GKSS container. The air was sampled at a flow rate of 1.2 L/min with a 0.45 mm PTFE filter in front of the sample inlet of the analyser.

The results of GEM measurements and ground-level ozone concentrations for the time period 16 June to 14 July are preliminary data. The arithmetic mean of all GEM measurements during this cruise lag is  $(1.6 \pm 0.1) \text{ ng m}^{-3}$  and is in good agreement with mean summer concentrations from other polar sites like Alert, Canada or Ny Ålesund, Svalbard.

Contaminations from the ships plume will be eliminated after the cruise according to the PODAS data of wind directions and wind speed relative to the ships course. In addition the second Tekran analyser in the wet lab was used to investigate the sea/air exchange of GEM during Arctic summer. The analyser was connected to a 20 l glas bottle, called "Equilibrator", indirectly measuring the Dissolved Gaseous Mercury (DGM) concentrations in the sea water with the help of the Henrys law constant.

We found that the Atlantic Ocean is a potential source for GEM in the atmosphere during this time of the year. The flux of GEM from the sea to the atmosphere was in the range of  $(0.1 \text{ to } 3) \text{ ng m}^{-3} \text{ h}^{-1}$  depending on the model used for calculation. We found significantly higher fluxes when we entered the most westerly part of the 75°N transect (1 - 3 July) where the ocean was covered with sea ice.

The oxidative properties of the lower atmosphere (which determine mercury speciation and thus transport) are also reflected in the profile of volatile organic compounds (VOCs) it contains. Dissolved organic carbon (DOC) in surface waters is thought to be the ultimate source of these VOCs over the open sea.

Air samples were taken for VOC analysis (McGill University). Water samples were taken for photochemical and photo oxidation experiments on surface water DOC, to further investigate whether these explain the VOCs found in the air samples. Altogether, 25 whole air samples (6 L) have been taken. Most of these (14) were taken along the 75°N transect (24 June - 3 July), to match the extensive water characterization of this transect. A further 7 were used to profile the transition from the North Sea (58°N, 16 June) to the Norwegian Sea (72°N, 22 June).

Water samples were taken to match the time/location of each air sample. To date, more than 50 samples have been taken (again, mostly along the 75°N transect) and

filtered (0.2  $\mu\text{m}$ ). The additional samples will serve as checks on the effects of sample size, storage and materials, sampling method (Niskins vs. Glass Sphere Water Samplers (GSWS) vs. RV *Polarstern's* in situ pump in the keel), as well as adding 3 intermediate and 4 deep water samples to the data set, which allows us to expose the analytical methods to a wider range of DOC.

Aerosols are important to this study because they represent another interface between the sea surface and the atmosphere, on which DOC may give volatile compounds through photochemistry. However, the cascade impactor used to sample them required long collection times and a favourable wind direction to avoid contamination by the ship itself. Still, 9 samples were collected, each consisting of 9 size fractions. Sampling times ranged from 6 to 40 hours, but were typically 12 to 24 hours.

Towards the end of the 75°N transect, snow was sampled on ice floes in the East Greenland Current to complement the air and water sampling by the air chemistry group. Samples were taken on 2 and 3 July at 74°58.08'N / 13°38.46'W and 75°08.52'N / 16°45.11'W, respectively. Four 250 ml-samples were collected by ultra-clean methods for mercury and radionuclide analysis. These will supplement the extensive snow sampling for these materials which will take place during ARK-XX/2. Four 1-l samples were collected for experiments on the photochemical generation of VOCs (to be done at McGill University). Finally, 40 l of snow were taken in GSWS on each occasion. These will be analysed for POPs by the BSH group.

## 6.2 Persistent organic pollutants (POPs)

By combining short-term atmospheric samples with the collection of representative water samples across different region of the North Atlantic / Arctic circle, answers are sought as to whether atmospheric transport or the marine phytoplankton productivity are controlling the transport and settling flux of persistent organic pollutants.

### Air Sampling

Four different modified High Volume air samplers were used to collect air on board of RV *Polastern* during ARK-XX/1. POPs such as polychlorinated biphenyls (PCBs), polybrominated dyphenyls ethers (PBDEs), organochlorine Pesticides (HCHs, HCBs, DDTs etc.), polyflourinated compounds (PFCs), Nonylphenol (NP), and combustion-derived polychlorinated dibenzo-p-dioxins, furans (PCDD/Fs) and Total Suspended Particulate (TSP) will be investigated. Totally 45 air samples were collected from Bremerhaven to Longyearbyen during the ARK-XX/1 (see Table 6.2.1 - 3). Table 6.2.1 shows samples collected using the Lancaster University High-Volume air sampler, which will be used to determine PCBs and PBDEs concentrations. Table 6.2.2 represents samples collected using the High Volume air sampler from University of Bremen and the samples collected for the determination of TSP (Total Suspended Particulate) using a TSP sampler belonging to Lancaster University. Samples from the Bremen Hi-vol will be used to investigate the concentration of dibenzo-p-dioxin and furans in the atmosphere. Table 6.2.3 shows sampling volumes

and locations for the samples taken with the GKSS High-Volume air sampler in order to determine PFCs and NP in air.

**Table 6.2.1:** Samples collection for the Lancaster High-Volume sampler during ARK-XX/1

Sample ID	Latitude	Longitude	Air volume (m <sup>3</sup> )	Comments
ARK-XX 1	55.5-58.5 N	7.1-4.8 E	287	North Sea
ARK-XX 2	58.6-61.1 N	4.7-3.99E	193	North Sea
ARK-XX 3	61.4-63.4 N	4.0-5.06 E	196	North Sea
ARK-XX 4	63.5-65.7 N	5.08-6.98 E	200	North Sea
ARK-XX 5	65.9-68.1 N	6.98-8.94 E	191	North Sea
ARK-XX 6	68.2-69.2 N	9.03-13.2 E	190	North Sea
ARK-XX 7	69.2-71.4 N	13.2-14.8 E	188	North Sea
ARK-XX 8	72.00 N	14.72E	199	HMMV
ARK-XX 9	72.00 N	14.72E	192	HMMV
ARK-XX 10	72.00 N	14.72E	196	HMMV
ARK-XX 11	71.1-74.6 N	16.6-10.6 E	365	75° Latitude transect
ARK-XX 12	74.6-74.55 N	10.6E-4.4W	411	75° Latitude transect
ARK-XX 13	75.0-76.2 N	4.5-3.4W	458	75° Latitude transect-LYB
ARK-XX 14	76.20-78.9 N	3.7W-5.4E	490	On the way to LYB
ARK-XX 15	79.4-79.8 N	4.2E-3.20	771	<i>Hausgarten</i>
ARK-XX 16	79.4-79.35N	3.2-5.11E	396	<i>Hausgarten</i>
ARK-XX FB1	68.1N	8.9E	Field blank	North Sea
ARK-XX FB2	69.2N	13.2 E	Field blank	North sea
ARK-XX FB3	72.0 N	14.7 E	Field blank	HMMV
ARK-XX FB4	74.5 N	4.4 W	Field blank	75° Latitude transect
ARK-XX FB5	79.4N	3.2 E	Field Blank	<i>Hausgarten</i>

**Table 6.2.2:** Samples collection for the Bremen High-Volume sampler and the TSP sampler during ARK-XX/1

Sample ID (Bremen High-VOL)	Sample ID (TSP sampler)	Latitude	Longitude	Flow rate (ft <sup>3</sup> /min)	Comments
ARK-XX R1	TSP ARK-XX 1	57.2-61.7 N	5.3-3.9E	13	North Sea
ARK-XX R2	No TSP sample	61.9-66.3 N	3.9-7.4 E	13	North Sea
ARK-XX R3	TSP ARK-XX 2	66.5-69.35 N	7.4-13.7 E	14	North Sea
ARK-XX R4	TSP ARK-XX 3	71.9-72.01N	14.72 E	19	HMMV
ARK-XX R5	TSP ARK-XX 4	71.10-74.6N	16.6-10.6E	20	To the 75°traverse
ARK-XX R6	TSP ARK-XX 5	74.6-74.55N	10.6E 4.3W	20	75°traverse
ARK-XX R7	TSP ARK-XX 6	75.0-76.1N	4.47-3.4W	19	75°traverse to LYB
ARK-XX R8	TSP ARK-XX 7	76.2-78.91	3.1W-5.1E	19	To LYB
ARK-XX R9	TSP ARK-XX 8	79.6 N-78.9	5.18E-4.8 E	20	<i>Hausgarten</i>
ARK-XX RFB1	TSP ARK-XX FB1	69.38N	13.85 E	Blank	North Sea
ARK-XX RFB2	TSP ARK-XX FB2	72.0 N	14.72 E	Blank	HMMV
ARK-XX RFB3	TSP ARK-XX FB3	74.6N	4.3W	Blank	75°traverse

**Table 6.2.3:** Samples collection for the GKSS High-Volume sampler during ARK-XX/1

Sample ID	Date	Latitude	Longitude	Volume (m <sup>3</sup> )	Comments
ARK XX-1	16/06/2004 - 21/06/2004	55.2°N - 72.0°N	6.5°E - 14.4°E	1114,6	Bremerhaven to HMMV
ARK XX-2	21/06/2004 - 23/06/2004	72.0°N - 71.2°N	14.4°E - 16.4°E	664,0	Continuous sampling at HMMV
ARK XX-3	23/06/2004 - 04/07/2004	71.3°N - 75.4°N	16.3°E - 8.2°W	913,2	75°N-traverse, sampling stopped during station times
ARK XX-4	04/07/2004 - 08/07/2004	75.5°N - 78.3°N	7.6°W - 5.5°E	911,2	Sampling continued at stations if relative wind direction was 270°-90° and true wind speed was at least 5 m/s
ARK XX-5	08/07/2004 - 11/07/2004	78.4°N - 79.4°N	5.5°E - 5.1°E	917,2	Continuous sampling despite low wind speed / wind from behind
ARK XX-6	11/07/2004 - 15/07/2004	79.4°N - ?	5.1°E - ?	?	Continuous sampling despite low wind speed / wind from behind

GFFs (Glass Fiber Filter) precombusted at 450 ° C overnight, were used to capture the particles and particle bound species, and two cylindrical 3 inch diameter polyurethane foam (PUF) adsorbents were used downstream to capture the gas-phase contaminants. Prior to use, the PUFs for the Lancaster and Bremen High-Volume sampler were cleaned with an Accelerated Solvent Extraction (ASE) system using dichloromethane (DCM) as solvent. After cleaning, the PUFs were desiccated under vacuum to remove excess solvent and stored frozen in pre-cleaned aluminum tins. The PUF adsorbent and XAD resin for NP and PFCs sampled with the GKSS high-vols were pre-cleaned by soxhlet extraction with acetone/hexane and ethyl acetate respectively. After samples collection, GFFs and PUFs (and XAD resin) were sealed and stored frozen until they will be analysed. Because low concentration levels are expected to be found in Arctic regions, all the pre-cleaning procedures was performed in a clean room at Lancaster University and GKSS.

The overall ship's track from the North Sea into the remote Arctic region is a great opportunity to monitor the air concentrations of POPs from source regions to polar areas. We expect to see spatial trends in air concentrations that provide some evidence for the global fractionation theory. It is generally assumed that the atmosphere can serve as pathway for the delivery of these pollutants to water and terrestrial surfaces. Therefore, POPs can undergo long-range atmospheric transport with high volatile compounds condensing in colder (polar) regions and less volatile compounds condensing in warmer regions close to sources. This will probably not occur in one step, but in a number of steps of volatilization followed by deposition, followed by seasonal fluctuations in temperature. The effect of this will be a relative enrichment of the more volatile compounds in cold areas. Criteria for global fractionation behaviour of chemicals are various physical-chemical properties such as vapour pressure, the octanol-air partition coefficient, the octanol-water partition coefficient and the Henry's Law Constant.

PCBs are a class of compounds with a variety of different physical-chemical processes. There are 209 congeners depending from the number of chlorine atoms on the molecule and the position that these atoms occupy on the molecule. Therefore, with all these differences in physical-chemical properties, PCBs are ideal to investigate and find evidence of the global fractionation theory. These properties are very dependent on temperature and will therefore greatly influence the global transport of POPs. The temperature dropping during this cruise track, from 11 °C to -2 °C is a rare opportunity to estimate the temperature dependence of POPs in the atmosphere.

Growth in interest on PBDE flame retardants has been as exponential as their apparent increase in the environment over the past 20-25 years in North America and Europe. Toxicological studies of limited PBDE congeners indicate that they are potential thyroid disruptors and developmental neurotoxicants. However, there is still very little information on PBDE contamination and its spatial trend over the regions of the world. The investigation, which will follow air sample collection on RV *Polarstern*, will attempt to comprehensively understand the spatial and temporal trend of contamination by PBDEs emerging compounds in the atmosphere.

Polyfluorinated organic acids and their derivatives are produced by industry in very large quantities and are used for many purposes. Perfluoroalkyl sulfonates are used e.g. as surfactants and surface protectors in carpets, leather, paper, packaging and upholstery. In addition, some sulfonated and carboxylated PFCs have been used in or as fire fighting foams, alkaline cleaners, shampoos, and insecticide formulations. Due to the large production quantities and the persistence in the environment, polyfluorinated compounds are meanwhile globally distributed. Perfluorooctanesulfonic acid (PFOS) has been detected in blood of ringed seals, other long chain perfluorinated chemicals have been detected in polar bears, arctic foxes, ringed seals, mink, birds and fishes collected in the Arctic.

Because of the findings of polyfluorinated compounds in Arctic biota samples, it is of special interest to investigate their long range transport. Due to their high polarity, a transport by the water phase is likely, especially since some of the PFCs have been found in North Sea water. Some precursors of PFOS and PFOA are highly volatile and can lead to an increased input of PFCs from the atmosphere to remote areas. The investigation of the wide scale distribution of polyfluorinated acids in the sea water of the North Sea and Arctic Ocean is a perfect complement to the simultaneous measurements in the atmosphere. The cruise was quite optimal for these investigations as it ranged from the likely sources (European continent) to remote areas without direct inputs.

Short-term air samples (12 hr) were collected in the North Sea, from Bremerhaven to Tromsø. These samples are useful to investigate the day-night cycle (if there is any) of PCBs over the ocean and whether the marine phytoplankton is controlling the atmospheric concentrations of POPs in the marine atmosphere. We were expecting to collect more short-term atmospheric samples during the 75° latitude transect and up to the *Hausgarten*, but this was not possible since the ship was stopping and starting most of the time. When taking an air sample good care should be taken to minimize the risk of contamination from the ship exhaust and this was quite impossible when the ship stopped and was not kept in the wind.

All the laboratory analysis of extractions and clean up will be performed in a clean room at Lancaster University, UK, and GKSS-Research Centre in Geesthacht, Germany. Field blanks were collected in order to define blank-based limit of detection (LOD) for each sampling matrix (PUF, XAD and GFF) as the average contaminant mass of field blanks plus 3 standard deviations.

### **Passive air sampling**

Five passive air samplers were deployed on board of the ship to look at the ship background concentrations of POPs. Passive samplers were deployed on the Peildeck near the hi-vol, in the GKSS container where matrix are treated before and after sampling, on the back of the ship, in the -30 °C freezer on the F-deck where air samples are stored and in the wet lab, where water sampling is performed.

Polyurethane Foam (PUF) samplers are used to passively sample air. The advantage of passive sampler compared with active samplers is that they are cheap because they are not power consuming and they are easy to deploy.

The surface of the PUF comes into contact with vapour phase species in the atmosphere and it will respond through three different steps:

- **Initial linear** uptake of the compound to the surface
- **A curvilinear portion** of the uptake as equilibrium is approaching
- **Equilibrium** between the air concentration and the surface.

The mass of the compound held by the surface when it is at equilibrium with the air will depend on:

1. **Temperature**
2. **Type of the surface**
3. **Physico-chemical properties of POPs.**

The uptake is also influenced by:

- The **size** or **capacity** of the subsurface compartment
- The **surface area**
- The **thickness** of the sampler.

These factors above can be varied depending on the compound of interest, the deployment/sampling time and the sensitivity of the analytical instrumentation. Time to reach equilibrium with the sampler device vary between compounds and increases with  $K_{oa}$ .

Previous studies on RV *Polarstern*, where passive sampler were also deployed, showed that the ship does not contribute to PCB contamination and this allowed us to conduct research on POPs on this research vessel even at very low concentration such as the Arctic regions. We expected to see the same results about the ship background contamination during this cruise leg.

### **Water Sampling**

Water sampling was performed simultaneously to the air sampling in order to investigate the mechanisms controlling the air-water exchange flux.

The water samples were taken from the clean seawater system (stainless steel pipe) of RV *Polarstern* (11 m depth) as well as directly from the surface water (20 m depth) with the glass sphere water samplers (GSWSs) from the BSH. We expect the air concentration of these compounds to be at equilibrium with the water concentration in the Arctic region, given the remoteness of this area. It is summarized in table 6.2.4 and figures 6.2.1 to 6.2.3.

The majority of samples have been extracted with solid phase adsorber columns based on styrene/divinylbenzole copolymer. A mixture of deuterated internal standards were added prior to extraction to control the extraction efficiency and to calculate the observed contaminants. Sample volumes of 10 liters and 30 liters were used for extraction to compare different factors of preconcentration. After pumping the seawater through the columns they were rinsed with pure water and dried with a gentle stream of nitrogen gas. Elution will be done after the cruise in the land based laboratory. One part of the taken replicate columns will be eluted with methanol as solvent for HPLC/MS/MS measurements, the other part will be eluted with a mixture of Hexane/Dichloromethane for GC/MS analysis.

At least 4 analytical runs per sample will be performed to detect and to quantify the whole list of expected contaminants. The main objective is the analysis of polyfluorinated compounds and some widely used pesticides, partly indicated as persistent organic pollutants.

Tab. 6.2.4

<b>ARK-XX/1 Sampling Overview for contaminants in Seawater (BSH)</b>			
<b>Sampling</b>	<b>Number of stations</b>	<b>Number of SPE-extractions</b>	<b>Number of LLE-extractions</b>
<b>Sampling locations winch</b>	<b>8</b>	<b>40</b>	<b>8</b>
<b>Sampling locations pipe</b>	<b>12</b>	<b>18</b>	<b>5</b>
<b>Snow samples</b>	<b>2</b>	<b>4</b>	<b>0</b>
Quality control, blanks		6	5
Quality control, recovery		4	0
<b>Total samples</b>	<b>22</b>	<b>62</b>	<b>13</b>

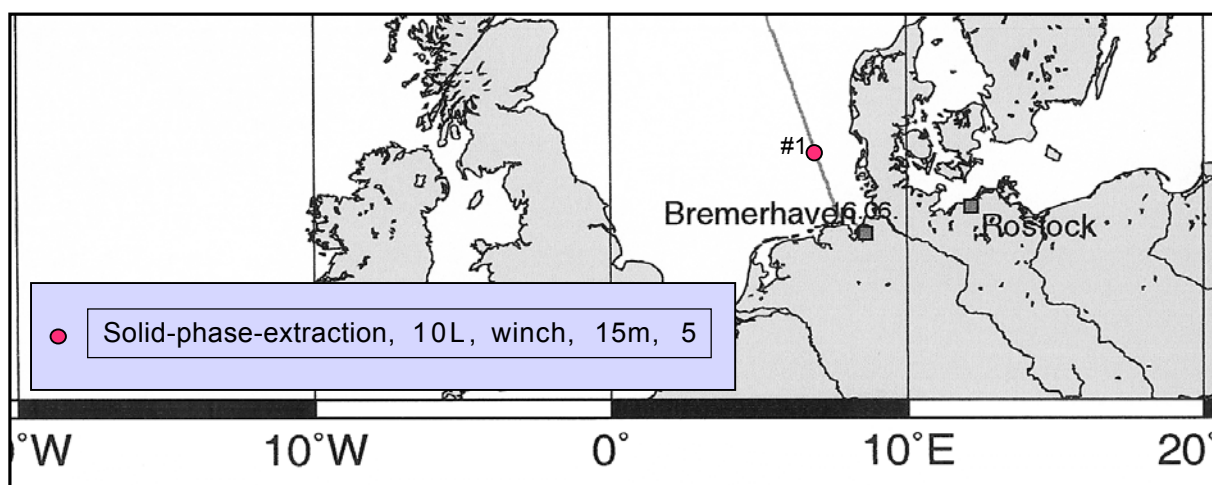


Fig. 6.2.1: Sampling locations for contaminants in seawater



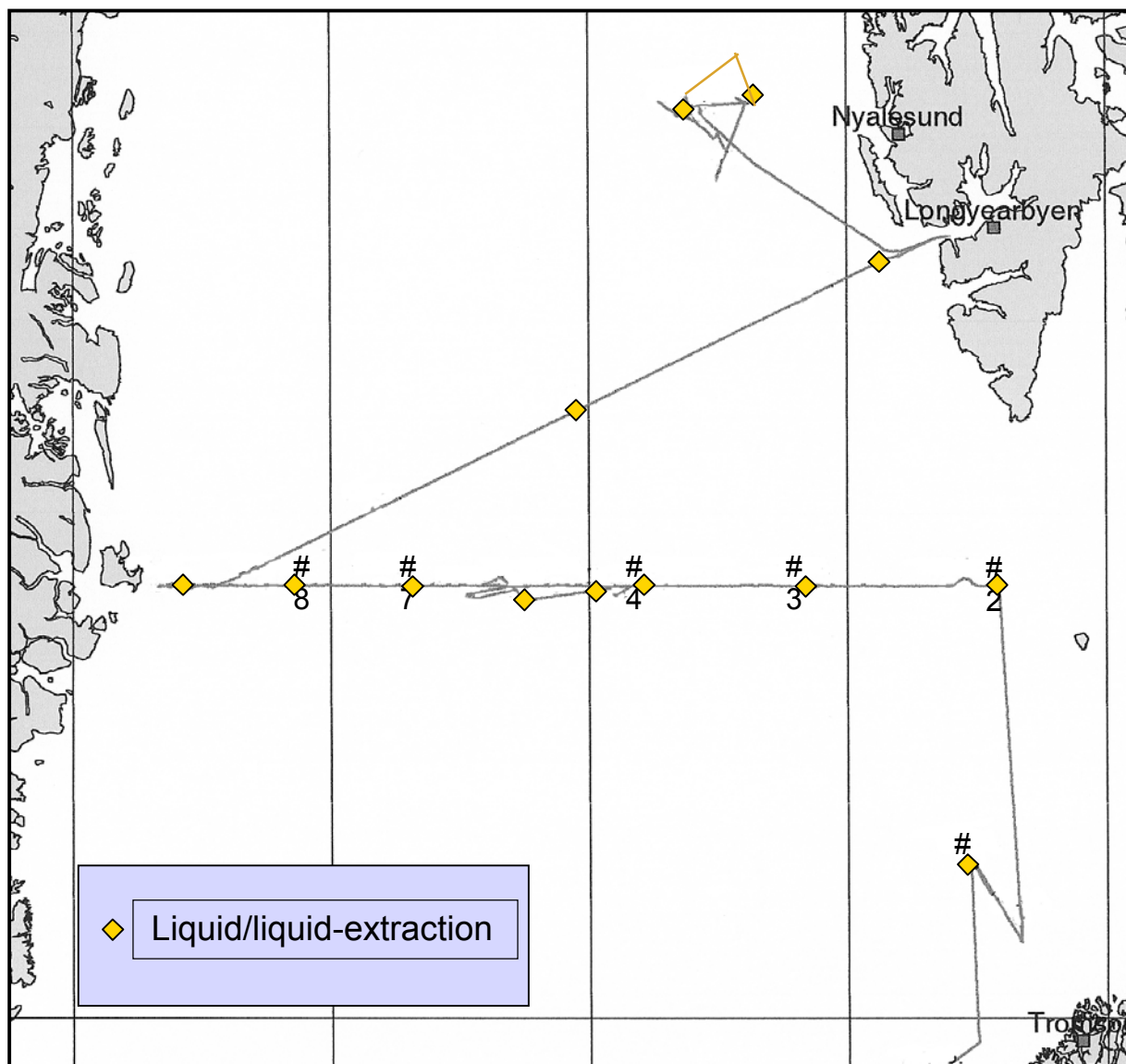


Fig. 6.3.3: Sampling locations from contaminants in seawater

## 7. SEDIMENT ACOUSTICS: ATLAS PARASOUND SYSTEM UPGRADE DS-1 TO DS-2

Gerhard Kuhn

On the transit from Bremerhaven to Tromsø the sea acceptance test for the newly installed Parasound system upgrade DS-2 was carried out. With this upgrade the hardware of the 1989 installed Parasound DS-1 system was replaced in a first stage of extension.

The Atlas Parasound is a permanently installed system on R/V *Polarstern*. It determines the water depth and with variable frequencies from 2.5 to 5.5 kHz it provides high-resolution information of the sedimentary layers up to a depth of 200 meters below sea floor.

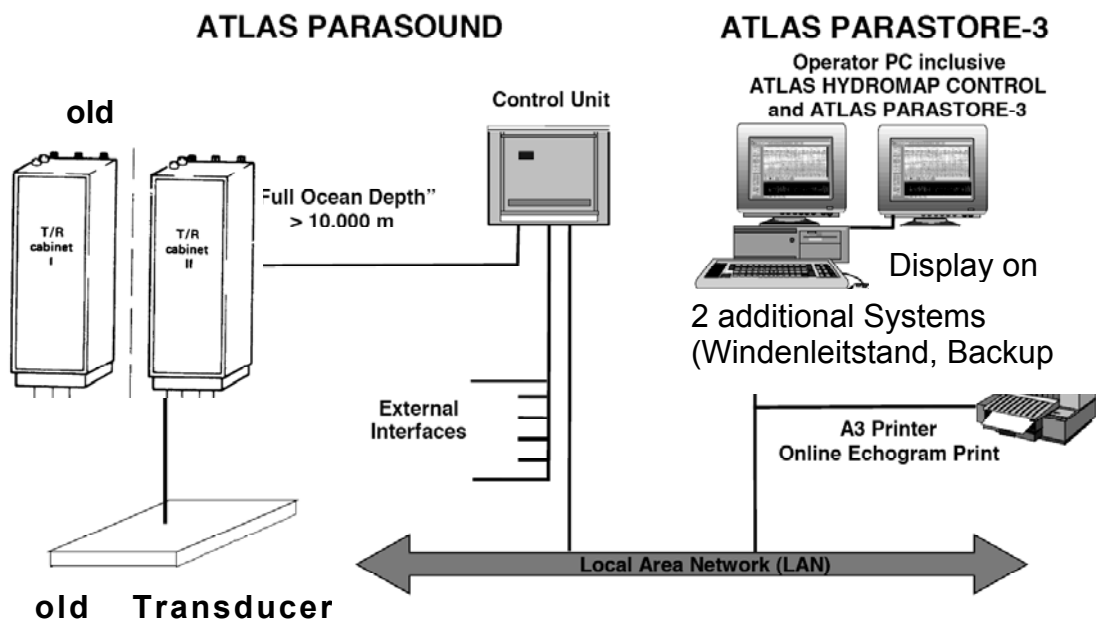


Fig. 7.1: System architecture of new ATLAS PARASOUND DS2 system (2004) with communication over local area network

After 4 days of trial the sea acceptance test was signed, but with some points to be fulfilled afterwards. Water depth was too low, time too short and sea state too calm to get realistic environmental conditions for testing the instrument. The crew left RV *Polarstern* on 20 and 22 June with helicopter flights to Tromsø.

---

## **APPENDIX**

**A.1 PARTICIPANTS**

**A.2 PARTICIPATING INSTITUTIONS**

**A.3 SHIP'S CREW**

**A.4 STATION LIST**

## A.1 PARTICIPANTS

<b>Name</b>	<b>Vorname/ First Name</b>	<b>Institut/ Institute</b>	<b>Beruf / Profession</b>
Bauerfeind	Eduard	AWI	Biologist
Baukau	Jana	GKSS	Student
Bergmann	Melanie	AWI	Biologist
Blöcker	Gerd	GKSS	Chemist
Büchner	Jürgen	HeliTransair	Pilot
Budéus	Gereon	AWI	Phys. oceanographer
Buldt	Klaus	DWD	Technician
Caba	Armando	GKSS	Engineer
Caliebe	Christina	BSH	Chemist
Cembella	Barbara	Optimare	Physicist
Cisewski	Boris	AWI	Phys. oceanographer
Dittmer	Martin	Atlas Hydrogr.	Technician
Ewert	Jörn	Atlas Hydrogr.	Technician
Falck	Eva	AWI	Chem.oceanographer.
Feickert	Janett	AWI	Student
Feldt	Oliver	HeliTransair	Technician
Gerull	Linda	AWI	Student
Gerwinski	Wolfgang	BSH	Engineer
Gioia	Rosalinda	University of Lancaster	Student
Hartig	Rüdiger	DWD	Meteorologist
Herr	Eberhard	HeliTransair	Pilot
Hudson	Edward	Uni Montreal	Chemist
Jahnke	Annika	GKSS	PhD student
Kaletzky	Arthur	University of Cambridge	Engineer
Kanzog	Corinna	AWI	Technician
Kattner	Lisa	AWI	Student
Kaufner	Helmke	Cinedesign	Writer
Kaufner	Peter	Cinedesign	Cameraman
Kolar	Ingrid	AWI	Student

<b>Name</b>	<b>Vorname/ First Name</b>	<b>Institut/ Institute</b>	<b>Beruf / Profession</b>
Kuhn	Gerhard	AWI	Geologist
Kulescha	Friedhelm	Oktopus	OFOS Techn.
Licari	Laetitia	AWI	Biologist
Niessen	Frank	AWI	Geologist
Otto	Juliane	AWI	Student
Partzsch	Kati	AWI	Student
Plugge	Rainer	AWI	Technician
Poppe	Ulrike	AWI	Geographer
Ronski	Stephanie	AWI	Phys. oceanographer
Sablotny	Burkhard	AWI	Technician
Schewe	Ingo	AWI	Biologist
Schmidt	Thomas	Fielax	IT engineer
Soltwedel	Thomas	AWI	Biologist
Temme	Christian	GKSS	Chemist
Wagner	Eberhard	Laeisz	Engineer
Xie	Zhiyong	GKSS	Chemist
Yousif	Khalaf	HeliTransair	Technician

---

## A.2 PARTICIPATING INSTITUTES

	<b>Adresse</b> <b>Address</b>
AWI	Stiftung Alfred-Wegener-Institut für Polar- und Meeresforschung in der Helmholtz- Gemeinschaft Postfach 12 01 61 27515 Bremerhaven
Atlas Hydrographic	Atlas Hydrographic Kurfürstenallee 130 28211 Bremen
BSH	Bundesamt für Seeschifffahrt und Hydrographie Wüstland 2 22589 Hamburg
Cinedesign	Cinedesign AV GmbH /NDR Carsten-Fock Weg 12 21129 Hamburg
DWD	Deutscher Wetterdienst Bernhard-Nocht Straße 76 20359 Hamburg
FIELAX	FIELAX Gesellschaft für wissenschaftliche Datenverarbeitung mbH Schifferstraße 10-14 27568 Bremerhaven
GKSS	Institut für Küstenforschung GKSS-Forschungszentrum Geesthacht GmbH Max-Planck-Straße 1 21502 Geesthacht
HeliTransair	HeliTransair GmbH Flugplatz 63329 Egelsbach

**Adresse  
Address**

---

Laeisz	Reederei F. Laeisz Bremerhaven Barkhausen-Str. 37 27568 Bremerhaven
Oktopus	Oktopus GmbH Wischhofstraße 1-3 Geb. 13 - Lager 24148 Kiel
OPTIMARE	Am Luneort 15a, 27572 Bremerhaven
University of Cambridge	University of Cambridge DAMTP-CMS Wilberforce Rd. Cambridge CB3 0WA England
University of Lancaster	Department of Environmental Science Lancaster University Lancaster, LA1 4YQ, UK England
University of Montreal	McGill University Department of Chemistry Otto Maass Building 801 Sherbrooke St.W. Montreal, Quebec H3A 2K6 Canada

---

### A.3 SCHIFFSBESATZUNG / SHIP'S CREW

No	NAME	RANK
01.	Domke, Udo	Master
02.	Schwarze, Stefan	1.Offc.
03.	Pluder, Andreas	Ch. Eng.
04.	Farysch, Bernd	Eng.
05.	Hartung, René	2.Offc.
06.	Peine, Lutz	2.Offc.
07.	Fallei, Holger	2.Offc.
08.	Krüger, Klaus-Jürgen	Doctor
09.	Hecht, Andreas	R.Offc.
10.	Delff, Wolfgang	1.Eng.
11.	Ziemann, Olaf	2.Eng.
12.	Kotnik, Herbert	2.Eng.
13.	Muhle, Heiko	Electr.
14.	Hoffmann, Mathias	FielaxElo
15.	Fröb, Martin	FielaxElo
16.	Muhle, Helmut	FielaxElo
17.	Piskorzynski, Andreas	FielaxElo
18.	Gerchow, Peter	FielaxElo
19.	Loidl, Reiner	Boatsw.
20.	Reise, Lutz	Carpenter
21.	Kaiser, Ralf	A.B.
22.	Pousada Martinez, Saturnio	A.B.
23.	Winkler, Michael	A.B.
24.	Guse, Hartmut	A.B.
25.	Hagemann, Manfred	A.B.
26.	Schmidt, Uwe	A.B.
27.	Vehlow, Ringo	A.B.
28.	Bäcker, Andreas	A.B.
29.	Preußner, Jörg	Storek.
30.	Ipsen, Michael	Mot-man
31.	Voy, Bernd	Mot-man
32.	Elsner, Klaus	Mot-man
33.	Hartmann,Ernst-Uwe	Mot-man
34.	Grafe, Jens	Mot-man
35.	Müller-Homburg, Ralf-Dieter	Cook
36.	Völske, Thomas	Cooksmate
37.	Silinski, Frank	Cooksmate
38.	Jürgens, Monika	1.Stwdess
39.	Wöckener, Martina	Stwdss/KS
40.	Czyborra, Bärbel	2.Stwdess
41.	Silinski, Carmen	2.Stwdess
42.	Gaude, Hans-Jürgen	2.Steward
43.	Möller, Wolfgang	2.Steward
44.	Huang, Wu-Mei	2.Steward
45.	Yu, Kwok, Yuen	Laundrym.
46.	Feiertag, Thomas	Fielax
47.	Brehme, Andreas	Fielax

## A.4 STATION LIST

Station	Date	Time	PositionLat	Position Lon	Depth (m)	Gear (Abbrev.)	Action
PS66/001-1	16.06.04	21:07	55° 0.05' N	7° 0.57' E	3.5	GSWS	to the water
PS66/001-1	16.06.04	21:50	54° 59.44' N	7° 1.17' E	23.3	GSWS	on Deck
PS66/002-1	21.06.04	07:05	72° 0.40' N	14° 43.40' E	1285.6	CTD/RO	surface
PS66/002-1	21.06.04	07:39	72° 0.30' N	14° 43.30' E	1283.6	CTD/RO	at depth
PS66/002-1	21.06.04	08:00	72° 0.37' N	14° 43.37' E	1282.4	CTD/RO	on deck
PS66/002-2	21.06.04	08:09	72° 0.38' N	14° 43.42' E	1283.3	MUC	surface
PS66/002-2	21.06.04	08:44	72° 0.38' N	14° 43.58' E	1280.3	MUC	at sea bottom
PS66/002-2	21.06.04	09:12	72° 0.37' N	14° 43.60' E	1280.8	MUC	on deck
PS66/002-3	21.06.04	09:21	72° 0.37' N	14° 43.64' E	1282.3	FLS	Start Track
PS66/002-3	21.06.04	09:35	72° 0.57' N	14° 46.48' E	1257.6	FLS	Course Change
PS66/002-3	21.06.04	09:53	71° 59.54' N	14° 45.31' E	1285.1	FLS	Information
PS66/002-3	21.06.04	10:54	72° 1.25' N	14° 44.66' E	1272.0	FLS	Course Change
PS66/002-3	21.06.04	11:03	72° 0.75' N	14° 44.98' E	1273.2	FLS	Course Change
PS66/002-3	21.06.04	11:05	72° 0.63' N	14° 44.86' E	1278.4	FLS	Information
PS66/002-3	21.06.04	11:43	72° 0.58' N	14° 44.66' E	1281.5	FLS	End of Track
PS66/003-1	21.06.04	12:09	72° 0.20' N	14° 43.63' E	1286.5	CTD	surface
PS66/003-1	21.06.04	12:36	72° 0.20' N	14° 43.70' E	1286.4	CTD	at depth
PS66/003-1	21.06.04	12:59	72° 0.21' N	14° 43.70' E	1287.1	CTD	on deck
PS66/003-2	21.06.04	13:09	72° 0.19' N	14° 43.61' E	1286.4	GSWS	to the water
PS66/003-2	21.06.04	14:11	72° 0.22' N	14° 43.67' E	1286.9	GSWS	on Deck
PS66/003-3	21.06.04	14:16	72° 0.20' N	14° 43.64' E	1286.5	MUC	surface
PS66/003-3	21.06.04	14:45	72° 0.23' N	14° 43.80' E	1286.9	MUC	at sea bottom
PS66/003-3	21.06.04	15:12	72° 0.21' N	14° 43.65' E	1286.4	MUC	on deck
PS66/003-4	21.06.04	15:22	72° 0.22' N	14° 43.67' E	1287.0	LANDER	surface
PS66/004-1	21.06.04	15:30	72° 0.29' N	14° 43.69' E	1285.7	FLS	Start Track
PS66/004-1	21.06.04	15:49	72° 0.79' N	14° 43.86' E	1286.7	FLS	Course Change
PS66/004-1	21.06.04	16:50	72° 0.56' N	14° 43.42' E	1292.0	FLS	Course Change
PS66/004-1	21.06.04	17:10	72° 0.12' N	14° 43.48' E	1286.3	FLS	Course Change
PS66/004-1	21.06.04	17:26	72° 0.28' N	14° 44.59' E	1286.6	FLS	Course Change
PS66/004-1	21.06.04	17:51	72° 0.14' N	14° 42.76' E	1285.4	FLS	Course Change
PS66/004-1	21.06.04	18:15	72° 0.22' N	14° 44.89' E	1284.3	FLS	Course Change
PS66/004-1	21.06.04	18:50	72° 0.54' N	14° 42.21' E	1292.8	FLS	End of Track
PS66/004-2	21.06.04	19:06	72° 0.00' N	14° 43.35' E	1287.9	CTD	surface
PS66/004-2	21.06.04	19:30	72° 0.01' N	14° 43.39' E	1287.3	CTD	at depth
PS66/004-2	21.06.04	19:53	72° 0.04' N	14° 43.72' E	1286.0	CTD	on deck
PS66/004-3	21.06.04	20:02	72° 0.02' N	14° 43.63' E	0.0	MUC	surface
PS66/004-3	21.06.04	20:44	72° 0.10' N	14° 43.58' E	1286.0	MUC	at sea bottom
PS66/004-3	21.06.04	21:11	72° 0.16' N	14° 43.72' E	1286.0	MUC	on deck
PS66/004-4	21.06.04	21:32	72° 0.35' N	14° 43.00' E	0.0	FLS	Start Track
PS66/004-4	21.06.04	21:37	72° 0.32' N	14° 43.42' E	0.0	FLS	Information
PS66/004-4	21.06.04	21:45	72° 0.33' N	14° 44.04' E	0.0	FLS	Course Change

Station	Date	Time	PositionLat	Position Lon	Depth (m)	Gear (Abbrev.)	Action
PS66/004-4	21.06.04	21:56	72° 0.23' N	14° 44.21' E	0.0	FLS	Information
PS66/004-4	21.06.04	22:01	72° 0.25' N	14° 43.86' E	0.0	FLS	Information
PS66/004-4	21.06.04	22:05	72° 0.26' N	14° 43.62' E	0.0	FLS	Information
PS66/004-4	21.06.04	22:09	72° 0.28' N	14° 43.28' E	0.0	FLS	Course Change
PS66/004-4	21.06.04	22:20	72° 0.14' N	14° 42.95' E	0.0	FLS	Information
PS66/004-4	21.06.04	22:37	72° 0.12' N	14° 44.04' E	0.0	FLS	Course Change
PS66/004-4	21.06.04	22:43	71° 59.99' N	14° 44.05' E	0.0	FLS	Information
PS66/004-4	21.06.04	22:54	72° 0.23' N	14° 43.90' E	0.0	FLS	Information
PS66/004-4	21.06.04	23:00	72° 0.38' N	14° 43.88' E	0.0	FLS	Course Change
PS66/004-4	21.06.04	23:10	72° 0.44' N	14° 43.69' E	0.0	FLS	Information
PS66/004-4	21.06.04	23:14	72° 0.35' N	14° 43.57' E	0.0	FLS	Information
PS66/004-4	21.06.04	23:23	72° 0.11' N	14° 43.39' E	0.0	FLS	Course Change
PS66/004-4	21.06.04	23:29	72° 0.01' N	14° 43.60' E	0.0	FLS	Information
PS66/004-4	21.06.04	23:42	72° 0.24' N	14° 43.67' E	0.0	FLS	Information
PS66/004-4	21.06.04	23:48	72° 0.39' N	14° 43.71' E	1282.6	FLS	End of Track
PS66/005-1	22.06.04	00:06	71° 59.96' N	14° 43.68' E	1289.1	CTD	surface
PS66/005-1	22.06.04	00:32	71° 59.99' N	14° 43.51' E	1289.5	CTD	at depth
PS66/005-1	22.06.04	00:50	72° 0.00' N	14° 43.55' E	1287.3	CTD	on deck
PS66/006-1	22.06.04	01:03	72° 0.12' N	14° 43.48' E	1285.9	CTD	surface
PS66/006-1	22.06.04	01:28	72° 0.15' N	14° 43.46' E	1287.8	CTD	at depth
PS66/006-1	22.06.04	01:44	72° 0.17' N	14° 43.49' E	1286.8	CTD	on deck
PS66/007-1	22.06.04	01:56	72° 0.31' N	14° 43.53' E	1286.0	CTD	surface
PS66/007-1	22.06.04	02:21	72° 0.33' N	14° 43.48' E	1285.1	CTD	at depth
PS66/007-1	22.06.04	02:37	72° 0.33' N	14° 43.56' E	1284.7	CTD	on deck
PS66/008-1	22.06.04	02:45	72° 0.45' N	14° 43.55' E	1284.2	CTD	surface
PS66/008-1	22.06.04	03:12	72° 0.46' N	14° 43.45' E	1283.1	CTD	at depth
PS66/008-1	22.06.04	03:27	72° 0.47' N	14° 43.54' E	0.0	CTD	on deck
PS66/009-1	22.06.04	03:33	72° 0.60' N	14° 43.49' E	1291.4	CTD	surface
PS66/009-1	22.06.04	03:59	72° 0.63' N	14° 43.55' E	1290.1	CTD	at depth
PS66/009-1	22.06.04	04:15	72° 0.65' N	14° 43.71' E	1288.8	CTD	on deck
PS66/010-1	22.06.04	04:31	72° 0.34' N	14° 44.05' E	1283.7	CTD/RO	surface
PS66/010-1	22.06.04	05:00	72° 0.23' N	14° 44.00' E	1285.5	CTD/RO	at depth
PS66/010-1	22.06.04	05:17	72° 0.24' N	14° 43.79' E	1286.2	CTD/RO	on deck
PS66/010-2	22.06.04	05:26	72° 0.22' N	14° 43.70' E	1285.8	CTD/RO	surface
PS66/010-2	22.06.04	05:53	72° 0.25' N	14° 43.75' E	1285.9	CTD/RO	at depth
PS66/010-2	22.06.04	05:59	72° 0.25' N	14° 43.75' E	1277.9	CTD/RO	at depth
PS66/010-2	22.06.04	06:25	72° 0.19' N	14° 43.76' E	1286.4	CTD/RO	on deck
PS66/010-3	22.06.04	06:33	72° 0.19' N	14° 43.78' E	1286.4	MUC	surface
PS66/010-3	22.06.04	07:19	72° 0.24' N	14° 43.93' E	1285.4	MUC	at sea bottom
PS66/010-3	22.06.04	07:50	72° 0.37' N	14° 44.26' E	1289.7	MUC	on deck
PS66/011-1	22.06.04	08:44	72° 0.24' N	14° 44.50' E	1287.2	AGT	surface
PS66/011-1	22.06.04	09:36	71° 58.48' N	14° 45.02' E	1287.4	AGT	AGT on ground

Station	Date	Time	PositionLat	Position Lon	Depth (m)	Gear (Abbrev.)	Action
PS66/011-1	22.06.04	09:57	71° 57.96' N	14° 44.92' E	1285.2	AGT	start trawl
PS66/011-1	22.06.04	10:15	71° 57.59' N	14° 44.93' E	1266.9	AGT	Information
PS66/011-1	22.06.04	10:26	71° 57.57' N	14° 44.84' E	1267.2	AGT	Stop Trawl
PS66/011-1	22.06.04	10:34	71° 57.51' N	14° 44.74' E	1269.1	AGT	Information
PS66/011-1	22.06.04	10:42	71° 57.37' N	14° 44.78' E	1273.4	AGT	start trawl
PS66/011-1	22.06.04	10:55	71° 57.16' N	14° 44.74' E	1251.5	AGT	Stop Trawl
PS66/011-1	22.06.04	11:29	71° 57.00' N	14° 44.60' E	1269.9	AGT	AGT off ground
PS66/011-1	22.06.04	12:02	71° 56.76' N	14° 44.55' E	1268.0	AGT	on deck
PS66/013-1	22.06.04	12:34	72° 0.07' N	14° 43.76' E	1285.7	CTD	surface
PS66/013-1	22.06.04	13:00	72° 0.06' N	14° 43.61' E	1285.8	CTD	at depth
PS66/013-1	22.06.04	13:24	72° 0.07' N	14° 43.66' E	1284.7	CTD	on deck
PS66/013-2	22.06.04	13:55	72° 0.16' N	14° 43.68' E	1286.9	MUC	surface
PS66/013-2	22.06.04	14:23	72° 0.11' N	14° 43.57' E	1286.7	MUC	at sea bottom
PS66/013-2	22.06.04	14:50	72° 0.09' N	14° 43.53' E	1287.3	MUC	on deck
PS66/014-1	22.06.04	15:13	71° 59.01' N	14° 45.04' E	1295.6	GKG	surface
PS66/014-1	22.06.04	15:34	71° 59.00' N	14° 45.02' E	1295.6	GKG	at sea bottom
PS66/014-1	22.06.04	15:56	71° 59.05' N	14° 45.06' E	1295.6	GKG	on deck
PS66/015-1	22.06.04	21:00	72° 0.72' N	14° 43.27' E	1290.0	CTD/RO	surface
PS66/015-1	22.06.04	21:26	72° 0.73' N	14° 43.40' E	1289.7	CTD/RO	at depth
PS66/015-1	22.06.04	21:54	72° 0.73' N	14° 43.35' E	1289.6	CTD/RO	on deck
PS66/015-2	22.06.04	22:05	72° 0.74' N	14° 43.35' E	1289.6	MUC	surface
PS66/015-2	22.06.04	23:14	72° 0.76' N	14° 43.66' E	1287.9	MUC	at sea bottom
PS66/015-2	22.06.04	23:40	72° 0.82' N	14° 43.68' E	1286.3	MUC	on deck
PS66/016-1	23.06.04	00:03	72° 0.26' N	14° 43.33' E	1285.2	CTD/RO	surface
PS66/016-1	23.06.04	00:29	72° 0.26' N	14° 43.34' E	1285.5	CTD/RO	at depth
PS66/016-1	23.06.04	00:46	72° 0.26' N	14° 43.40' E	1285.6	CTD/RO	on deck
PS66/017-1	23.06.04	00:52	72° 0.31' N	14° 43.52' E	1284.8	CTD	surface
PS66/017-1	23.06.04	01:20	72° 0.33' N	14° 43.52' E	1284.4	CTD	at depth
PS66/017-1	23.06.04	01:36	72° 0.34' N	14° 43.54' E	1284.3	CTD	on deck
PS66/018-1	23.06.04	02:14	71° 55.98' N	14° 43.53' E	1302.4	CTD	surface
PS66/018-1	23.06.04	02:41	71° 56.03' N	14° 43.53' E	1288.1	CTD	at depth
PS66/018-1	23.06.04	02:57	71° 55.98' N	14° 43.43' E	1290.1	CTD	on deck
PS66/019-1	23.06.04	03:18	71° 57.96' N	14° 43.78' E	1311.6	CTD	surface
PS66/019-1	23.06.04	03:46	71° 57.94' N	14° 43.55' E	1312.5	CTD	at depth
PS66/019-1	23.06.04	04:00	71° 57.92' N	14° 43.73' E	1311.6	CTD	on deck
PS66/020-1	23.06.04	04:36	72° 2.49' N	14° 43.35' E	1214.8	CTD/RO	surface
PS66/020-1	23.06.04	05:01	72° 2.46' N	14° 43.64' E	1263.2	CTD/RO	at depth
PS66/020-1	23.06.04	05:16	72° 2.45' N	14° 43.66' E	1262.9	CTD/RO	on deck
PS66/021-1	24.06.04	05:27	74° 59.95' N	15° 50.15' E	266.8	CTD/RO	surface
PS66/021-1	24.06.04	05:35	75° 0.02' N	15° 50.10' E	266.4	CTD/RO	at depth
PS66/021-1	24.06.04	05:47	75° 0.02' N	15° 50.34' E	264.4	CTD/RO	on deck
PS66/021-2	24.06.04	05:52	75° 0.01' N	15° 50.35' E	264.0	GSWS	to the water

Station	Date	Time	PositionLat	Position Lon	Depth (m)	Gear (Abbrev.)	Action
PS66/021-2	24.06.04	06:02	75° 0.00' N	15° 50.51' E	263.2	GSWS	to the water
PS66/021-2	24.06.04	06:46	74° 59.92' N	15° 49.63' E	274.0	GSWS	on Deck
PS66/022-1	24.06.04	08:00	75° 0.06' N	15° 10.24' E	1016.8	CTD/RO	surface
PS66/022-1	24.06.04	08:22	75° 0.04' N	15° 10.15' E	1019.2	CTD/RO	at depth
PS66/022-1	24.06.04	08:45	75° 0.05' N	15° 10.45' E	1014.8	CTD/RO	on deck
PS66/023-1	24.06.04	10:08	75° 4.33' N	14° 30.93' E	1282.4	CTD/RO	surface
PS66/023-1	24.06.04	10:34	75° 4.23' N	14° 30.43' E	1291.2	CTD/RO	at depth
PS66/023-1	24.06.04	11:02	75° 4.17' N	14° 29.77' E	1300.8	CTD/RO	on deck
PS66/024-1	24.06.04	12:15	74° 59.97' N	13° 52.11' E	1800.8	CTD/RO	surface
PS66/024-1	24.06.04	12:50	75° 0.02' N	13° 51.83' E	1798.8	CTD/RO	at depth
PS66/024-1	24.06.04	13:22	74° 60.00' N	13° 51.98' E	1799.6	CTD/RO	on deck
PS66/025-1	24.06.04	14:35	74° 60.00' N	13° 12.77' E	1938.0	CTD/RO	surface
PS66/025-1	24.06.04	15:13	75° 0.06' N	13° 12.64' E	1915.2	CTD/RO	at depth
PS66/025-1	24.06.04	15:52	75° 0.03' N	13° 12.41' E	1968.0	CTD/RO	on deck
PS66/026-1	24.06.04	17:04	75° 0.00' N	12° 35.29' E	2180.8	CTD/RO	surface
PS66/026-1	24.06.04	17:46	74° 59.92' N	12° 36.10' E	2181.2	CTD/RO	at depth
PS66/026-1	24.06.04	18:24	74° 59.70' N	12° 36.09' E	2186.0	CTD/RO	on deck
PS66/027-1	24.06.04	19:38	75° 0.13' N	11° 55.69' E	2335.6	CTD/RO	surface
PS66/027-1	24.06.04	20:22	74° 59.88' N	11° 56.15' E	2332.8	CTD/RO	at depth
PS66/027-1	24.06.04	21:00	74° 59.60' N	11° 56.22' E	2334.0	CTD/RO	on deck
PS66/028-1	24.06.04	22:11	75° 0.23' N	11° 18.48' E	2450.4	CTD/RO	surface
PS66/028-1	24.06.04	22:56	74° 59.95' N	11° 18.15' E	2455.2	CTD/RO	at depth
PS66/028-1	24.06.04	23:32	74° 59.70' N	11° 18.26' E	2458.4	CTD/RO	on deck
PS66/029-1	25.06.04	00:42	75° 0.07' N	10° 38.93' E	2534.8	CTD/RO	surface
PS66/029-1	25.06.04	01:29	75° 0.03' N	10° 38.91' E	2534.8	CTD/RO	at depth
PS66/029-1	25.06.04	02:09	74° 59.92' N	10° 39.33' E	2533.6	CTD/RO	on deck
PS66/030-1	25.06.04	03:29	74° 59.97' N	9° 59.87' E	2579.2	CTD/RO	surface
PS66/030-1	25.06.04	04:17	74° 59.82' N	9° 59.95' E	2580.4	CTD/RO	at depth
PS66/030-1	25.06.04	04:51	74° 59.73' N	10° 0.21' E	2580.0	CTD/RO	on deck
PS66/031-1	25.06.04	06:07	75° 0.17' N	9° 21.99' E	2594.0	CTD/RO	surface
PS66/031-1	25.06.04	06:56	74° 59.89' N	9° 21.80' E	2593.6	CTD/RO	at depth
PS66/031-1	25.06.04	07:38	74° 59.64' N	9° 21.83' E	2594.0	CTD/RO	on deck
PS66/032-1	25.06.04	08:54	75° 0.29' N	8° 44.09' E	2663.2	CTD/RO	surface
PS66/032-1	25.06.04	09:40	74° 59.99' N	8° 44.18' E	2664.8	CTD/RO	at depth
PS66/032-1	25.06.04	10:18	74° 59.71' N	8° 44.38' E	2667.2	CTD/RO	on deck
PS66/032-2	25.06.04	10:25	74° 59.66' N	8° 44.44' E	2667.6	GSWS	to the water
PS66/032-2	25.06.04	11:12	74° 59.28' N	8° 44.66' E	2669.6	GSWS	on Deck
PS66/033-1	25.06.04	12:24	75° 0.14' N	8° 4.71' E	3533.6	CTD/RO	surface
PS66/033-1	25.06.04	13:30	74° 60.00' N	8° 4.60' E	3528.0	CTD/RO	at depth
PS66/033-1	25.06.04	14:19	74° 59.89' N	8° 4.31' E	3523.6	CTD/RO	on deck
PS66/034-1	25.06.04	15:32	74° 59.97' N	7° 26.15' E	2473.6	CTD/RO	surface
PS66/034-1	25.06.04	16:20	74° 59.74' N	7° 26.29' E	2476.8	CTD/RO	at depth

Station	Date	Time	PositionLat	Position Lon	Depth (m)	Gear (Abbrev.)	Action
PS66/034-1	25.06.04	17:00	74° 59.74' N	7° 26.77' E	2477.6	CTD/RO	on deck
PS66/035-1	25.06.04	18:11	75° 0.27' N	6° 47.24' E	2233.6	CTD/RO	surface
PS66/035-1	25.06.04	18:55	75° 0.41' N	6° 47.63' E	2174.8	CTD/RO	at depth
PS66/035-1	25.06.04	19:22	75° 0.36' N	6° 47.61' E	2191.2	CTD/RO	on deck
PS66/036-1	25.06.04	20:33	75° 0.31' N	6° 8.73' E	2798.4	CTD/RO	surface
PS66/036-1	25.06.04	21:25	75° 0.20' N	6° 8.47' E	2811.6	CTD/RO	at depth
PS66/036-1	25.06.04	21:58	75° 0.16' N	6° 8.47' E	2814.0	CTD/RO	on deck
PS66/037-1	25.06.04	23:08	74° 60.00' N	5° 30.37' E	3131.6	CTD/RO	surface
PS66/037-1	26.06.04	00:06	74° 59.79' N	5° 29.91' E	3120.0	CTD/RO	at depth
PS66/037-1	26.06.04	00:50	74° 59.66' N	5° 29.83' E	3120.0	CTD/RO	on deck
PS66/038-1	26.06.04	01:58	74° 59.94' N	4° 52.03' E	3236.0	CTD/RO	surface
PS66/038-1	26.06.04	02:59	74° 59.74' N	4° 51.68' E	3240.0	CTD/RO	at depth
PS66/038-1	26.06.04	03:38	74° 59.58' N	4° 51.73' E	3241.2	CTD/RO	on deck
PS66/039-1	26.06.04	04:44	75° 0.06' N	4° 14.26' E	3098.8	CTD/RO	surface
PS66/039-1	26.06.04	05:43	74° 59.96' N	4° 13.96' E	3093.2	CTD/RO	at depth
PS66/039-1	26.06.04	06:20	74° 59.99' N	4° 14.18' E	3102.0	CTD/RO	on deck
PS66/040-1	26.06.04	07:30	75° 0.02' N	3° 35.21' E	3482.4	CTD/RO	surface
PS66/040-1	26.06.04	08:34	74° 60.00' N	3° 35.09' E	3480.4	CTD/RO	at depth
PS66/040-1	26.06.04	09:24	74° 59.94' N	3° 35.03' E	3479.2	CTD/RO	on deck
PS66/041-1	26.06.04	10:40	74° 60.00' N	2° 55.96' E	2519.2	CTD/RO	surface
PS66/041-1	26.06.04	11:27	75° 0.02' N	2° 55.82' E	2518.4	CTD/RO	at depth
PS66/041-1	26.06.04	12:03	75° 0.09' N	2° 55.95' E	2508.4	CTD/RO	on deck
PS66/041-2	26.06.04	12:13	75° 0.15' N	2° 55.95' E	2500.0	GSWS	to the water
PS66/041-2	26.06.04	12:56	75° 0.15' N	2° 56.80' E	2510.8	GSWS	on Deck
PS66/042-1	26.06.04	14:10	74° 59.96' N	2° 16.80' E	2955.6	CTD/RO	surface
PS66/042-1	26.06.04	15:06	74° 59.79' N	2° 16.99' E	2960.4	CTD/RO	at depth
PS66/042-1	26.06.04	15:42	74° 59.82' N	2° 16.71' E	2959.6	CTD/RO	on deck
PS66/043-1	26.06.04	17:56	74° 59.98' N	0° 59.23' E	3775.6	CTD/RO	surface
PS66/043-1	26.06.04	19:05	75° 0.08' N	0° 57.95' E	3776.0	CTD/RO	at depth
PS66/043-1	26.06.04	19:52	75° 0.28' N	0° 57.33' E	3775.6	CTD/RO	on deck
PS66/044-1	26.06.04	20:49	74° 54.05' N	1° 13.50' E	3778.8	CTD/RO	surface
PS66/044-1	26.06.04	21:59	74° 54.04' N	1° 13.47' E	3778.4	CTD/RO	at depth
PS66/044-1	26.06.04	22:46	74° 53.98' N	1° 13.35' E	3778.4	CTD/RO	on deck
PS66/045-1	26.06.04	23:09	74° 53.06' N	1° 7.02' E	3778.8	CTD/RO	surface
PS66/045-1	27.06.04	00:18	74° 53.02' N	1° 6.89' E	3778.8	CTD/RO	at depth
PS66/045-1	27.06.04	01:05	74° 52.98' N	1° 6.80' E	3778.8	CTD/RO	on deck
PS66/046-1	27.06.04	01:27	74° 52.01' N	1° 13.44' E	3778.4	CTD/RO	surface
PS66/046-1	27.06.04	02:36	74° 51.96' N	1° 13.18' E	3778.8	CTD/RO	at depth
PS66/046-1	27.06.04	03:23	74° 51.91' N	1° 13.60' E	3778.8	CTD/RO	on deck
PS66/047-1	27.06.04	03:43	74° 53.03' N	1° 19.83' E	3778.4	CTD/RO	surface
PS66/047-1	27.06.04	04:53	74° 52.94' N	1° 19.22' E	3778.8	CTD/RO	at depth
PS66/047-1	27.06.04	05:41	74° 52.87' N	1° 18.98' E	3778.4	CTD/RO	on deck

Station	Date	Time	PositionLat	Position Lon	Depth (m)	Gear (Abbrev.)	Action
PS66/048-1	27.06.04	06:04	74° 55.06' N	1° 19.73' E	3777.6	CTD/RO	surface
PS66/048-1	27.06.04	07:15	74° 54.95' N	1° 19.70' E	3778.0	CTD/RO	at depth
PS66/048-1	27.06.04	08:01	74° 54.96' N	1° 19.66' E	3777.6	CTD/RO	on deck
PS66/049-1	27.06.04	08:33	74° 55.01' N	1° 6.97' E	3778.4	CTD/RO	surface
PS66/049-1	27.06.04	09:43	74° 54.99' N	1° 6.61' E	3778.4	CTD/RO	at depth
PS66/049-1	27.06.04	10:29	74° 54.97' N	1° 6.94' E	3778.4	CTD/RO	on deck
PS66/050-1	27.06.04	10:52	74° 54.00' N	1° 0.38' E	3778.4	CTD/RO	surface
PS66/050-1	27.06.04	12:14	74° 53.96' N	1° 0.45' E	3778.4	CTD/RO	at depth
PS66/050-1	27.06.04	13:01	74° 53.96' N	1° 0.65' E	3778.4	CTD/RO	on deck
PS66/051-1	27.06.04	13:33	74° 52.03' N	1° 0.48' E	3778.0	CTD/RO	surface
PS66/051-1	27.06.04	14:39	74° 51.86' N	0° 59.74' E	3778.4	CTD/RO	at depth
PS66/051-1	27.06.04	15:26	74° 51.90' N	0° 59.76' E	3778.4	CTD/RO	on deck
PS66/052-1	27.06.04	15:47	74° 53.02' N	0° 53.90' E	3778.0	CTD/RO	surface
PS66/052-1	27.06.04	16:58	74° 52.99' N	0° 54.03' E	3778.0	CTD/RO	at depth
PS66/052-1	27.06.04	17:44	74° 52.99' N	0° 53.75' E	3778.4	CTD/RO	on deck
PS66/053-1	27.06.04	18:10	74° 53.63' N	1° 3.47' E	3780.0	CTD/RO	surface
PS66/053-1	27.06.04	19:21	74° 53.55' N	1° 3.43' E	3779.2	CTD/RO	at depth
PS66/053-1	27.06.04	20:15	74° 53.61' N	1° 3.09' E	3779.2	CTD/RO	on deck
PS66/054-1	27.06.04	21:32	75° 0.04' N	1° 37.99' E	3130.0	CTD/RO	surface
PS66/054-1	27.06.04	22:31	75° 0.06' N	1° 38.08' E	3125.2	CTD/RO	at depth
PS66/054-1	27.06.04	23:19	75° 0.04' N	1° 38.22' E	3122.0	CTD/RO	on deck
PS66/055-1	28.06.04	06:04	74° 50.48' N	2° 28.02' W	3700.0	MOR	Hydrophone into the water
PS66/055-1	28.06.04	06:09	74° 50.53' N	2° 28.03' W	3700.4	MOR	released
PS66/055-1	28.06.04	06:27	74° 50.44' N	2° 28.31' W	3700.0	MOR	released
PS66/055-1	28.06.04	06:42	74° 50.47' N	2° 28.45' W	3700.0	MOR	on the surface
PS66/055-1	28.06.04	06:59	74° 50.37' N	2° 28.29' W	3699.6	MOR	action
PS66/055-1	28.06.04	08:03	74° 50.82' N	2° 27.35' W	3702.0	MOR	on deck
PS66/055-1	28.06.04	08:04	74° 50.82' N	2° 27.33' W	3702.4	MOR	releaser on deck
PS66/055-1	28.06.04	08:05	74° 50.83' N	2° 27.31' W	3702.4	MOR	mooring on deck
PS66/055-2	28.06.04	09:04	74° 50.39' N	2° 29.30' W	3699.2	MOR	surface
PS66/055-2	28.06.04	10:35	74° 50.39' N	2° 28.86' W	3699.6	MOR	surface
PS66/055-2	28.06.04	10:46	74° 50.39' N	2° 28.80' W	3699.2	MOR	surface
PS66/055-2	28.06.04	10:51	74° 50.39' N	2° 28.76' W	3699.2	MOR	surface
PS66/055-2	28.06.04	10:56	74° 50.39' N	2° 28.73' W	3699.2	MOR	on the ground
PS66/055-2	28.06.04	10:56	74° 50.39' N	2° 28.73' W	3699.2	MOR	released
PS66/055-2	28.06.04	10:58	74° 50.39' N	2° 28.71' W	3699.2	MOR	Hydrophone on Deck
PS66/056-1	28.06.04	13:28	75° 5.13' N	3° 27.44' W	3667.2	MOR	Hydrophone into the water
PS66/056-1	28.06.04	13:30	75° 5.13' N	3° 27.39' W	3666.8	MOR	released
PS66/056-1	28.06.04	13:31	75° 5.14' N	3° 27.37' W	3666.8	MOR	on the surface
PS66/056-1	28.06.04	13:32	75° 5.14' N	3° 27.33' W	3667.2	MOR	Hydrophone on

Station	Date	Time	PositionLat	Position Lon	Depth (m)	Gear (Abbrev.)	Action
PS66/056-1	28.06.04	13:45	75° 4.86' N	3° 27.72' W	3667.6	MOR	Deck action
PS66/056-1	28.06.04	13:47	75° 4.85' N	3° 27.72' W	3667.2	MOR	action
PS66/056-1	28.06.04	13:59	75° 4.85' N	3° 27.54' W	3667.2	MOR	action
PS66/056-1	28.06.04	15:11	75° 4.99' N	3° 26.06' W	3668.0	MOR	action
PS66/056-1	28.06.04	15:14	75° 4.99' N	3° 25.99' W	3668.0	MOR	mooring on deck
PS66/057-1	28.06.04	16:01	75° 4.92' N	3° 27.28' W	3667.6	MOR	action
PS66/057-1	28.06.04	16:05	75° 4.91' N	3° 27.27' W	3667.2	MOR	action
PS66/057-1	28.06.04	16:33	75° 4.88' N	3° 27.42' W	3667.6	MOR	action
PS66/057-1	28.06.04	17:06	75° 4.87' N	3° 27.65' W	3667.6	MOR	on deck
PS66/057-1	28.06.04	17:51	75° 4.90' N	3° 27.68' W	3667.6	MOR	surface
PS66/057-1	28.06.04	18:06	75° 4.93' N	3° 27.49' W	3667.6	MOR	surface
PS66/057-1	28.06.04	19:14	75° 4.95' N	3° 27.37' W	3668.0	MOR	surface
PS66/057-1	28.06.04	19:21	75° 4.95' N	3° 27.33' W	3668.0	MOR	surface
PS66/057-1	28.06.04	19:28	75° 4.93' N	3° 27.33' W	3668.0	MOR	surface
PS66/057-1	28.06.04	19:35	75° 4.95' N	3° 27.27' W	3668.4	MOR	on the ground
PS66/057-1	28.06.04	19:37	75° 4.96' N	3° 27.25' W	3668.0	MOR	releaser on deck
PS66/058-1	28.06.04	21:05	74° 59.97' N	4° 7.94' W	3643.6	CTD/RO	surface
PS66/058-1	28.06.04	22:12	74° 59.97' N	4° 7.88' W	3643.2	CTD/RO	at depth
PS66/058-1	28.06.04	23:04	74° 59.95' N	4° 7.61' W	3643.2	CTD/RO	on deck
PS66/059-1	29.06.04	00:15	75° 0.01' N	3° 30.12' W	3665.6	CTD/RO	surface
PS66/059-1	29.06.04	01:24	74° 59.77' N	3° 29.83' W	3668.4	CTD/RO	at depth
PS66/059-1	29.06.04	02:10	74° 59.76' N	3° 29.65' W	3669.2	CTD/RO	on deck
PS66/060-1	29.06.04	03:23	74° 59.99' N	2° 51.22' W	3693.2	CTD/RO	surface
PS66/060-1	29.06.04	04:32	74° 59.92' N	2° 50.72' W	3693.6	CTD/RO	at depth
PS66/060-1	29.06.04	05:20	74° 59.68' N	2° 51.24' W	3694.0	CTD/RO	on deck
PS66/061-1	29.06.04	08:33	74° 55.36' N	4° 37.96' W	3616.0	MOR	Hydrophone into the water
PS66/061-1	29.06.04	08:34	74° 55.36' N	4° 37.95' W	3616.0	MOR	released
PS66/061-1	29.06.04	08:35	74° 55.37' N	4° 37.95' W	3616.4	MOR	on the surface
PS66/061-1	29.06.04	08:50	74° 54.99' N	4° 38.13' W	3614.8	MOR	action
PS66/061-1	29.06.04	08:52	74° 54.99' N	4° 38.16' W	3614.8	MOR	on deck
PS66/061-1	29.06.04	08:53	74° 54.99' N	4° 38.17' W	3614.8	MOR	on deck
PS66/061-1	29.06.04	09:00	74° 55.00' N	4° 38.21' W	3614.8	MOR	on deck
PS66/061-1	29.06.04	09:55	74° 55.04' N	4° 38.05' W	3615.2	MOR	on deck
PS66/061-1	29.06.04	09:56	74° 55.04' N	4° 38.05' W	3615.2	MOR	on deck
PS66/061-2	29.06.04	10:05	74° 55.05' N	4° 38.01' W	3614.8	MOR	surface
PS66/061-2	29.06.04	10:10	74° 55.05' N	4° 37.98' W	3615.2	MOR	surface
PS66/061-2	29.06.04	11:16	74° 55.01' N	4° 38.02' W	3615.2	MOR	surface
PS66/061-2	29.06.04	11:27	74° 55.01' N	4° 38.00' W	3614.8	MOR	surface
PS66/061-2	29.06.04	11:35	74° 55.02' N	4° 37.99' W	3614.8	MOR	surface
PS66/061-2	29.06.04	11:36	74° 55.02' N	4° 38.00' W	3614.8	MOR	surface

Station	Date	Time	PositionLat	Position Lon	Depth (m)	Gear (Abbrev.)	Action
PS66/061-2	29.06.04	11:40	74° 55.00' N	4° 38.08' W	3614.8	MOR	surface
PS66/061-2	29.06.04	11:45	74° 54.97' N	4° 38.11' W	3614.4	MOR	released
PS66/061-2	29.06.04	11:45	74° 54.97' N	4° 38.11' W	3614.4	MOR	on the ground
PS66/061-2	29.06.04	11:47	74° 54.97' N	4° 38.08' W	3614.4	MOR	Hydrophone on Deck
PS66/062-1	29.06.04	13:11	74° 53.20' N	4° 38.01' W	3614.8	MOR	surface
PS66/062-1	29.06.04	13:35	74° 53.22' N	4° 38.06' W	3614.8	MOR	surface
PS66/062-1	29.06.04	14:24	74° 53.22' N	4° 38.03' W	3614.4	MOR	surface
PS66/062-1	29.06.04	14:39	74° 53.19' N	4° 38.06' W	3614.4	MOR	surface
PS66/062-1	29.06.04	14:40	74° 53.19' N	4° 38.06' W	3614.4	MOR	on the ground
PS66/062-1	29.06.04	14:43	74° 53.19' N	4° 38.05' W	3614.4	MOR	slipped
PS66/063-1	29.06.04	15:16	74° 51.29' N	4° 37.89' W	3616.4	MOR	surface
PS66/063-1	29.06.04	15:34	74° 51.28' N	4° 37.93' W	3617.2	MOR	surface
PS66/063-1	29.06.04	16:25	74° 51.29' N	4° 37.88' W	3617.2	MOR	surface
PS66/063-1	29.06.04	16:42	74° 51.31' N	4° 37.83' W	3617.2	MOR	surface
PS66/063-1	29.06.04	16:47	74° 51.30' N	4° 37.86' W	3617.2	MOR	on the ground
PS66/063-1	29.06.04	17:00	74° 51.27' N	4° 37.95' W	3617.2	MOR	on the ground
PS66/063-1	29.06.04	17:01	74° 51.27' N	4° 37.95' W	3617.2	MOR	on deck
PS66/064-1	29.06.04	20:54	74° 59.97' N	2° 12.95' W	3639.6	CTD/RO	surface
PS66/064-1	29.06.04	22:02	74° 59.95' N	2° 12.92' W	3642.0	CTD/RO	at depth
PS66/064-1	29.06.04	22:55	74° 59.97' N	2° 12.96' W	3639.2	CTD/RO	on deck
PS66/065-1	30.06.04	02:41	75° 0.07' N	0° 21.22' E	3772.4	CTD/RO	surface
PS66/065-1	30.06.04	03:52	75° 0.05' N	0° 21.04' E	3772.4	CTD/RO	at depth
PS66/065-1	30.06.04	04:45	74° 59.87' N	0° 21.23' E	3772.8	CTD/RO	on deck
PS66/066-1	30.06.04	06:09	75° 0.10' N	0° 18.20' W	3764.8	CTD/RO	surface
PS66/066-1	30.06.04	07:19	75° 0.12' N	0° 18.50' W	3764.8	CTD/RO	at depth
PS66/066-1	30.06.04	08:13	75° 0.08' N	0° 18.64' W	3764.8	CTD/RO	on deck
PS66/067-1	30.06.04	09:30	75° 0.08' N	0° 56.11' W	3678.4	CTD/RO	surface
PS66/067-1	30.06.04	10:37	75° 0.12' N	0° 56.30' W	3671.2	CTD/RO	at depth
PS66/067-1	30.06.04	11:28	75° 0.15' N	0° 56.72' W	3650.4	CTD/RO	on deck
PS66/068-1	30.06.04	12:47	74° 59.98' N	1° 34.68' W	3730.8	CTD/RO	surface
PS66/068-1	30.06.04	13:57	75° 0.10' N	1° 34.59' W	3730.0	CTD/RO	at depth
PS66/068-1	30.06.04	14:53	75° 0.13' N	1° 34.68' W	3730.0	CTD/RO	on deck
PS66/069-1	30.06.04	19:20	74° 59.96' N	4° 47.58' W	3613.9	CTD/RO	surface
PS66/069-1	30.06.04	20:24	75° 0.06' N	4° 47.18' W	3614.4	CTD/RO	at depth
PS66/069-1	30.06.04	21:11	75° 0.07' N	4° 47.10' W	3614.8	CTD/RO	on deck
PS66/070-1	30.06.04	22:22	74° 59.93' N	5° 25.34' W	3576.4	CTD/RO	surface
PS66/070-1	30.06.04	23:28	75° 0.02' N	5° 25.15' W	3576.0	CTD/RO	at depth
PS66/070-1	01.07.04	00:15	75° 0.02' N	5° 25.37' W	3576.0	CTD/RO	on deck
PS66/071-1	01.07.04	01:27	74° 60.00' N	6° 3.77' W	3526.4	CTD/RO	surface
PS66/071-1	01.07.04	02:32	75° 0.18' N	6° 4.12' W	3526.0	CTD/RO	at depth
PS66/071-1	01.07.04	03:31	75° 0.18' N	6° 4.08' W	3526.0	CTD/RO	on deck
PS66/072-1	01.07.04	04:43	74° 59.80' N	6° 42.86' W	3490.4	CTD/RO	surface

Station	Date	Time	PositionLat	Position Lon	Depth (m)	Gear (Abbrev.)	Action
PS66/072-1	01.07.04	05:50	74° 59.96' N	6° 43.18' W	3490.4	CTD/RO	at depth
PS66/072-1	01.07.04	06:37	75° 0.10' N	6° 42.91' W	3490.4	CTD/RO	on deck
PS66/072-2	01.07.04	06:44	75° 0.10' N	6° 42.90' W	3490.4	GSWS	to the water
PS66/072-2	01.07.04	07:20	75° 0.10' N	6° 43.05' W	3490.4	GSWS	on Deck
PS66/073-1	01.07.04	08:34	74° 59.92' N	7° 21.94' W	3439.2	CTD/RO	surface
PS66/073-1	01.07.04	09:39	74° 59.99' N	7° 22.18' W	3439.0	CTD/RO	at depth
PS66/073-1	01.07.04	10:22	74° 59.98' N	7° 22.21' W	3439.2	CTD/RO	on deck
PS66/074-1	01.07.04	11:34	74° 59.91' N	8° 1.16' W	3400.0	CTD/RO	surface
PS66/074-1	01.07.04	12:39	75° 0.02' N	8° 1.25' W	3399.9	CTD/RO	at depth
PS66/074-1	01.07.04	13:31	75° 0.10' N	8° 1.09' W	3400.0	CTD/RO	on deck
PS66/075-1	01.07.04	14:58	74° 59.99' N	8° 40.25' W	3360.0	CTD/RO	surface
PS66/075-1	01.07.04	16:00	75° 0.05' N	8° 39.94' W	3359.5	CTD/RO	at depth
PS66/075-1	01.07.04	16:40	75° 0.06' N	8° 40.09' W	3359.8	CTD/RO	on deck
PS66/076-1	01.07.04	17:51	74° 59.95' N	9° 18.82' W	3298.5	CTD/RO	surface
PS66/076-1	01.07.04	18:55	74° 59.87' N	9° 19.08' W	3298.0	CTD/RO	at depth
PS66/076-1	01.07.04	19:36	75° 0.02' N	9° 18.84' W	3297.6	CTD/RO	on deck
PS66/077-1	01.07.04	20:44	74° 59.92' N	9° 57.17' W	3221.2	CTD/RO	surface
PS66/077-1	01.07.04	21:45	74° 59.96' N	9° 57.16' W	3221.6	CTD/RO	at depth
PS66/077-1	01.07.04	22:36	75° 0.04' N	9° 57.18' W	3218.4	CTD/RO	on deck
PS66/078-1	01.07.04	23:44	74° 59.97' N	10° 35.98' W	3072.4	CTD/RO	surface
PS66/078-1	02.07.04	00:45	75° 0.05' N	10° 35.88' W	3070.0	CTD/RO	at depth
PS66/078-1	02.07.04	01:24	75° 0.06' N	10° 35.82' W	3069.6	CTD/RO	on deck
PS66/079-1	02.07.04	02:17	74° 59.93' N	11° 1.84' W	2742.0	CTD/RO	surface
PS66/079-1	02.07.04	03:11	74° 59.93' N	11° 2.12' W	2738.8	CTD/RO	at depth
PS66/079-1	02.07.04	03:45	74° 59.91' N	11° 2.03' W	2740.4	CTD/RO	on deck
PS66/080-1	02.07.04	04:35	74° 59.92' N	11° 28.42' W	2328.0	CTD/RO	surface
PS66/080-1	02.07.04	05:22	74° 59.75' N	11° 28.19' W	2338.0	CTD/RO	at depth
PS66/080-1	02.07.04	06:01	74° 59.57' N	11° 28.05' W	2349.2	CTD/RO	on deck
PS66/081-1	02.07.04	06:50	74° 59.87' N	11° 52.32' W	1908.4	CTD/RO	surface
PS66/081-1	02.07.04	07:27	74° 59.82' N	11° 53.27' W	1897.2	CTD/RO	at depth
PS66/081-1	02.07.04	07:53	74° 59.82' N	11° 54.00' W	1883.6	CTD/RO	on deck
PS66/082-1	02.07.04	08:28	74° 59.95' N	12° 9.26' W	1537.2	CTD/RO	surface
PS66/082-1	02.07.04	08:59	74° 59.94' N	12° 9.58' W	1530.4	CTD/RO	at depth
PS66/082-1	02.07.04	09:26	74° 59.96' N	12° 9.66' W	1527.6	CTD/RO	on deck
PS66/082-2	02.07.04	09:33	74° 59.98' N	12° 9.66' W	1526.0	GSWS	to the water
PS66/082-2	02.07.04	10:13	74° 59.97' N	12° 10.14' W	1517.2	GSWS	on Deck
PS66/083-1	02.07.04	10:57	74° 59.92' N	12° 21.53' W	1254.4	CTD/RO	surface
PS66/083-1	02.07.04	11:22	74° 59.96' N	12° 21.74' W	1246.0	CTD/RO	at depth
PS66/083-1	02.07.04	11:44	75° 0.02' N	12° 21.92' W	1235.6	CTD/RO	on deck
PS66/084-1	02.07.04	12:27	75° 0.02' N	12° 31.22' W	1011.6	CTD/RO	surface
PS66/084-1	02.07.04	12:48	75° 0.03' N	12° 30.97' W	1012.0	CTD/RO	at depth
PS66/084-1	02.07.04	13:11	74° 59.99' N	12° 31.11' W	1012.8	CTD/RO	on deck

Station	Date	Time	PositionLat	Position Lon	Depth (m)	Gear (Abbrev.)	Action
PS66/085-1	02.07.04	14:00	74° 59.80' N	12° 44.66' W	915.2	CTD/RO	surface
PS66/085-1	02.07.04	14:14	74° 59.64' N	12° 45.01' W	912.0	CTD/RO	at depth
PS66/085-1	02.07.04	14:32	74° 59.38' N	12° 45.39' W	932.0	CTD/RO	on deck
PS66/086-1	02.07.04	16:27	74° 59.82' N	13° 9.30' W	234.0	CTD/RO	surface
PS66/086-1	02.07.04	16:32	74° 59.78' N	13° 9.35' W	236.0	CTD/RO	at depth
PS66/086-1	02.07.04	16:44	74° 59.68' N	13° 9.48' W	235.0	CTD/RO	on deck
PS66/087-1	02.07.04	18:41	74° 59.74' N	13° 40.16' W	187.0	CTD/RO	surface
PS66/087-1	02.07.04	18:48	74° 59.69' N	13° 40.27' W	187.0	CTD/RO	at depth
PS66/087-1	02.07.04	18:56	74° 59.63' N	13° 40.39' W	187.0	CTD/RO	on deck
PS66/088-1	02.07.04	21:12	75° 0.10' N	14° 20.10' W	6.0	CTD/RO	surface
PS66/088-1	02.07.04	21:18	75° 0.07' N	14° 20.08' W	148.0	CTD/RO	at depth
PS66/088-1	02.07.04	21:25	75° 0.03' N	14° 20.10' W	149.0	CTD/RO	on deck
PS66/089-1	03.07.04	00:39	75° 0.05' N	15° 2.17' W	112.0	CTD/RO	surface
PS66/089-1	03.07.04	00:44	75° 0.03' N	15° 2.15' W	110.0	CTD/RO	at depth
PS66/089-1	03.07.04	00:49	75° 0.00' N	15° 2.16' W	106.0	CTD/RO	on deck
PS66/090-1	03.07.04	03:15	74° 59.90' N	15° 40.04' W	195.0	CTD/RO	surface
PS66/090-1	03.07.04	03:22	74° 59.84' N	15° 40.07' W	196.0	CTD/RO	at depth
PS66/090-1	03.07.04	03:31	74° 59.80' N	15° 39.91' W	189.0	CTD/RO	on deck
PS66/091-1	03.07.04	06:13	75° 0.07' N	16° 24.49' W	146.0	CTD/RO	surface
PS66/091-1	03.07.04	06:23	75° 0.03' N	16° 24.40' W	331.0	CTD/RO	at depth
PS66/091-1	03.07.04	06:37	75° 0.02' N	16° 24.41' W	332.0	CTD/RO	on deck
PS66/092-1	03.07.04	09:31	75° 3.36' N	16° 44.37' W	289.0	CTD/RO	surface
PS66/092-1	03.07.04	09:40	75° 3.33' N	16° 44.67' W	288.0	CTD/RO	at depth
PS66/092-1	03.07.04	09:50	75° 3.37' N	16° 44.84' W	289.0	CTD/RO	on deck
PS66/093-1	06.07.04	12:17	79° 3.40' N	4° 18.96' E	2430.4	MOR	action
PS66/093-1	06.07.04	12:24	79° 3.39' N	4° 18.88' E	2432.0	MOR	Hydrophone into the water
PS66/093-1	06.07.04	12:40	79° 3.41' N	4° 19.81' E	0.0	MOR	action
PS66/093-1	06.07.04	12:43	79° 3.43' N	4° 19.92' E	0.0	MOR	released
PS66/093-1	06.07.04	13:04	79° 3.81' N	4° 20.49' E	0.0	MOR	Hydrophone on Deck
PS66/093-1	06.07.04	13:08	79° 3.90' N	4° 20.60' E	0.0	MOR	action
PS66/093-1	06.07.04	13:20	79° 3.39' N	4° 18.74' E	0.0	MOR	Hydrophone into the water
PS66/093-1	06.07.04	13:23	79° 3.42' N	4° 18.83' E	0.0	MOR	Hydrophone on Deck
PS66/093-1	06.07.04	13:24	79° 3.43' N	4° 18.89' E	0.0	MOR	on the surface
PS66/093-1	06.07.04	13:48	79° 3.67' N	4° 19.32' E	0.0	MOR	action
PS66/093-1	06.07.04	13:49	79° 3.68' N	4° 19.34' E	0.0	MOR	on deck
PS66/093-1	06.07.04	13:55	79° 3.83' N	4° 19.53' E	0.0	MOR	mooring on deck
PS66/094-1	06.07.04	14:20	79° 3.88' N	4° 11.54' E	0.0	MOR	Hydrophone into the water
PS66/094-1	06.07.04	14:29	79° 3.92' N	4° 11.71' E	0.0	MOR	action
PS66/094-1	06.07.04	14:32	79° 3.96' N	4° 11.67' E	0.0	MOR	released

Station	Date	Time	PositionLat	Position Lon	Depth (m)	Gear (Abbrev.)	Action
PS66/094-1	06.07.04	14:39	79° 4.08' N	4° 11.78' E	0.0	MOR	released
PS66/094-1	06.07.04	14:44	79° 4.17' N	4° 12.03' E	0.0	MOR	Hydrophone on Deck
PS66/094-1	06.07.04	14:52	79° 4.33' N	4° 12.47' E	2428.4	MOR	action
PS66/094-1	06.07.04	15:24	79° 3.95' N	4° 11.17' E	2460.0	MOR	on the surface
PS66/094-1	06.07.04	15:47	79° 4.17' N	4° 12.06' E	2439.6	MOR	mooring on deck
PS66/095-1	06.07.04	16:22	79° 1.06' N	4° 19.77' E	2587.2	MOR	Hydrophone into the water
PS66/095-1	06.07.04	16:26	79° 1.13' N	4° 20.00' E	2582.8	MOR	action
PS66/095-1	06.07.04	16:32	79° 1.29' N	4° 20.11' E	2574.0	MOR	released
PS66/095-1	06.07.04	16:36	79° 1.40' N	4° 20.21' E	2565.6	MOR	on the surface
PS66/095-1	06.07.04	17:06	79° 1.44' N	4° 21.22' E	2554.8	MOR	on deck
PS66/095-1	06.07.04	17:27	79° 1.56' N	4° 22.24' E	2544.4	MOR	on deck
PS66/095-1	06.07.04	17:44	79° 1.58' N	4° 23.19' E	2538.7	MOR	on deck
PS66/095-1	06.07.04	17:53	79° 1.66' N	4° 23.60' E	2531.2	MOR	on deck
PS66/095-1	06.07.04	17:59	79° 1.73' N	4° 23.89' E	2526.0	MOR	mooring on deck
PS66/096-1	06.07.04	18:32	79° 4.32' N	4° 19.36' E	2338.0	CTR	hydrophon into water
PS66/096-1	06.07.04	18:42	79° 4.53' N	4° 19.79' E	2316.4	CTR	released
PS66/096-2	06.07.04	19:04	79° 4.41' N	4° 20.03' E	2322.0	OFOS	surface
PS66/096-2	06.07.04	19:21	79° 4.40' N	4° 20.09' E	2321.9	OFOS	on deck
PS66/096-1	06.07.04	19:40	79° 4.36' N	4° 20.00' E	2325.9	CTR	on surface
PS66/096-1	06.07.04	20:00	79° 4.66' N	4° 19.41' E	2310.4	CTR	mooring alongside
PS66/096-1	06.07.04	20:05	79° 4.73' N	4° 19.49' E	2302.8	CTR	on deck
PS66/096-1	06.07.04	20:08	79° 4.78' N	4° 19.57' E	2297.2	CTR	on deck
PS66/096-3	06.07.04	20:15	79° 4.89' N	4° 19.71' E	2284.4	CTR	to water
PS66/096-3	06.07.04	20:20	79° 4.95' N	4° 19.93' E	2279.2	CTR	to water
PS66/096-3	06.07.04	20:24	79° 4.99' N	4° 20.11' E	2277.1	CTR	slipped
PS66/096-4	06.07.04	20:40	79° 4.95' N	4° 20.27' E	2277.6	LANDER	surface
PS66/096-4	06.07.04	20:42	79° 4.94' N	4° 20.25' E	2278.0	LANDER	released
PS66/097-1	06.07.04	21:18	79° 0.96' N	4° 20.00' E	2588.8	CTD/RO	surface
PS66/097-1	06.07.04	22:09	79° 1.01' N	4° 19.88' E	2588.0	CTD/RO	at depth
PS66/097-1	06.07.04	22:48	79° 0.99' N	4° 19.79' E	2588.8	CTD/RO	on deck
PS66/098-1	06.07.04	23:18	79° 4.07' N	4° 8.84' E	2486.8	LANDER	surface
PS66/099-1	06.07.04	23:50	79° 6.01' N	4° 23.29' E	2337.2	OFOS	surface
PS66/099-1	07.07.04	00:39	79° 5.98' N	4° 23.08' E	2337.6	OFOS	at depth
PS66/099-1	07.07.04	05:30	79° 6.02' N	4° 34.50' E	2054.8	OFOS	Start Hoisting
PS66/099-1	07.07.04	06:13	79° 5.95' N	4° 37.35' E	2017.7	OFOS	on deck
PS66/100-1	07.07.04	06:46	79° 4.14' N	4° 50.61' E	2020.9	CTD/RO	surface
PS66/100-1	07.07.04	07:25	79° 4.19' N	4° 51.15' E	2008.0	CTD/RO	at depth
PS66/100-1	07.07.04	07:52	79° 4.17' N	4° 51.26' E	2015.5	CTD/RO	on deck
PS66/100-2	07.07.04	08:01	79° 4.02' N	4° 50.60' E	2051.2	MUC	surface

Station	Date	Time	PositionLat	Position Lon	Depth (m)	Gear (Abbrev.)	Action
PS66/100-2	07.07.04	08:44	79° 4.02' N	4° 50.25' E	2050.8	MUC	at sea bottom
PS66/100-2	07.07.04	09:24	79° 4.05' N	4° 50.08' E	2044.4	MUC	on deck
PS66/101-1	07.07.04	10:05	79° 7.80' N	4° 54.68' E	1542.4	CTD/RO	surface
PS66/101-1	07.07.04	10:24	79° 7.79' N	4° 54.70' E	1542.4	CTD/RO	Information
PS66/101-1	07.07.04	10:54	79° 7.78' N	4° 54.43' E	1547.1	CTD/RO	at depth
PS66/101-1	07.07.04	11:15	79° 7.75' N	4° 54.25' E	1552.0	CTD/RO	on deck
PS66/101-2	07.07.04	11:22	79° 7.75' N	4° 54.18' E	1553.5	MUC	surface
PS66/101-2	07.07.04	11:54	79° 7.76' N	4° 54.07' E	1554.0	MUC	at sea bottom
PS66/101-2	07.07.04	12:27	79° 7.72' N	4° 53.66' E	1564.8	MUC	on deck
PS66/102-1	07.07.04	14:01	79° 8.52' N	6° 6.25' E	1292.4	CTD/RO	surface
PS66/102-1	07.07.04	14:28	79° 8.39' N	6° 6.79' E	1288.8	CTD/RO	at depth
PS66/102-1	07.07.04	14:48	79° 8.32' N	6° 7.13' E	1285.9	CTD/RO	on deck
PS66/103-1	07.07.04	15:22	79° 10.16' N	5° 48.87' E	1384.3	AGT	surface
PS66/103-1	07.07.04	16:12	79° 9.24' N	5° 54.86' E	1335.9	AGT	AGT on ground
PS66/103-1	07.07.04	16:32	79° 8.97' N	5° 56.35' E	1323.9	AGT	start trawl
PS66/103-1	07.07.04	17:04	79° 8.62' N	5° 58.24' E	1310.3	AGT	Start hoisting
PS66/103-1	07.07.04	17:26	79° 8.56' N	5° 58.20' E	1309.3	AGT	AGT off ground
PS66/103-1	07.07.04	18:04	79° 8.51' N	5° 57.88' E	1307.6	AGT	on deck
PS66/104-1	07.07.04	18:40	79° 8.02' N	6° 5.76' E	1280.8	MUC	surface
PS66/104-1	07.07.04	19:06	79° 7.99' N	6° 5.46' E	1280.8	MUC	at sea bottom
PS66/104-1	07.07.04	19:33	79° 7.95' N	6° 5.48' E	1278.8	MUC	on deck
PS66/105-1	07.07.04	23:00	78° 37.39' N	5° 2.82' E	2350.3	GKG	surface
PS66/105-1	07.07.04	23:43	78° 37.30' N	5° 3.22' E	2346.0	GKG	at sea bottom
PS66/105-1	08.07.04	00:17	78° 37.31' N	5° 3.79' E	2342.0	GKG	on deck
PS66/106-1	08.07.04	00:42	78° 37.00' N	5° 0.08' E	2363.6	OFOS	surface
PS66/106-1	08.07.04	01:35	78° 36.97' N	5° 0.33' E	2363.2	OFOS	at depth
PS66/106-1	08.07.04	05:02	78° 37.02' N	5° 9.90' E	2350.4	OFOS	Start Hoisting
PS66/106-1	08.07.04	05:45	78° 36.79' N	5° 10.74' E	2350.0	OFOS	on deck
PS66/107-1	08.07.04	06:01	78° 36.48' N	5° 4.62' E	2340.7	BL_P	hydrophon surface
PS66/107-1	08.07.04	06:21	78° 36.59' N	5° 4.55' E	2340.0	BL_P	released
PS66/107-1	08.07.04	06:33	78° 36.70' N	5° 4.75' E	2340.7	BL_P	on deck
PS66/107-1	08.07.04	06:55	78° 36.49' N	5° 4.96' E	2340.4	BL_P	hydrophon surface
PS66/107-1	08.07.04	07:10	78° 36.60' N	5° 5.16' E	2340.4	BL_P	released
PS66/107-1	08.07.04	07:14	78° 36.64' N	5° 5.29' E	2340.4	BL_P	released
PS66/107-1	08.07.04	07:17	78° 36.67' N	5° 5.40' E	2340.4	BL_P	on deck
PS66/108-1	08.07.04	07:44	78° 37.60' N	5° 2.64' E	2356.7	MUC	surface
PS66/108-1	08.07.04	08:30	78° 37.50' N	5° 3.16' E	2349.0	MUC	at sea bottom
PS66/108-1	08.07.04	09:13	78° 37.23' N	5° 2.83' E	2348.4	MUC	on deck
PS66/109-1	08.07.04	09:35	78° 35.00' N	5° 4.98' E	2335.3	CTD/RO	surface
PS66/109-1	08.07.04	10:11	78° 34.92' N	5° 5.62' E	2333.6	CTD/RO	at depth
PS66/109-1	08.07.04	10:43	78° 34.78' N	5° 5.93' E	2331.6	CTD/RO	on deck

Station	Date	Time	PositionLat	Position Lon	Depth (m)	Gear (Abbrev.)	Action
PS66/110-1	08.07.04	11:27	78° 35.08' N	5° 4.09' E	2342.0	MOR	surface
PS66/110-1	08.07.04	11:30	78° 35.08' N	5° 4.17' E	2341.6	MOR	surface
PS66/110-1	08.07.04	11:33	78° 35.07' N	5° 4.31' E	2340.8	MOR	surface
PS66/110-1	08.07.04	11:41	78° 35.05' N	5° 4.50' E	2339.6	MOR	surface
PS66/110-1	08.07.04	11:56	78° 35.01' N	5° 4.85' E	2336.4	MOR	surface
PS66/110-1	08.07.04	12:20	78° 35.06' N	5° 5.58' E	2335.2	MOR	surface
PS66/110-1	08.07.04	12:38	78° 35.06' N	5° 5.66' E	2336.0	MOR	surface
PS66/110-1	08.07.04	12:45	78° 35.05' N	5° 5.67' E	2336.0	MOR	surface
PS66/110-1	08.07.04	12:48	78° 35.05' N	5° 5.61' E	2335.6	MOR	slipped
PS66/110-1	08.07.04	12:48	78° 35.05' N	5° 5.61' E	2335.6	MOR	on the ground
PS66/111-1	08.07.04	13:13	78° 36.42' N	5° 5.21' E	2340.0	MOR	surface
PS66/111-1	08.07.04	13:15	78° 36.42' N	5° 5.28' E	2340.0	MOR	slipped
PS66/112-1	08.07.04	14:39	78° 46.84' N	5° 19.68' E	2468.4	CTD/RO	surface
PS66/112-1	08.07.04	15:27	78° 46.89' N	5° 19.51' E	2473.2	CTD/RO	at depth
PS66/112-1	08.07.04	16:05	78° 46.85' N	5° 19.79' E	2467.6	CTD/RO	on deck
PS66/112-2	08.07.04	16:13	78° 46.83' N	5° 19.82' E	2466.4	MUC	surface
PS66/112-2	08.07.04	17:00	78° 46.79' N	5° 19.99' E	2460.0	MUC	at sea bottom
PS66/112-2	08.07.04	17:44	78° 46.79' N	5° 20.43' E	2450.8	MUC	on deck
PS66/113-1	08.07.04	18:47	78° 55.18' N	5° 0.57' E	2629.2	CTD/RO	surface
PS66/113-1	08.07.04	19:39	78° 55.22' N	5° 2.82' E	2623.2	CTD/RO	at depth
PS66/113-1	08.07.04	20:12	78° 55.33' N	5° 4.53' E	2627.2	CTD/RO	on deck
PS66/113-2	08.07.04	20:29	78° 55.08' N	4° 57.87' E	2639.6	MUC	surface
PS66/113-2	08.07.04	21:18	78° 55.03' N	4° 59.73' E	2634.8	MUC	at sea bottom
PS66/113-2	08.07.04	22:09	78° 54.98' N	5° 1.65' E	2629.6	MUC	on deck
PS66/114-1	09.07.04	01:20	79° 3.67' N	3° 39.48' E	3128.0	CTD/RO	surface
PS66/114-1	09.07.04	02:10	79° 3.80' N	3° 39.66' E	3124.0	CTD/RO	at depth
PS66/114-1	09.07.04	02:53	79° 3.77' N	3° 39.75' E	3121.2	CTD/RO	on deck
PS66/114-2	09.07.04	03:00	79° 3.78' N	3° 39.38' E	3122.4	MUC	surface
PS66/114-2	09.07.04	03:57	79° 3.78' N	3° 39.25' E	3136.0	MUC	at sea bottom
PS66/114-2	09.07.04	04:58	79° 3.67' N	3° 37.07' E	3279.2	MUC	on deck
PS66/115-1	09.07.04	05:41	79° 5.03' N	4° 6.23' E	2491.6	CTD/RO	surface
PS66/115-1	09.07.04	06:01	79° 5.03' N	4° 6.38' E	2490.0	CTD/RO	at depth
PS66/115-1	09.07.04	06:19	79° 5.00' N	4° 6.60' E	2489.2	CTD/RO	on deck
PS66/116-1	09.07.04	06:47	79° 3.34' N	4° 19.00' E	2435.6	LANDER	Information
PS66/116-1	09.07.04	06:56	79° 3.45' N	4° 19.27' E	2427.6	LANDER	Information
PS66/116-1	09.07.04	07:12	79° 3.37' N	4° 19.41' E	2431.6	LANDER	Information
PS66/116-1	09.07.04	07:23	79° 3.63' N	4° 20.10' E	2405.6	LANDER	Information
PS66/116-1	09.07.04	07:26	79° 3.68' N	4° 20.24' E	2400.0	LANDER	Information
PS66/116-1	09.07.04	07:29	79° 3.73' N	4° 20.43' E	2392.8	LANDER	Information
PS66/116-1	09.07.04	07:32	79° 3.78' N	4° 20.62' E	2385.6	LANDER	Information
PS66/116-1	09.07.04	07:42	79° 3.87' N	4° 20.57' E	2375.6	LANDER	Information
PS66/116-1	09.07.04	07:46	79° 3.92' N	4° 20.56' E	2371.6	LANDER	Information

Station	Date	Time	PositionLat	Position Lon	Depth (m)	Gear (Abbrev.)	Action
PS66/116-1	09.07.04	07:57	79° 3.98' N	4° 21.11' E	2358.4	LANDER	Information
PS66/116-1	09.07.04	08:08	79° 4.04' N	4° 21.04' E	2351.2	LANDER	Information
PS66/116-1	09.07.04	08:09	79° 4.05' N	4° 21.03' E	2350.4	LANDER	Information
PS66/116-1	09.07.04	08:33	79° 5.09' N	4° 20.19' E	2277.2	LANDER	Information
PS66/116-1	09.07.04	08:54	79° 5.57' N	4° 20.60' E	2336.4	LANDER	Information
PS66/116-1	09.07.04	08:56	79° 5.59' N	4° 20.65' E	2336.8	LANDER	on Deck
PS66/117-1	09.07.04	09:28	79° 5.08' N	4° 5.13' E	2502.8	MUC	surface
PS66/117-1	09.07.04	10:14	79° 5.00' N	4° 4.98' E	2507.6	MUC	at sea bottom
PS66/117-1	09.07.04	11:00	79° 4.60' N	4° 4.81' E	2524.0	MUC	on deck
PS66/118-1	09.07.04	12:02	79° 11.15' N	3° 40.26' E	3329.6	AGT	surface
PS66/118-1	09.07.04	13:43	79° 10.07' N	3° 49.31' E	2422.0	AGT	AGT on ground
PS66/118-1	09.07.04	14:20	79° 9.75' N	3° 52.21' E	2377.2	AGT	start trawl
PS66/118-1	09.07.04	14:50	79° 9.50' N	3° 54.53' E	2425.2	AGT	Stop Trawl
PS66/118-1	09.07.04	15:10	79° 9.58' N	3° 54.89' E	2425.2	AGT	AGT off ground
PS66/118-1	09.07.04	16:32	79° 9.79' N	3° 56.07' E	2426.8	AGT	on deck
PS66/119-1	09.07.04	17:18	79° 4.89' N	4° 5.89' E	2500.8	GKG	surface
PS66/119-1	09.07.04	17:52	79° 4.95' N	4° 5.50' E	2503.6	GKG	at sea bottom
PS66/119-1	09.07.04	18:38	79° 5.01' N	4° 5.84' E	2496.4	GKG	on deck
PS66/119-2	09.07.04	18:47	79° 5.01' N	4° 6.32' E	2490.8	LANDER	surface
PS66/119-3	09.07.04	19:18	79° 4.92' N	4° 5.73' E	2501.2	MUC	surface
PS66/119-3	09.07.04	20:09	79° 5.00' N	4° 5.18' E	2505.2	MUC	at sea bottom
PS66/119-3	09.07.04	20:57	79° 4.87' N	4° 5.08' E	2510.8	MUC	on deck
PS66/120-1	09.07.04	21:27	79° 1.98' N	4° 10.72' E	2623.2	OFOS	surface
PS66/120-1	09.07.04	22:23	79° 1.99' N	4° 10.27' E	2626.4	OFOS	at depth
PS66/120-1	10.07.04	02:53	79° 3.87' N	4° 17.71' E	2406.0	OFOS	Start Hoisting
PS66/120-1	10.07.04	03:38	79° 3.76' N	4° 17.38' E	2418.0	OFOS	on deck
PS66/121-1	10.07.04	04:40	79° 3.54' N	3° 35.53' E	3530.4	CTD/RO	surface
PS66/121-1	10.07.04	05:43	79° 3.47' N	3° 36.51' E	3360.8	CTD/RO	at depth
PS66/121-1	10.07.04	06:30	79° 3.49' N	3° 36.94' E	3355.6	CTD/RO	on deck
PS66/121-2	10.07.04	06:45	79° 3.51' N	3° 34.62' E	3560.0	MUC	surface
PS66/121-2	10.07.04	07:46	79° 3.51' N	3° 34.62' E	3560.8	MUC	at sea bottom
PS66/121-2	10.07.04	08:52	79° 3.82' N	3° 33.78' E	3574.8	MUC	on deck
PS66/122-1	10.07.04	09:05	79° 3.30' N	3° 29.00' E	4004.8	CTD/RO	surface
PS66/122-1	10.07.04	10:20	79° 3.53' N	3° 28.69' E	0.0	CTD/RO	at depth
PS66/122-1	10.07.04	11:14	79° 3.61' N	3° 28.79' E	4090.8	CTD/RO	on deck
PS66/122-2	10.07.04	11:25	79° 3.62' N	3° 28.85' E	0.0	MUC	surface
PS66/122-2	10.07.04	12:41	79° 3.56' N	3° 28.57' E	4089.6	MUC	at sea bottom
PS66/122-2	10.07.04	13:57	79° 3.37' N	3° 28.57' E	4024.8	MUC	on deck
PS66/123-1	10.07.04	14:18	79° 3.89' N	3° 20.69' E	0.0	CTD/RO	surface
PS66/123-1	10.07.04	15:52	79° 3.81' N	3° 20.14' E	5103.6	CTD/RO	at depth
PS66/123-1	10.07.04	16:58	79° 3.87' N	3° 21.15' E	4762.8	CTD/RO	on deck
PS66/123-2	10.07.04	17:08	79° 3.85' N	3° 21.24' E	4948.8	MUC	surface

Station	Date	Time	PositionLat	Position Lon	Depth (m)	Gear (Abbrev.)	Action
PS66/123-2	10.07.04	19:12	79° 3.79' N	3° 18.76' E	5109.6	MUC	at sea bottom
PS66/123-2	10.07.04	20:45	79° 3.39' N	3° 18.03' E	5061.2	MUC	on deck
PS66/124-1	10.07.04	21:40	79° 7.91' N	2° 50.63' E	5569.6	CTD/RO	surface
PS66/124-1	10.07.04	23:10	79° 7.98' N	2° 50.95' E	5570.4	CTD/RO	at depth
PS66/124-1	11.07.04	00:32	79° 7.94' N	2° 50.92' E	5569.2	CTD/RO	on deck
PS66/124-2	11.07.04	00:40	79° 7.95' N	2° 51.07' E	5570.0	MUC	surface
PS66/124-2	11.07.04	02:21	79° 8.02' N	2° 50.64' E	5570.8	MUC	at sea bottom
PS66/124-2	11.07.04	04:07	79° 6.80' N	2° 57.04' E	5529.6	MUC	on deck
PS66/125-1	11.07.04	06:31	79° 17.00' N	4° 18.87' E	2410.4	CTD/RO	surface
PS66/125-1	11.07.04	07:16	79° 17.05' N	4° 19.01' E	2411.6	CTD/RO	at depth
PS66/125-1	11.07.04	07:49	79° 17.14' N	4° 19.36' E	2413.6	CTD/RO	on deck
PS66/125-2	11.07.04	07:52	79° 17.17' N	4° 19.46' E	2414.8	MUC	surface
PS66/125-2	11.07.04	08:44	79° 17.00' N	4° 19.96' E	2402.4	MUC	at sea bottom
PS66/125-2	11.07.04	09:29	79° 16.77' N	4° 20.08' E	2391.2	MUC	on deck
PS66/126-1	11.07.04	10:54	79° 24.68' N	4° 41.57' E	2548.0	CTD/RO	surface
PS66/126-1	11.07.04	11:42	79° 24.70' N	4° 41.83' E	2548.0	CTD/RO	at depth
PS66/126-1	11.07.04	12:19	79° 24.65' N	4° 41.55' E	2545.6	CTD/RO	on deck
PS66/126-2	11.07.04	12:25	79° 24.61' N	4° 41.70' E	2544.0	MUC	surface
PS66/126-2	11.07.04	13:13	79° 24.60' N	4° 41.89' E	2544.0	MUC	at sea bottom
PS66/126-2	11.07.04	14:04	79° 24.64' N	4° 42.28' E	2545.2	MUC	on deck
PS66/127-1	11.07.04	15:29	79° 35.97' N	5° 9.91' E	2788.8	CTD/RO	surface
PS66/127-1	11.07.04	16:23	79° 36.01' N	5° 9.70' E	2791.2	CTD/RO	at depth
PS66/127-1	11.07.04	17:04	79° 35.99' N	5° 9.48' E	2794.4	CTD/RO	on deck
PS66/127-2	11.07.04	17:12	79° 35.97' N	5° 9.41' E	2794.4	MUC	surface
PS66/127-2	11.07.04	18:03	79° 35.93' N	5° 9.50' E	2790.8	MUC	at sea bottom
PS66/127-2	11.07.04	18:53	79° 36.00' N	5° 10.33' E	2786.8	MUC	on deck
PS66/127-3	11.07.04	19:12	79° 35.93' N	5° 10.53' E	2784.0	MUC	surface
PS66/127-3	11.07.04	20:02	79° 35.99' N	5° 10.56' E	2784.0	MUC	at sea bottom
PS66/127-3	11.07.04	21:00	79° 35.94' N	5° 9.41' E	2793.2	MUC	on deck
PS66/127-4	11.07.04	21:30	79° 35.75' N	5° 8.99' E	2796.4	OFOS	surface
PS66/127-4	11.07.04	22:18	79° 35.90' N	5° 9.93' E	2787.6	OFOS	at depth
PS66/127-4	12.07.04	03:05	79° 34.10' N	5° 15.18' E	2661.2	OFOS	Start Hoisting
PS66/127-4	12.07.04	03:56	79° 33.95' N	5° 13.03' E	2711.6	OFOS	on deck
PS66/127-5	12.07.04	04:15	79° 35.99' N	5° 9.83' E	2789.6	GKG	surface
PS66/127-5	12.07.04	05:07	79° 35.90' N	5° 9.96' E	2788.8	GKG	at sea bottom
PS66/127-5	12.07.04	05:57	79° 35.92' N	5° 10.51' E	2784.4	GKG	on deck
PS66/127-6	12.07.04	06:26	79° 35.93' N	5° 10.55' E	2783.6	MOR	action
PS66/127-6	12.07.04	06:29	79° 35.93' N	5° 10.55' E	2782.4	MOR	action
PS66/127-6	12.07.04	06:31	79° 35.93' N	5° 10.56' E	2781.6	MOR	action
PS66/127-6	12.07.04	06:42	79° 35.94' N	5° 10.74' E	2782.8	MOR	action
PS66/127-6	12.07.04	06:52	79° 35.93' N	5° 10.71' E	2783.6	MOR	action
PS66/127-6	12.07.04	07:14	79° 35.96' N	5° 10.09' E	2788.8	MOR	action

Station	Date	Time	PositionLat	Position Lon	Depth (m)	Gear (Abbrev.)	Action
PS66/127-6	12.07.04	07:33	79° 35.98' N	5° 9.88' E	2790.4	MOR	action
PS66/127-6	12.07.04	07:45	79° 35.98' N	5° 9.90' E	2791.2	MOR	action
PS66/127-6	12.07.04	07:50	79° 35.98' N	5° 9.86' E	2790.0	MOR	on the ground
PS66/127-6	12.07.04	07:54	79° 35.98' N	5° 9.89' E	2790.0	MOR	releaser on deck
PS66/128-1	12.07.04	10:14	79° 15.80' N	5° 39.69' E	1703.2	AGT	surface
PS66/128-1	12.07.04	11:15	79° 16.68' N	5° 43.66' E	1722.8	AGT	AGT on ground
PS66/128-1	12.07.04	11:46	79° 17.07' N	5° 45.50' E	1727.6	AGT	start trawl
PS66/128-1	12.07.04	12:16	79° 17.44' N	5° 47.29' E	1730.8	AGT	Stop Trawl
PS66/128-1	12.07.04	12:36	79° 17.42' N	5° 47.47' E	1728.4	AGT	AGT off ground
PS66/128-1	12.07.04	13:31	79° 17.43' N	5° 48.13' E	1720.4	AGT	on deck
PS66/129-1	12.07.04	16:38	79° 0.96' N	4° 19.02' E	2594.0	MOR	action
PS66/129-1	12.07.04	16:40	79° 0.97' N	4° 19.17' E	2593.2	MOR	action
PS66/129-1	12.07.04	16:41	79° 0.96' N	4° 19.23' E	2592.4	MOR	action
PS66/129-1	12.07.04	16:48	79° 0.90' N	4° 19.38' E	2594.4	MOR	action
PS66/129-1	12.07.04	17:00	79° 0.90' N	4° 19.72' E	2593.6	MOR	action
PS66/129-1	12.07.04	17:16	79° 0.95' N	4° 20.05' E	2589.6	MOR	action
PS66/129-1	12.07.04	17:23	79° 0.97' N	4° 20.19' E	2588.4	MOR	action
PS66/129-1	12.07.04	17:37	79° 0.99' N	4° 20.47' E	2585.6	MOR	action
PS66/129-1	12.07.04	17:42	79° 0.99' N	4° 20.56' E	2585.2	MOR	action
PS66/129-1	12.07.04	17:43	79° 0.99' N	4° 20.58' E	2585.2	MOR	surface
PS66/129-1	12.07.04	17:48	79° 0.99' N	4° 20.61' E	2584.4	MOR	on the ground
PS66/129-1	12.07.04	17:49	79° 0.99' N	4° 20.62' E	2584.4	MOR	slipped
PS66/129-1	12.07.04	17:50	79° 0.99' N	4° 20.64' E	2584.0	MOR	Hydrophone on Deck
PS66/129-1	12.07.04	17:51	79° 0.99' N	4° 20.66' E	2584.0	MOR	releaser on deck
PS66/130-1	12.07.04	20:52	79° 20.78' N	5° 55.08' E	1778.4	GSWS	to the water
PS66/130-1	12.07.04	21:22	79° 20.74' N	5° 55.08' E	1776.8	GSWS	on Deck
PS66/130-2	12.07.04	21:30	79° 20.73' N	5° 55.11' E	1776.8	OFOS	surface
PS66/130-2	12.07.04	22:06	79° 20.74' N	5° 55.03' E	1778.8	OFOS	at depth
PS66/130-2	13.07.04	02:05	79° 19.22' N	5° 49.93' E	1776.4	OFOS	Start Hoisting
PS66/130-2	13.07.04	02:42	79° 19.03' N	5° 50.16' E	1766.8	OFOS	on deck
PS66/131-1	13.07.04	05:52	79° 3.34' N	4° 19.27' E	2433.2	LANDER	Information
PS66/131-1	13.07.04	05:58	79° 3.31' N	4° 19.57' E	2434.4	LANDER	Information
PS66/131-1	13.07.04	06:03	79° 3.29' N	4° 19.57' E	2435.6	LANDER	Information
PS66/131-1	13.07.04	06:31	79° 5.01' N	4° 21.20' E	2278.8	LANDER	Information
PS66/131-1	13.07.04	06:33	79° 5.04' N	4° 21.29' E	2280.8	LANDER	surface
PS66/131-1	13.07.04	06:36	79° 5.07' N	4° 21.36' E	2283.6	LANDER	released
PS66/131-1	13.07.04	07:13	79° 5.01' N	4° 21.42' E	2280.8	LANDER	Information
PS66/131-1	13.07.04	07:34	79° 5.28' N	4° 20.71' E	2293.2	LANDER	on Deck
PS66/131-1	13.07.04	07:39	79° 5.26' N	4° 21.18' E	2298.4	LANDER	on Deck
PS66/132-1	13.07.04	08:11	79° 4.78' N	4° 6.25' E	2498.8	LANDER	Information
PS66/132-1	13.07.04	08:23	79° 4.60' N	4° 6.90' E	2498.4	LANDER	Information

Station	Date	Time	PositionLat	Position Lon	Depth (m)	Gear (Abbrev.)	Action
PS66/132-1	13.07.04	08:26	79° 4.62' N	4° 7.04' E	2496.4	LANDER	Information
PS66/132-1	13.07.04	08:29	79° 4.64' N	4° 7.16' E	2494.0	LANDER	Information
PS66/132-1	13.07.04	08:37	79° 4.63' N	4° 7.25' E	2493.6	LANDER	released
PS66/132-1	13.07.04	08:55	79° 4.37' N	4° 7.80' E	2496.4	LANDER	Information
PS66/132-1	13.07.04	09:12	79° 4.45' N	4° 8.19' E	2489.6	LANDER	Information
PS66/132-1	13.07.04	09:36	79° 5.20' N	4° 8.36' E	2452.0	LANDER	Information
PS66/132-1	13.07.04	09:38	79° 5.20' N	4° 8.46' E	2436.8	LANDER	on Deck
PS66/133-1	13.07.04	10:07	79° 6.48' N	4° 20.84' E	2334.0	OFOS	surface
PS66/133-1	13.07.04	10:14	79° 6.46' N	4° 20.67' E	2334.0	OFOS	on deck
PS66/133-1	13.07.04	10:28	79° 6.49' N	4° 20.54' E	2333.0	OFOS	surface
PS66/133-1	13.07.04	11:13	79° 6.51' N	4° 20.32' E	2333.0	OFOS	at depth
PS66/133-1	13.07.04	15:19	79° 8.57' N	4° 20.00' E	2052.0	OFOS	Start Hoisting
PS66/133-1	13.07.04	16:12	79° 8.93' N	4° 24.18' E	1922.0	OFOS	on deck
PS66/134-1	13.07.04	17:06	79° 4.90' N	4° 5.52' E	2510.0	LANDER	surface
PS66/135-1	13.07.04	17:16	79° 4.82' N	4° 5.33' E	2516.0	CTR	to water
PS66/135-1	13.07.04	17:29	79° 4.72' N	4° 5.43' E	2510.0	CTR	to water
PS66/136-1	13.07.04	17:37	79° 4.55' N	4° 5.66' E	2512.8	CTR	to water
PS66/136-1	13.07.04	17:40	79° 4.54' N	4° 5.75' E	2512.4	CTR	information
PS66/136-1	13.07.04	17:43	79° 4.55' N	4° 5.83' E	2511.2	CTR	to water
PS66/136-1	13.07.04	17:45	79° 4.55' N	4° 5.88' E	2510.8	CTR	slipped
PS66/137-1	13.07.04	21:09	78° 46.77' N	6° 14.59' E	2280.4	MUC	surface
PS66/137-1	13.07.04	21:57	78° 46.75' N	6° 15.05' E	2272.0	MUC	at sea bottom
PS66/137-1	13.07.04	22:45	78° 46.92' N	6° 14.80' E	2280.8	MUC	on deck
PS66/138-1	13.07.04	23:47	78° 46.92' N	6° 55.38' E	1539.2	MUC	surface
PS66/138-1	14.07.04	00:24	78° 46.89' N	6° 54.98' E	1541.6	MUC	at sea bottom
PS66/138-1	14.07.04	00:56	78° 46.83' N	6° 55.13' E	1540.0	MUC	on deck
PS66/139-1	14.07.04	01:45	78° 46.86' N	7° 24.81' E	1199.2	MUC	surface
PS66/139-1	14.07.04	02:12	78° 46.83' N	7° 25.04' E	1198.0	MUC	at sea bottom
PS66/139-1	14.07.04	02:38	78° 46.90' N	7° 25.83' E	1195.2	MUC	on deck
PS66/140-1	14.07.04	04:34	78° 35.15' N	8° 20.56' E	1036.0	MUC	surface
PS66/140-1	14.07.04	05:01	78° 35.36' N	8° 18.73' E	1044.0	MUC	at sea bottom
PS66/140-1	14.07.04	05:24	78° 35.41' N	8° 19.12' E	1035.2	MUC	on deck

# **ARK-XX/2**

**16.07. - 29.08.2004**

**Longyearbyen - Tromsø**

**Fahrtleiter / Chief Scientist**

**Peter Lemke**

**Koordinator / Coordinator**

**Eberhard Fahrbach**



---

## CONTENTS

<b>1.</b>	<b>Zusammenfassung und Fahrtverlauf</b>	<b>67</b>
	<b>Introduction and Itinerary</b>	<b>69</b>
<b>2.</b>	<b>Weather conditions</b>	<b>73</b>
<b>3.</b>	<b>Oceanography: Flow through Fram Strait and in the entrance to the Arctic Ocean</b>	<b>78</b>
<b>4.</b>	<b>Sea Ice - Geophysical characteristics north of Fram Strait</b>	<b>94</b>
	4.1    Sea ice conditions along cruise track	95
	4.2    Electromagnetic Induction	96
	4.3    Cryoelectrics (DC Multi-electrode Resistivity)	100
	4.4    Ground Penetrating Radar	102
	4.5    Remote Sensing Products	103
	4.6    Results	118
<b>5.</b>	<b>Air chemistry: Study of air, sea, snow and ice contamination for mercury (HG) and selected persistent organic pollutants (POPS)</b>	<b>137</b>
	5.1    Scientific programme	137
	5.2    Introduction	137
	5.3    Experiments	138
	5.4    Results	140
<b>6.</b>	<b>Bathymetry</b>	<b>149</b>
<b>7.</b>	<b>Petrologic and tectonic evolution of the Lena Trough and western Gakkel Ridge</b>	<b>153</b>
	7.1    Summary	153
	7.2    Introduction	155
	7.3    Data and Sample Collection Methods	158
	7.4    Dredging Results	164
	7.5    Sample preparation and data collection	173

**Appendix 209**

<b>A.1</b>	<b>Participants</b>	<b>210</b>
<b>A.2</b>	<b>Participating Institutes</b>	<b>212</b>
<b>A.3</b>	<b>Schiffsbesatzung / Ship's Crew</b>	<b>214</b>
<b>A.4</b>	<b>Station list ARK-XX/2</b>	<b>215</b>

---

# 1. ZUSAMMENFASSUNG UND FAHRTVERLAUF

Peter Lemke  
Alfred Wegener Institute, Bremerhaven

POLARSTEN ist am 16. Juli 2004 in Longyearbyen (Spitzbergen) planmäßig ausgelaufen, um in der Framstraße und nördlich davon ozeanographische, petrologische, bathymetrische, meereisphysikalische und luftchemische Untersuchungen zu machen (Abb. 1.1).

Die ozeanographischen Arbeiten hatten zum Ziel, den Wassermassen- und Wärmeaustausch zwischen Nordpolarmeer und Atlantik und die Zirkulation in der Framstraße und weiter nördlich zu untersuchen. Dafür wurden ein CTD-Schnitt bei 78°50'N von Spitzbergen bis 11°27,5'W ausgeführt, sowie Wasserproben genommen, um Spurenstoffe zu messen. Zwölf im letzten Jahr auf diesem Schnitt ausgelegte Verankerungen und zwei PIES (Pressure Inverted Echo Sounder) wurden aufgenommen, und zehn Verankerungen mit neuem Gerät wieder ausgelegt. Ein PIES konnte nicht aufgenommen werden. An zwei Verankerungen fehlte der Top-Auftrieb. Eine dieser Verankerungen tauchte nicht vollständig auf, wurde trotzdem erfolgreich aus 600 m Tiefe geborgen. Eine weitere Verankerung konnte nicht ausgelöst werden (beide Auslöser waren defekt) und wurde ebenfalls – mit Ankergewicht – aus dem Meer gefischt. Außerdem wurde die komplizierte Struktur des Ein- und Ausstroms nördlich der Framstraße durch drei vollständige hydrographische Schnitte untersucht.

Inhalt der petrologischen Arbeiten war die detaillierte Beprobung und Kartierung des sich effektiv am langsamsten spreizenden Mittelozeanischen Rückens der Welt: Gakkel-Rücken und Lena-Trog. Zehn Dredge-Stationen waren am Gakkel-Rücken erfolgreich, wobei sehr wertvolle, junge Peridotite gesammelt wurden. Achtundzwanzig Dredge-Stationen wurden im Lena Trog durchgeführt. Eine dieser Stationen erbrachte wertvolles Material von einem Black Smoker (Lucky B).

Im Verlauf der bathymetrischen Arbeiten wurde das bis heute von FS *Polarstern* systematisch mit Fächersonar vermessene Gebiet im Bereich der Framstraße deutlich nach Norden erweitert. Ziel war die Erfassung des geologisch bedeutenden Übergangs vom Lena Trog zum Gakkel Rücken. Das dabei neu erfasste Gebiet hat eine Ausdehnung von 100.000 km<sup>2</sup> und ermöglicht die zusammenhängende Kartierung der Eurasisch - Nordamerikanischen Plattengrenze zwischen Framstraße und Gakkel-Rücken. Im Bereich des Gakkel-Rückens wurde das im Jahr 2001 kartierte Gebiet um zwei Profile (je 220 km) entlang des Rückens erweitert.

Die meereisphysikalischen Arbeiten waren als Vorbereitung zur Validation für CryoSat-Messungen gedacht. Ein umfangreiches Programm, das sowohl Helikopterflüge mit unterschiedlichen Messinstrumenten (EM-Bird (Elektromagnetische

Eisdickenmessung), Laser Altimeter, Video), als auch Untersuchungen direkt auf dem Meereis einschloss, wurde in der Region nördlich der Framstraße durchgeführt. Messungen an 27 Stationen setzen die bisherigen Beobachtungen aus den Jahren 1991, 1996, 1998 und 2001 fort. Das Sea Ice Monitoring System (SIMS) ist während der Eisfahrt aus seiner Aufhängung heraus gebrochen und ins Wasser gefallen, konnte aber geborgen werden. Die Eisarbeiten wurden durch häufigen Nebel erschwert. Das galt insbesondere für das Zusammentreffen mit der R.R.S. *James Clark Ross*, als nur ein 2 km langes EM-Bird Profil geflogen werden konnte. Stattdessen wurde ein umfangreiches Bodenprogramm auf dem Meereis mit Bohrungen und EM-Kajak Messungen durchgeführt.

Während der gesamten Fahrtroute fanden umfassende Studien zur Luftchemie statt. Es ging dabei um die Bestimmung von Spurenkonzentrationen organischer Schadstoffe und Quecksilberspezies, wobei insbesondere der Austausch zwischen Luft, Eis/Schnee und Wasser und die Rolle des Ferntransportes und damit das Nachliefern organischer Schadstoffe in die arktischen Regionen untersucht wurden. Insgesamt wurden dafür 218 Luft-, Wasser-, Schnee-, Eis- und Sedimentproben genommen.

Ein besonderes Ereignis war die 24-stündige Unterbrechung des Forschungsprogramms zur umweltfreundlichen Entsorgung der russischen Driftstation *NP-32* (Fig. 1.2, 1.3). Diese Aktion war sehr erfolgreich durch die ausgezeichnete Zusammenarbeit zwischen der *RV Polarstern*-Besatzung und den Wissenschaftlern. Nach sehr erfolgreicher Beendigung der Arbeiten lief *RV Polarstern* am 29. August 2004 in Tromsø ein.

## INTRODUCTION AND ITINERARY

RV *Polarstern* left port in Longyearbyen as planned on 16 July, 2004 to perform oceanographic, petrologic, bathymetric, sea ice and air chemistry studies in and north of Fram Strait (Fig. 1.1).

The oceanographic work was dedicated to investigate the water mass and heat exchange between the Arctic and the North Atlantic with special emphasis on the circulation in and north of Fram Strait. A hydrographic section along 78°50'N was taken from Spitzbergen to 11°27.5'W, and water samples for tracer determination were collected. Twelve oceanographic moorings and two PIES (Pressure Inverted Echo Sounders), which have been deployed along this section last year, were recovered, and twelve moorings were re-deployed. One PIES could not be recovered. Two moorings had the top buoyancy missing. One of these moorings did not surface and had to be fished out from 600 m depth. Another mooring could not be released (both releasers didn't work) and was finally fished out, including the anchor weight. In addition, the complex structure of the inflow and outflow north of Fram Strait has been investigated through three hydrographic sections, which all could be finished.

The goal of the petrological work was to conduct a detailed sampling and mapping campaign on the effectively slowest-spreading mid-ocean ridge on Earth: Western Gakkel Ridge and Lena Trough. Ten dredge stations were occupied on Gakkel Ridge, and very valuable young peridotites were collected. Twenty-eight dredge stations were successfully taken in Lena Trough, including a valuable haul from a black smoker (Lucky B).

The bathymetric activities substantially expanded the area in Fram Strait already surveyed by RV *Polarstern* during former expeditions further to the north, with special emphasis to register the geologically and oceanographically important transition from the Spitsbergen Deep over Lena Trough to the Gakkel Ridge. The recorded area has an expanse of 100,000 km<sup>2</sup> and connects previously mapped areas of the Eurasian-North-American plate boundaries between Fram Strait and Gakkel Ridge. In the region of Gakkel Ridge, the previously mapped region was extended by two more profiles (each 220 km long) along the ridge.

The sea ice work was undertaken as a preparatory activity for the international calibration and validation initiative for CryoSat measurements. A diverse programme including helicopter flights carrying various measurement instruments (EM-Bird (Electro Magnetic ice thickness measurements), laser altimeter, video camera) and direct measurements on the ice surface was performed in the region north of Fram Strait. Measurements on 27 stations added to a series of observations from 1991, 1996, 1998 and 2001. The Sea Ice Monitoring System (SIMS) broke off from the bow and fell into a lead, but could be recovered. The ice work was strongly limited by the

frequent occurrence of fog. This was especially true for the meeting with the R.R.S. *James Clark Ross*, where only a 2 km long EM-Bird profile could be flown, in addition to a substantial surface sea ice programme with drilling and EM-kayak work.

During the entire cruise an extensive air chemistry programme was performed. The main interest was the detection of trace organic contaminants and mercury species, with special emphasis on the exchange between air, ice/snow and water and the role of the long-range transport and hence the delivery of organic pollutants to the Arctic region. In total 218 air, water, snow, ice and sediment samples have been taken.

A special incident was the 24-hour interruption of the research programme in order to remove harmful waste from the abandoned Russian drifting station *NP-32* (Fig. 1.2, 1.3). This operation was very successful due to the excellent cooperation between crew and scientists. After the conclusion of the work programme RV *Polarstern* steamed towards Tromsø and reached port on 29 August, 2004. Despite the challenging weather and ice conditions, the cruise was very successful.

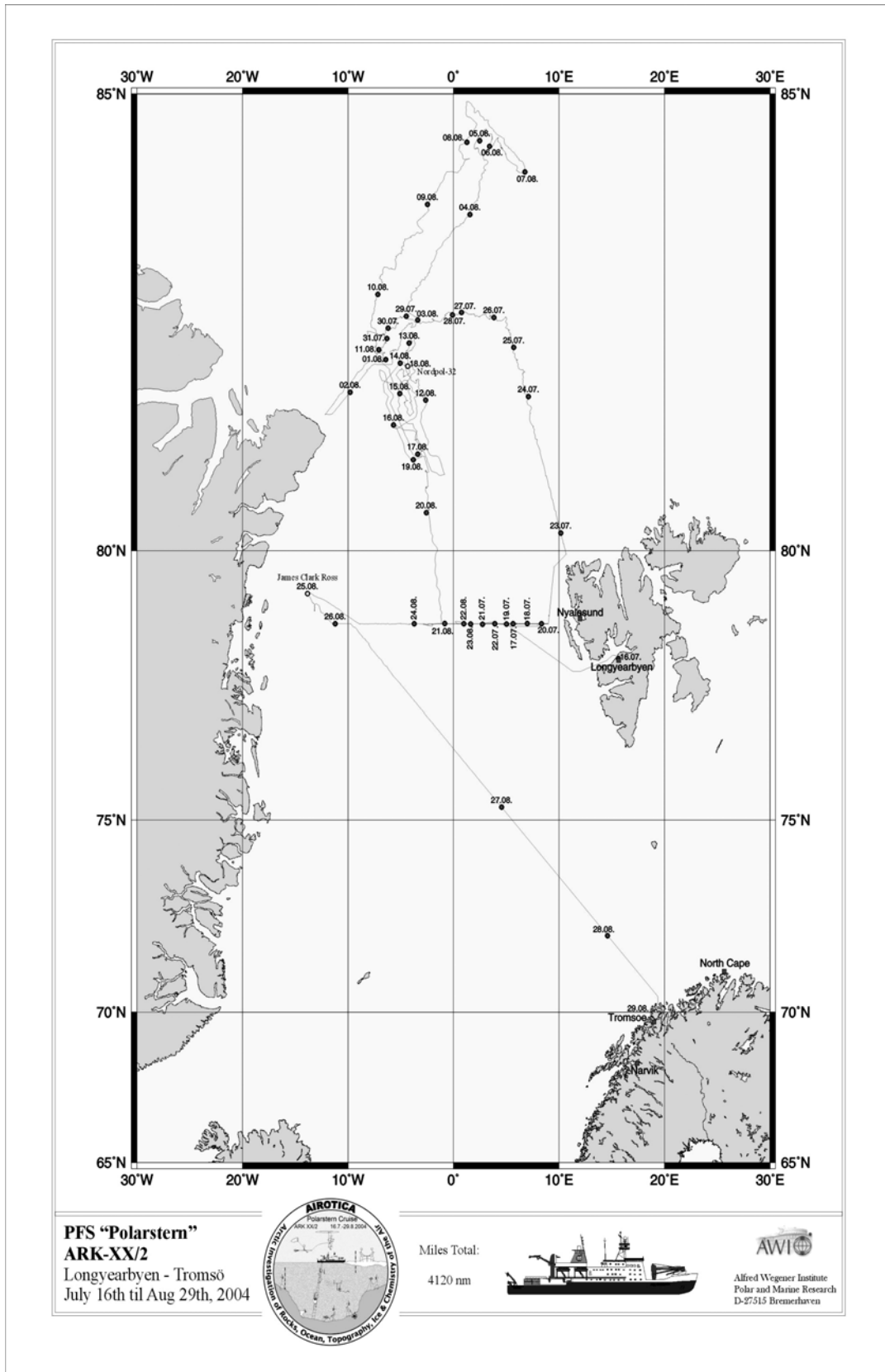


Fig. 1.1: Cruise track during ARK-XX/2



*Fig. 1.2: The destroyed and abandoned Russian Drifting Research Station NP-32*



*Fig. 1.3: Waste removal from the NP-32 ice floe*

---

## 2. WEATHER CONDITIONS

RV *Polarstern* weighed anchor in Isfjord outside Longyearbyen, Svalbard, in the evening of 16 July, 2004 and sailed under a clear sky with good visibility to its first operational area, off the northeast coast of Svalbard at about 79°N, where the first station work was carried out the following day.

At that time a large high pressure zone extended from central Europe over Finland and Russia to Siberia, while Iceland and the Norwegian Sea were under the influence of several lows. A stable high was located over Greenland for the whole cruise, and mostly a weak trough or occasionally a complete low over the northeast coast of Greenland. This synoptic situation caused steady southerly winds, which brought warm and humid air from southern regions to our working area. These condensed to form a cover of fog or low stratus clouds which generally hindered operations until a change in the weather on 2 August. The distribution of weather variables and a time-series of air temperature are displayed in figures 2.1 to 2.4.

From 17 to 23 July, operations were located in the eastern part of Fram Strait and, in a brief period of improved conditions, included some helicopter flights to Longyearbyen and a nearby glacier. Except for some fields of light drifting ice during the passage out of Isfjord, all this was done on a calm, ice-free sea, but mostly under poor visibility conditions and a deep cloud ceiling.

On 23 July the vessel steered northwards with a southwest wind, at times strong to gale force blowing, and encountered the edge of the pack ice at about 81.5°N during the night of 24 July.

From there the RV *Polarstern* moved slowly northward, breaking through occasional heavy pack ice, while carrying out station works and making continuous measurements up to a latitude of 84.9°N, which was reached on 8 August. During this period and especially up to 1 August, continuous fog interrupted helicopter operations and made navigating in the ice much more difficult.

On 2 August a low was located to the northeast of RV *Polarstern* and the wind veered between southwest and northwest, bringing good visibility. With this change of the weather situation, the supply of very warm and humid air, which caused almost continuous fog, was over. However, the incoming air from Greenland or Arctic ice regions was still partly saturated and thus the generally good visibility and partly sunny or clear skies were interrupted from time to time with incoming fog patches. But in general, navigating in the ice became less difficult and helicopter flights could be carried out more regularly.

RV *Polarstern* reached its northernmost point of 84.9°N on the morning of 8 August and since then has moved slowly southward under the same, i.e. generally good

weather conditions doing further station works and continuous soundings and measurements.

Early on 16 August the RV *Polarstern* came across an abandoned ice station. The ship stopped and made an inspection, and it turned out to be the Russian meteorological station *North Pole 32*, which was evacuated on 5 March, 2004 after a storm broke and deformed the floe.

On 16 and 17 August the ship continued its scientific work moving slowly southward but came back to the station area during 18th. At that time dense fog made navigation difficult and helicopter flights, planned to locate the drifting station again, could only be done after a delay. But by early 19 August, *North Pole 32* had been cleared up and, especially, all fuel drums, both full and empty, were removed from the ice. So the ship moved south again, continuing its scientific work. A synoptic weather map for 19 August 2004 is shown in figure 2.5.

On 20 August weather was calm and from there on, until 24 August, the waters free of ice. The next day the ship reached the first of several moorings of the AWI, which had been deployed in a line along at about 79°N. At that time a low, approaching from south, brought northerly to north-easterly winds of 6 Bft, 3 m wave height and temporarily fog. Until 23 August the low passed our working area, causing weak variable winds on 22 August, but increasing southwest wind up to Bft 6 for a while during the next day. From 24 to 26 August operations were carried out with weak variable winds and mostly dense fog.

On 25 August RV *Polarstern*, meanwhile back in partly thick pack ice again, met the British research vessel R.R.S. *James Clark Ross* on the position 79.3°N 09.6°W.

On 26 August the last station works have been carried out at the position 78.8°N 09.6°W and RV *Polarstern* steamed to Tromsø, where the ship arrived on 29 August and terminated leg no. 2 of its 20th cruise to the Arctic.

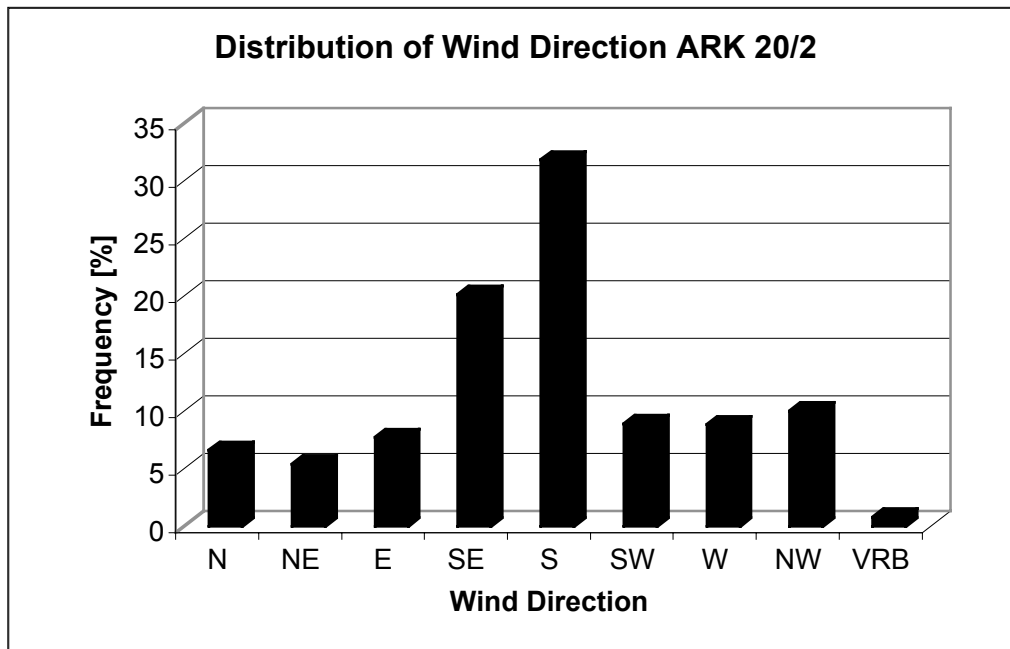


Fig. 2.1: Distribution of wind direction during ARK-II/2

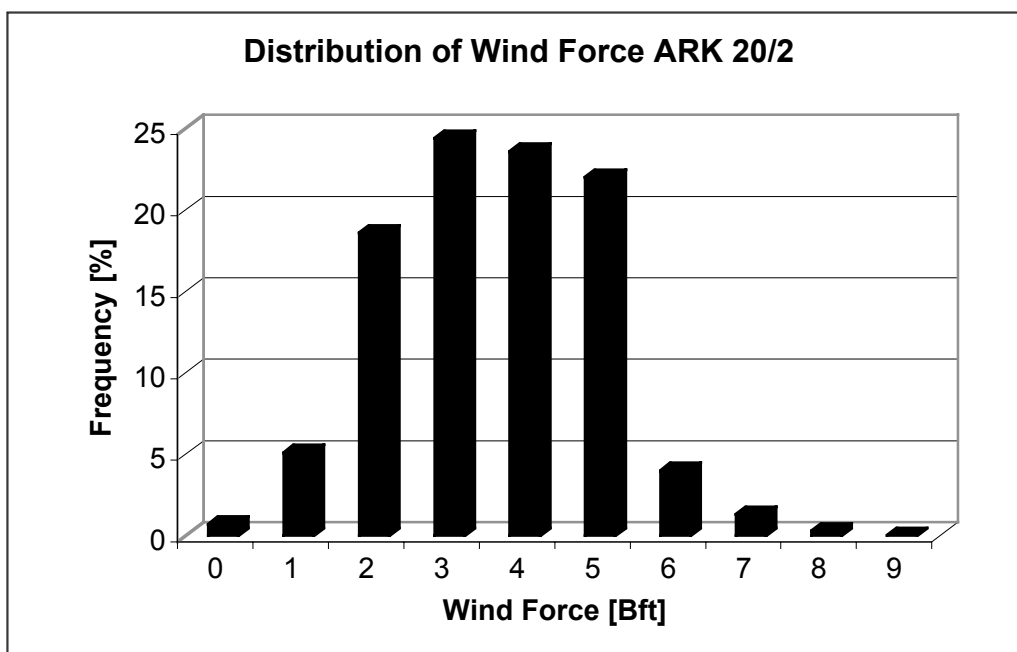


Fig. 2.2: Distribution of wind force during ARK-XX/2

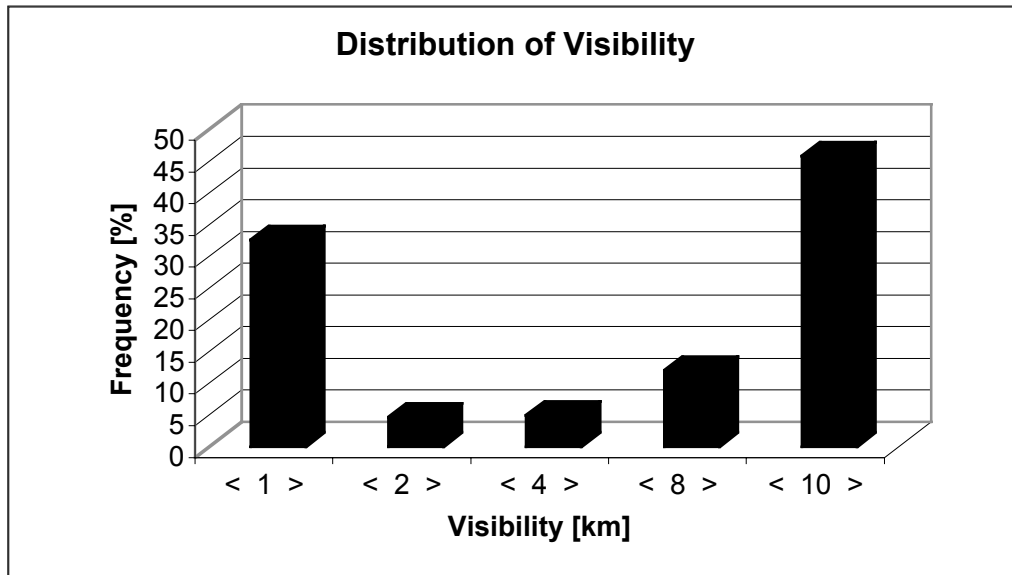


Fig. 2.3: Distribution of visibility during ARK-XX/2

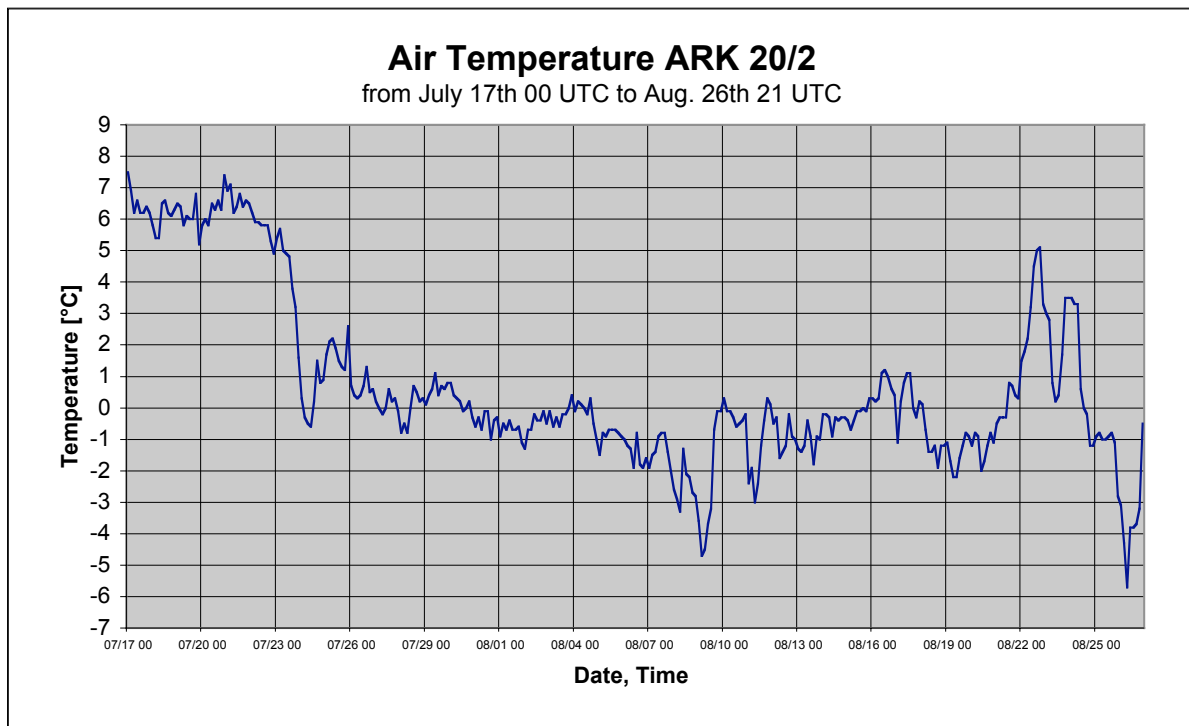


Fig. 2.4: Time-series of air temperature during ARK-XX/2

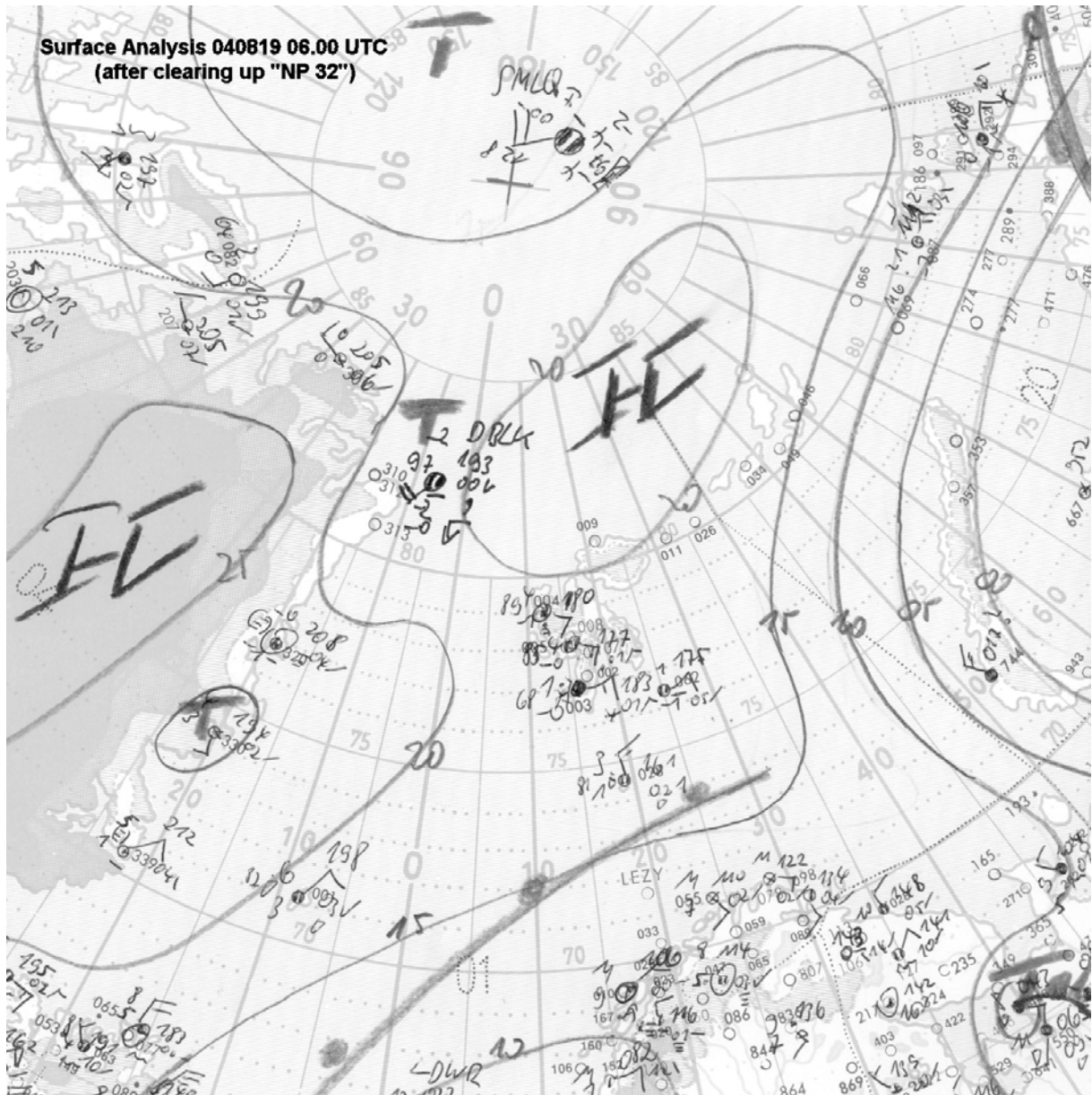


Fig. 2.5: Surface analysis of 19 August 2004, 6:00 UTC, after clearing up NP-32

---

### 3. OCEANOGRAPHY: FLOW THROUGH FRAM STRAIT AND IN THE ENTRANCE TO THE ARCTIC OCEAN

Agnieszka Beszczynska-Möller<sup>1)</sup>, Kerstin Fieg<sup>1)</sup>, Wolfgang Hayek<sup>1)</sup>, Ekkehard Schütt<sup>1)</sup>, Andreas Wisotzki<sup>1)</sup>, Marika Marnela<sup>2)</sup>, Matthias Monsees<sup>3)</sup>, Harald Rohr<sup>3)</sup>, Oliver Zenk<sup>3)</sup>, Helmut Schwegler<sup>4)</sup>

<sup>1)</sup>Alfred Wegener Institute, Bremerhaven

<sup>2)</sup>Finnish Institute of Marine Research, Helsinki

<sup>3)</sup>Optimare, Bremerhaven

<sup>4)</sup>University Bremen, Bremen

#### Background

Exchanges between the North Atlantic and the Arctic Ocean result in the most dramatic water mass conversions in the World Ocean: warm and saline Atlantic waters, flowing through the Nordic Seas into the Arctic Ocean, are modified by cooling, freezing and melting to become shallow fresh waters, ice and saline deep waters. The outflow from the Nordic Seas to the south provides the initial driving of the global thermohaline circulation cell. Knowledge of these fluxes and understanding of the modification processes is a major prerequisite for the quantification of the rate of overturning within the large circulation cells of the Arctic and the Atlantic Oceans, and is also a basic requirement for understanding the role of these ocean areas in climate variability on interannual to decadal time-scales.

The Fram Strait represents the only deep connection between the Arctic Ocean and the Nordic Seas. Just as the freshwater transport from the Arctic Ocean is of major influence on convection in the Nordic Seas and further south, the transport of warm and saline Atlantic water affects the water mass characteristics in the Arctic Ocean, which has consequences for the internal circulation and possibly influences also ice and atmosphere.

The complicated topographic structure of the Fram Strait leads to a splitting of the West Spitsbergen Current carrying Atlantic Water northward into at least three branches. One current branch follows the shelf edge and enters the Arctic Ocean north of Svalbard. This part has to cross the Yermak Plateau which poses a sill for the flow with a depth of approximately 700 m. A second branch flows northward along the north-western slope of the Yermak Plateau and the third one recirculates immediately in Fram Strait at about 79°N. Evidently, the size and strength of the different branches largely determine the input of oceanic heat to the inner Arctic Ocean. The East Greenland Current, carrying water from the Arctic Ocean southwards has a concentrated core above the continental slope.

It is our aim to measure the oceanic fluxes through Fram Strait and to determine their variability on seasonal to decadal time scales. Since 1997, year-round velocity, temperature and salinity measurements have been carried out in Fram Strait with

moored instruments. Hydrographic sections exist since 1980. Through a combination of both data sets estimates of mass, heat and salt fluxes through the strait have been obtained. Fluxes of nutrients and tracers like the oxygen isotope  $O^{18}$  could only be determined occasionally. From 1997 to 2000 intensive fieldwork was undertaken in the framework of the European Union project "VEINS" (Variability of Exchanges in Northern Seas). After the end of VEINS it was maintained under national programmes. Since 2003, the work has been carried out as part of the international Programme "ASOF" (Arctic-Subarctic Ocean Flux Study) and is partly funded in the ASOF-N project by the European Union "Energy, Environment and Sustainable Development" Programme as Proposal No EVK2-2001-00215 (ASOF-N). The mooring line is maintained in close co-operation with the Norwegian Polar Institute and the University of Hamburg. The results of the measurements will be used in combination with regional models, to investigate the nature and origin of the transport fluctuations on seasonal to decadal time scales.

### Work at Sea

The oceanographic work at sea during ARK-XX/2 included two main activities: the recovery and redeployment of the array of moorings and measurements of CTD (Conductivity, Temperature, Depth) profiles. Two main hydrographic sections were measured, the standard section in Fram Strait at  $78^{\circ}50'N$  which has been occupied regularly since 1997, and the long section started from the northern tip of Svalbard and continued across the Yermak Plateau, western part of the Nansen Basin, the Nansen-Gakkel Ridge up to the Greenland coast. The latter section had been rarely surveyed before, the last time during the RV *Polarstern* cruise ARK-XIII in 1997. During ARK-XX/2 it was for the first time that the CTD section covered the whole entrance from the northern Fram Strait to the Arctic Ocean.

The mooring array extends through the deep part of the Fram Strait from the eastern to the western shelf edge and was expanded in 2003 to the East Greenland shelf. Five Norwegian moorings and two from the University of Hamburg will be recovered by RV *Lance* in September 2004 between  $3^{\circ}$  and  $12^{\circ}30'W$ .

RV *Polarstern* recovered 12 moorings east of  $3^{\circ}W$  which had been deployed in autumn 2003 during ARK-XIX/4b along  $78^{\circ}50'N$  (Fig. 3.1). Each mooring carried 3 to 7 instruments including rotor and acoustic current meters from Aanderaa Instruments and Falmouth Scientific Inc. (FSI), acoustic current profilers from RD Instruments, temperature and salinity probes from Sea-Bird Electronics Inc. (Sea-Bird) and two bottom pressure recorders from Sea-Bird.

The mooring work was split into two parts to avoid the tight time schedule for the preparing of new deployments. During the first week of the cruise 8 of 12 moorings were redeployed in the eastern part of Fram Strait. The remaining four western moorings were recovered and deployed at the end of the cruise. Most of the work occurred under favourable weather conditions and in ice free waters. The use of the Posidonia system for those moorings which were equipped with Posidonia capable releases was of a great help and assured a safe recovery. Of two moorings which had lost their top buoys during the measuring period, only one, F6-7, was buoyant

enough to reach the surface after releasing. The second mooring, F5-6, ascended only to ca. 600 m and remained neutral in the water column. This mooring had to be redeployed twice in 2003 due to the broken wire and the amount of floatations was less than originally planned. Due to the Posidonia transponder at F5-6, its position was determined with a high accuracy and except one current meter the complete mooring was dredged out. Unfortunately a sound source of the Laboratoire d'Océanographie Dynamique et de Climatologie LODYC of the Pierre et Marie Curie University (UPMC) based in Paris which had been deployed at the mooring F5-6 was recovered in a very poor condition. It seems that this damage took place some time before the recovery.

During the second part of the cruise the mooring F15-2 had also to be recovered by dredging because of the failure of both releasers. Most likely they had been damaged by a hit against the ship's board during the last year's deployment. This mooring was equipped with the Posidonia transponder, but the device was not responding to the ship system. Eventually, all instruments at F15-2 were recovered together with the anchor, however most of the ropes were severely damaged.

In spite of required dredging, the mooring recovery rate was 100 %. 69 of 75 previously deployed instruments delivered the data, therefore producing a rate of 92 % for the data obtained. One current meter was lost during the dredging, two FSI instruments recorded no data, one recorded only part of data and one Aanderaa device was flooded. The rotor of a second Aanderaa current meter had been lost during deployment and no current speed was recorded. The temperature records from all RCM 11 current meters are incorrect but most likely this problem is due to a bug in the Aanderaa software during conversion to engineering units and binary data are still valid. The recovered and deployed instruments and the obtained data are summarized in tables 3.1 and 3.2. The distribution of the instruments in the moorings is displayed in figure 3.2.

The positions of the deployed moorings were kept as closely as possible to the original ones. The instrumentation agrees in general to the one of the recovered moorings (Table 3.2). Some additional instruments were added in order to obtain better vertical resolution and additional information by new sensor types. Each mooring carries 3 to 8 instruments. Four moorings are equipped with bottom pressure recorders from Sea-Bird Electronics to obtain changes of the sea level inclination indicative of barotropic velocity changes. Two moorings are equipped with the upward looking ADCPs (Acoustic Doppler Current Profiler). At two moorings in the West Spitsbergen Current the near-bottom Sea-Bird temperature, salinity and pressure sensors are coupled with two transmissiometers.

In 2003 three pressure inverted echo sounders (PIES Model 6.1E) manufactured at the University of Rhode Island were deployed on the transect for the first time. By combining historical hydrography with the acoustic travel time measurements they give the opportunity to obtain time series of full water column profiles of temperature and specific volume anomaly. They can be used to estimate the baroclinic flow and the heat transport. During ARK-XX/2 two of three deployed PIES were recovered at moorings F6-7 and F8-6. The instrument deployed next to mooring F2-7 was not able to interrogate with acoustic command system and thus could not be released.

Because of the delayed delivery of new PIES to RV *POLARSTERN*, their deployment took place during the next leg of the cruise, ARK-XX/3. All new instruments will be equipped with the Posidonia transponders, which should decrease the risk of loss. The experience gained during recovery of the last two PIES suggests that interrogating the instrument with acoustic commands and releasing should take place under maximum quiet ship conditions, i.e. the engine should be decoupled.

Two so-called pop-up floats from Denkmanufaktur, Großenkneten, were built into the moorings for the second time. After a predefined time, the instruments, which contain a data memory and a satellite transmitter will be released from the mooring and ascend to the surface. Then they will transmit the data, which were downloaded from the instrument to which they were connected, via satellite (Iridium) to land. This technology, which is still in an experimental stage, will enable early data access and thus secure data coverage in order to approach to a near real-time availability of data from moored instruments. However, the first pop-up buoys deployed in 2003 failed to send the data via Iridium, and some improvements were made by their manufacturer to ensure proper work of buoys deployed during this cruise. All moorings were also equipped with satellite transponders at the top flotation.

The CTD measurements along the Fram Strait section occurred mostly during the nights between mooring work and, similar to the mooring work, were split into two periods. Therefore the sequence of stations is rather irregular. The northern section Spitsbergen-Greenland was measured continuously. Altogether 97 CTD profiles were taken at 96 stations (Fig. 3.1, Table 3.3). Two CTD systems from Sea-Bird Electronics Inc SBE911+ were used. Mainly SN 561 with duplicate T and C sensors (temperature sensors SBE3, SN 2685 and 2678, conductivity sensors SBE4, SN 2325 and 2618 and pressure sensor Digiquartz 410K-105 SN 75659) were in service. For the control of the temperature sensors a SBE35 RT digital reversing thermometer, SN 27 was applied. The CTD was connected to a SBE32 Carousel Water Sampler, SN 273 (24 12-litre bottles). Additionally, Benthos Altimeter Model 2110-2, and Wetlabs C-Star Transmissiometer SN 403 were mounted on the carousels. For the first time along the Fram Strait section the SBE 43 dissolved oxygen sensor was used. The SBE 43 uses a membrane polarographic oxygen detector in its oxygen sensor. The algorithm to compute oxygen concentration requires also measurements of temperature, salinity and pressure. When the oxygen sensor is interfaced with a Sea-Bird CTD, all of these parameters are measured by the system. 242 water samples were measured onboard with Winkler titration for a calibration of the oxygen sensor. A concentration of chlorophyll a was also measured by the Dr Haardt fluorometer, SN 8060. During the cruise 481 water samples were collected at 37 stations to measure concentrations of barium and nutrients. At the same stations 317 water samples for stable isotopes,  $\delta^{18}\text{O}$  and  $\delta^{13}\text{C}$ , were taken. In addition 14 water samples at 50 l were collected at 5 stations in the eastern part of Fram Strait for technetium measurements. The sampling scheme is indicated in the list of CTD stations (Table 3.3).

Underway measurements with a ship-borne narrow band 150 kHz ADCP from RD Instruments and a Sea-Bird SBE45 thermo-salinograph measurements were conducted along the transect to supply temperature, salinity and current data at a much higher spatial resolution than given through the moorings. Two thermo-

salinographs were in use, one in 6 m depth in the bow thruster's tunnel and one in 11 m depth in the keel. Both instruments are controlled by taking water samples which are measured on board.

### **Preliminary Results**

The data from the moored instruments were read out from the memories but need to be carefully processed in Bremerhaven. Therefore no results can be given here. First insight into the raw data is promising, especially with a good data coverage in the recirculation area. The evaluation of the hydrographic data occurred on the basis of preliminary data available on board. The post-cruise calibration might result in minor changes.

The temperature and salinity sections across the Fram Strait are shown in figure 3.3. The main core of northward flowing warm and saline Atlantic Water is found at the eastern side of the transect in shallow to intermediate layers. The West Spitsbergen Current is visible at the eastern slope by downward sloping isolines. The Atlantic Water (AW) reaches significantly further to the west than during previous years. On the western side, the cold and low saline Polar Waters of the East Greenland Current can be seen. As compared to the last year the Atlantic Water layer extends farther to the west and is also slightly deeper. In the main core of the West Spitsbergen Current above the slope this change is less pronounced, while the branch of the WSC shifted towards the open sea, and in the recirculation area the amount of AW is significantly greater (Fig. 3.3c). The part of the section occupied by AW (defined with  $T > 2^{\circ}\text{C}$  and  $S > 34.92$ ) in 2004 is 30 % greater than measured in 2003. Also its mean temperature is higher by  $0.2^{\circ}\text{C}$  than last year. In the outer branch of the WSC the isotherm  $2^{\circ}\text{C}$  was shifted down from ca 450 m in 2003 to up to 650 m in 2004. Water with temperature above  $1.5^{\circ}\text{C}$  and slightly increased salinity can be found so far west as up to the slope of the Greenland shelf.

At the same time there is a surface layer of freshened water with salinity within a range 33-34.8, spread above the AW layer across the entire central and eastern Fram Strait. While in previous years this freshening occurred only in single spots, in 2004 the surface low salinity layer with an average thickness of 30-60 m thick extends continuously across the strait. There is also a strong vertical gradient of salinity at its lower boundary, decoupling the AW layer from the atmospheric influence. Except single spots there is no temperature drop in the freshened surface layer. One of the possible explanations can be related to the big amounts of melting ice observed in Fram Strait in 2004.

The second CTD section covers the whole entrance from the northern Fram Strait to the Arctic Ocean, going from the northern tip of Svalbard across the Yermak Plateau, the western part of the Nansen Basin, crossing the Nansen-Gakkel Ridge and continuing over the shelf of Greenland up to the coast (Fig. 3.4). The Svalbard branch of the West Spitsbergen Current, turning east over the archipelago and crossing a sill of the Yermak Plateau is clearly distinguished as a core of the warm (above  $3^{\circ}\text{C}$ ) and highly saline (above 34.98) water. Another, much weaker, core with slightly increased temperature and salinity represents the WSC branch flowing along the north-western flank of the Yermak Plateau. Due to shallow depths and strong

tidal mixing the water column over the Yermak Plateau is significantly colder and less saline than in both inflow branches. Less saline and very cold Polar Surface Water occupies the upper 200 m and the thickness of this layer increases westward from the Yermak Plateau. The westernmost bulk of low salinity water (<33) with temperatures around  $-1^{\circ}\text{C}$  suggests that it could origin from the Canadian Basin. The water samples taken for tracer analysis during ARK-XX/2 should help to distinguish between the Polar Water masses of different origin. The low saline surface layer is also characterised by a significant increase of dissolved oxygen while clear minimum is associated with the warm and saline WSC core in the eastern part of the section. Another oxygen minimum can be found in the subsurface layer near the Greenland shelf slope.

To identify the longer-term variability, time series of mean temperatures and salinities for typical water masses were derived for two depth intervals (5 - 30 m and 50 – 500 m) (Fig. 3.5). Three characteristic areas were distinguished in relation to the main flows: the West Spitsbergen Current (WSC) between the shelf edge and  $5^{\circ}\text{E}$ , the Return Atlantic Current (RAC) between  $3^{\circ}\text{W}$  and  $5^{\circ}\text{E}$ , and Polar Water in the East Greenland Current (EGC) between  $3^{\circ}\text{W}$  and the Greenland Shelf. The temperature of the near surface layer in the West Spitsbergen Current continued slight decrease which was also observed last year which might be affected by seasonal variability. However, the temperature stays high in comparison to the late 1980s. The temperature of the water of the Return Atlantic Current significantly increased since last year in both layers. Mean salinities observed in the West Spitsbergen Current were close to those measured last year while those of Return Atlantic Current increased further. The strong decrease of the mean salinities in the East Greenland Current, which was observed in 2002, is fully compensated indicating a rather high interannual variability or aliasing of the seasonal signal but no clear long-period trend. The mean temperature in the EGC increased slightly in both layers. However, since the data were collected in different seasons from spring to autumn, they are affected by the annual cycle which is most pronounced in the upper layers. In summary the surface layers show a rather heterogeneous picture most likely due to the seasonal transition in late fall as well as to the rather stormy weather. The conditions in the intermediate layer tended further to warmer and more saline values with the strongest change found in the recirculation area in the central part of Fram Strait.

Tab. 3.1: Moorings recovered during ARK-XX/2

Moor- ing	Latitude Longitude	Water depth (m)	Date and time of first record	Instrument type	Serial number	Instr. depth (m)	Record length
F1-6	78° 49.93' N 08° 39.90' E	244 (248)	2003-09-26 12:00	AVTP	11890	60	297.3
			2003-09-26 12:00	SBE 37	226	61	297.3
			2003-09-26 12:00	AVTCP	9998	232	297.3
F2-7	78° 50.14' N 08° 19.87' E	778 (797)	2003-09-26 14:00	AVTP	10925	72	297.1
			2003-09-26 14:00	SBE 37	447	74	297.1
			2003-09-26 14:00	ACM Coast	1563	159	297.1
			2003-09-26 14:00	AVTP	10929	264	297.1
				ACM	1386	466	3)
			2003-09-26 14:00	SBE 37	1233	766	297.1
			2003-09-26 14:00	AVT	9186	772	297.1
2003-09-26 14:00	SBE 16	630	778	297.1			
F3-6	78° 50.06' N 07° 59.65' E	1011 (1037)	2003-09-26 16:00	AVTP	9193	71	297.0
			2003-09-26 16:00	SBE 37	216	73	297.0
			2003-09-26 16:00	ACM Coast	1566	158	297.0
			2003-09-26 16:00	AVTP	10928	263	297.0
			2003-09-26 16:00	ACM	1388	765	297.0
			2003-09-26 16:00	AVT	6854	990	297.0
F4-6	78° 49.96' N 07° 00.02' E	1432	2003-09-26 18:00	SBE 37 P	1230	72	295.6
			2003-09-24 10:44	ADCP	951	101	295.6
			2003-09-26 18:00	AVTCP	9214	258	295.6
			2003-09-26 18:00	AVT	9391	764	295.6
			2003-09-26 18:00	ACM	1392	1266	166.3
			2003-09-26 18:00	AVT	9180	1411	295.6
F5-6	78° 49.95' N 06° 00.13' E	2417	2003-10-02 00:00	SBE 37	241	72	289.5
			2003-10-02 00:00	AVTP	9204	81	289.5
				ACM Coast	1568	273	2)
				LODYC SQ		513	4)
			2003-10-02 00:00	AVTCP	12330	768	289.5
			2003-10-02 00:00	ACM/CTD	1471	1270	289.5
	ACM/CTD	1448	2016	3)			
2003-10-02 00:00	AVT	9188	2391	289.5			
F6-7	78° 49.81' N 05° 01.24' E	2645	2003-09-27 14:00	AVTP	10005	47	293.7
			2003-09-27 14:00	SBE 37	227	49	293.7
			2003-09-27 14:00	AVTP	10927	253	293.7
			2003-09-27 14:00	AVTCP	12325	759	293.7
			2003-09-27 14:00	RCM 11	20	2625	293.7
			2003-09-27 14:00	SBE 16	631	2631	293.7
PIES C	78° 49.93' N 05° 00.87' E	2712	2003-09-27 11 :22	C-PIES	74	2712	299.1
F7-5	78° 49.99' N 04° 00.05' E	2292	2003-09-27 10:00	AVTP	10003	81	297.8
			2003-09-27 10:00	SBE16	1167	83	297.8
			2003-09-27 10:00	AVTCP	12326	273	5)16.1
			2003-09-27 10:00	AVT	9769	779	297.8
			2003-09-27 10:00	AVT	9770	2265	297.8
F8-6	78° 50.04' N 02° 48.11' E	2441	2003-09-29 10:00	AVTP	9763	68	295.9
			2003-09-29 10:00	SBE 16	1975	70	295.9
			2003-09-29 10:00	AVTCP	12324	270	295.9
			2003-09-29 10:00	AVT	11937	771	295.9
			2003-09-29 10:00	AVT	9767	1517	295.9
			2003-09-29 10:00	RCM 11	212	2423	295.9
			2003-09-23 20:21	SBE 26	227	2429	303.5

3. OCEANOGRAPHY: FLOW THROUGH FRAM STRAIT AND IN THE ENTRANCE TO THE ARCTIC OCEAN

Moor- ing	Latitude Longitude	Water depth (m)	Date and time of first record	Instrument type	Serial number	Instr. depth (m)	Record length
PIES W	78° 49.87' N 02° 47.59' E	2505	2003-09-25 16 :20	PIES	58	2505	297.3
F15-2	78° 49.99' N 01° 36.64' E	2497	2003-09-28 14:00	AVTP	10541	46	329.9
			2003-09-28 14:00	SBE 37 P	1607	48	329.9
			2003-09-28 14:00	AVTP	10926	257	329.9
			2003-09-28 14:00	AVTP	8037	758	329.9
			2003-09-28 14:00	AVT	10496	1504	329.9
			2003-09-28 14:00	RCM 11	214	2480	329.9
F16-2	78° 50.10' N 00° 24.03' E	2531	2003-09-29 12:00	AVTP	10539	66	327.7
			2003-09-29 12:00	SBE 37 P	242	68	327.7
			2003-09-29 12:00	AVTP	7727	262	327.7
			2003-09-29 12:00	AVT	9182	763	327.7
			2003-09-29 12:00	AVT	10497	1509	327.7
			2003-09-29 12:00	RCM 11	215	2515	327.7
F9-5	78° 50.30' N 00° 48.69' W	2610	2003-09-29 20:00	AVTCP	9200	61	326.6
			2003-09-29 20:00			63	326.6
			2003-09-29 20:00	SBE 37 P	243		
			2003-09-29 20:00	AVTCP	9785	252	326.6
			2003-09-29 20:00	AVT	10532	753	326.6
			2003-09-26 16:00	RCM 11	216	1499	297.0
			2003-09-29 20:00	RCM 11	26	2585	326.6
			2003-09-23 19:50	SBE 26	228	2591	335.8
F10-6	78° 49.89' N 02° 00.04' W	2663	2003-09-30 20:00	ACM	1385	61	325.3
			2003-09-30 20:00			62	325.3
			2003-09-28 14:00	SBE 37 P	244		
			2003-09-30 20:00	ADCP-UP	1561	281	327.8
						779	<sup>1)</sup>
			2003-09-30 20:00	AVTCP	9211		325.3
			2003-09-30 20:00	RCM11	219	1535	325.3
			2003-09-30 20:00	RCM11	25	2641	325.3

Abbreviations:

ADCP	RDI Inc. self contained acoustic doppler current profiler
ACM	Falmouth Scientific Inc. 3-dimensional acoustic current meter
AVTCP	Aanderaa current meter with temperature, conductivity and pressure sensor
AVTP	Aanderaa current meter with temperature and pressure sensor
AVT	Aanderaa current meter with temperature sensor
RCM 11	Aanderaa Doppler current meter with temperature sensor
SBE 16	Seabird Electronics SBE16 recording temperature, conductivity, and pressure
SBE 26	Seabird Electronics SBE26 bottom pressure recorder
SBE 37	Seabird Electronics SBE37 recording temperature and conductivity and optionally pressure (SBE 37 P)
PIES	Pressure Inverted Echosounder (optionally with current meter C-PIES)

Remarks :

- <sup>1)</sup> Rotor lost
- <sup>2)</sup> Instrument lost.
- <sup>3)</sup> Instrument failure, no data.
- <sup>4)</sup> Instrument damaged.
- <sup>5)</sup> Instrument flooded, no data.

Tab. 3.2: Moorings deployed during ARK-XX/2

Moorings	Latitude Longitude	Water depth (m)	Date and time of first record	Instrument type	Serial number	Instr. depth (m)
F1-7	78° 49.94' N 08° 39.84' E	244 (248)	03.05.2004 12:00 17.07.2004 13:00 17.07.2004 13:00 03.05.2004 12:00	AVTP SBE 37 SBE 37 AVTP	8048 221 217 9402	61 63 226 232
F2-8	78° 50.14' N 08° 19.64' E	778 (795)	03.05.2004 12:00 17.07.2004 13:00 03.05.2004 12:00 17.07.2004 13:00 03.05.2004 12:00 19.07.2004 14:44	AVTP SBE 37 AVT SBE 16 AVT SBE 26	8050 212 3517 2419 9403 258	59 61 255 771 773 778
F3-7	78° 50.30' N 07° 59.55' E	1011 (1036)	03.05.2004 12:00 17.07.2004 12:00 03.05.2004 12:00 03.05.2004 12:00 03.05.2004 12:00 17.07.2004 16:00	AVTP SBE 37P AVTP RCM 11 RCM 11 SBE 16/Trans	8403 1228 9786 294 295 2421/446	60 62 252 753 999 1001
F4-7	78° 50.17' N 07° 00.01' E	1432 (1458)	17.07.2004 12:00 17.07.2004 17:20 03.05.2004 12:00 03.05.2004 12:00 17.07.2004 16:00 03.05.2004 12:00	SBE 37 CTD ADCP AVTPC RCM 11 SBE 16/Trans RCM 11	1229 1368 9213 296 2418/435 297	63 93 249 755 1419 1421
F5-7	78° 49.93' N 06° 00.10' E	2412 (2467)	03.05.2004 12:00 17.07.2004 15:00 03.05.2004 12:00 03.05.2004 12:00 03.05.2004 12:00 03.05.2004 12:00	AVT SBE 16 AVTP AVTP RCM 11 RCM 11	6856 2414 8417 9212 298 311	61 63 253 749 1505 2401
F6-8	78° 49.80' N 05° 01.33' E	2644 (2693)	03.05.2004 12:00 19.97.2004 10:00 03.05.2004 12:00 03.05.2004 12:00 03.05.2004 12:00 03.05.2004 12:00 17.07.2004 15 :00	AVT SBE 16 AVTP AVTP RCM 11 RCM 11 SBE 16	9179 1253 9192 9997 312 313 1978	59 61 255 751 1507 2638 2644
F7-6	78° 49.99' N 04° 00.03' E	2292 (2339)	19.07.2004 20:00 21.07.2004 11:00 19.07.2004 20:00 19.07.2004 16:00 19.07.2004 20:00 19.07.2004 16:00	AVT SBE 16 AVTP RCM 11 AVTP RCM11	9184 2413 9194 314 12332 315	61 63 253 759 1503 2281
F8-7	78° 50.05' N 02° 48.09' E	2441 (2491)	19.07.2004 20 :00 21.07.2004 11 :00 19.07.2004 20 :00 19.07.2004 22 :00	AVT SBE 16 AVTP AVTP	9185 2415 9195 9219	60 62 247 753
			19.07.2004 22 :00 20.07.2004 16 :00 21.07.2004 10 :00	AVTP AVT SBE 26	12328 10530 259	1499 2435 2441
F15-3	78° 50.00' N 01° 36.59' E	2498 (2546)	31.07.2004 10 :00 09.08.2004 10 :00 27.07.2004 18 :00 27.07.2004 18 :00	AVT SBE 16 ACM ACM	9187 2416 1391 1389	57 59 248 249

Mooring	Latitude Longitude	Water depth (m)	Date and time of first record	Instrument type	Serial number	Instr. depth (m)
			31.07.2004 10 :00 31.07.2004 10 :00 31.07.2004 10 :00	AVTP AVT AVT	10492 10531 9206	755 1501 2487
F16-3	78° 50.05' N 00° 23.81' E	2530 (2581)	31.07.2004 10 :00 09.08.2004 10 :00 31.07.2004 10 :00 31.07.2004 10 :00 27.07.2004 18 :00 27.07.2004 18 :00 31.07.2004 12 :00	AVTP SBE 16 AVTP AVT ACM ACM RCM 11	9207 1976 10872 9782 1442 1443 20	59 61 251 757 1502 1503 2519
F9-6	78° 50.33' N 00° 48.74' W	2609 (2662)	31.07.2004 12 :00 12.07.2004 18 :00 31.07.2004 12 :00 31.07.2004 12 :00 27.07.2004 18 :00 27.07.2004 18 :00 31.07.2004 12 :00 09.08.2004 10 :00	AVTP SBE 16 AVTP RCM 11 ACM ACM RCM 11 SBE 16	10002 1977 11889 217 1447 1449 212 1979	58 60 250 756 1506 1507 2603 2609
F10-7	78° 49.88' N 02° 00.06' W	2663 (2717)	31.07.2004 12 :00 09.08.2004 10:00 21.08.2004 20 :14 31.07.2004 12 :00 27.07.2004 18 :00 31.07.2004 12 :00	AVTP SBE 16 ADCP-UP AVTP ACM AVTP	11888 2422 1561 11613 1450 12333	61 63 253 750 1505 2652

Tab. 3.3: CTD stations carried out during ARK-XX/2

File	Station	Cast	Latitude	Longitude	Depth	PMax	Date			Water samples				
							Day	Month	Year	$\delta^{18}\text{O}$	$\delta^{13}\text{C}$	Barium	Nutr.	Tech.
14401.dat	144	1	78.833	5.079	2622	2662	17	7	2004					
14501.dat	145	1	78.834	5.334	2574	2613	18	7	2004					
14601.dat	146	1	78.834	5.662	2528	2565	18	7	2004					
14701.dat	147	1	78.830	5.921	2457	2494	18	7	2004					
15001.dat	150	1	78.833	6.167	2319	2350	18	7	2004					
15101.dat	151	1	78.834	6.502	1931	1953	18	7	2004					
15201.dat	152	1	78.834	6.912	1526	1540	19	7	2004					
15301.dat	153	1	78.834	7.167	1323	1338	19	7	2004					
15401.dat	154	1	78.833	7.492	1147	1157	19	7	2004					
15501.dat	155	1	78.833	7.912	1041	1052	19	7	2004					
16101.dat	161	1	78.833	9.004	214	212	19	7	2004					
16201.dat	162	1	78.833	8.827	232	232	19	7	2004					
16301.dat	163	1	78.834	8.715	254	253	19	7	2004					
16401.dat	164	1	78.834	8.604	387	387	19	7	2004					
16501.dat	165	1	78.834	8.495	577	580	19	7	2004					
16601.dat	166	1	78.833	8.367	739	744	19	7	2004					
16701.dat	167	1	78.833	8.196	900	907	20	7	2004					

File	Station	Cast	Latitude	Longitude	Depth	PMax	Date			Water samples				
							Day	Month	Year	$\delta^{18}\text{O}$	$\delta^{13}\text{C}$	Barium	Nutr.	Tech.
17301.dat	173	1	78.833	2.826	2436	2472	21	7	2004					
17701.dat	177	1	78.833	3.161	2386	2420	21	7	2004					
17801.dat	178	1	78.835	3.400	2320	2353	21	7	2004					
17901.dat	179	1	78.832	3.744	2228	2259	21	7	2004					
18001.dat	180	1	78.834	4.000	2286	2318	21	7	2004					
18101.dat	181	1	78.833	4.401	2368	2402	22	7	2004					
18201.dat	182	1	78.834	4.751	2609	2653	22	7	2004					
18701.dat	187	1	79.948	10.714	315	312	23	7	2004					
18801.dat	188	1	80.110	10.426	508	509	23	7	2004					
18901.dat	189	1	80.267	10.172	596	598	23	7	2004					
19001.dat	190	1	80.429	9.899	677	680	23	7	2004					
19101.dat	191	1	80.589	9.628	1231	1243	23	7	2004					
19201.dat	192	1	80.753	9.351	979	987	23	7	2004					
19301.dat	193	1	80.912	9.072	595	597	23	7	2004					
19401.dat	194	1	81.073	8.781	968	976	23	7	2004					
19501.dat	195	1	81.232	8.490	718	722	23	7	2004					
19601.dat	196	1	81.390	8.197	793	797	24	7	2004					
19701.dat	197	1	81.552	7.898	828	833	24	7	2004					
19801.dat	198	1	81.714	7.543	821	825	24	7	2004					
19901.dat	199	1	81.876	7.246	769	774	24	7	2004					
20001.dat	200	1	82.031	6.958	740	744	24	7	2004					
20101.dat	201	1	82.194	6.667	1073	1082	24	7	2004					
20201.dat	202	1	82.369	6.648	2301	2336	25	7	2004					
20301.dat	203	1	82.510	5.963	3324	3383	25	7	2004					
20401.dat	204	1	82.676	5.579	3612	3678	25	7	2004					
20501.dat	205	1	82.840	5.243	4024	4101	25	7	2004					
20601.dat	206	1	82.978	4.915	4023	4102	26	7	2004					
20701.dat	207	1	82.995	3.548	3835	3907	26	7	2004					
20801.dat	208	1	82.996	2.208	3395	3453	27	7	2004					
20901.dat	209	1	83.036	0.764	3651	3718	27	7	2004					
21001.dat	210	1	83.016	-0.620	3689	3756	28	7	2004					
21101.dat	211	1	82.964	-2.023	3341	3398	29	7	2004					
21201.dat	212	1	82.928	-3.252	2449	2484	29	7	2004					
21301.dat	213	1	82.997	-4.685	2518	2556	29	7	2004					
21601.dat	216	1	82.872	-5.503	2914	2961	30	7	2004					
21801.dat	218	1	82.885	-6.197	4189	4274	30	7	2004					
22001.dat	220	1	82.746	-6.402	4646	4744	31	7	2004					
22201.dat	222	1	82.608	-7.352	3967	4041	1	8	2004					
22501.dat	225	1	82.495	-8.219	3140	3193	1	8	2004					
22601.dat	226	1	82.370	-8.972	3033	3083	1	8	2004					
22701.dat	227	1	82.246	-9.784	2866	2911	2	8	2004					
22801.dat	228	1	82.121	-10.581	2355	2390	2	8	2004					
22901.dat	229	1	81.992	-11.373	226	225	2	8	2004					
23001.dat	230	1	81.866	-12.156	218	217	2	8	2004					

3. OCEANOGRAPHY: FLOW THROUGH FRAM STRAIT AND IN THE ENTRANCE TO THE ARCTIC OCEAN

File	Station	Cast	Latitude	Longitude	Depth	PMax	Date			Water samples				
							Day	Month	Year	$\delta^{18}\text{O}$	$\delta^{13}\text{C}$	Barium	Nutr.	Tech.
24201.dat	242	1	84.633	1.174	4051	4129	8	8	2004					
24501.dat	245	1	82.115	-2.720	2610	2648	12	8	2004					
24701.dat	247	1	82.716	-4.161	2100	2128	13	8	2004					
25811.dat	258	11	81.361	-3.387	3235	3290	17	8	2004					
26501.dat	265	1	78.835	-1.120	2574	2613	21	8	2004					
26601.dat	266	1	78.835	-1.423	2634	2675	21	8	2004					
26702.dat	267	2	78.833	-1.989	2661	2704	21	8	2004					
26802.dat	268	2	78.839	-0.805	2609	2651	21	8	2004					
26901.dat	269	1	78.832	-0.501	2635	2678	21	8	2004					
27001.dat	270	1	78.836	-0.208	2592	2632	21	8	2004					
27101.dat	271	1	78.833	0.095	2578	2616	21	8	2004					
27201.dat	272	1	78.833	0.688	2441	2477	22	8	2004					
27301.dat	273	1	78.833	1.004	2433	2469	22	8	2004					
27402.dat	274	2	78.837	0.397	2531	2571	22	8	2004					
27501.dat	275	1	78.832	1.297	2473	2509	22	8	2004					
27701.dat	277	1	78.832	1.561	2492	2530	22	8	2004					
27801.dat	278	1	78.834	1.921	2505	2543	22	8	2004					
27901.dat	279	1	78.834	2.257	2488	2526	22	8	2004					
28001.dat	280	1	78.835	2.584	2469	2503	23	8	2004					
28201.dat	282	1	78.834	-1.750	2657	2699	23	8	2004					
28301.dat	283	1	78.832	-2.393	2612	2650	24	8	2004					
28401.dat	284	1	78.833	-2.859	2525	2562	24	8	2004					
28601.dat	286	1	78.833	-3.339	2339	2372	24	8	2004					
28701.dat	287	1	78.832	-3.719	2091	2118	24	8	2004					
28801.dat	288	1	78.832	-4.148	1757	1779	24	8	2004					
28901.dat	289	1	78.835	-4.580	1383	1398	24	8	2004					
29001.dat	290	1	78.835	-5.001	1016	1026	24	8	2004					
29101.dat	291	1	78.832	-5.439	602	605	24	8	2004					
29201.dat	292	1	78.834	-6.305	300	299	24	8	2004					
29301.dat	293	1	78.834	-7.159	229	227	24	8	2004					
29401.dat	294	1	78.832	-8.012	183	180	25	8	2004					
29501.dat	295	1	78.831	-8.873	240	238	25	8	2004					
29701.dat	297	1	78.835	-11.469	248	246	26	8	2004					
29801.dat	298	1	78.834	-10.602	380	379	26	8	2004					
29901.dat	299	1	78.832	-9.736	216	211	26	8	2004					

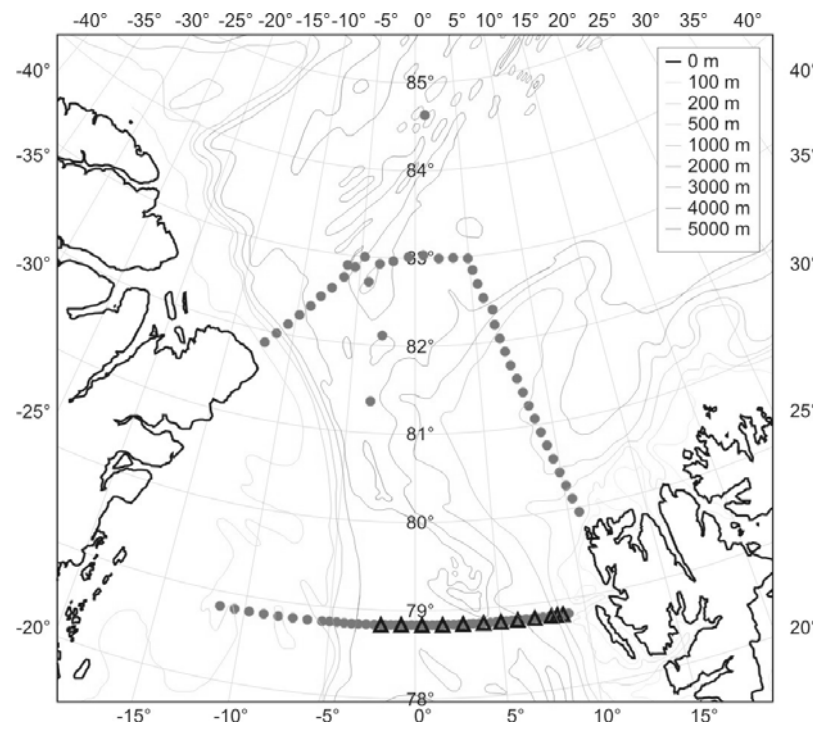


Fig. 3.1: Map with the position of moorings (triangles) and CTD stations (dots) taken during ARK-XX/2

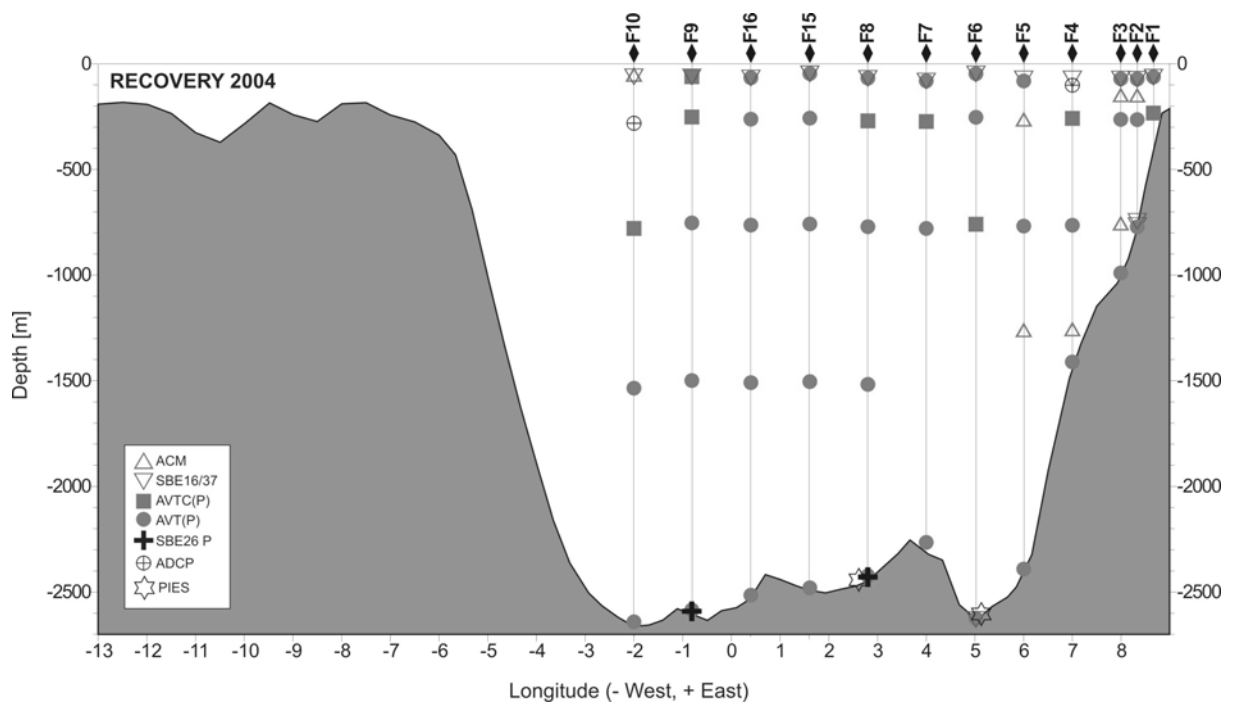


Fig. 3.2: Transect across Fram Strait with the moored instruments recovered during ARXX/2

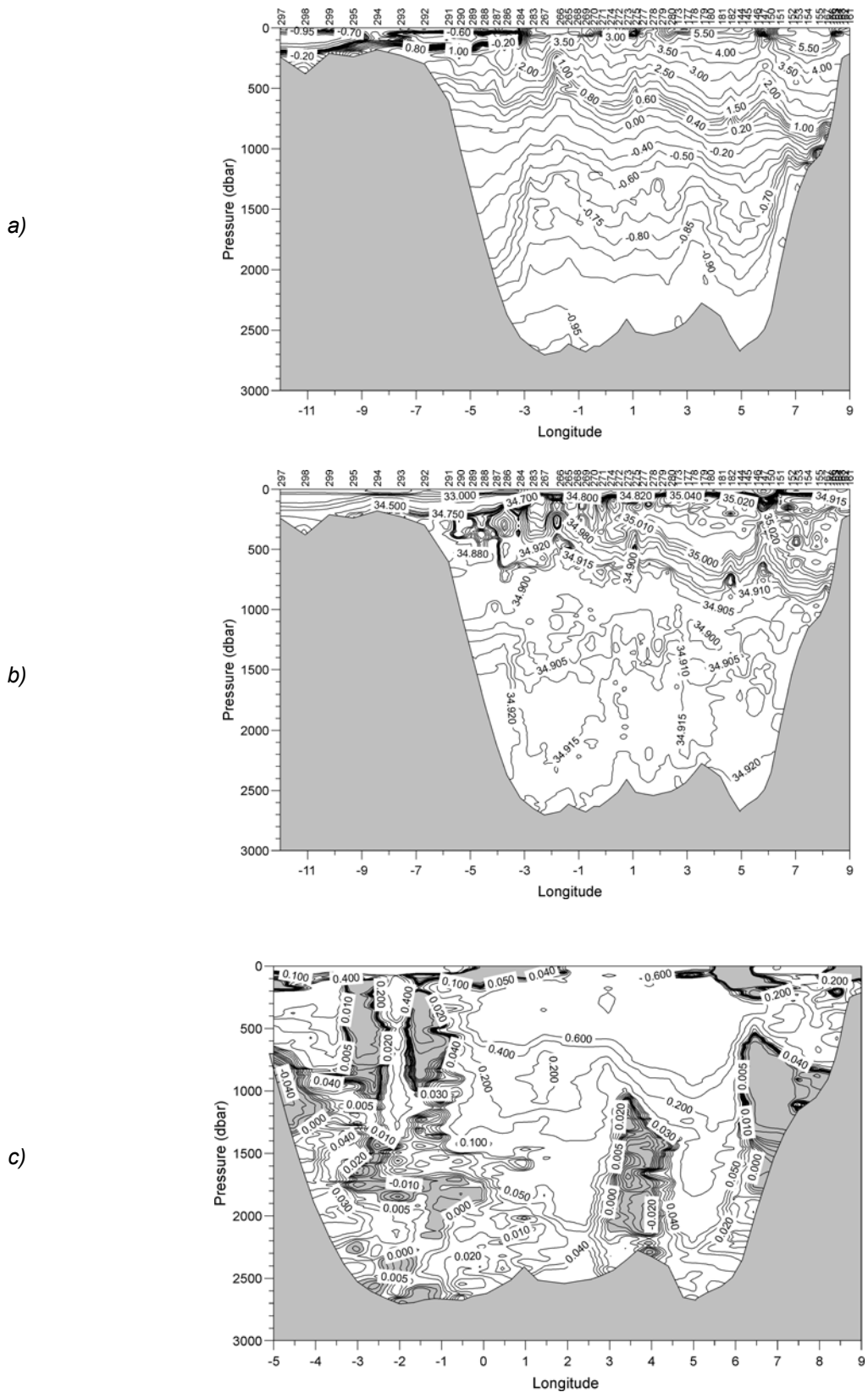


Fig. 3.3: Vertical distribution of potential temperature (a) and salinity (b) across the Fram Strait measured during ARK-XX/2 and temperature difference between 2003 and 2004 (c)

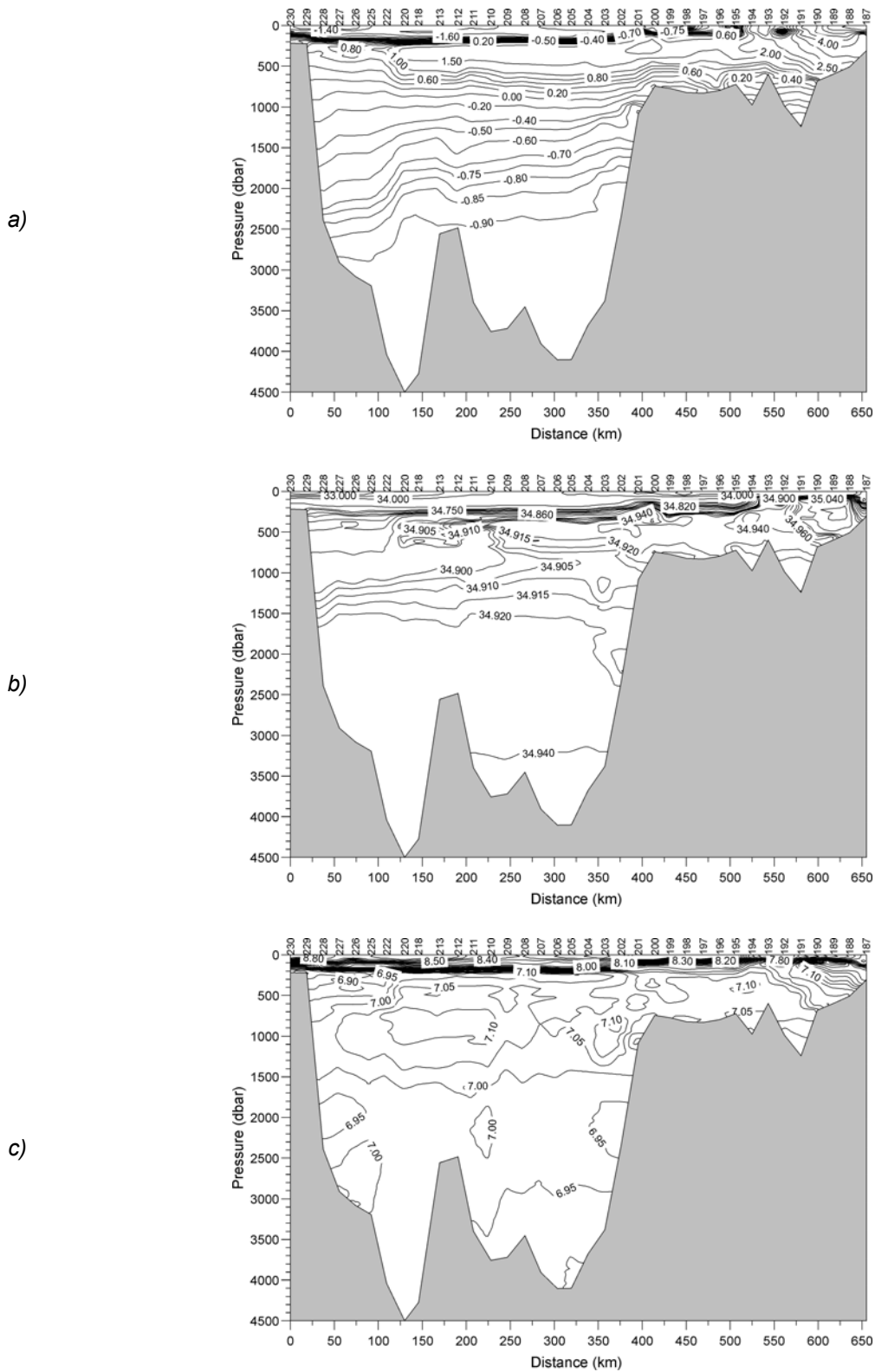


Fig. 3.4: Vertical distributions of potential temperature (a), salinity (b) and dissolved oxygen (c) at the section Greenland-Spitsbergen during ARK-XX/2

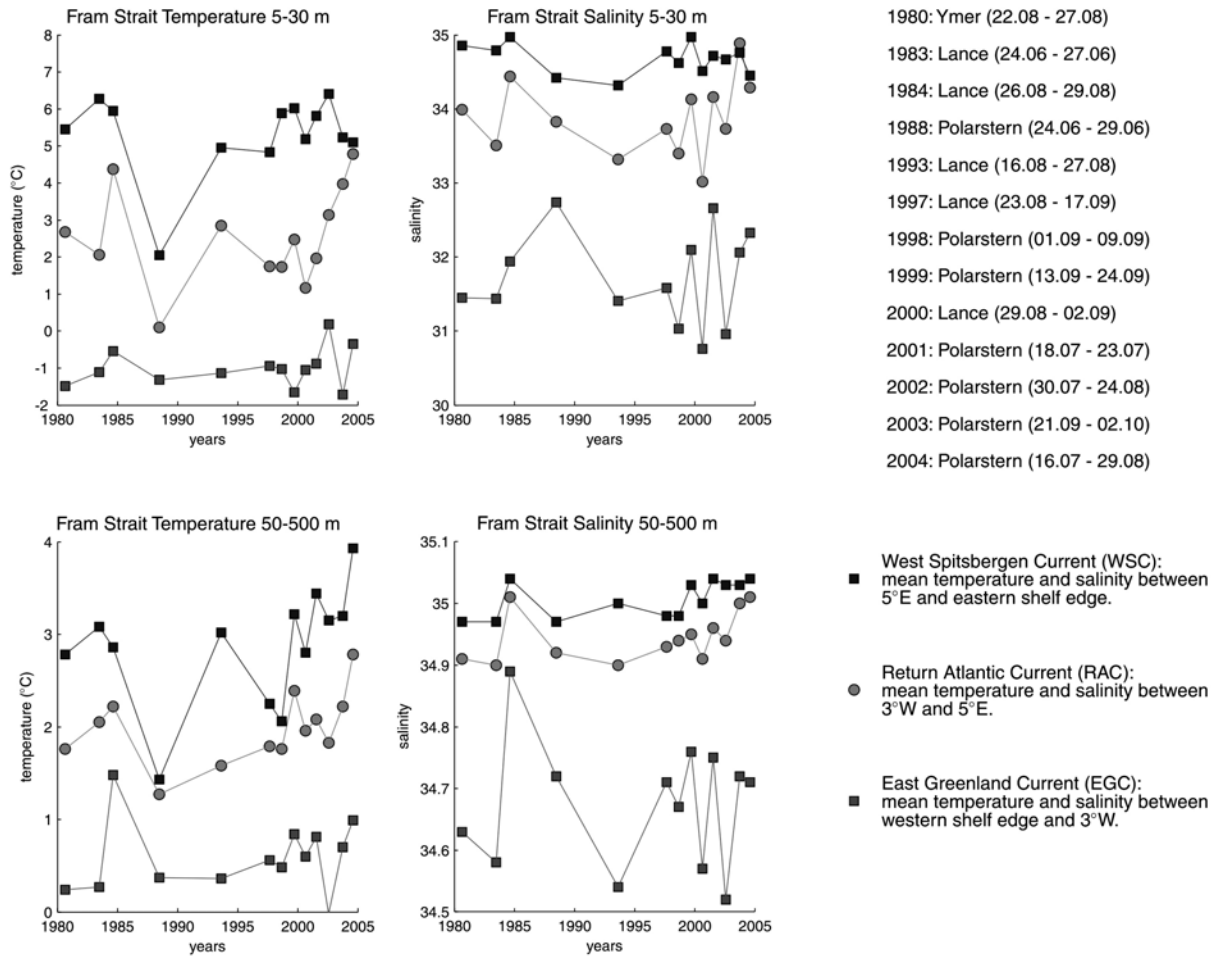


Fig. 3.5: The variations of the Fram Strait mean temperatures and salinities in the West Spitsbergen Current (WSC), Return Atlantic Current (RAW) and East Greenland Current (EGC)

---

## 4. SEA ICE - GEOPHYSICAL CHARACTERISTICS NORTH OF FRAM STRAIT

Thomas Busche<sup>1)</sup>, David Flinspach<sup>1)</sup>, Jan Lieser<sup>1)</sup>, Torge Martin<sup>1)</sup>, Andreas Pfaffling<sup>1)</sup>, Carola von Saldern<sup>1)</sup>, John Bishop<sup>2)</sup>, Gunnar Spreen<sup>3)</sup>

<sup>1)</sup>Alfred Wegener Institute, Bremerhaven

<sup>2)</sup>University of Tasmania, Sandy Bay

<sup>3)</sup>University Bremen, Bremen

The main objective of the sea ice physics measurements during the *RV Polarstern* cruise ARK-XX/2 was to provide a comprehensive data set for the validation and interpretation of remote sensing information and the AWI Helicopter-borne Electromagnetic induction sensor (HEM-Bird).

Satellites carry a variety of instruments for monitoring the changing surface conditions of the Earth. For polar regions, especially radar, microwave, and optical sensors are suitable to gain information on the sea ice cover, for example roughness, concentration, and surface temperature. Radar and microwave signals are able to travel through the atmosphere without major interference with the atmospheric constituents and, therefore, provide information irrespective of cloud cover or sunlight illumination. However, a weather filter has to be applied to the microwave data, depending on the frequency used. In contrast, remote sensing information in the visible spectrum are always dependent on cloud-free conditions and sun illuminated regions.

During the cruise near real-time data from Advanced Synthetic Aperture Radar (ASAR) and Advanced Microwave Scanning Radiometer (AMSR-E) were received and processed regularly onboard the ship and provided valuable information for route planning and ship's navigation (see Section 4.5). Also, the activities included pre-launch ground truth data collection for the upcoming CryoSat satellite mission, which is a dedicated radar altimeter mission for large scale monitoring of the global ice sheets and sea ice thickness. This mission will complement the existing remote sensing techniques and is scheduled to start in October 2005.

The ground truth data were collected using both, helicopter borne instruments as well as direct measurements on single sea ice floes. The helicopters operated from *RV Polarstern* provided the platform for large scale surveys carrying the AWI HEM-Bird for sea ice thickness measurements (see Section 4.2) together with a nadir looking video system from which the melt pond coverage of sea ice will be deduced later. Direct measurements of sea ice floes consisted of ground based EM ice thickness measurements, drillings, multi electrode DC electric resistivity readings (cryo-electric), ground penetrating radar, and leveling. These direct measurements are also used as extensive ground validation of the HEM-Bird.

Finally, the first inter-comparison of an upward looking sonar and a HEM-Bird was carried out during a 12-hour ice station near the Greenland coast together with an

Autonomous Underwater Vehicle (AUV), which was operated from the British research ship R.R.S. *James Clark Ross*. The location of a landfast sea ice area provided a perfect situation to compare the two systems, which operate at very different speeds.

#### 4.1 Sea ice conditions along cruise track

Jan Lieser, Torge Martin  
Alfred Wegener Institute (AWI)

Hourly standardized visual observations have been performed from the ship's bridge by the ship's members of the sea ice group, who were kindly supported by Marika Marnela (Finnish Institute for Marine Research, Finland) and Wolfgang Hayek (University of Bremen, Germany). The surrounding of the ship was described with different variables, such as ice concentration, typical ice thickness, melt pond size and coverage, floe and lead size, and ridge information (size and spacing). Additionally, photos showing the views to port side, ahead and starboard were taken whenever weather situation allowed. All this information will be available from the AWI website soon after return.

The left panel of figure 4.1 displays sea ice concentration during the cruise. The ship entered ice covered waters northwest of Spitsbergen and performed a transect along  $83^{\circ}\text{N}$  in high ice concentrations. After a detour to the northern coast of Greenland sailing in almost open waters the ship encountered again high ice concentration north of approximately  $82.6^{\circ}\text{N}$ , but faced favourable travelling conditions in leads and polynyas up to almost  $85^{\circ}\text{N}$ . The right panel shows the observed melt pond coverage during the cruise. By the end of July and during August the melt pond coverage was on an almost constant level between 30 and 40 %.

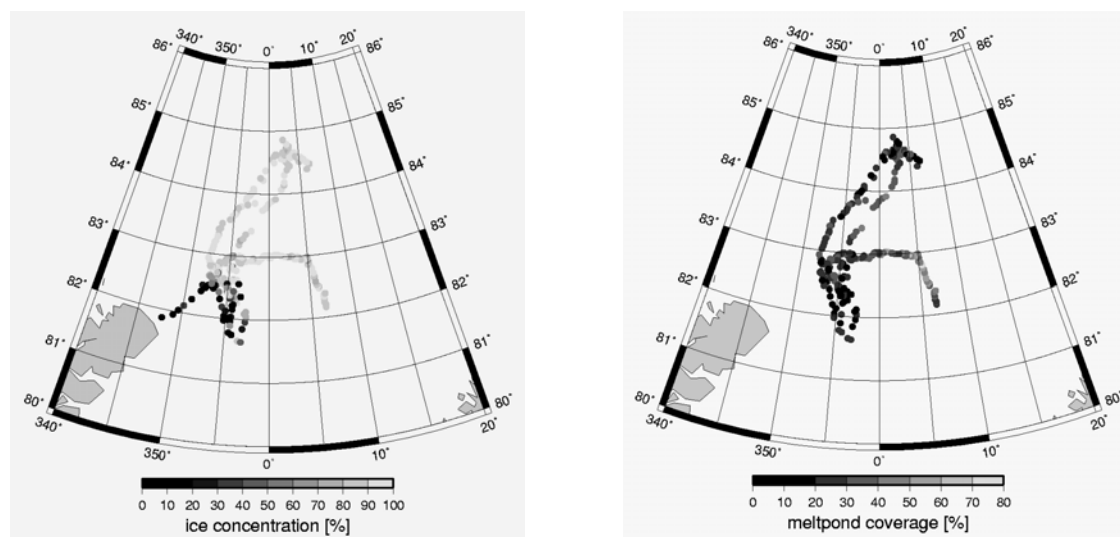


Fig. 4.1: Sea ice conditions during the cruise as observed by the observer team. The left panel indicates ice concentration, the right panel shows melt pond coverage.

## 4.2 Electromagnetic Induction

Andreas Pfaffling  
Alfred Wegener Institute

Extensive ice thickness profiling was carried out by means of electromagnetic induction (EMI) using different platforms. The technique allows for continuous high accuracy measurements, performed either directly from the ice surface or from above, e.g. by means of the ship or helicopters.

With EMI, a low-frequency EM field is generated by a transmitter coil. This primary field induces electrical eddy currents in the water, which in turn result in a secondary EM field. The ratio between those fields is measured by a receiver coil. As the strength of any EM field decreases with distance to the source, the secondary field decreases with increasing distance between the EM instrument and the water underneath the ice. Thus, the thicker the ice is, the weaker the secondary field becomes.

During ARK-XX/2 we deployed a hierarchy of different means of EM soundings: Ground-based measurements have proven to provide very accurate data (Section 4.2.1). Their calibration is evaluated by means of accompanying drill-hole measurements. However, ground-based measurements are only possible on single, thick floes, and the profile lengths are very limited. Another possibility is to perform continuous ship borne measurements along the ship's track (4.2.3). These would provide the most extensive data en-route whereas, ice thicknesses along a ship's track is never representative for a particular ice regime, as the ship usually follows leads with open water or new ice. The only instrument which delivers the true ice thickness distribution is AWI's helicopter towed EMI device known as HEM-BIRD. Section 4.2.2 provides a closer description of the airborne ice thickness sensor. The following summarizes the usage of the several instruments during ARK-XX/2, whereas more detailed first results are presented in section 4.6.

### 4.2.1 Ground based EM sea ice thickness measurements

Carola von Saldern, Andreas Pfaffling  
Alfred Wegener Institute

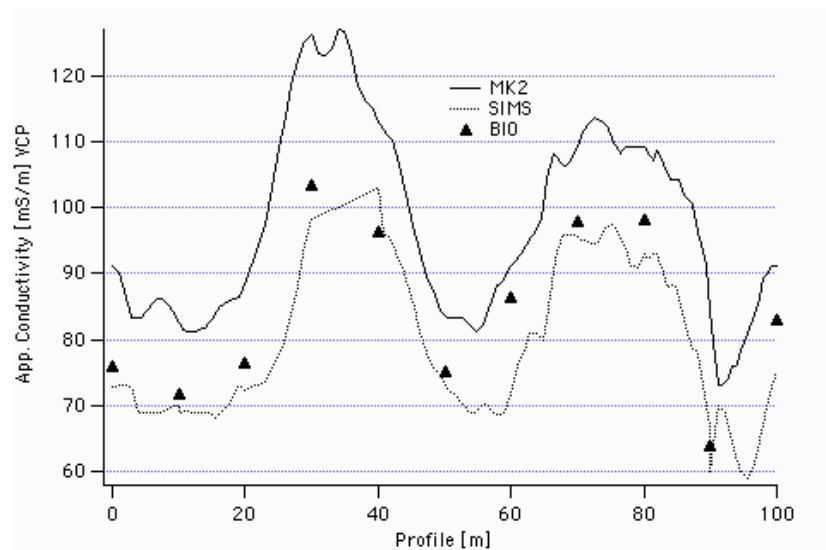
Ground-based measurements have been performed on single ice floes using a Geonics EM31 instrument. Floes have been entered either from the ship or by helicopter.

The EM31 operates at a frequency of 9.8 kHz with a coil spacing of 3.66 m. The EM31 provides high accuracy data and the processing procedures are well established. The EM31 was partly placed into a Prijon kayak serving as amphibic sledge, to enable measurements over melt ponds and to shelter the instrument. When the floe was entered via helicopter, the EM31 was mounted on a small pulka sledge, as the kayak could not easily be transported with the helicopter.

EM measurements were performed continuously with tie-points every 5 to 50 meter depending on the length of the profile. For some floes the GPS position was logged together with the EM31 data using the new Allegro data logger for the EM31. The profiles were mainly laid along straight lines besides some GPS based random walking profiles, including level and deformed ice. The EM profiles were validated by means of drill-hole measurements.

As a result of the drowning of the SIMS (see 4.2.3) a comparison of the three EM31's on board was carried out at the first ice station, which showed a disagreement between the readings due to bad calibration of the devices, which is illustrated in figure 4.2.1.

*Fig. 4.2.1: Measured apparent conductivities along the same profile acquired with three EM31 instruments*



This effect was also observed during a sea ice cruise to the Antarctic. To maintain consistency of the data, all following measurements were carried out with the same EM31 device, the MK2.

To transform the measured apparent conductivity into values for the ice thickness, the well-known negative-exponential relation was used.

With the new Allegro data logger it was possible to log the GPS positions of selected measurements. An example of a random walk over an ice floe is shown in figure 4.2.2 The black dot indicates the starting point. The ice drift is clearly visible, since start and end point of the track were in fact at the same position on the floe but appear as separate points on the track plot.

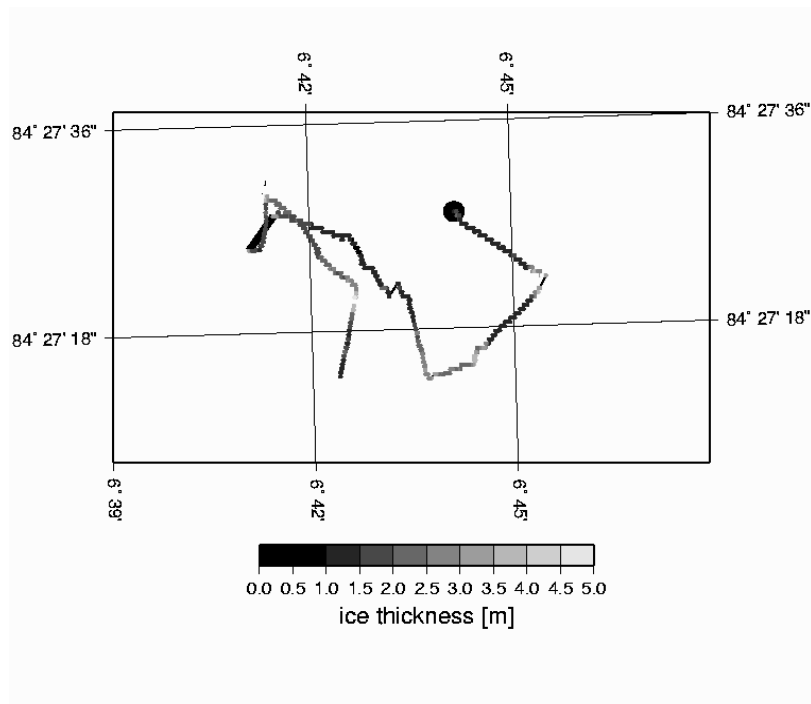


Fig. 4.2.2: GPS positions for the measurement track from 7 August 2004

#### 4.2.2 Helicopter borne EM

Andreas Pfaffling, David Flinspach  
Alfred Wegener Institute, Bremerhaven

AWI's helicopter borne EM ice thickness sensor (HEM-BIRD) was operated with the RV *Polarstern* BO105 helicopters during 13 flights. The bird is 3.5 m long, has a diameter of 35 cm, and weighs around 100 kg. It is towed 20 m below the helicopter, at an operation altitude of 10 to 15 m above the ice surface with a speed of 60 knots. Take-off and landing were conducted from the helicopter deck. The bird was successfully landed directly into a special cart which could also be used for transport and storage on board. The bird operates at 3.68 and 112 kHz, with coil spacings of 2.77 and 2.05 m, respectively. A DGPS antenna and a laser altimeter are also included. The DGPS base station was set up on the ice, when flights and ice stations were coincident. The base station was also established on deck as an attempt to provide a moving DGPS station, still capable of improving height accuracy. Flights were performed along triangles with 40 - 60 km side length as well as long transects up to 100 km in length across the marginal ice zone. At each turning point, the helicopter ascended to an altitude of 300 feet to allow for internal calibration and nulling of the bird. One flight was complemented by an intense ground validation along five parallel 150 m long profiles 10 m apart during the 12 h ice station on August 13 for validation and footprint analysis. A nadir video camera was operated during all bird flights to document ice conditions below the system. On some flights the video footage was taken from the second helicopter at high altitude to get a wider swath of the profile. Geo-referenced digital still photographs were also taken to

document general ice conditions. Subsequently they were included into an html linked map projection allowing for easy geocoded image browsing.

For a better understanding of the HEM systems base level drift the bird was landed on a Svalbard glacier on 22 July and tested there to study its behaviour on a practically non-conducting halfspace.

### 4.2.3 Sea Ice Monitoring System

Jan Lieser  
Alfred Wegener Institute, Bremerhaven

The Sea Ice Monitoring System (SIMS) is another realization of the electromagnetic induction technique in combination with a laser altimeter for monitoring the sea ice thickness especially along the ship's track. The RV *Polarstern* SIMS is suspended from the ship's crane in front of the bow at a height of approximately 4 to 5 meters above the surface. It is mounted in a wooden box together with some electronics for synchronization of the components. If the system is not in use it is stored in a metal box on the port side inside the bow area.

For this cruise the SIMS was installed during the first day in ice on 23 July. During the first hour after installation the wooden attachment, which keeps the SIMS at the bows hook, broke apart and the system fell off into the sea and was completely flooded.



*Fig. 4.2.3: Recovery of the Sea Ice Monitoring System*

This was observed by the ship's officer on the bridge. The SIMS was recovered from the sea and all components were flushed extensively with fresh water and MilliQ-water for cleaning. This helped to prevent serious damage of the EM-31 system,

which functioned accurately during the following sea ice stations. The laser altimeter could not be tested during the cruise and, therefore, the SIMS was not installed back on the ship's bow for the rest of the expedition. Back home the laser altimeter proved to work properly, too.

### 4.3 Cryoelectrics (DC Multi-electrode Resistivity)

David Flinspach<sup>1)</sup>, John Bishop<sup>2)</sup>

<sup>1)</sup>Alfred Wegener Institute, Bremerhaven

<sup>2)</sup>University of Tasmania, Sandy Bay

A 'Tomoplex' multi-electrode (50) dc resistivity system was kindly lent by Leipzig University to investigate the electrical structure of sea-ice. The equipment consisted of two transmitter- receiver systems (each system consisting of one blue metal box) and 2 reels of cables each with 25 electrode 'take-outs' spaced 5 m apart. The software used to run the system ('Tomo128verS43.exe') was input into two AWI 'Husky' field computers and AWI had 50 stainless steel electrodes made up.

A number of problems were initially encountered and these are briefly described below so that the next users of this promising method may benefit from our experiences. No useful results were obtained during the first test on the ice with the only diagnostic message 'constant current error' showing on the screen. A number of bench tests were then made which established that one of the systems was apparently not working or not working as well (this was then put aside and not further used) and that one of the Huskies was not properly communicating with the Tomoplex. Later it was also found that the 1-25 electrode socket on the working Tomoplex had some corroded pins and was not functioning properly (sockets 51-75 and 76-100 were used for subsequent surveys). The attached appendix describes which instruments worked and which didn't. Concerning the comment on the current, the option changes the current being applied but not the 'fixed' current in the control programme.

The bench test used the circuit shown in figure 4.3.1 below and various positions were tried for the reference electrode, both internal and external. On the ice, we eventually settled on an external electrode beside the system.

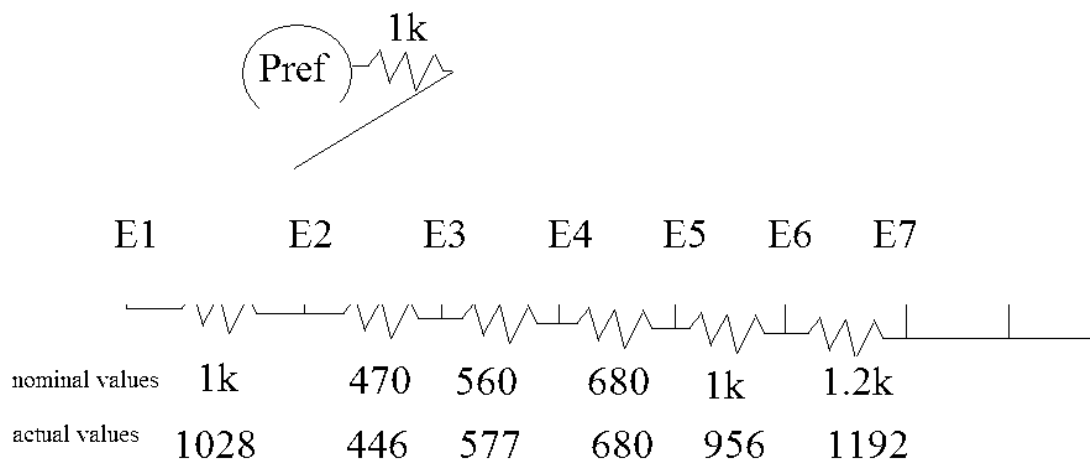


Fig. 4.3.1. Bench circuit used to test the Tomoplex. The first seven takeouts on the cable were attached E1 to E7 as shown with the Pref attached to E1 through a 1k resistor. A series of Wenner array readings were then made across the resistors and the difference of the two potential readings, P1 and P2, gave the correct resistances.

As well as bench tests, a test 'tank' (a large plastic box) was filled with sea water and a plywood float with a line of 25 nails at 2 cm intervals was set up. A Wenner set up of some 92 readings was then made. The readings along the edges of the array were not valid but the central values were close to 0.16 ohm.m, i.e. about half the actual value. The discrepancy may be in the geometry – i.e. the tank was closer to a 'quarter-space' than a 'half-space'.

Further tests were made on the ice with increasing success and acceptable results were obtained on the two 12-hour ice stations (4.6.1). The main problem with this equipment appears to be its power – voltage levels: it does not have enough of either to overcome the high contact impedances of hard 'dry' snow or ice. It also does not seem to have the sensitivity needed to record the low voltages recorded at large spacings when the conductive sea water is the major contributor to the section. On THE floe (Ice Station I), salt and salty water was added to lower the contact impedance. This worked in the short term but the salt melted the ice around the electrodes, increasing the impedance in the longer term. On the OTHER floe (Ice Station II), meltpond (i.e. very fresh) water was frequently added to the electrodes and better results were obtained, but the deepest readings are mostly very noisy or just wrong (e.g., negative).

At THE floe, line 2 of the grid was occupied and a 50 electrode grid set up with a 0.25 m spacing occupying the interval between 68 and 80 m read with various Wenner control files. The array was then expanded to a 1 m spacing and reread with the same control files. The resulting data (resistance) files were processed to apparent resistivities and input into a demonstration version of Loke's 2D resistivity inversion programme. This allows 3 iterations and produces an acceptable first-pass result. Further processing using the full programme is required to complete the

process and to implement the topography. The preliminary results have had the bad data points removed and are shown in chapter 4.6.1.

At the OTHER floe, line 3 of the grid was occupied and a 50 electrode grid with a 2 m spacing between 30 m and 130 m and as noted above, rather better results were obtained. Again, the results and the inversion of the edited data are shown in chapter 4.6.1.

#### 4.4 Ground Penetrating Radar

Thomas Busche<sup>1)</sup>, Andreas Pfaffling<sup>1)</sup>,  
 Gunnar Spreen<sup>2)</sup> <sup>1)</sup>Alfred Wegener Institute, Bremerhaven  
<sup>2)</sup> University of Bremen, Bremen

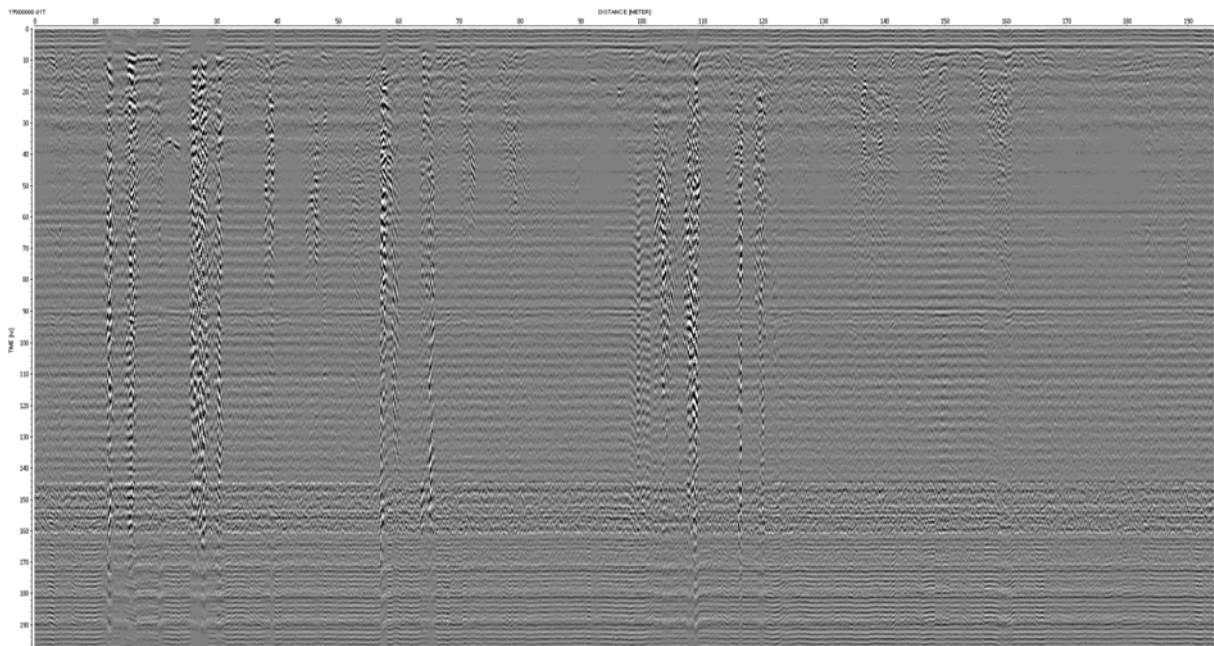


*Fig. 4.4.1: Radar profile with applied Filters from 3 August 2004. No clear ice water boundary is visible. The measurement was derived with a 500 MHz antenna. The x-axis shows the distance in meters, the y-axis the travel time in nanoseconds.*

During ARK-XX/2 a RAMAC GPR instrument (MALA GeoScience) was taken to the sea ice to contribute information on the sea ice properties particularly ice and snow thickness. In contrast to EM induction methods (see Section 4.2), GPR systems use a high frequency (> 50 MHz) electromagnetic pulse comparable with a seismic explosion or air gun, which travels inside the media. If there are changes of the dielectric properties of the media on distinct horizons the EM pulse is partly reflected and returns to the receiver antenna of the system. An example for such a horizon would be the ice underside where the media changes from ice to water or the snow-ice interface. During a GPR survey such a wave travel experiment (shot) is recorded

every 10 cm along the profile. Once the antenna has transmitted the EM impulse the receiver starts to acquire the returning signals for some nanoseconds. For interpretation the signal traces of every shot are plotted next to each other in a radargram (Fig. 4.4.1). The grayscale displays the amplitude of the received waveform. The propagation velocity depends on the dielectric permittivity of the media. The reflectivity is related to changes in the dielectric properties, determining the velocity. Apart from the wave travel velocity, the damping of the wave depends on the conductivity of the media and the antenna frequency (50 MHz up to 1.5 GHz). Damping increases with frequency and conductivity. Figure 4.4.1 shows the radargram for a GPR measurement made on 3 August 2004. A 500 MHz antenna was used. This was the lowest antenna frequency available on the cruise. No dominant reflector is visible in figure 4.4.1 and this was the situation for all measurements made during ARK-XX/2. The most likely explanation is, that the EM pulse is damped out before it reaches the ice water interface. Under the summer conditions of ARK-XX/2 (16 July to 29 August 2004) the ice was warm and therefore water saturated. The first few centimetres of the snow-ice layer contain a lot of liquid water. The penetration depth of electromagnetic waves with 500 MHz frequency in freshwater is 19 cm and for the other available antenna with 800 MHz just 7 cm (calculated with equation from A. Stogryn, IEEE Trans. on MW Theory and Techniques, August 1971). For slight saline water like the melted ice water the penetration depth is even lower. It is very likely that an equivalent water content is reached in the ice before the EM pulse got back from its travel through the ice to the water interface and back to the surface. Due to this experience it can be stated that the GPR method at frequencies above 500 MHz is not usable under Arctic summer conditions. An approach with an lower frequency antenna may be more successful under summer conditions but will reduce the lateral resolution of the method.

## 4.5 Remote Sensing Products

### 4.5.1 Video Survey

Thomas Busche<sup>1)</sup>, Gunnar Spreen<sup>2)</sup>

<sup>1)</sup>Alfred Wegener Institute, Bremerhaven

<sup>2)</sup>University of Bremen, Bremen

During the ARK-XX/2 campaign 18 video flights have been carried out. Twelve together with the helicopter borne EM measurement (HEM-Bird, see chapter 4.2.2) and 6 flights only with the video camera mounted to the helicopter. Date, time and height of the flights are given in table 4.5.1.1, an overview over the locations of the flights is shown in figure 4.5.1.1.

#### Video System Description

The video measuring system consists of a Mini-DV consumer camera (Sony DCR-VX 2000) which is mounted in a special designed metal box (see Fig. 4.5.1.2). The box is insulated and has a heating inside to keep the temperature in the box on a constant level above zero degree Celsius. The power supply cable for the heating and a data cable for the video stream leave the box through a cut-out and enter the helicopter through the back door (see Fig. 4.5.1.2). The camera itself is operated by

accumulator. Inside the helicopter the cable for the heating is connected to the board power supply and the video cable with a portable video recorder with included display (Sony GV-D 1000, see Fig. 4.5.1.3). The display was used to monitor the camera functionality during the flight. The video data was stored on Mini-DV tapes with this video recorder. Additionally, a cable remote control can be connected to the video camera to control the zoom level, but this was not used during this survey.

To get the correct position information for the video data two hand-held GPS (Global Positioning System) receivers were used (Garmin etrex Summit and Magellan Meridian Platinum). One of them was always operated during the flight. The GPS data from the EM-Bird measurements could be used for geolocation, too. The only connection between the video and GPS data is the time information. The recorded video stream contains time, date and information about some major camera parameters. The time information can be connected with the GPS time data to get the right position for every recorded frame. It is crucial to adapt the time of the video recorder clock to the GPS time before the flight to get accurate geolocation information.

The autofocus of the camera was turned off during all flights. The parameters for shutter, exposure and white balance were changed between the flights (see Table 4.5.1.2). To automatically evaluate the video data it is required that the brightness and contrast of the data stays almost constant during the flight. The first flight (28 July 2004) was done with automatic shutter and exposure control. This caused the video to get overexposed for some seconds when the flight track crossed a water-ice edge. The brightness and contrast is highly variable in this first video, therefore the parameters for shutter, exposure and white balance were kept constant for the following flights. This method has the disadvantage that changes in the illumination conditions like a weather change from sunny to cloudy cause variations in the brightness and contrast, but these changes are much less pronounced than with the automatic settings. A second problem occurred during later flights: The mounting of the camera inside the metal box could shift the focal length ring in front of the lens. This caused a false focal length setting for flight 7 and maybe the end of flight 3. After flight 7 this problem was solved. All other flights show good results and should be usable for analyses.

Two exemplary video images for different helicopter flight heights are shown in figure 4.5.1.4.

### **AMSR-E Sea Ice Concentration Validation**

At the Institute for Environmental Physics at the University of Bremen a sea ice concentration algorithm for spaceborne passive microwave measurements near 90 GHz was developed. This algorithm (ARTIST sea ice (ASI) algorithm) was also adapted to measurements of the Advanced Microwave Scanning Radiometer for EOS (AMSR-E) on board the AQUA satellite. See chapter 4.5.3 for more information on the sea ice concentration product.

To validate the obtained sea ice concentrations from the ASI algorithm it is necessary to have some ground truth measurements for comparison with the satellite data. The

ASI algorithm can then be adapted to *in-situ* data to represent the real sea ice concentrations best.

The helicopter video data are suitable to get these ground truth data. The footprint of the AMSR-E 89 GHz measurements is approximately 5 km. To get a significant comparison between *in-situ* and satellite data the *in-situ* data have to cover several measurements of the satellite measurements. The helicopter flight track lengths differ between the flights. A typical track length is a triangle with 40 km legs. Therefore every flight crosses more than 20 measurements of the satellite sensor. The covered width of the video data is dependent on the flight height. 6 video survey flights at higher altitudes were performed. These video data have a covered ground width of approximately 1 km. The other flights done together with the HEM-Bird have only a width of tens of meters (30 to 50 m). The high video flights with 1 km width give good ground truth information of the ice cover even at the low resolution of the satellite data. The video data of one flight covers the area of more than 4 satellite measurements. This should be a good representation of the ice cover in the survey region. The lower video flights are still expected to represent the ice concentration quite well as they cross a sufficient number of satellite data measurements and the anisotropy of the ice concentration in one footprint of the AMSR-E measurement is expected to be small.

To get ice concentrations from the video data several processing steps are necessary:

1. Read in the video data from tape to the hard disk of a computer.
2. Convert the video stream to single image files. The video data consists of 25 images per second. Due to the great overlap of consecutive images not every image of the video stream has to be extracted. How many images per second have to be extracted depends on the flight height. (For the high video flights just one image per second was extracted.)
3. Find the right GPS position for every extracted image. This is done by calculating the recording time of the image from the recording time of the first image of the video data which is saved on the tapes. The recording time is then joined with the corresponding GPS data for that time.
4. Classify the image in three classes: "water", "ice" and "melt ponds". For the ice concentration only the classes "water" and "ice" would be necessary. But to obtain information on the influence of the melt pond coverage on the satellite derived ice concentration a third class for melt ponds is needed.

The ice concentrations found thereby can then be compared to the AMSR-E ice concentrations calculated with the ASI algorithm. If the ASI results do not match the *in-situ* ice concentrations the algorithm can be adapted to the results.

**Tab. 4.5.1.1:** Date and approximate height information of the 18 performed video survey flights during ARK-XX/2. Information about the video camera parameters used are given in table 4.5.1.2.

Flight number	Date	Video start	Video stop	Height [ft]	EM-Bird	Comment
1	28. Jul 04	10:05:48	11:21:22	~100	x	Overexposed after water ice crossings.
2	31. Jul 04	10:01:18	10:52:03	250 - 3000		Tandem flight with 2nd helicopter with HEM-Bird.
3	31. Jul 04	12:18:28	13:23:28	250 - 4000		Video is getting blurred in the second half of the flight.
4	2. Aug 04	15:07:26	16:21:38	~100	x	
5	2. Aug 04	21:08:26	22:20:13	300 - 3500		
6a	3. Aug 04	08:41:30	08:54:23	~100	x	Short flight due to HEM-Bird failure, retry in the afternoon.
6b	3. Aug 04	16:43:04	17:23:06	~100	x	Last part of video is defect.
7	4. Aug 04	11:05:00		~100	x	Unusable, vibrations caused wrong focal length alignment.
8	4. Aug 04	16:37:29	18:06:45	~100	x	
9	6. Aug 04	13:45:29	15:02:09	~100	x	
10	7. Aug 04			~100	x	
11	8. Aug 04	09:13:03	10:12:02	3500		
12	8. Aug 04			~100	x	
13	9. Aug 04			~100	x	
14	9. Aug 04	11:14:38	12:15:40	3500		
15	11. Aug 04	10:13:29	11:24:39	~100	x	
16	12. Aug 04	17:33:13	18:44:41	3500		Tandem flight with 2nd helicopter with HEM-Bird.
17a	13. Aug 04	13:47:55	13:57:13	~100	x	2. ice station 'the OTHER floe', first try
17b	13. Aug 04	14:04:15	14:18:58	~100	x	2. ice station 'the OTHER floe', second try
18	14. Aug 04	12:14:29	13:33:22	~100	x	

**Tab. 4.5.1.2:** Camera parameters for all flights. The manual white balance setting was fixed to the correct white balance value for an ice floe measured from on board the ship.

Flight Number	Autofocus	Prog. Scan	Steady Shot	Shutter	Exposure	white balance
1	off + infinity	on	on	automatic	automatic	automatic
2 - 7	off + infinity	on	on	1/1000	F 4.8	fixed
8 - 18	off + infinity	on	on	1/1250	F 4.8	fixed

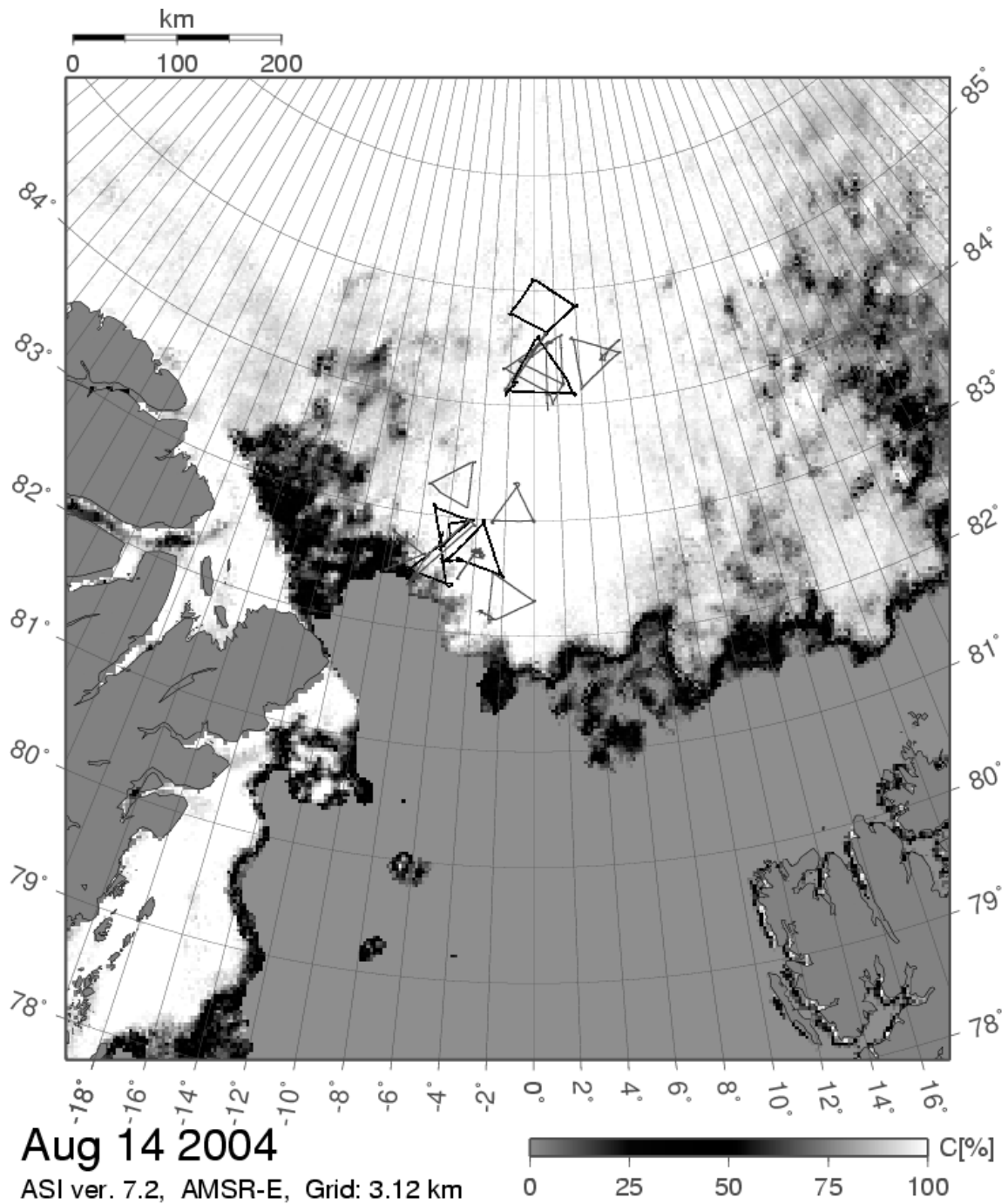


Fig. 4.5.1.1: Flight tracks of the 18 performed video flights between 2004/07/28 and 2004/08/14. Additional to the EM-Bird flights (see chapter 4.2.2) six extra video flights had been carried out (including two tandem flights with both helicopters). The parameters of the flights are given in table 4.5.1.1. In the background the sea ice concentration on 9 August 2004 is shown.



*Fig. 4.5.1.2: Video camera in a metal box mounted below the helicopter. The cables to the interior of the helicopter used for the temperature stabilization of the box and for the video stream to the video recorder are visible, too.*



*Fig. 4.5.1.3: Video recorder with display in the interior of the helicopter. From here the video recording could be started and stopped and with the display the correct functionality of the camera was monitored.*

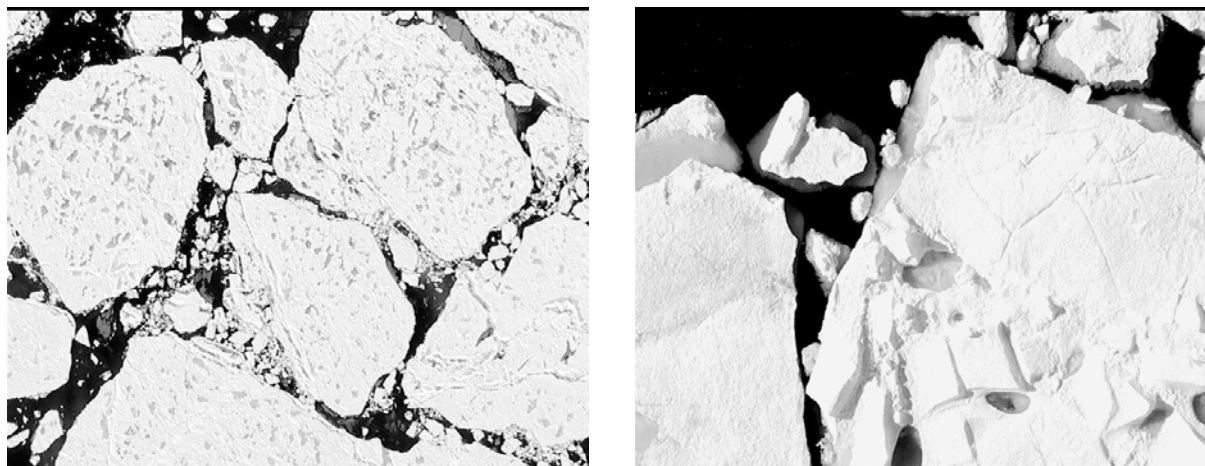


*Fig. 4.5.1.4: Example of an image recorded from approximately 1 km height (left), and 75 m height (right). The images were extracted from the video data. Water, ice and melt ponds are distinguishable in both images. In the right image some ice below the water surface is visible. It has a similar colour and therefore representation in feature space as some of the melt ponds.*

#### **4.5.2 Near Real Time Synthetic Aperture Radar Images**

Thomas Busche  
Alfred Wegener Institute, Bremerhaven

The remote sensing activities during ARK-XX/2 are a contribution to the SITHOS Project (Sea Ice Thickness Observing System) whose overall objective is to develop a European monitoring system for sea ice thickness and related parameters. They are a continuation of the successful measuring campaign CryoVex2003 that was conducted in the framework of the project during ARK-XIX/1 in March and April 2003 in the European Arctic, in the Barents Sea and Fram Strait under winter sea ice conditions. CryoVex2003 was the first pre-launch validation experiment for the CryoSat mission of the European Space Agency (ESA). During ARK-XX/2 this validation initiative and efforts for the Cryosat Mission was continued in summer sea ice conditions. As during CryoVex2003 imaging radar data from the Advanced Synthetic Aperture Radar (ASAR) from the European satellite ENVISAT, received on board RV *Polarstern* in near real-time after image acquisition, are of special interest for mission planning and also ship navigation. The satellite images are co-financed by the ICEMON initiative, a consortium of institutions and companies to bundle the efforts to implement a coherent European operational oceanography system for the high latitudes, consisting of sea ice, meteorological and oceanographic services. For the AWI sea ice physics group HEM-Bird helicopter flights coincident to image data taken within the satellite frames are essential for algorithm development and the comparison of thickness and laser profile data to the radar signatures.

### **Image Data Processing and Delivery**

Due to mission planning and the time schedule for programming the satellite data taken at ESA's ground control segment the SAR imagery has been ordered from the Norwegian processing facility KSAT three weeks in advance of the start of ARK-XX/2. The frame coordinates have been derived from the planned ship route, taking into account the main areas for geological sampling at the Gakkel Ridge and in the northern part of the Lena Trough around the Aurora site. For both areas, which were planned to be the main areas for detailed geophysical fieldwork on ice floes and HEM-Bird helicopter flights small time series of high resolution ASAR images in the Image Mode Precision (IMP) with start from 26 July to 2 August and 3 August to 7 August, respectively, have been ordered. The nominal resolution of the Image Mode data is around 25 m with an imaged area that covers 100 km x 100 km. This spatial resolution gives the opportunity to detect features on the ice floes, like ridges and melt ponds and also small leads in the surrounding ice field. The utilization of the image data with lower spatial resolution (~75 m) but higher coverage (400 km x 400 km) in the Wide Swath Mode (WSM) was mainly the reconnaissance of general ice conditions and also the detection of the ice edge on the transit to the main study areas.

The near real time images being processed at KSAT within two to three hours after acquisition were placed on a ftp server. At AWI the raw images have been geocoded to a conformal map projection and prepared for transmission through the communication bottleneck of the IRIDIUM system in order to reduce transmission time and costs. Therefore the image data has been scaled from a original size of around 50 to 80 Megabytes in a 16-bit resolution to 15 Mb in 8-bit one and further compressed to a file size of 70 kilobytes using the JPEG2000 standard, a wavelet image compression technique. Unfortunately, this high compression ratios are accompanied by a remarkable loss of detail and radiometric resolution cannot be avoided. Near real time images were sent after processing to RV *Polarstern* via email attachment. Table 4.5.2.1 shows a list of ordered near real time data, and with the exception of the scene from 8 August all images were acquired and also successfully sent to the ship. Time between image acquisition and reception on board RV *Polarstern* was normally in the order of 6 to 20 hours, so the most of them could be used on the following day. On board the vessel digital maps were created with an overlay of the ship track and position and also for orientation with points of special interest e.g. the planned geological sampling sites. The maps were deposited after creation on the ship's file server to make them available to the scientists and the ship's command.

Tab. 4.5.2.1: ENVISAT ASAR Image Products ordered by AWI at KSAT, Norway

ASAR Product Name	Polarization	Orbit	Date	Acquisition Time (UTC)	Scene Centre Latitude (deg, min)	Scene Centre Longitude (deg, min)	HEM-Bird-Flight
ASA_WSM_1P	HH	12506	2004/07/21	18:18:19	82,44	13,24	NO
ASA_WSM_1P	HH	12531	2004/07/23	12:16:18	82,32	6,21	NO
ASA_IMP_1P	HH	12575	2004/07/26	14:02:39	82,47	-5,56	NO
ASA_IMP_1P	HH	12589	2004/07/27	13:31:17	82,50	-7,36	NO
ASA_IMP_1P	HH	12604	2004/07/28	14:39:44	82,49	-7,01	NO
ASA_IMP_1P	HH	12618	2004/07/29	14:08:23	82,47	-7,22	NO
ASA_IMP_1P	HH	12635	2004/07/30	18:36:18	82,56	-5,33	NO
ASA_IMP_1P	HH	12649	2004/07/31	18:04:56	82,55	-6,04	NO
ASA_IMP_1P	HH	12660	2004/08/01	12:34:02	83,00	-6,12	NO
ASA_IMP_1P	HH	12678	2004/08/02	18:42:03	82,56	-6,60	YES
ASA_IMP_1P	HH	12690	2004/08/03	14:50:44	84,41	1,15	NO
ASA_IMP_1P	HH	12703	2004/08/04	12:39:17	84,25	2,30	YES (2x)
ASA_IMP_1P	HH	12720	2004/08/05	17:07:42	84,29	5,26	NO
ASA_IMP_1P	HH	12732	2004/08/06	13:16:24	84,33	4,18	YES*
ASA_IMP_1P	HH	12750	2004/08/07	19:24:54	84,17	4,55	NO
ASA_WSM_1P	HH	12760	2004/08/08	12:13:25	82,32	7,04	NO
ASA_WSM_1P	HH	12775	2004/08/09	13:22:24	82,32	-10,11	NO
ASA_WSM_1P	HH	12808	2004/08/11	20:38:08	79,53	-7,30	NO
ASA_WSM_1P	HH	12836	2004/08/13	19:34:54	79,53	8,18	NO
ASA_WSM_1P	HH	12989	2004/08/24	12:11:33	79,39	-5,49	NO

\* Image not acquired

## Results

Altogether three coincident helicopter flights have been successfully performed within the satellite frames during ARK-XX/2. Mostly bad weather conditions, especially low visibility due to fog, prevented more measurement flights. On some days, due to time delay, the frames were out of reach for the helicopters. Figure 4.5.2.1 shows a digital map of a high resolution SAR image from 5 August 2004 produced on board the ship. The image shows an area around the Gakkel Ridge, sampling sites for dredging are labelled and highlighted with red crosses, the track of RV *Polarstern* the following day from 6 August 2004 and the actual ship position are marked with crosses. The maps assisted in the search for leads and ice free sampling locations.

ENVISAT ASAR Image Mode Precision  
 Near Realtime 04/08/05 UTC 17:07:42: Polarstern Position 04/08/06 UTC 09:09

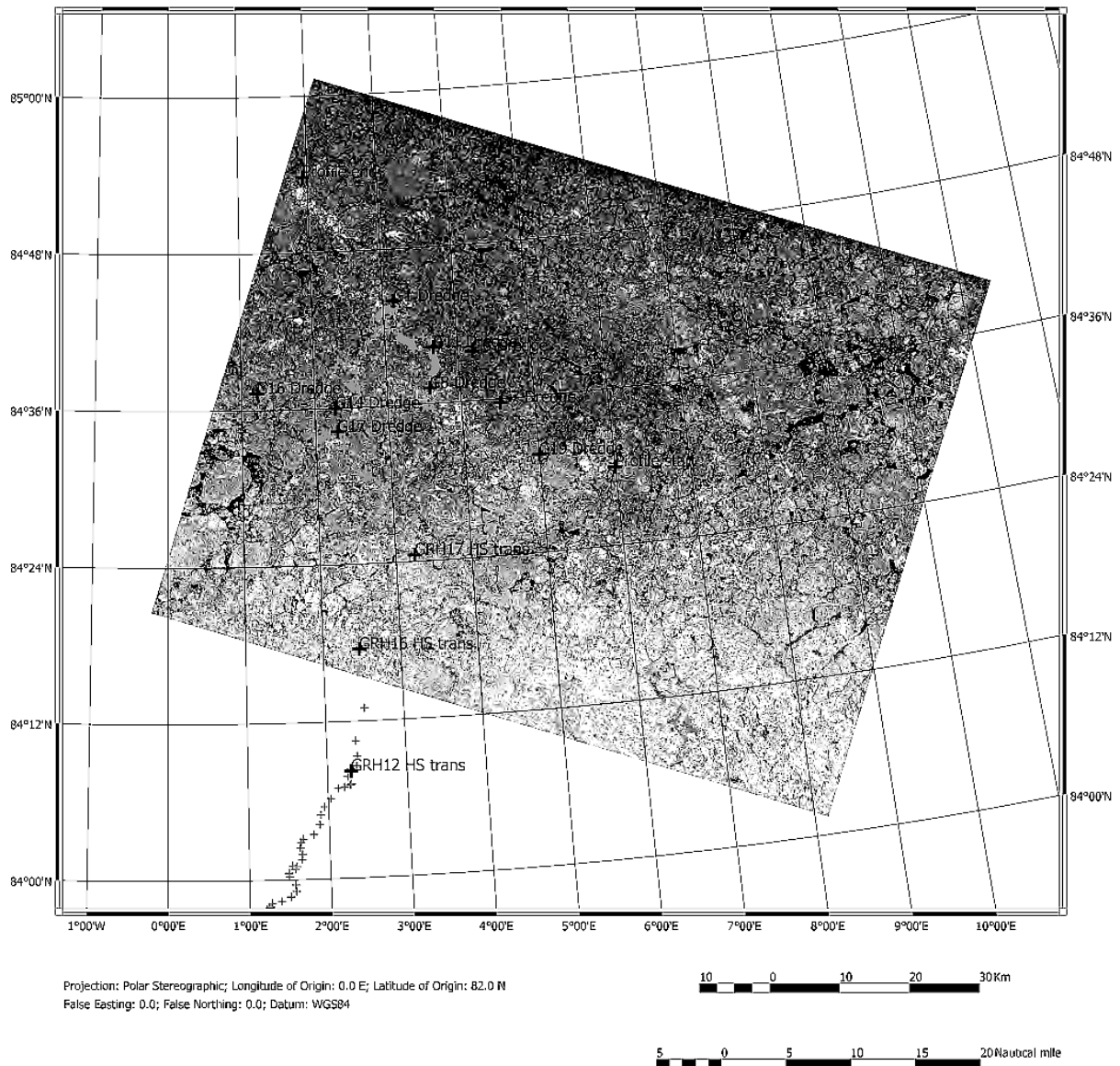
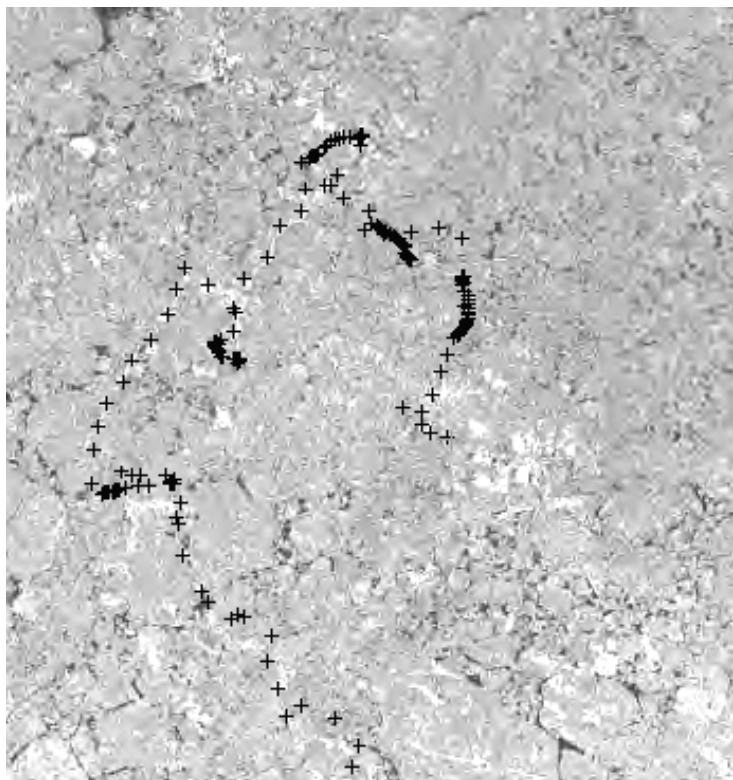


*Fig. 4.5.2.1: Digital map produced on board RV Polarstern showing an ENVISAT ASAR scene from 04/08/05 with geological sampling points, ship track and position*

Although the image compression is very high and the loss of detail is apparent, the ship's course through the ice is visible in some scenes as can be seen in figure 4.5.2.2, a zoom-in into the SAR scene from 5 August 2004. But an identification of single ridges is not possible in this compression state. A detailed analysis of the SAR data on the basis of calibrated images with full radiometric and spatial resolution will be performed in the future, the extraction of ridge statistics is also planned. For cruises in the near future the processing chain and delivery will be fully automated at AWI in order to shorten delivery times.

Fig. 4.5.2.2: Zoom-in into  
ENVISAT ASAR scene  
04/05/08



### 4.5.3 AMSR-E

Gunnar Spreen  
University of Bremen

The AMSR-E data is used to calculate sea ice concentrations, which are used mainly for two purposes during this cruise:

1. Ship navigation,
2. Validation of the ASI sea ice concentration algorithm for AMSR-E measurements.

The Advanced Microwave Scanning Radiometer for EOS (AMSR-E) on board NASA's AQUA satellite is a radiometer measuring the thermal radiation of the Earth at 6 different microwave frequencies (7, 11, 19, 24, 37 and 89 GHz). For each frequency the horizontal and vertical polarisation of the radiation is measured separately.

The advantage of passive microwave measurement in comparison to optical sensors is the independence of daylight and clouds. It measures continuously all the year round and the Arctic regions are completely covered with measurements every day at least once. The main disadvantage is the coarse resolution of the measurements which is 5 km minimum.

On this cruise the 89 GHz channels are used to calculate the sea ice concentration with the ARTIST Sea Ice (ASI) algorithm [Kaleschke et al., 2001; Spreen, 2004]. Moreover this algorithm includes the use of different combinations of the 19, 24 and 37 GHz channels to eliminate the atmospheric influence over open water, which may cause spurious ice concentrations.

The spatial resolution of the radiometer measurement on the earth surface depends on the frequency used, the higher the frequency the higher the spatial resolution. The ASI algorithm has been selected because it provides a resolution more than three times better than traditional sea ice concentration algorithms like the NASA-TEAM or the BOOTSTRAP algorithm (5 km instead of more than 15 km spatial resolution). A disadvantage is the more pronounced atmospheric influence at 89 GHz, which is compensated for within the ASI algorithm. The combination of the ASI sea ice concentration algorithm and AMSR-E data provides the best spatial resolution for sea ice data retrieved from passive microwave sensors available today. For example the widely used NASA-TEAM sea ice concentrations calculated from SSM/I data provide only a spatial resolution of approximately 33 km.

The measured value of a microwave radiometer is the brightness temperature of the corresponding area of the earth surface (sensor footprint). The brightness temperature is defined as the product of the emissivity and the physical temperature of an object. AMSR-E brightness temperature data were transferred to RV *Polarstern* via email every day of the cruise. This is essential for having full control over the results of the ice concentration algorithm as adjustments on the algorithm can be made on board. To keep the data size small it is necessary to preprocess the data before sending it via e-mail. AMSR-E raw antenna count data files are received at the Institute of Environmental Physics of the University Bremen near real time from the National Snow and Ice Data Center (NSIDC), Boulder, USA. Every morning the physical brightness temperatures are calculated and the swath data of the day before are interpolated on a polar stereographic grid, which covers the operational area of ARK-XX/2 (see Fig. 4.5.3.1). The grid spacing is 3.125 km for the two 89 GHz channels and 12.5 km for the other 4 lower frequency channels used. The temperature resolution is slightly reduced to keep the file size small and finally compressed as Portable Network Graphic (PNG). The total data amount of all 6 grids is reduced to approximately 170 kB by these efforts. They are sent to RV *Polarstern* by an e-mail robot every morning at 6 UTC. Of all days of the cruise the data receiving failed 2 times only and on one day it was delayed to the following day. However, it has to be mentioned that the data receiving caused some difficulties for the radio operator via the IRIDIUM satellite connection which had to be used north of approximately 80 degree latitude. The IRIDIUM connection has a nominal data throughput of 2400 bit per second which results in a transfer time of approximately 12 minutes for the data, but unfortunately the data connection was regularly not very stable and therefore the transfer time was drastically increased.

There have been two main applications for the AMSR-E sea ice concentration data during this cruise: First, it was used for ship navigation and scientific planning purposes. The daily calculated ice concentration maps like figure 4.5.3.1 and figure 4.5.3.2 were distributed via the board network and belonged to the data pool of the 'Bordwetterwarte' (meteorological station). Thereby the master or the officer in charge

on the bridge had access to the sea ice maps and can use them for their navigational planning. It is important to know when the ship will reach the ice edge and if the travelling route is free of choice. RV *Polarstern* can navigate through areas with low ice concentrations by use of these maps. This can drastically reduce the overall travel time and fuel consumption. Ice ramming has to be done by RV *Polarstern* more often in regions with high ice concentration than in regions with low ice concentration. This persistent ramming whereby the ship has to sail forward and back again with all machines running causes an immense fuel consumption.

The quality and usefulness of the maps were discussed with the master for further improvement of the representation of the data.

Additionally the maps were used for scientific planning. The oceanographers needed to know if their moorings were below the ice cover and where the CTD work had to be performed in the ice. Together with the ASAR data (Section 4.5.2) the AMSR-E sea ice maps were used by the petrologists for their dredge station planning. And finally the sea ice physicists used the maps for planning the helicopter flights with the HEM-Bird and the video camera.

The second application was the validation of the ASI algorithm with ground truth video data. See section 4.5.1 for a detailed description of the performed validation study. There are two major input parameters for the ASI algorithm: the 100 % ice coverage tie point (Pice) and the open water tie point (POW). The values of these two tie points determine the curve shape of the third order polynomial, which represents the ice concentration between 0 % and 100 %. To prevent over- or underestimation of the real ice concentration some ground truth data are needed to find the best tie points. Additionally, the influence of the atmosphere and the melt pond coverage of the ice on the ASI algorithm will be evaluated and thereby the sensibility of the algorithm can be estimated. As a first step the tie points were adapted manually on board the ship to best represent the observable ice situation seen from the ship and the helicopter flights. The previously used tie points POW=47 K and Pice=11.7 K (Version 5.2) were changed to POW=50 K and Pice=9 K (Version 7.2). With the aid of the video data the best tie points for the cruise duration shall be found. These tie points then should be representative for Arctic summer conditions and the error of the algorithm, which is expected to be highest during summer melting condition can be estimated by sensitivity studies.

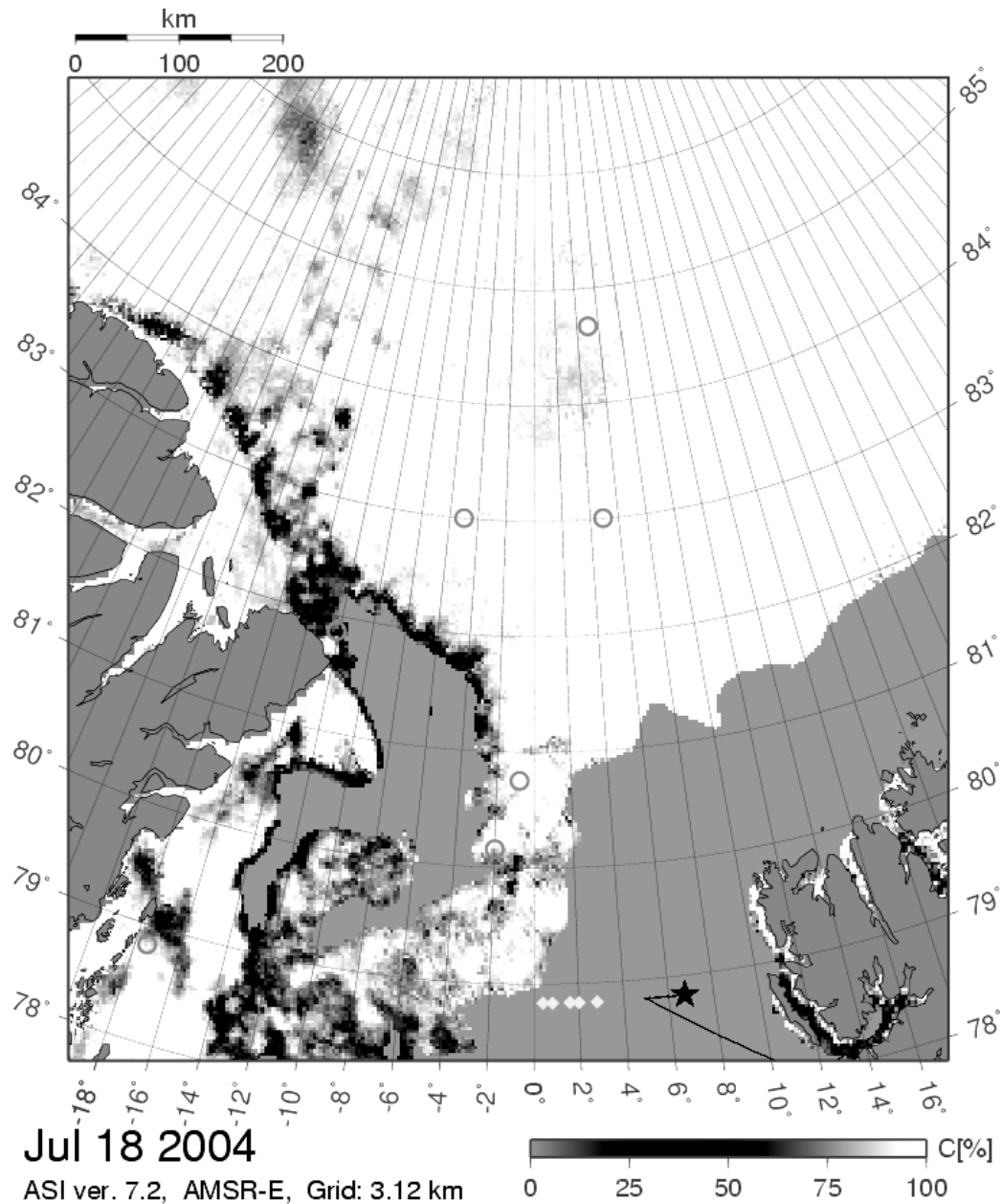


*Fig. 4.5.3.1: AMSR-E sea ice concentration map showing the ice situation at the beginning of cruise ARK-XX/2. For this cruise an adapted version of the ASI algorithm was used for the calculation. Some important points like the moorings (rhombuses), scientific stations (circles) and the position and track of RV Polarstern (star) are marked.*

Already calculated and projected sea ice concentration maps like for example figure 4.5.3.1 and figure 4.5.3.2 will be made available for future cruises of RV *Polarstern*. The data will be sent daily in compressed form to RV *Polarstern* as image file and then benefit can be taken from the validations made on the cruise.

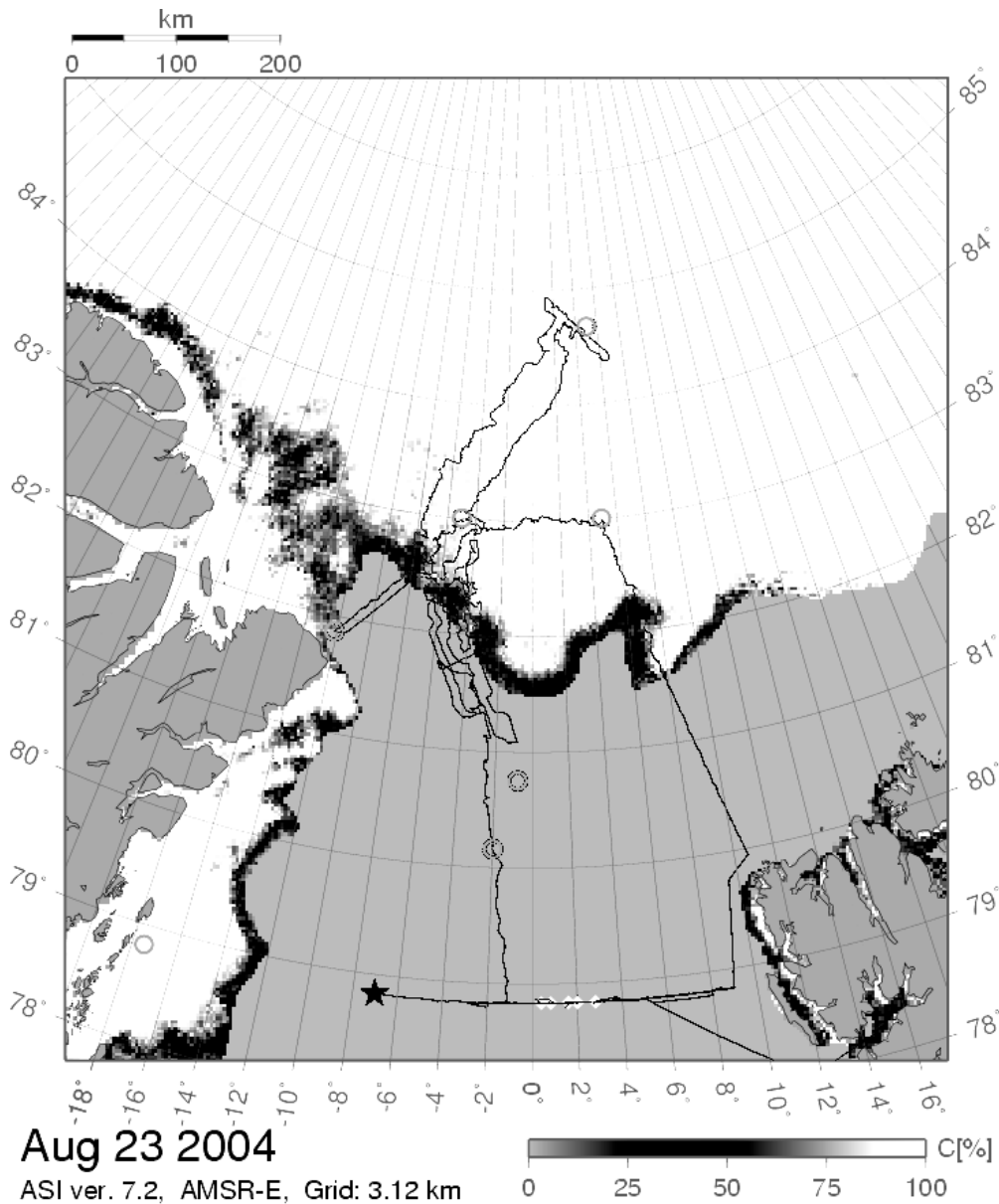


*Fig. 4.5.3.2: Sea ice concentration map showing the ice situation at the end of cruise ARK-XX/2. The large tongue of ice east of Greenland visible in figure 4.5.3.1 has completely melted during the cruise.*

### Literature

- Kaleschke, L. and C. Lüpkes and T. Vihma and J. Haarpaintner and A. Bochert and J. Hartmann and G. Heygster: SSM/I Sea Ice Remote Sensing for Mesoscale Ocean-Atmosphere Interaction Analysis. *Can J. Rem. Sens.*, 27(5): 526—537, 2001.
- Spreen, G.: Meereisfernerkundung mit dem satellitengestützten Mikrowellenradiometer AMSR(-E) - Bestimmung der Eiskonzentration und Eiskante unter Verwendung der 89 GHz-Kanäle. Diplomarbeit, Fachbereich Physik der Universität Hamburg, angefertigt am Institut für Umweltphysik, Universität Bremen, 2004.

## 4.6 Results

John Bishop<sup>1)</sup>, Thomas Busche<sup>2)</sup>, David Flinspach<sup>2)</sup>, Jan Lieser<sup>2)</sup>, Torge Martin<sup>2)</sup>, Andreas Pfaffling<sup>2)</sup>, Carola von Saldern<sup>2)</sup>, Gunnar Spreen<sup>3)</sup>

1) University of Tasmania, Sandy Bay  
 2) Alfred Wegener Institute, Bremerhaven  
 3) University of Bremen, Bremen

### 4.6.1 Sea ice stations

During this cruise several sea ice floes have been investigated. For four of these stations the ship was tied alongside the floe and on further five stations scientists and equipment have been brought by helicopter. The locations of these floe stations are shown in figure 4.6.1.1.

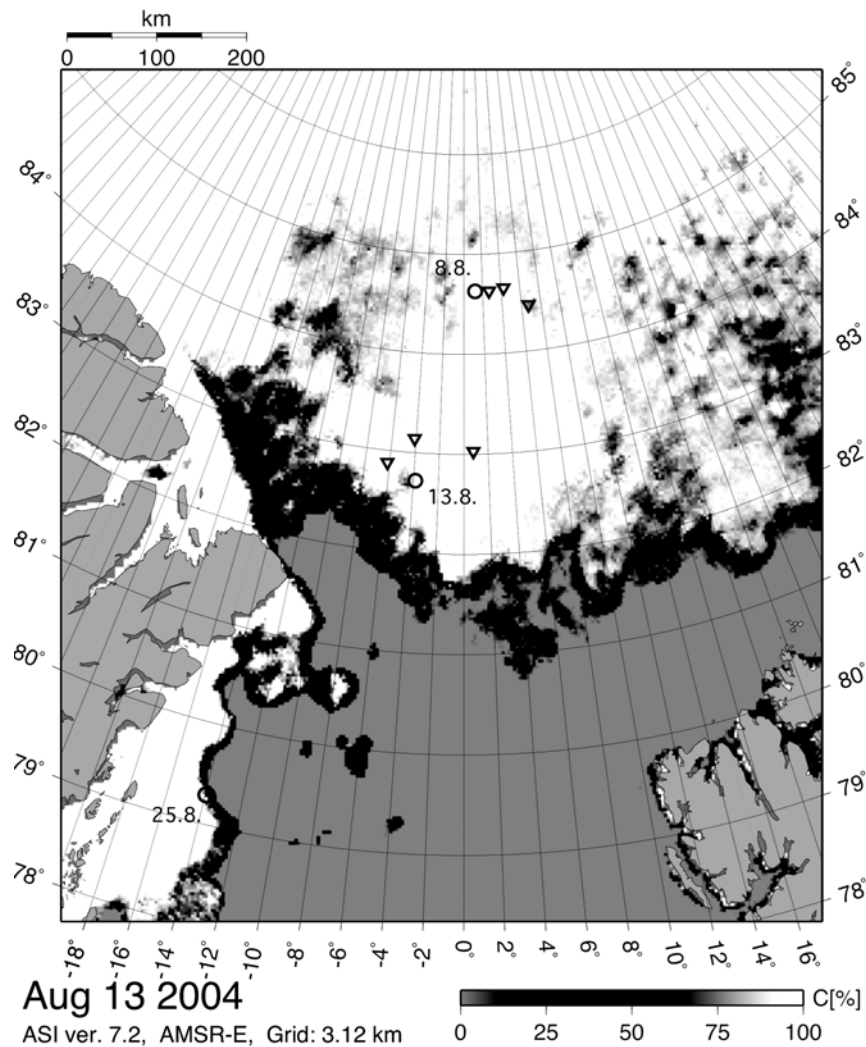


Fig. 4.6.1.1: Locations of sea ice ground work during ARK-XX/2. Triangles and circles show short and long stations respectively.

In general on the ice electromagnetic induction (EM31), ground penetrating radar (GPR), drilling and resistivity (cryo-electrics, CE) methods as well as augers, core drills and snow sticks have been applied in order to measure the ice and snow thickness and internal ice structure (CE). Being the best established geophysical device for ground based sea ice thickness profiling, the EM31 yielded very satisfactory results during ARK-XX/2. In total, over 8000 measurements were obtained with the EM31 during the cruise, both on floes ice and on fast ice. Figure 4.6.1.2 displays the thickness distribution obtained from 5634 EM31 conductivity measurements on pack ice. The mean ice thickness is  $2.60 \pm 1.03$  m. The modal distribution is 2.0 m. The minimum and maximum ice thickness values are 0.94 m and 9.84 m, respectively.

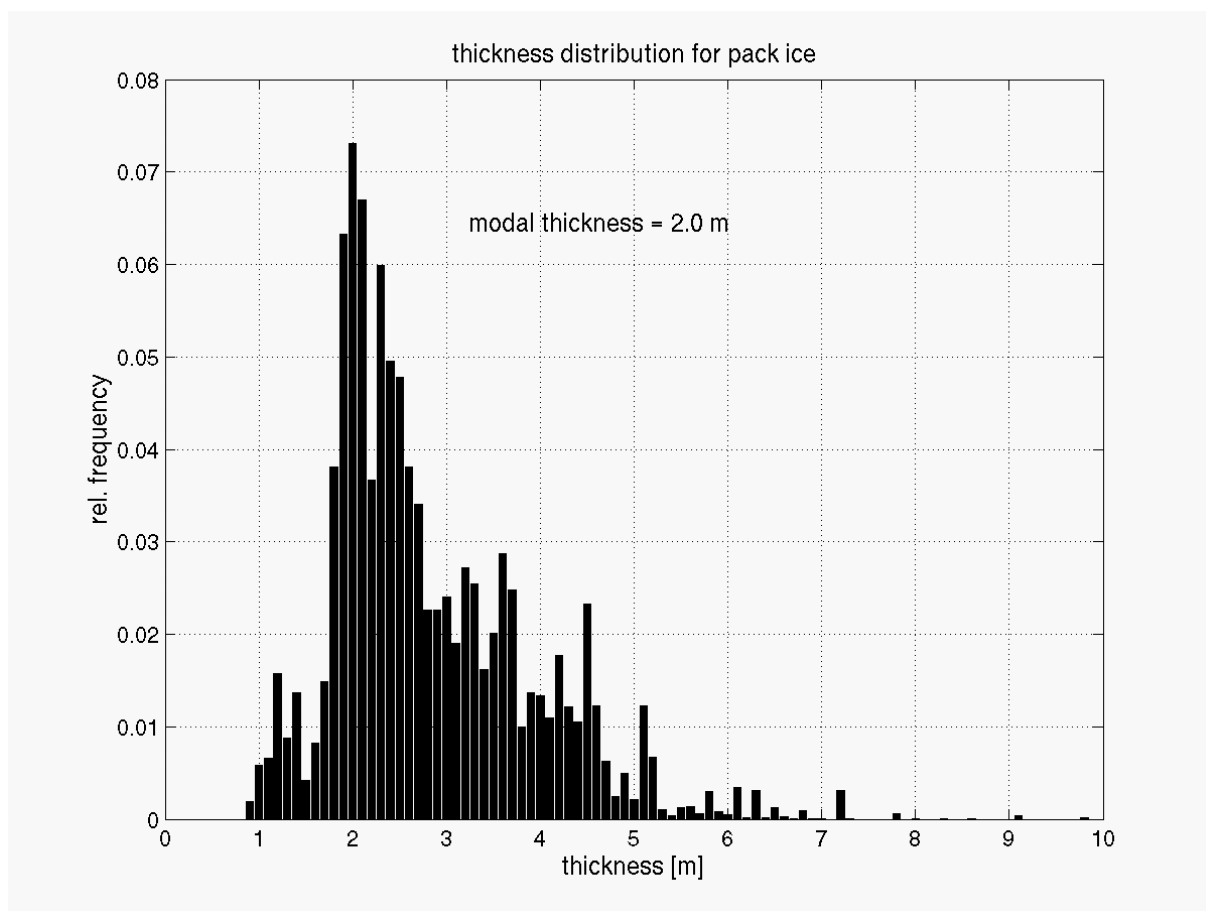


Fig. 4.6.1.2: Thickness distribution of pack ice obtained with the EM3

Two of the ship stations lasted for 12 hours. On both of these stations an ice surface profile including snow thickness has additionally been taken by levelling. An ice core was taken at the second 12 hr station. Concluding the cruise a joint sea ice station with a science team on board the British research vessel R.R.S. *James Clark Ross* served as a third long ice station.

The long ice stations will be described in the following chapters in more detail.

### 4.6.1 THE floe

The first 12-hour ice floe station started on Sunday, 8 August, at 11 am. A floe meeting all the requirements was found at 84°38'N and 001°12'E. We were searching for a floe of acceptable level ice thickness (around 2 m) and a 2-dim weathered ridge structure. The whole experiment aimed at the validation and footprint analysis of the HEM-Bird (4.2.2). However, due to bad weather and technical problems it was not possible to realize bird flights over the floe in the planned extent.

During both 12 h stations a rectangular grid of 40 m x 150 m was set up with five lines 10 m apart. Along these lines, the measurements have been made with different spatial resolution. After setting up the grid GPR measurements started, as long as the snow layer was undisturbed. Then several groups supported by all different work groups aboard went for CE, EM31, levelling and snow thickness measurements. After ensuring that electrical techniques would not have been disturbed, the drilling teams started. Drilling started with a hole spacing of 25 m. Later on spacing was reduced especially on the ridge down to only 1 m.

The positioning of the grid relative to the ship can be seen in figure 4.6.1.3.

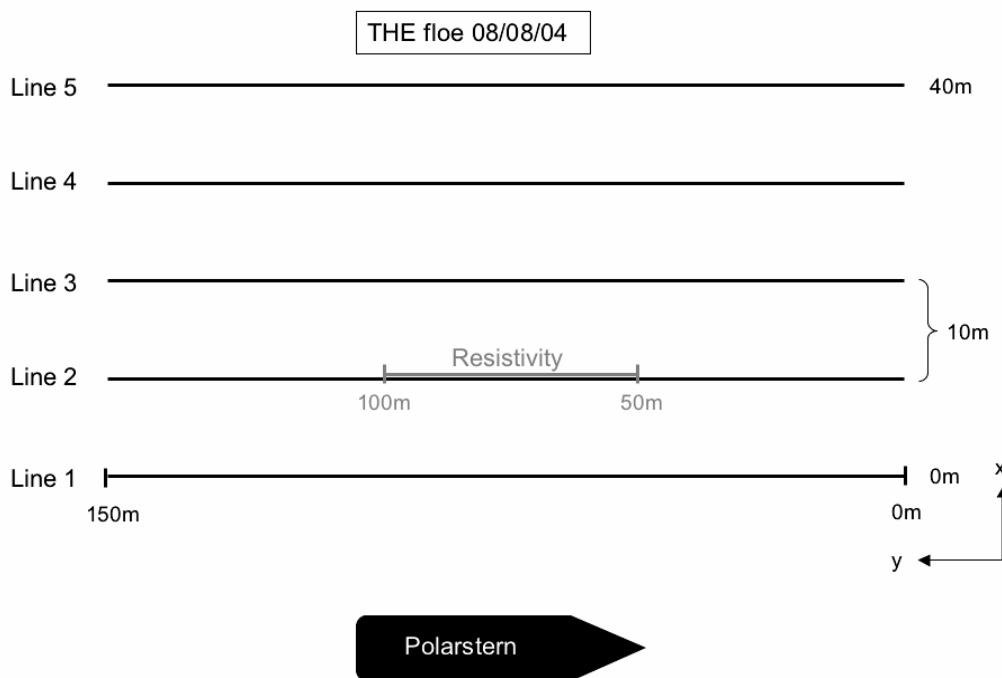


Fig. 4.6.1.3: Positioning of the measurement grid relative to the ship  
Position of CE is marked.

## Levelling

The levelling was carried out with a laser stationed on a tripod giving a horizontally levelled plane. The surveyor's pole shows the distance between the ice surface and this plane, if zeroed on the water level the device directly measures the freeboard of the floe. The spacing of the two outer and the middle lines and on the ridge was 1 m, lines 2 and 4 were measured with a spacing of 2 m.

From these data, and thickness measurements of EM31 and drilling a contour-plot of the grid was derived (see Fig. 4.6.1.4).

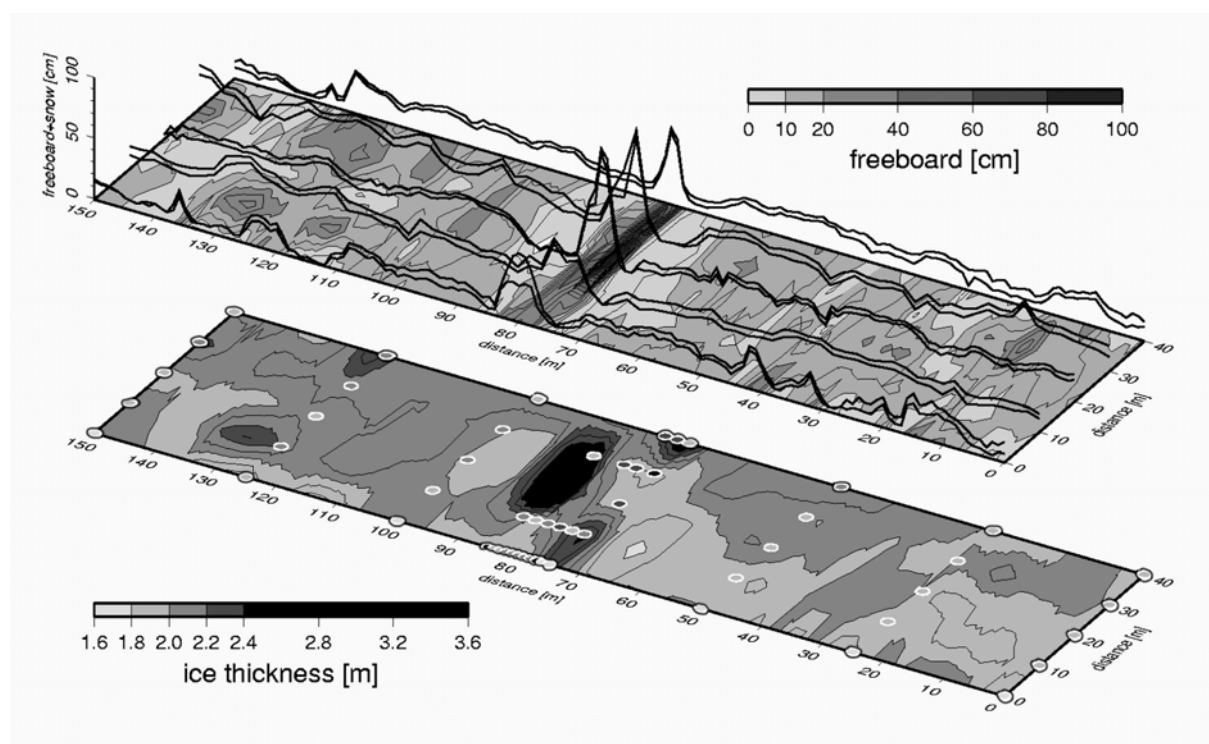


Fig. 4.6.1.4: Surface and ice underside profiles of THE floe within the grid.

**Upper panel:** contours of levelled freeboard and 1-dim cross sections of freeboard (black) and snow thickness (grey) along the five grid lines. **Lower panel:** total ice thickness measured with the EM31 as a contour map and drill hole measurements as filled circles (same colour bar).

## Kayak EM31

The EM31 MK2 instrument was placed inside the kayak and pulled over the ice floe, thereby attempting to go at a constant speed. EM31 measurements were obtained in two ways. Each of the five profile lines was first measured in automatic mode. In addition, tie points marked by flags on all profile lines were measured in manual mode in order to obtain better statistics for comparison with the drill-hole data. GPS positions were recorded for all measurement points with the use of the Allegro data logger.

The automatic measurements yielded 640 data points. The resulting thickness distribution is shown in figure 4.6.1.5 for bins of width 10 cm. The mean thickness was found to be  $2.05 \pm 0.15$  m. Minimum and maximum thickness values are 1.75 and 3.17 m, respectively. The mode of the distribution is found at 2.0 m.

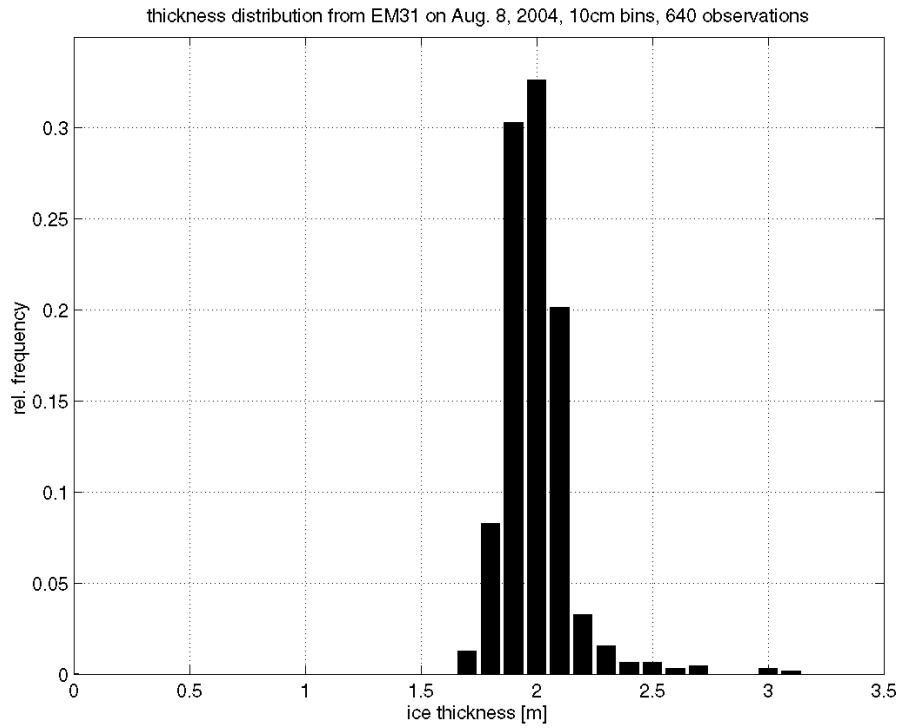


Fig. 4.6.1.5: Thickness distribution for the ice station on 8 August 2004

Figure 4.6.1.6 shows a comparison of the ice thickness obtained from the EM31 with the drilled thicknesses for the second line along the profile ( $x=10$ ). There is a good correspondence between the drill-hole thickness and the EM31 thickness for the level ice. Around the ridge, however, there are some deviations due to the larger footprint of the EM31.

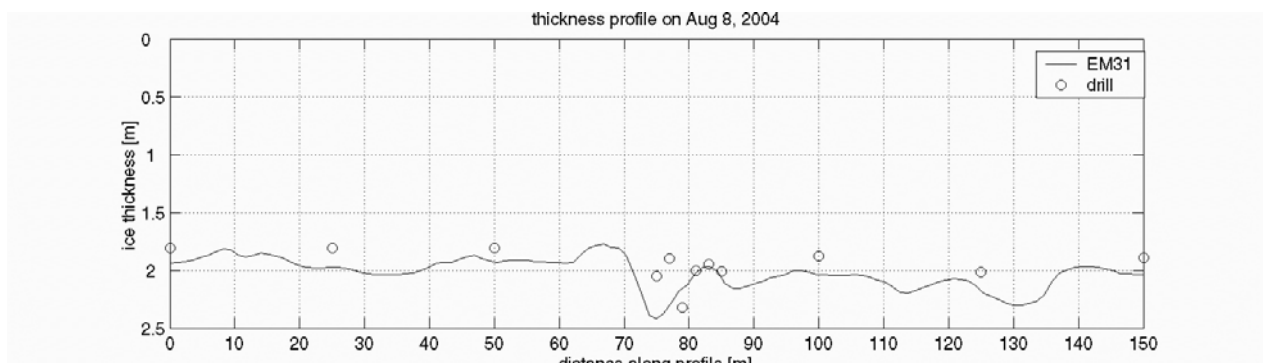


Fig. 4.6.1.6: Comparison of drilled ice thickness and EM31 thickness along line

### Cryoelectrics

A combination of multi-electrode arrays employing 50 electrodes with a 0.25 m electrode spacing between 68 m and 80 m and then expanded to a 1 m spacing between 50 m and 100 m, was used for measurements on line 2 of the grid set up at Ice Station I (THE floe). All 398 combinations of the Wenner array were tried but many measurements were either too noisy or failed to produce a reasonable value (e.g., a negative resistivity). A description of the equipment used is given in 4.3 'Cryoelectrics' of this report. Figure 4.6.1.7 below shows the data and the results of the preliminary interpretation for Line 2 of Sea Ice Station I.

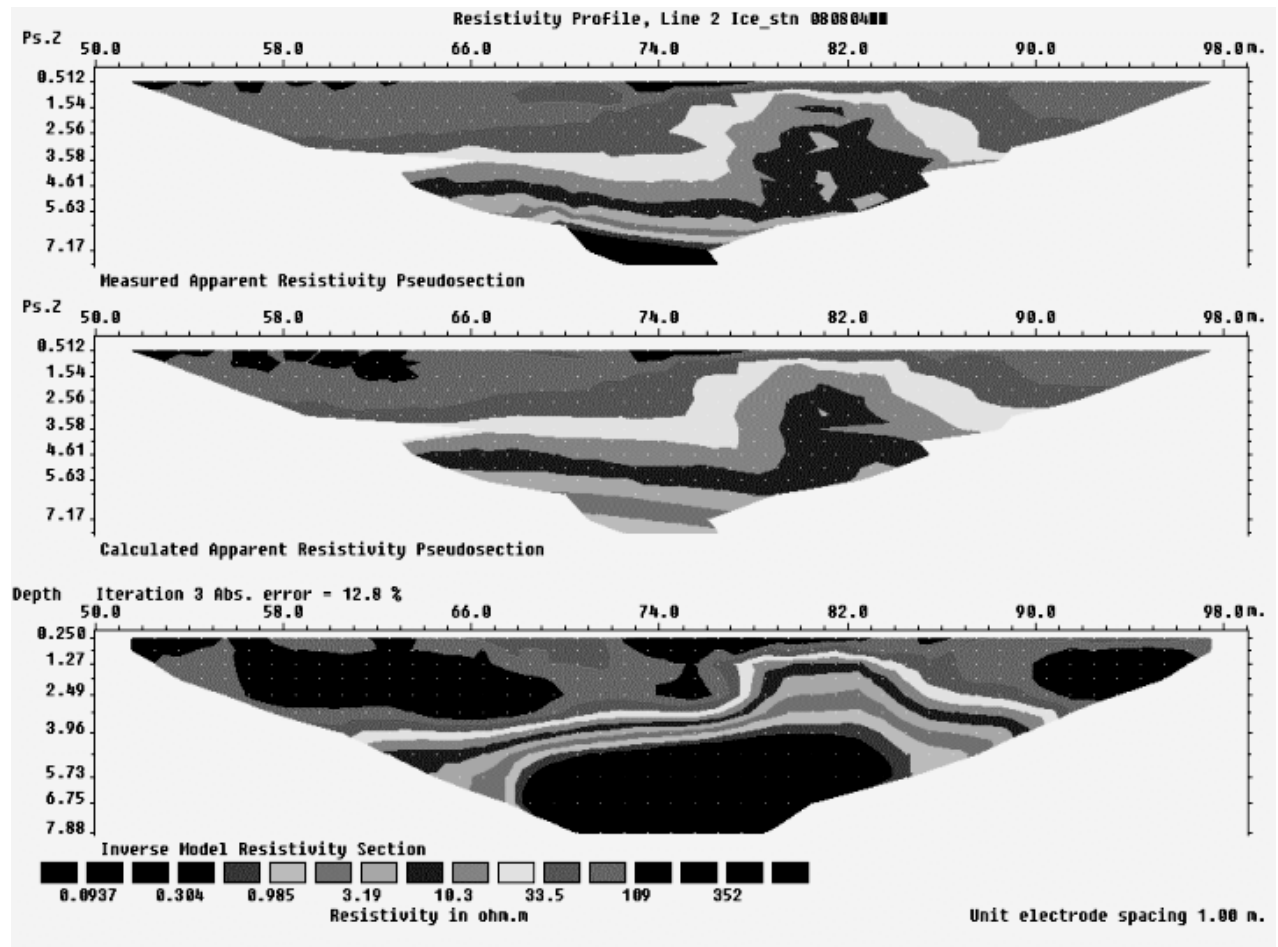
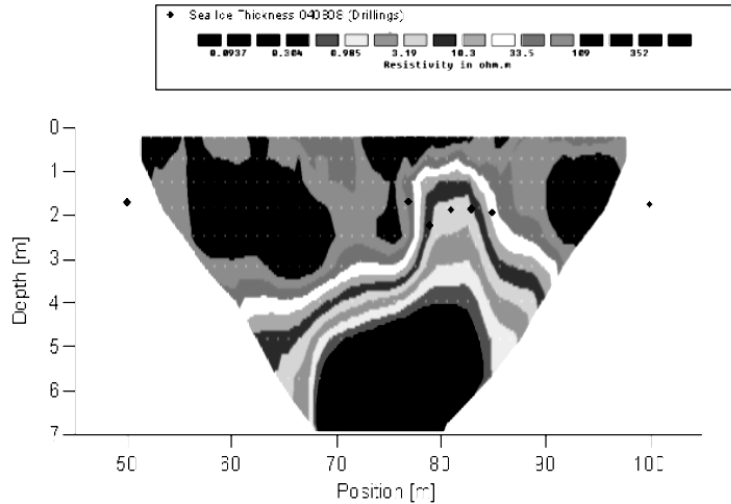


Fig. 4.6.1.7: Top is a pseudosection of the edited apparent resistivities processed from the recorded resistances. Bottom is the preliminary 2D inversion (3 iterations only) of the top data showing a conductive sea water at depth and a sea-ice of variable resistivity (30-300 ohm.m) and thickness (~1-5 m). The centre figure is the calculated response from the bottom model and a comparison between this and the observed data (top) gives a measure of the 'goodness-of-fit' of the model to the data (i.e., quite satisfactory). The increasing depth to the sea water at the edges of the section are most probably due to a combination of poor data at depth and an inadequate or inappropriate inversion routine. See further comment in figure 4.6.1.15.

Fig. 4.6.1.8:  
 A replotting of the 2D model in figure 4.5.1.7 with the sea-ice depths determined by augering superimposed. The agreement is reasonable but the information is rather sparse, especially in the region 55-70 m and again at ~90 m. This profile is over a simple ridge centred at ~75 m and this section indicates a thinner zone immediately adjacent to the sail. The data needs to be re-modelled incorporating the topography and comparing the result to the EM31 derived ice thickness.



**4.6.1.2 The OTHER floe**

The second 12-hour ice floe station was carried out on Friday, 13 August, after a polar bear disturbed our floe preparations the day before. A floe most acceptable was found at 82°72'N and 003°84'W. The selection of the floe was complicated due to the high coverage of melt ponds, which were slightly refrozen and quite a trap for scientists. Measurements were also partly complicated due to strong winds.

Preliminary GPR data processing showed that neither ice nor snow thickness could be measured. As expected the high water content of the warm summer sea ice attenuated the GPR pulses and therefore no reflections could be sensed. Consequently GPR measurements weren't carried out on the OTHER floe.

The positioning of the grid relatively to the ship can be seen in figure 4.6.1.9.

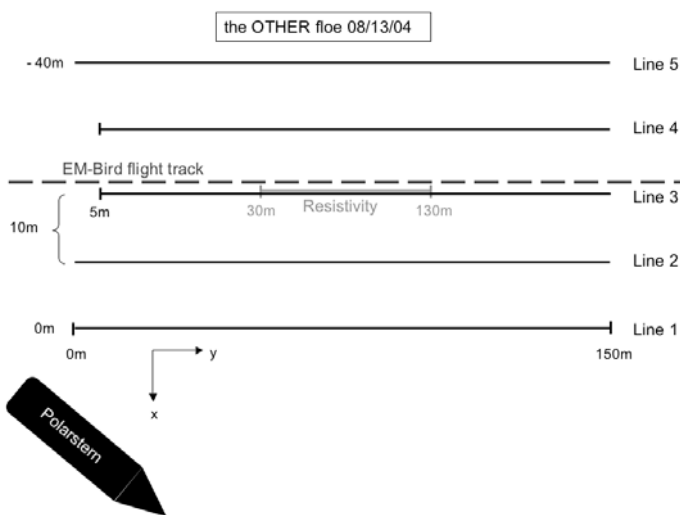


Fig. 4.6.1.9: Positioning of the measurement grid relative to the ship. Position of CE and Bird flight track are marked. Note that lines 3 and 4 start at 5 m, position 0 m was covered with a large melt pond.

### Levelling

Spacing of levelling was 2 m along the profile and 1 m on the ridge. Larger gaps had to be left where the grid lines crossed melt ponds. In this case the last and the first restart point of the levelling track were taken on the thin ice cover of the refrozen pond.

Results of levelling, EM31 measurements and drillings are integrated in figure 4.6.1.10.

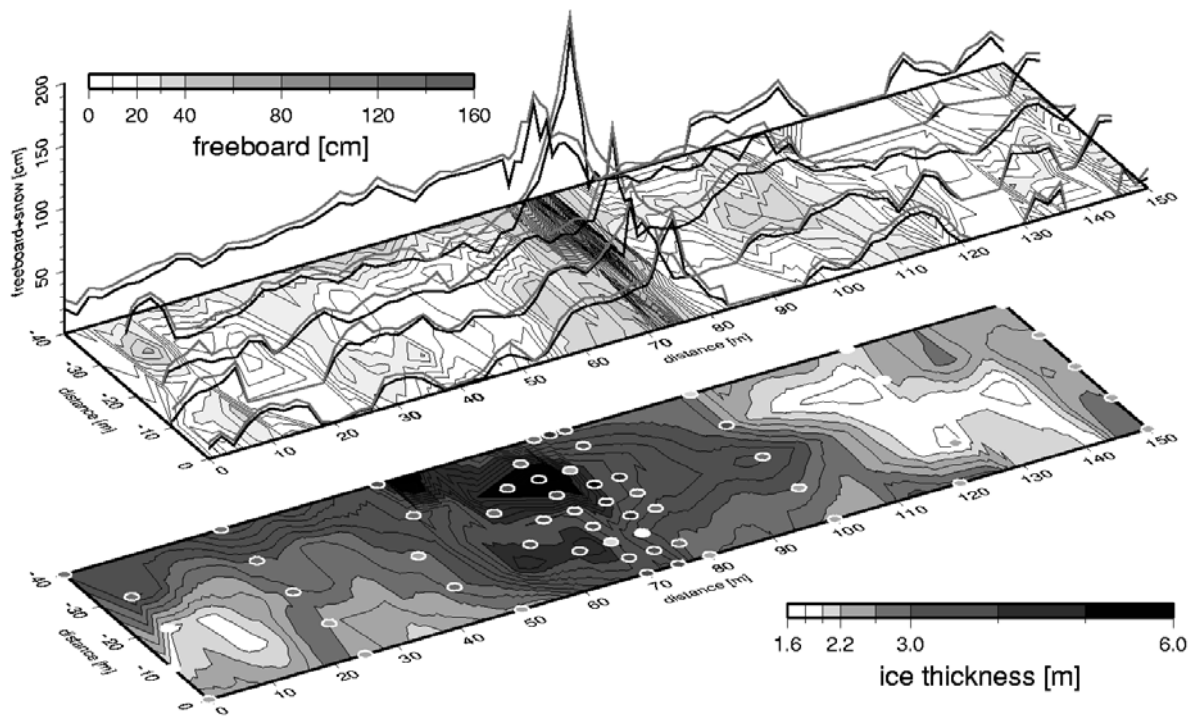


Fig. 4.6.1.10: Surface and ice underside profiles of the OTHER floe within the grid. **Upper panel:** contours of levelled freeboard and 1-dim cross sections of freeboard (black) and snow thickness (grey) along the five grid lines. Data points positioned on melt ponds have been linear interpolated. **Lower panel:** total ice thickness measured with the EM31 as a contour map and drill hole measurements as filled circles (same colour bar).

### Kayak EM31

The EM31 MK2 instrument was placed inside the kayak and pulled over the ice floe. Measurements were obtained in several ways. Each of the five profile lines was measured twice in automatic mode (both directions), and tie points marked by flags were also measured in manual mode to enable validation with the drill-hole data. In addition, measurements were taken at each of the first 25 electrodes on the resistivity line ( $x = -20$ ,  $y = 25-100$ ) to obtain statistics for a comparison with the resistivity data. GPS position data were logged automatically for all measurements.

The ice thickness distribution derived from the measurements is shown in figure 4.6.1.11. The mean thickness was found to be  $2.79 \pm 0.72$  m. Minimum and maximum thickness values are 1.66 and 6.55 m, respectively. The modal thickness is 2.4 m.

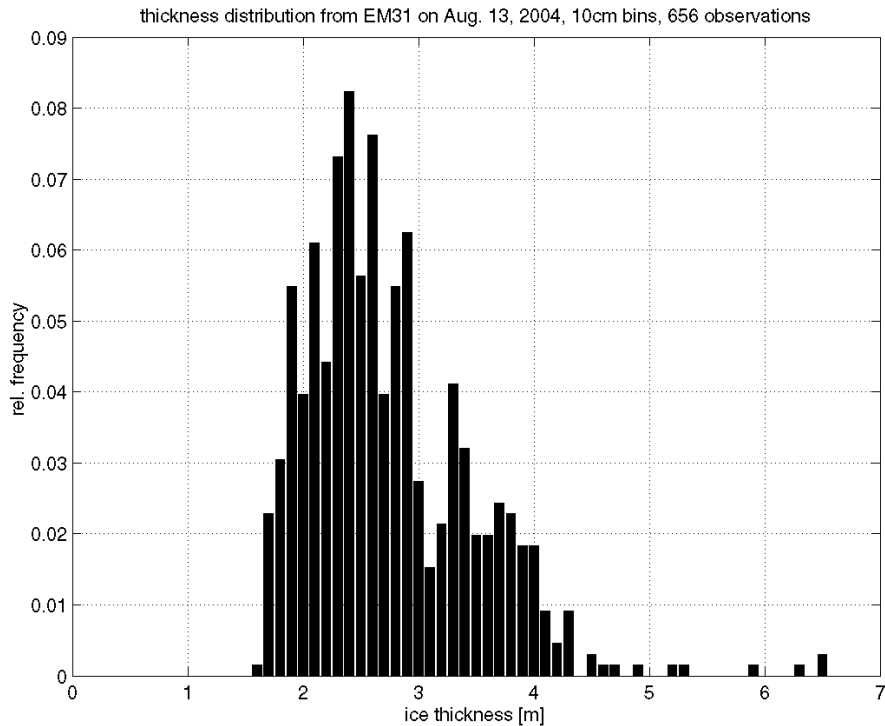


Fig. 4.6.1.11: Thickness distribution for the ice station on 13 August 2004

Figure 4.6.1.12 shows the thickness profile obtained from the central line (#3) of the station grid ( $x=-20$ ) in comparison with the drill-hole data. In the EM31 profile, the pressure ridge is clearly visible, and also a meltpond near the end of the profile. The thickness of this profile obtained from the EM31 ranged from 1.65 m at the thinnest location to 4.41 m at the pressure ridge. It appears that the EM31 considerably overestimated the ice thickness of the ridge compared to the drilling arising from the different footprints as mentioned in 4.6.1.1. Note in figure 4.6.1.12 that the drillings along the adjacent grid lines show comparable thicker ice sensed by the EM.

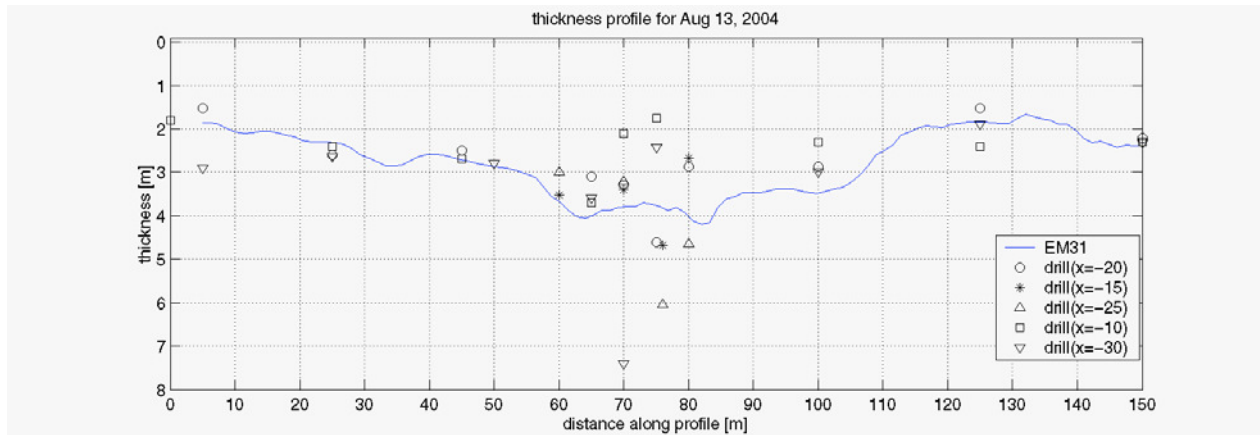


Fig. 4.6.1.12: Thickness profile along centre line (#3,  $x=-20$  m). Corresponding auger thicknesses are marked with circles, while the data from adjacent drillings is denoted with further symbols to illustrate the variability along the ridge.

### Heli EM

In spite of very bad flying weather due to dense fog and therefore visibility below 50 m, fortunately RV *Polarstern*'s fearless helicopter pilots agreed to fly the EM-bird along the grid profiles. Nevertheless, the experiment had to be abandoned after some attempts due to icing on helicopter and bird. However, first analysis of the data shows very good agreement between Heli EM and ground based thickness estimation (Fig. 4.6.1.13).

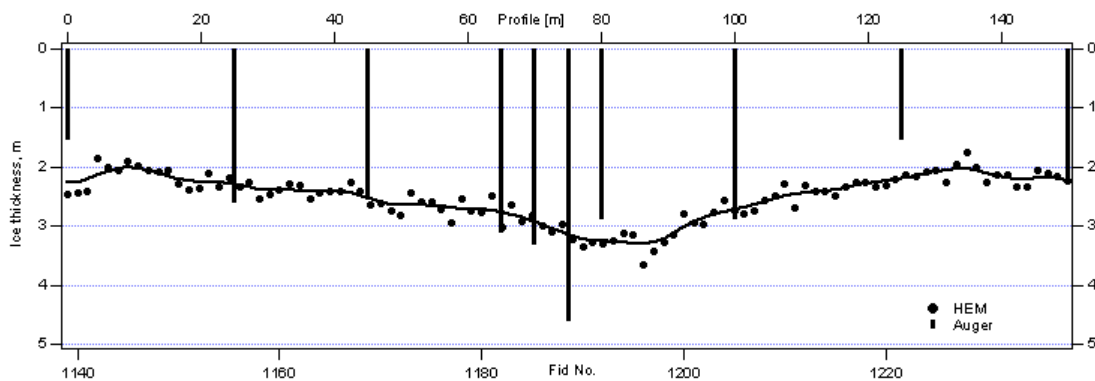


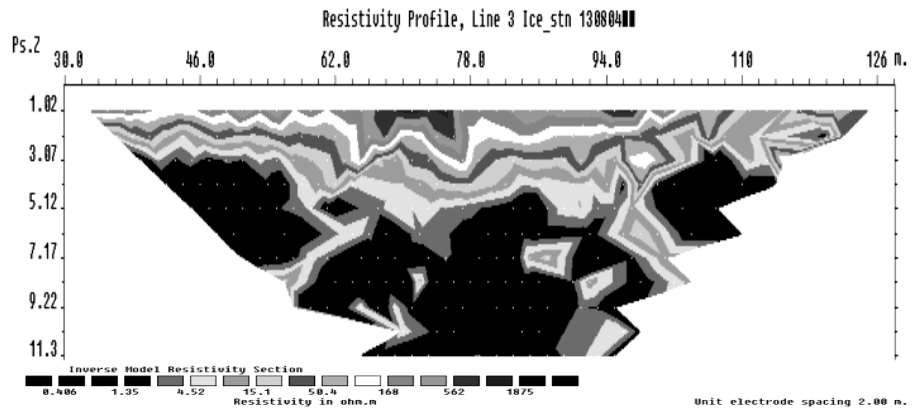
Fig. 4.6.1.13: Ice thickness profile along the centre line (#3) of the grid. Black bars denote auger thickness compared to HEM derived measures plotted as a line with markers. Markers show the single measurements whereas the line arises from a binomial smoothing accounting to the bird's footprint size.

While the level ice thickness is estimated fairly accurate by the bird, the ridge draft is underestimated as expected. However, the ridge is sensed by the Heli EM though it has a very small width and depth compared to the surrounding level ice. As the positions of the bird data are only time interpolated as a quick first result, the position of the ridge centre mismatches slightly.

**Cryoelectrics**

Fifty electrodes at a two metre spacing were set up on the centre line (#3) between 30 m and 130 m. Resistances were measured using all possible 398 Wenner array readings, and processed as in 1.

*Fig. 4.6.1.14  
Recorded and edited data converted to apparent resistivity and plotted as a pseudosection, showing a variable thickness of (relatively) resistive sea ice at the surface with an underlying conductive sea water. This latter should have a reasonably uniform resistivity, but the greater the apparent depth, the noisier the data.*



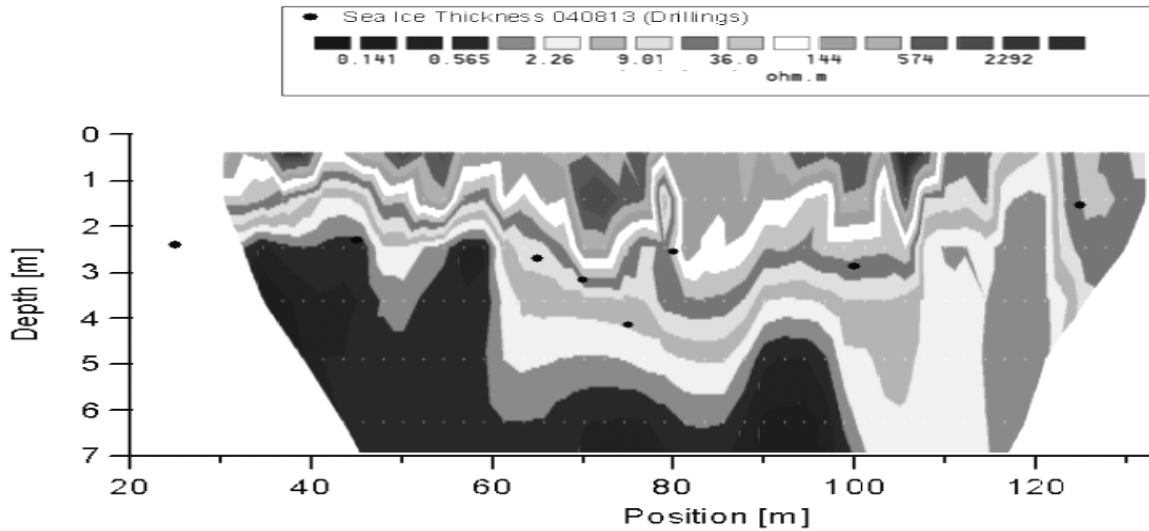


Fig. 4.6.1.15.: The inverted section (i.e., with real depths) for the data in figure 4.6.14 plus auger depths. The true sea water resistivity is  $\sim 0.4 \text{ ohm.m}$  and the bulk of the ice is  $50\text{-}150 \text{ ohm.m}$ . The results are in good agreement with the thickness of the sea ice determined by the auger drilling. Further inversion (more iterations, different routines) is required and, particularly, reprocessing with the topography.

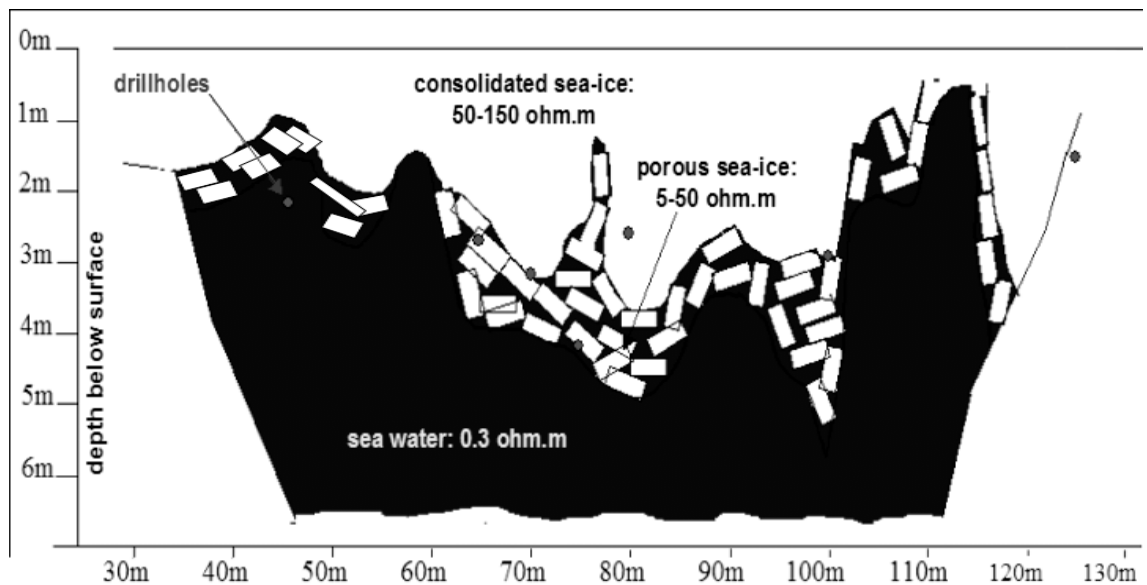


Fig. 4.6.1.16.: The above inverted section (Fig. 4.6.1.15) has been interpreted to show areas of consolidated and more resistive ice and more porous zones of less-resistive ice. Further experimentation with better data (obtained from better instrumentation) and different inversion routines is expected to produce even more confident definition of sea ice structure.

**Ice core**

In the end an ice core has been drilled on the 3rd line at about 83 m next to the ridge. The core has been sawn into pieces of about 10 cm length. Then slices of longitudinal sections were photographed under polarized light in order to investigate the crystal structure of the ice. From this, conclusions on growth conditions can be drawn. Density and salinity of each of these pieces has been measured (see Fig. 6.4.1.17)

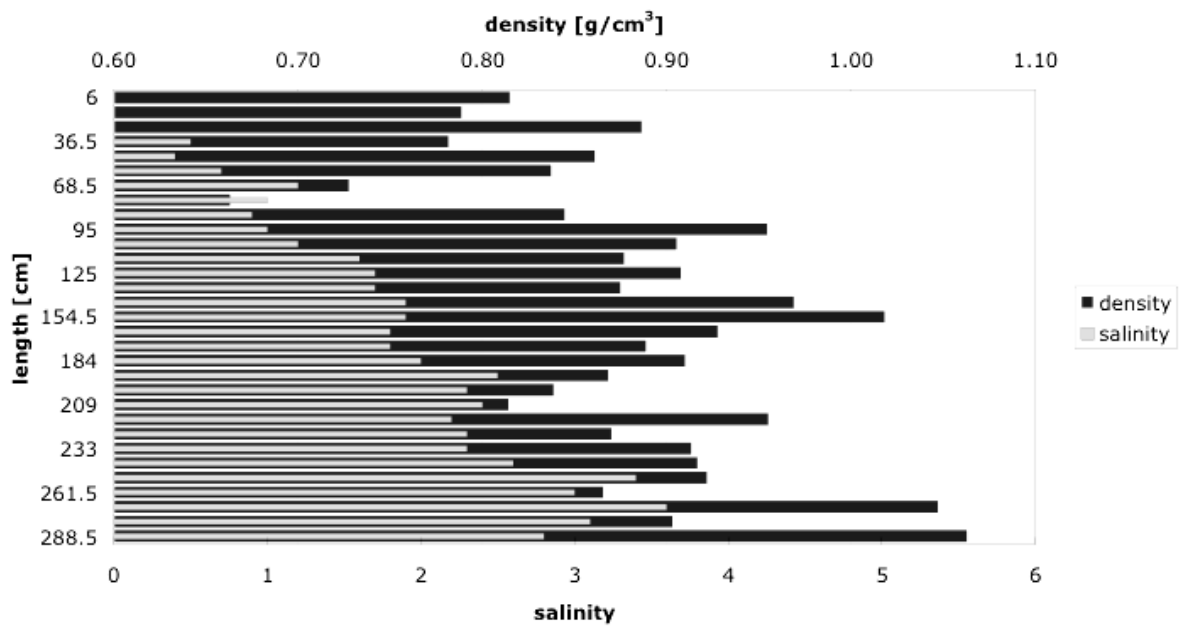


Fig. 4.6.1.17: Vertical density and salinity profiles from melted core samples

**4.6.1.3 The JCR station**

The ice station on 25 August 2004 took place near the Greenland coast and work was done in collaboration with scientists from the British research vessel R.R.S. *James Clark Ross*. On this occasion, it was possible to obtain ice thickness measurements of fast ice. The thickness distribution for 1828 measurements is displayed in figure 4.6.1.18. The mean thickness was found to be  $1.56 \pm 0.55$  m, the minimum thickness 0.91 m and the maximum thickness 7.52 m. The mode of the distribution is 1.2 m.

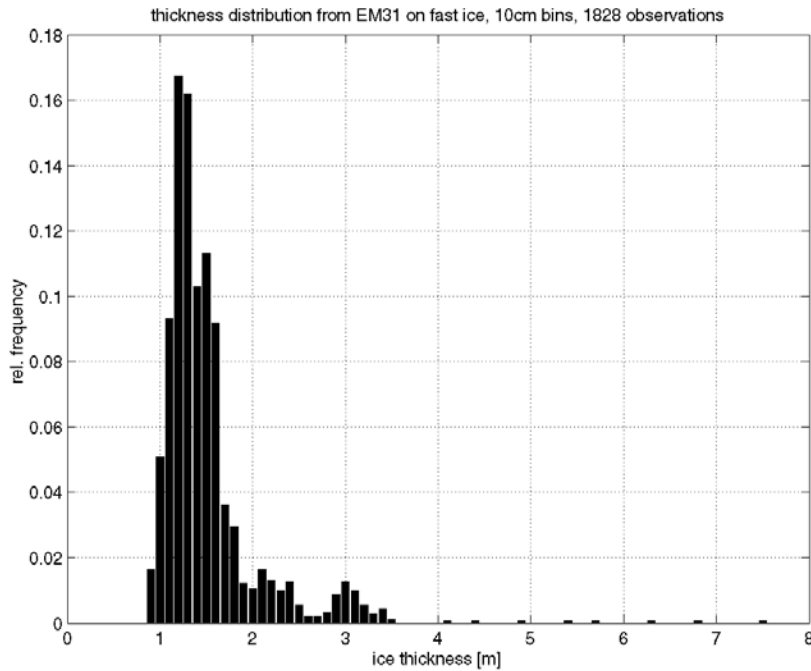


Fig. 4.6.1.18: Thickness distribution of fast ice on August 25, 2004

A comparison of the ice thickness derived from the EM31 and the drilling data provided by the team of the R.R.S. *James Clark Ross* is shown in figure 4.6.1.19. The profile shown is the centre line (# 1), on which coincident resistivity measurements were obtained. The comparison shows a rather good agreement, taking onto account that drillings and EM readings were not always taken on exactly the same position. Further assessment of the EM31 is illustrated in figure 4.6.1.20. Comparing the ice thickness distributions derived from the different methods proves the accurate level ice thickness estimation by means of electromagnetic induction.

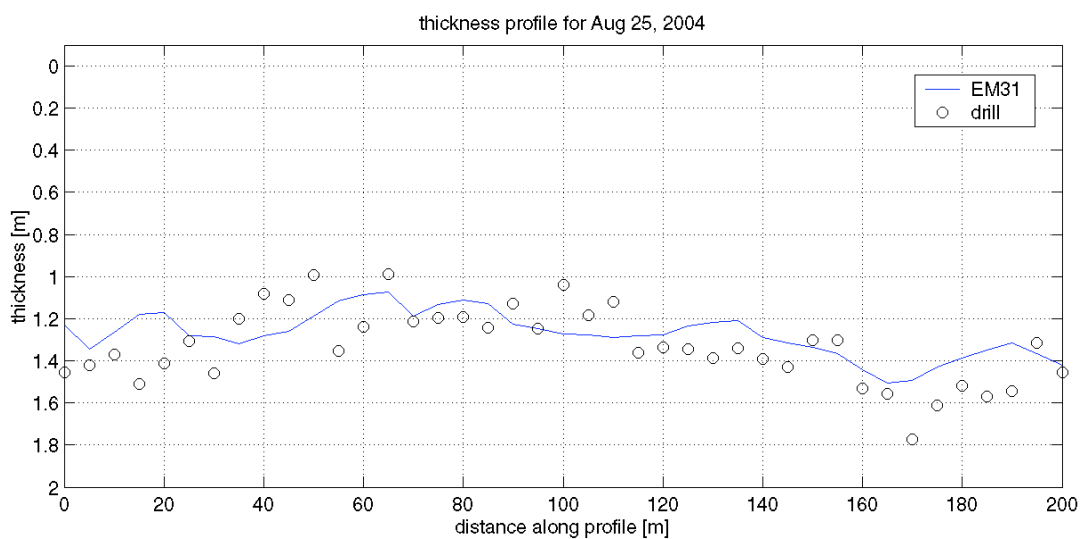
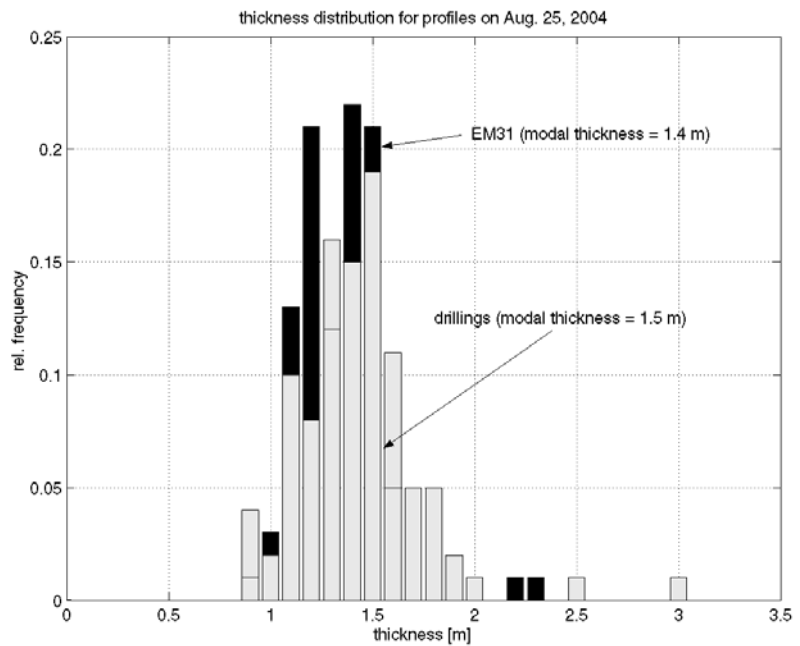


Fig. 4.6.1.19: Thickness profile for line 1 on August 25, 2004

Fig. 4.6.1.20: Auger and EM thickness distributions for line #1 shown in figure 4.6.1.19



## 4.6.2 Regional sea ice results

As introduced in 4.2.2 the HEM system is capable to determine the sea ice thickness via electromagnetic induction. However, the laser altimeter data can be processed solely to retrieve freeboard and pressure ridge sail height statistics. The following two subchapters deal with HEM ice thickness and laser altimeter results, respectively.

### 4.6.2.1 Ice thickness distribution in northern Fram Strait

Although we had to deal with the unsuitable weather conditions of the Arctic summer, we were lucky enough to find flying weather at least every second day from the 2 to 14 August while RV *Polarstern* was operating north of Fram Strait from 82°N up to 85°N at longitudes from 8°W to 8°E.

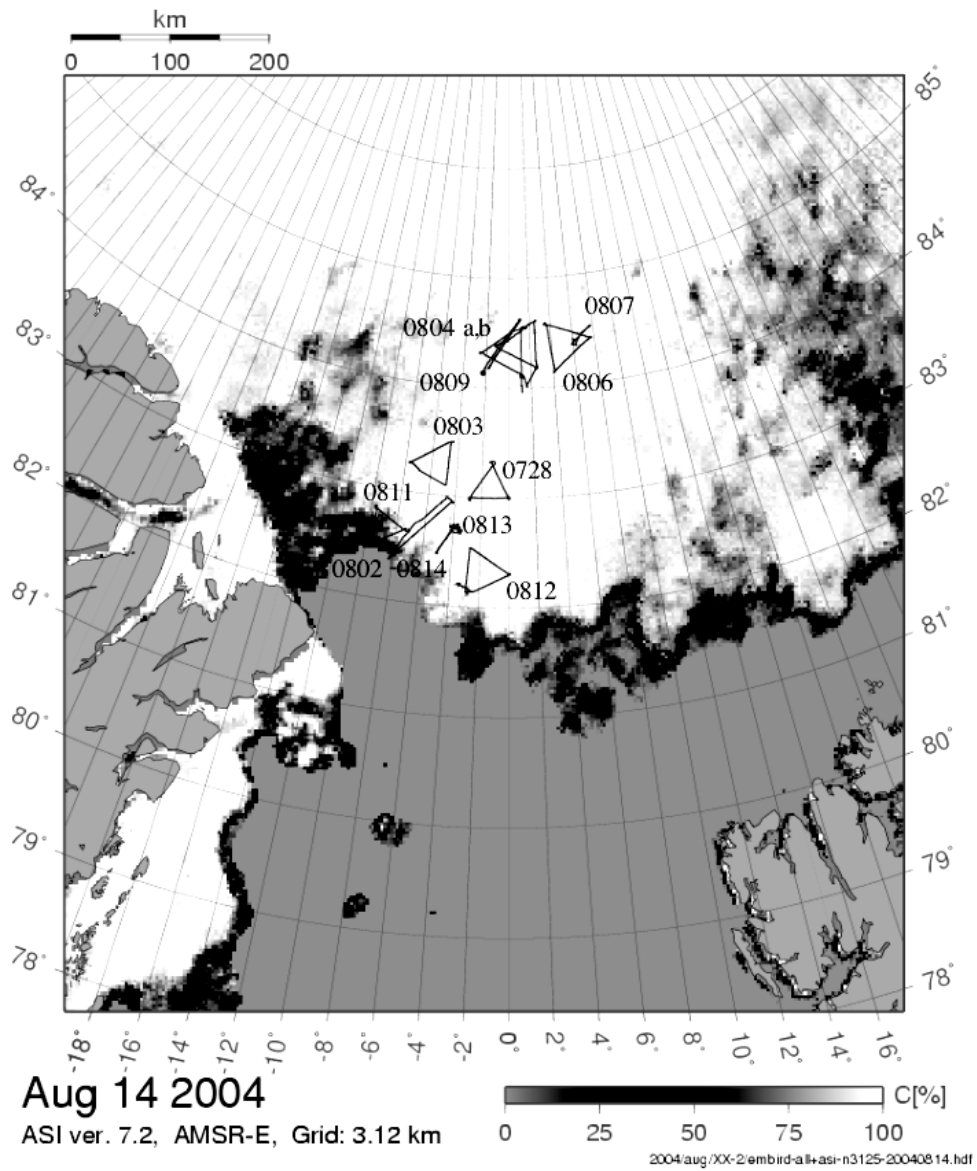
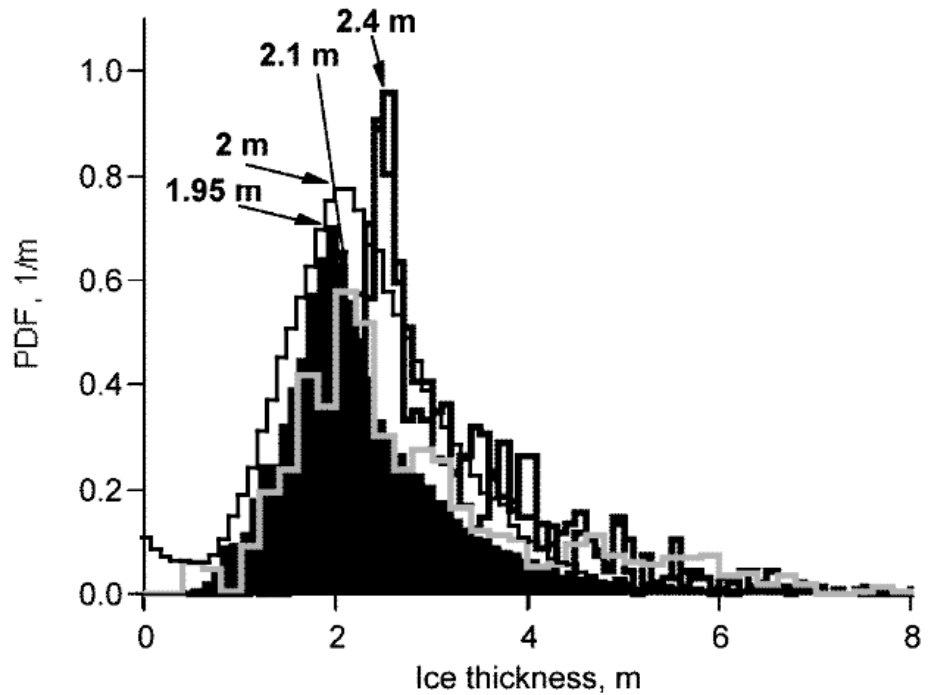


Fig. 4.6.2.1: Ground tracks of all HEM flights during ARK-XX/2

Fig. 4.6.2.2: Observed ice thickness distributions from the years 1991, '96, '98, 2001 and 2004 denoted by their modal thickness of 2.4, 2.4, 2.1, 1.95 and 2.0 m, respectively



To compare the results of ARK-XX/2 to the observed decrease in ice thickness from 1991 to 2001 the thickness distribution was computed using the thickness profiles acquired on 28 July and 3, 4, 6, 12 and 14 August (Fig. 4.6.2.2). Measurements over the marginal sea ice zone were not taken into account. As the profiles on 4 and 9 as well as on 6 and 7 August were over the same region, only data from 4 and 6 were considered respectively.

#### 4.6.2.2 EM-Bird Laser flights

The EM-Bird (see 4.2.2) is equipped with a laser altimeter, which operates at a frequency of 100 Hz. Considering a flight speed of ~60 kn this means a data point spacing of 30 cm. The gained data are adjusted from the vertical helicopter movement by several filtering methods. From these altimeter data a freeboard height, ridge height, width and spacing is derived. Freeboard is the part of the vertical oriented floe thickness, in which is above water level. Ridges are dams of dynamical deformed sea ice, which broken blocks are piled up in a line with a cross-section of triangular shape. Ridges are divided into a sail above water level and keels below.

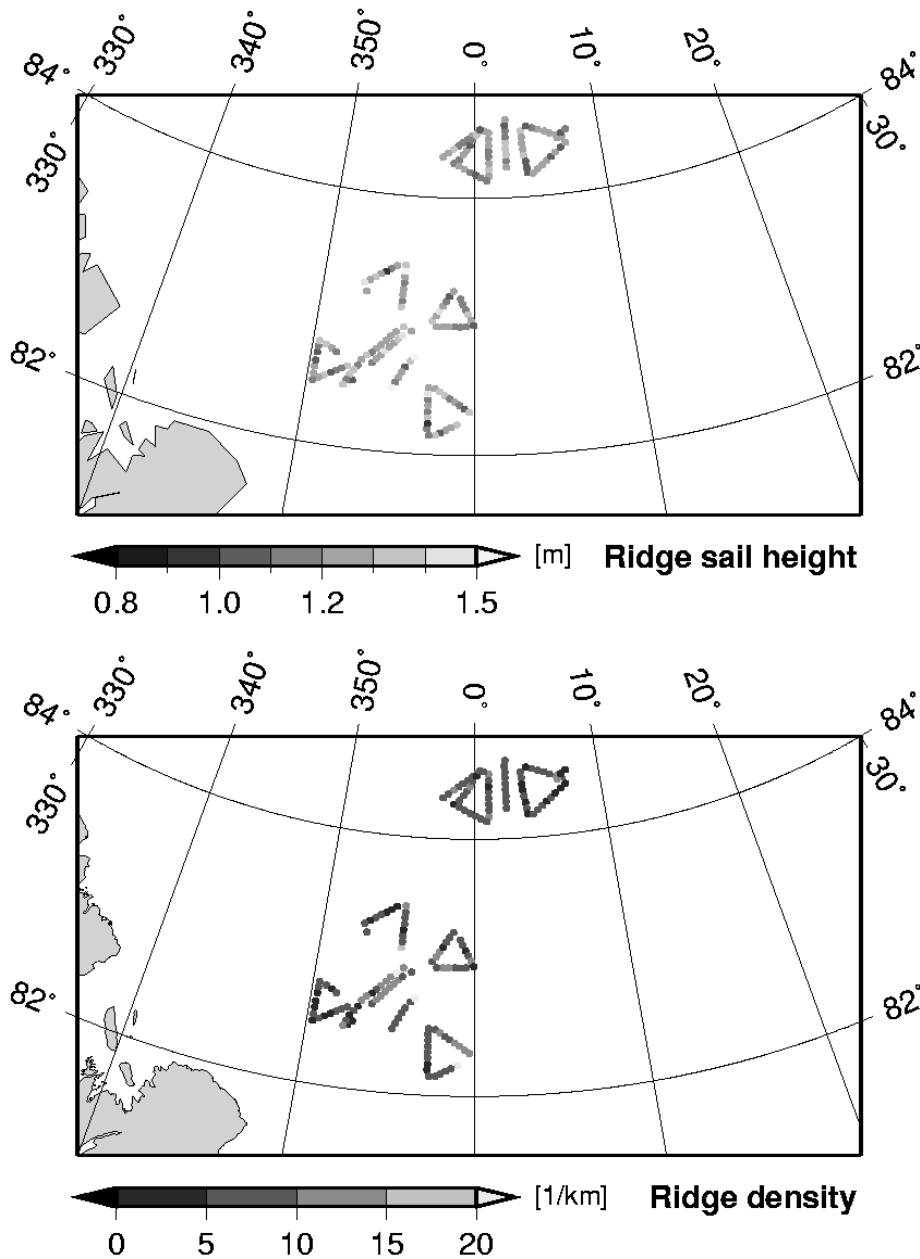


Fig. 4.6.2.3: Ridge sail heights and ridge density as derived from EM-Bird-laser data

Sail heights of up to 10 m have been measured in the Arctic, whereas keel drafts are 3 - 4 times deeper on average. About 70 % of the Arctic sea ice volume is stored in such dynamically grown features. In figure 4.6.2.3 ridge sail height and ridge density are shown as an average along 5 km legs. Compared to other regions of the Arctic or to winter conditions the sampled region during this cruise shows a moderate ridge density, but with a remarkable mean sail height.

**Appendix: Cryoelectrics Bench Test Notes (31/7/04)**

Bench tests were made of the Leipzig Tomoplex equipment on RV *Polarstern* (31/7/04) and the following conclusions were made:

1. SET UP:

A small 4 electrode (Wenner type) set up was made as:-

C1 1kohm P1 800ohm P2 1Kohm C2 ie, approximating sea ice conditions.

with C1 at electrode 1, C2 at electrode 4, P1 at electrode 3, P2 at electrode 4 and Pref 0 (ie ext.).

It was found that #Box# EO152 worked very well with an input current of 1mA, ton=toff=1ms with a trigger level of 111 (ie 11.1mV) using the '207' Husky (now labelled 'tomo compatible').

'Worked' means that values of 800 ohms were obtained for P2 (P1 recorded values of ~40 milliohms).

The other box (EO151) did not work with these settings and neither did the other Husky.

Currents ranging from 1 to 50 mA gave good results, but changing the current in the 'tomo' programme did not actually change it !!!!! To actually change the current, you have to edit the \*.prm file. (p.s. This should read to PERMANENTLY change the current.)

EO152 worked with both internal and external batteries and worked with a range of on and off times from 0.2 to 3secs, and a range of trigger levels from 1 (ie 0.1mv) to 222 (ie 22.2mV). Current levels above 50 mA did not work.

The file 'wnr\_t1t1.prm (copied below) worked satisfactorily in the lab (yet to be tried in the field).

```

none
wfmt1t1.dat
0
111
1
1.000000 4.000000 1.000000 1.000000 1.000000 4.000000 0.000000 2.000000
3.000000 0.000000 0.000000 0.000000 0.000000 0.000000 0.000000 0.000000
0.000000 0.000000 0.000000 0.000000 0.000000 0.000000 0.000000

```

JB/DF  
31-7-04

---

## 5. AIR CHEMISTRY: STUDY OF AIR, SEA, SNOW AND ICE CONTAMINATION FOR MERCURY (HG) AND SELECTED PERSISTENT ORGANIC POLLUTANTS (POPS)

Katrine Aspmo<sup>1</sup>, Christophe Ferrari<sup>2</sup>,  
Xavier Fain<sup>2</sup>, Pierre-Alexis Gauchard<sup>2</sup>,  
Rainer Lohmann<sup>3</sup>, Luca Nizzetto<sup>2</sup>

<sup>1</sup>Norwegian Institute for Air Research, Kjeller  
<sup>2</sup>Laboratoire de Glaciologie et Geophysique de  
L'environnement, Saint Martin d'Herès  
<sup>3</sup>University of Bremen, Bremen

### 5.1 Scientific programme

Several international leading groups of Environmental Atmospheric Chemistry were joining the RV *Polarstern* on ARK-XX/2 (2004) for measurement of trace organic contaminants and mercury species in remote environments of the Northern Hemisphere, so as to investigate the environmental cycling and fate of key global pollutants. These pollutants emitted by anthropogenic sources (and also natural sources for mercury) were found during the last years at high concentrations in the food chain. Understanding their distribution in the different reservoirs of the Arctic could help to better assess the pathways between these reservoirs and the food chain. RV *Polarstern* has been found to be well suited to act as a 'clean ship' for the sampling of these trace compounds. The research programme for atmospheric chemistry group during ARK-XX/2 was focused on three major topics:

1. Determination of mercury speciation and Persistent Organic Pollutants (POPs) speciation (i.e. gaseous versus particulate) in the atmosphere during Arctic summer
2. Determination of Hg in air, melt pond water, sea ice, snow and sediments so as to define the stocks of Hg in Arctic environment
3. Determination of sea to atmosphere fluxes for mercury and sea to atmosphere partition for POPs.

### 5.2 Introduction

Mercury (Hg) is present in the environment in various chemical forms and can be transformed to methyl mercury. This organic form constitutes the most hazardous species of mercury. In the atmosphere, Gaseous Elemental Mercury (GEM) is the predominant form with concentration about  $\sim 1.5 \text{ ng/m}^3$  and has a lifetime of about one year (Slemr et al., 1985), but some oxidized species of mercury (Hg(II)) are

found at lower concentrations ( $\sim\text{pg}/\text{m}^3$ ), as Particulate Mercury (PM) and Reactive Gaseous Mercury (RGM). These species are more reactive and soluble than GEM and can be deposited faster onto Earth surface (Lu et al., 2001). Hg (II) is predominant in aquatic reservoirs (e.g. oceans, lakes, cloud water) where it can be easily transformed into methylmercury. This mercury species can accumulate the food chain in Arctic environments, especially in fish and sea mammals. Consequently, native human populations are exposed to this toxic pollutant (Wheatley et al., 1995, Girard et al., 1995).

Reactivity of GEM in the atmosphere is weak except under special conditions in which GEM can be rapidly oxidized. These fast atmospheric processes known as Atmospheric Mercury Depletion Events (AMDE) have been observed in various places in Arctic regions in Canada (Schroeder et al., 1998, Poissant et al., 2001), U.S.A. (Alaska) (Lindberg, 2001), Norway (Berg et al., 2001), Greenland (Skov et al., 2002), and in Antarctica (Ebinghaus et al., 2002) in spring. During this fast concomitant depletion of mercury and ozone, concentrations of Hg can be strongly enhanced in the snow surface as the result of deposition of oxidized forms of Hg (Lu et al., 2001, Berg et al., 2003, Lindberg et al., 2002).

In contrast to mercury, there are no natural sources of persistent organic pollutants (POPs), but only anthropogenic ones, such as incinerators, from which dioxins are emitted, pesticides (DDT, Lindan), which have been widely used, and other substances, which are produced in large quantities, such as flame-retardants, shampoo and other cleaning agents. Because of the longevity of these compounds and their large amounts of production, POPs are globally distributed and have also reached the polar regions. POPs are fat-soluble, and accumulate in organisms causing toxic reactions at the end of the food chain, e.g. in humans. The concentration of various POPs is only a few picograms ( $10^{-12}$  g) per cubic meter air or litre water. Therefore, large volume samples are taken (e.g. 1000 litre water, 500 to 1000 cubic meter air), which are later analysed in clean-labs.

By combining short-term atmospheric samples with the collection of representative water samples across different region of the North Atlantic / Arctic circle, answers are sought as to whether atmospheric transport or the marine phytoplankton productivity are controlling the transport and settling flux of persistent organic pollutants.

### **5.3 Experiments**

Two Tekran gas-phase mercury vapour analysers (Model 2537A) were installed on RV *Polarstern* for the determination of GEM in the Arctic atmosphere. RGM was also measured with a Tekran 1130 (automated technique) mercury speciation unit, which gave one Tekran 2537A mercury vapour analyser the ability to concurrently monitor both GEM and RGM species in ambient air at the  $\text{pg}/\text{m}^3$  level. The other Tekran mercury vapour analyser was also installed for both GEM, RGM (manual technique) measurements so as to compare the two techniques. The manual technique is also able to measure Particulate Mercury (PM), the third term of atmospheric mercury

speciation. The sample inlets were located on the upper deck of RV *Polarstern* in front of the GKSS container. The air was sampled at a flow rate of 1.2 L/min with a 0.45 mm PTFE filter in front of the sample inlet of the analyser.

Atmospheric ozone was measured during that cruise, as this oxydant is involved in mercury atmospheric reactivity. Furthermore, atmospheric particles were continuously monitored so as to have their number with time and their size distribution. Atmospheric particles offered important surfaces for heterogeneous chemistry for both active halogen formation from sea salts aerosols and mercury oxydation into RGM and PM. Two optical techniques were used for their monitoring. In order to describe as best as possible the air masses that were sampled for Hg, Ozone and POPs, we also collected for 24 hours sampling time atmospheric aerosols for ion-determination (chlorine, bromine, nitrate, sulfate, potassium, sodium...) and also for radionucleides determination. These filters will be measured in Grenoble (France) for  $^{210}\text{Pb}$ ,  $^{10}\text{Be}$  and  $^{210}\text{Po}$ . The concentrations of these elements will give us, combined with the air mass back trajectories, the origin of the air mass and in a certain extent its "chemical age".

In addition a third Tekran analyser in the wet lab was used to investigate the sea/air exchange of GEM during Arctic summer. The analyser was connected to a 20 L glas bottle, called "Equilibrator", indirectly measuring the Dissolved Gaseous Mercury (DGM) concentrations in the sea water with the help of the Henry's law constant. In addition to these sea to atmosphere fluxes, we collected during a CTD profile, sea water for depth profiles for Hg and heavy metals. Furthermore, we took the opportunity to also sample sea water for better understanding the possible Hg emissions from a hydrothermal deep ocean volcano.

Snow and melt pond water, have been collected during the cruise during helicopter flights far from the vessel for Hg, ions, heavy metals determination.

During the first sea ice station (84.615°N, 1.112 °W), two sea ice cores have been drilled for Hg, ionic balance determination when we will be back to Grenoble. They will be first decontaminated using a well-established procedure already tested for ice cores originating from polar ice caps or temperate glaciers.

Deep ocean sediments have been collected from 27 dredges. Sediments will be analyzed after water elimination and chemical treatment.

Four different modified high-volume air samplers were used to collect air on board of RV *Polarstern* during ARK-XX/2. POPs such as polychlorinated biphenyls (PCBs), polybrominated diphenylethers (PBDEs), organochlorine pesticides (such as HCHs, HCBs, and DDTs), polyflourinated compounds (PFCs), Nonylphenol (NP), and combustion-derived polycyclic aromatic hydrocarbons (PAHs) and polychlorinated dibenzo-p-dioxins and dibenzofurans (PCDD/Fs) and total suspended particulates (TSP) were investigated.

## 5.4 Results

### 5.4.1 Mercury speciation in the Arctic

#### a) Atmospheric speciation of Mercury

The results of GEM measurements for the time period from 17 July to 10 August are preliminary data (Fig. 5.1). The three instruments used for GEM monitoring were in excellent agreement as reported in figure 5.1. The concentration increased from 1.4 to 2 ng/m<sup>3</sup> during the period of time studied. The arithmetic mean of all GEM measurements during this cruise leg is  $(1.7 \pm 0.3)$  ng/m<sup>3</sup> and is in good agreement with mean summer concentrations from other polar sites like Alert, Canada or Ny Ålesund, Svalbard. Contaminations from the ship's plume will be eliminated after the cruise according to the PODAS data of wind directions and wind speed relative to the ship's course.

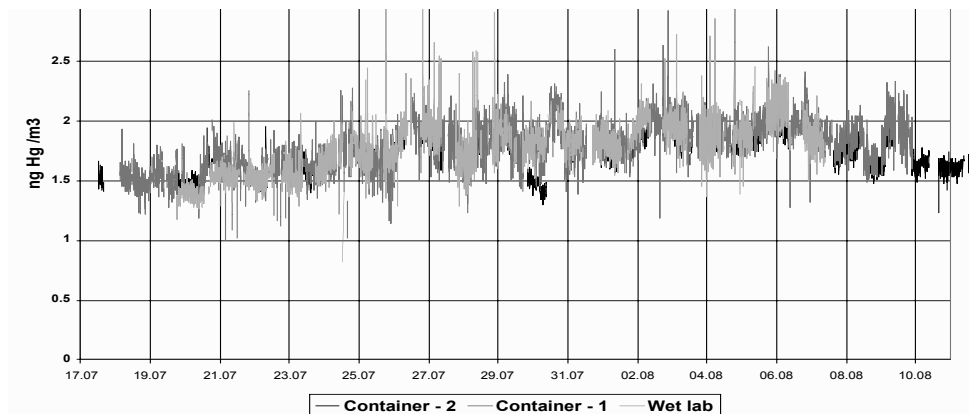


Fig. 5.1: GEM concentrations from 17 July to 10 August with three instruments

The GEM concentration during the cruise seemed to change with latitude, more precisely with the presence of sea ice, where GEM concentrations seemed to increase. This assumption has to be studied in detail, but snow surfaces (i.e. which cover the ice) are known to be a source of GEM to the atmosphere (Dommergue et al., 2003 a,b, Ferrari et al., 2004 ). For RGM and PM, concentrations were very low during all the cruise (see Fig. 5.2), most of the time below the detection limit of the methods. The two techniques for RGM give both low levels (i.e. < 5-10 pg/m<sup>3</sup>).

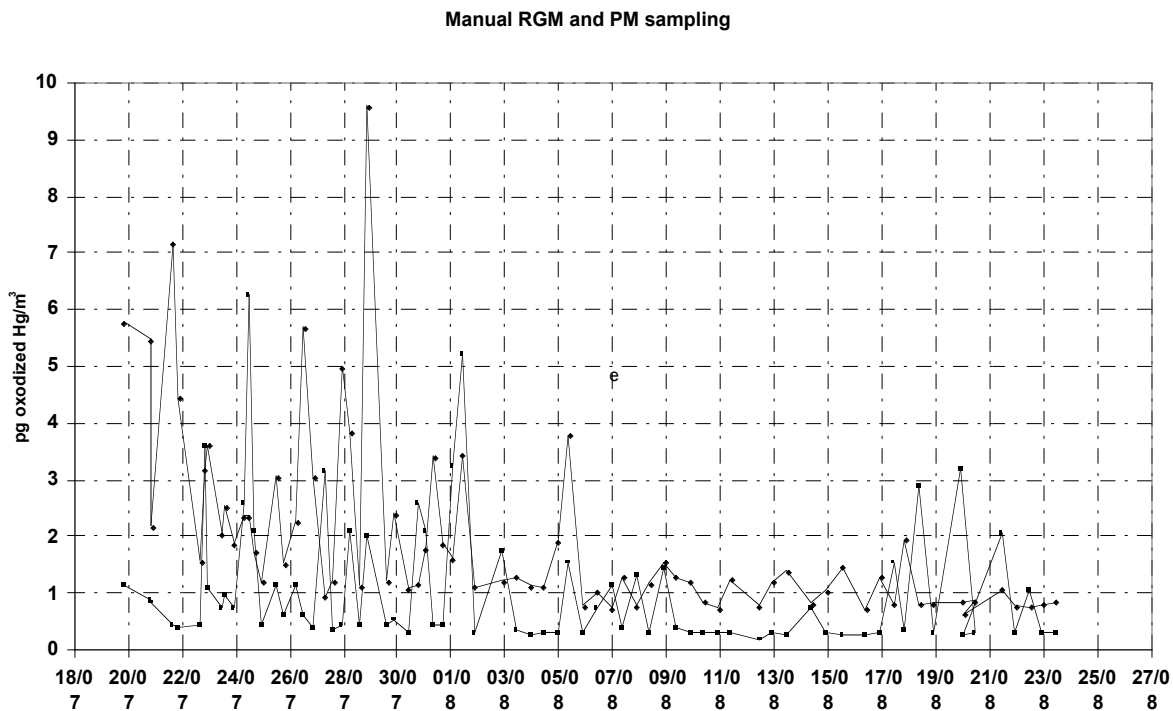


Fig. 5.2: Atmospheric Mercury speciation from 18 July to 24 August for RGM (manual method) and PM

Preliminary results indicated some long stable time periods for ozone and sharp decreases in concentration. It is too early to discuss in details these results as we need to eliminate contamination due to the vessel and helicopters. Their fingerprint is characterized by drops in ozone (due to NO emissions) and peaks in particles (see Fig. 5.3).

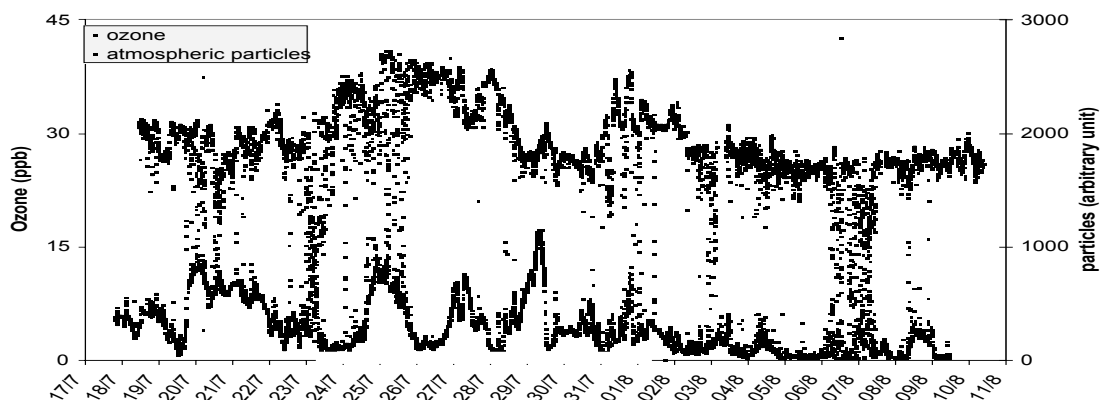


Fig. 5.3: Ozone and atmospheric particles from 17 July to 10 August

## b) Sea to atmosphere flux of Mercury

Sea to atmosphere flux for mercury determination is not based on direct flux measurement but derived from (1) difference in concentration from atmosphere above the sea surface and a derived dissolved gaseous mercury concentration in the first cm of the sea, (2) a mass transfer coefficient. The flux is obtained using the following formula:

$$F = k \frac{(c_{atm} - c_{equ})}{H}$$

Where F is the flux expressed in ng/m<sup>2</sup>/h, k the mass transfer coefficient (m/h), C<sub>atm</sub> the GEM concentration above the sea surface, C<sub>equ</sub> the equilibration concentration reached in our system, directly linked to the dissolved GEM concentration (ng/m<sup>3</sup>), and H the Hg Henry's law constant.

Preliminary results indicated that Hg fluxes from the sea to the atmosphere were about ~ (0.04-6.5) ng/m<sup>2</sup>/h which is in good agreement with evasion fluxes measured over the Pacific ocean (Fig. 5.4). Fluxes did not seem to be correlated with solar irradiation, water or air temperature, but this has to be studied in more detail. When we entered the ice we observed that GEM dissolved concentration was far more important than in open sea. The sea ice acted as a lid, preventing the Hg emission. An other explanation could be that under the ice, some GEM sources, chemical and/or biological, led to the GEM saturation of water.

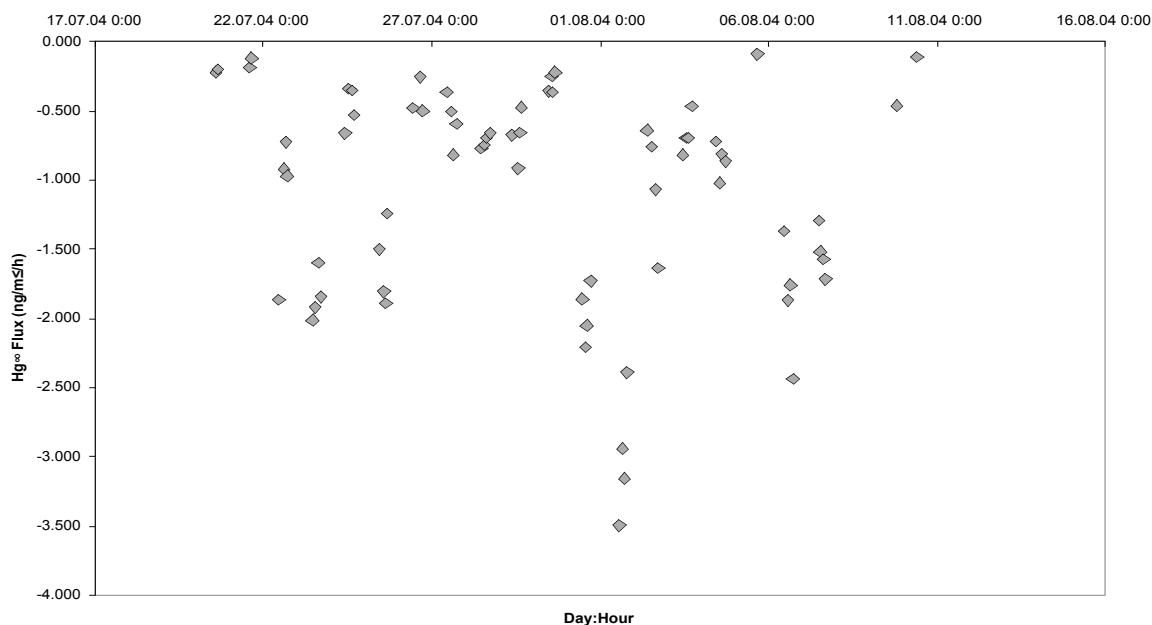


Fig. 5.4: GEM fluxes from the sea to the atmosphere from 21 July to 11 August 2004

## c) Sea water profile for Mercury

In order to assess the ocean water content for Hg, we took the opportunity offered by the oceanographers doing CTD measurements. We were also interested in researching temperature profile anomalies in the water column deep in the ocean corresponding to hydrothermal exhausts from a deep ocean volcano. Our aim was to sample water for Hg determination and to estimate whether this volcanic activity can be a source of mercury. In the atmosphere, volcanic emission is the main natural source for Hg.

The CTD has been done on 17 August (81°21.82'N, 3°3.40'W), and we collected water at the bottom (2239 m), ~ 2000 m, ~ 1800 m, ~ 1700 m, ~ 1500 m and ~ 1000 m for Hg analysis, which will be done in our respective institutes. Hg determination in exhaust plumes from deep ocean volcanoes has never been done before.

## d) Snow, melt pond water, sediments and sea-ice cores

Snow and melt water samples have been collected mostly around 83°N and 84°N as described in figure 5.5. About 200 ml of water in the pond and 500 ml of snow was collected at each sampling place. These samples will be analysed in Grenoble and Oslo for mercury, heavy metals and major ions. Hg will be measured using cold vapour atomic absorption (or fluorescence) spectrometry, which is a really sensitive technique for low mercury levels. These results will allow us to understand if important concentrations of mercury are found in surface snow and melt pond water corresponding to winter to summer deposition. We will then have a better idea if snow is the main pathway for Arctic contamination for mercury. Sediments have been sampled during the different dredges (see Fig. 5.5) for Hg determination so as to assess the stock of Hg contained in deep Arctic Ocean. This will be done for the first time. Finally, in order to assess the stock of Hg stored in the sea-ice, the two ice cores sampled during the first sea-ice station will be analyzed for Hg in Grenoble.

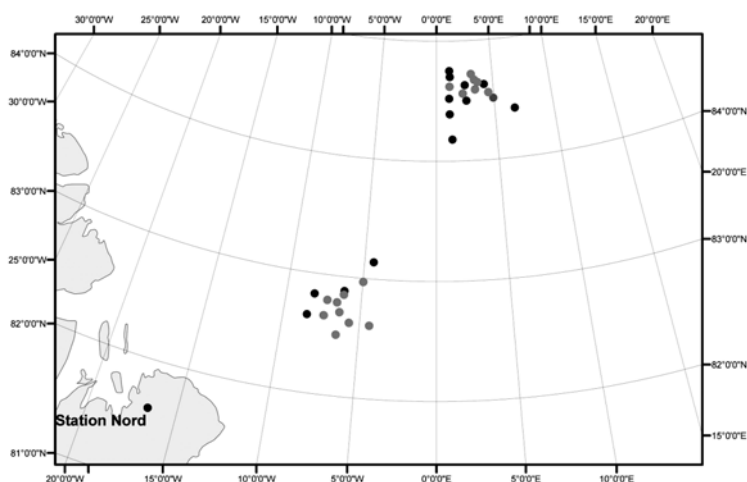


Fig. 5.5 : Snow and melt pond water sampling sites (black) and sediment sampling localisations (grey spots)

#### 5.4.2 Persistent organic pollutants (POPs)

A grand total of more than 75 air samples were collected from Longyearbyen to Tromsø during the ARK-XX/2 (see Tables 5.1 - 5.5). Most samples were collected for analysis of PAHs and PCDD/Fs (25), TSP (25) and PCBs/ OC pesticides (21). Sampling was continued for PFCs (4 samples with ca. 1000 m<sup>3</sup> each) and NPs (2 samples, each with ca. 2200 m<sup>3</sup>). The samples will be analysed in clean laboratories once returned to the different institutions. In each case, air samples were separated by a combination of filter and adsorbent into the fraction of POPs on particles (retained by the filters) and the gaseous fraction (retained by the adsorbent).

To take genuine air samples on a ship is not easy, since it emits pollutants like a small village with its 100 inhabitants, and these pollutants are not of interest in our studies. To sample clean ambient air, the sampling devices were located on the observation deck high up at the front of the ship. Measurements were taken only under head-wind conditions (i.e. relative wind coming from 270 – 360°, and 0 – 90°) with relative wind speeds exceeding 3 m/s. Under unfavourable conditions like aft-winds, the emissions of the helicopters, the ship's engine, incinerator and outgassing from the ship's inside would disturb the measurements. The majority of samples were composed of these 'clean' sampling intervals, which were integrated until a large enough air volume had been collected. During unfavourable wind conditions, the samplers were switched off and the filters covered by lids. A few so-called 'dirty' samples were also collected (see tables) – these will be used to assess the degree to which the ship's outgassing actually influenced the atmospheric concentrations of the various POPs investigated. Sampling was continuous for 'dirty' samples, hence no attention was paid to relative wind direction or speed. The air sampling was complemented by taking several field blanks, i.e. samples in which the sampling media were exposed to the routine handling and deployment without actually sampling any large air volumes. These so-called 'field blanks' are important to derive the detection limits for the air samples based on the contamination incurred during the shipment and handling of the sampling media.

Parallel to the air sampling, representative water samples were collected in the wet lab from the stainless steel direct seawater inlet from the keel of the ship at 11 m depth.

Table 5.1 shows samples collected using the Lancaster University High-Volume air sampler, which will be used to determine concentrations of PCBs, OC-pesticides and PBDEs.

**Tab. 5.1:** Sampling times, locations and duration and flow for the determination of PCB and OC-pesticides (to be analysed by Lancaster University, Lancaster)

Sample ID	Start Date	Stop Date	Hours	MH	Type		
RG 50	17 jul 04	18:50	21 jul 04	20:15	20.8	54"	
RG 51	21 jul 04		21 jul 04		0.0	FB	FB
RG 52	21 jul 04	22:30	23 jul 04	8:50	15.0	54"-56"	
RG 53	23 jul 04	10:00	24 jul 04	14:00	9.2	52"-53"	
RG 54	24 jul 04	17:40	25 jul 04	19:30	24.9	52"-53"	Dirty
RG 55	25 jul 04	8:05	28 jul 04	5:30	20.0	56"-58"	
RG 56	28 jul 04		28 jul 04		0.0	FB	FB
RG 57	28 jul 04	12:50	31 jul 04	20:30	27.4	54"-60"	
RG 58	31 jul 04	21:57	01 aug 04	19.4	16.3	56"-61"	Dirty
RG 59	01 aug 04	18:05	02 aug 04	8:15	14.2	60"	
RG 60	02 aug 04	10:30	03 aug 04	15:00	19.8	58"-54"	Dirty
RG 61	03 aug 04	15:35	08 aug 04	0:20	23.4	56"-54"	
RG 62	08 aug 04	1:10	10 aug 04	10:30	21.7	57"-61"	
RG 63	10 aug 04	17:10	10 aug 04	22:05	17.3	51"-52"-51"	Dirty
RG 64	10 aug 04	22:35	13 aug 04	20:10	26.2	59"-56"	
RG 65	13 aug 04	20:55	15 aug 04	11:25	18.5	58"-56"-53"	
RG 66	15 aug 04		15 aug 04		0.0	FB	FB
RG 67	15 aug 04	15:45	17 aug 04	9:10	19.6	53"-55"	
RG 69	17 aug 04	11:20	18 aug 04	9:10	8.1	54"	
RG 70	19 aug	4:10	20 aug 04	22:05	18.3	58"	
RG 71	21 aug 04	1:02	22 aug 04	5:20	21.3	58"-56"	
RG 75	22 aug 04	7:10	Running				

Table 5.2 represents samples collected using the High Volume air sampler from University of Bremen and the samples collected for the determination of TSP concentrations using a TSP sampler belonging to Lancaster University (Table 5.3). For selected samples during the 2nd half of ARK-XX/2, short-term samples (ca. 10 hours each) were taken to investigate the distribution of PAHs and PCDD/Fs between the gas and particulate phase (abbreviated as GP). For these samples, a back-up filter was deployed to determine the degree of breakthrough of particles and the amount of gaseous adsorption to a clean filter. For these samples, conditions were chosen with high relative humidity (90 – 100 %), as this minimizes the adsorption of gas phase POPs to clean filters.

Samples from the Bremen Hi-vol will be used to investigate the concentration of PAHs and PCDD/Fs in the atmosphere.

**Tab. 5.2:** Sampling times, locations and air volumes for determination of PAH and PCDD/Fs (to be analysed by Bremen University)

	sample N°	start date	stop date	start location	stop location	V (m <sup>3</sup> )
	RL AIR 100	20.07.04 11:45	21.07.04 20:05	78.50 N, 08.20 E	78.50 N, 03.24 E	677
FB	RL AIR 101	21.07.04 22:30	field blank	78.50 N, 02.54 E		
	RL AIR 102	21.07.04 22:30	23.07.04 8:50	78.50 N, 02.54 E	79.58 N, 10.39 E	546
	RL AIR 103	23.07.04 10:00	24.07.04 14:00	80.07 N, 10.26 E	82.07 N, 06.51 E	260
Dirty!	RL AIR 104	24.07.04 18:05	25.07.04 19:30	82.17 N, 06.35 E	82.50 N, 05.16 E	816
	RL AIR 105	25.07.04 20:20	28.07.04 5:30	82.50 N, 05.15 E	83.00N, 00.00W	670
FB	RL AIR 106	25.07.04 22:50	field blank	83.00N, 00.00W		
	RL AIR 107	25.07.04 12:50	31.07.04 20:30	83.00 N, 00.07 W	82.39 N, 06.44 W	758
Dirty!	RL AIR 108	31.07.04 22:00	01.08.04 17:25	82.37 N, 06.49 W	82.30 N, 07.43 W	639
	RL AIR 109	01.08.04 18:05	02.08.04 8:15	82.30 N, 08.13 W	81.52 N, 12.10 W	512
Dirty!	RL AIR 110	02.08.04 10:30	03.08.04 15:00	81.59 N, 10.46 W	82.58 N, 03.28 W	643
	RL AIR 111	03.08.04 15:35	08.08.04 0:35	83.03 N, 04.30 W	84.55 N, 01.44 E	730
	RL AIR 112	08.08.04 1:10	10.08.04 10:30	84.55 N, 01.44 E	83.18 N, 06.58 W	557
Dirty!	RL AIR 113	10.08.04 17:10	15.08.04 15:10	82.59 N, 07.44 W	82.01 N, 04.36 W	615
	RL AIR 114	10.08.04 22:35	13.08.04 20:25	82.48 N, 07.12 W	82.43 N, 03.58 W	840
GP	RL AIR 115	13.08.04 20:55	14.08.04 10:20	82.43 N, 03.58 W	82.28 N, 05.01 W	254
GP	RL AIR 116	15.08.04 24:25	15.08.04 11:25	82.24 N, 04.53 W	82.06 N, 05.10 W	275
GP	RL AIR 117	15.08.04 15:45	16.08.04 14:05	82.01 N, 04.36 W	81.43 N, 05.35 W	295
GP	RL AIR 118	16.08.04 14:05	17.08.04 9:10	81.42 N, 07.14 W	81.22 N, 03.15 W	290
GP	RL AIR 119	17.08.04 23:20	19.08.04 12:00	81.22 N, 03.23 W	82.23 N, 03.37 W	277
GP	RL AIR 120	19.08.04 16:10	19.08.04 12:00	81.17 N, 06.15 W	81.17 N, 03.58 W	244
GP	RL AIR 121	19.08.04 14:10	20.08.04 22:05	81.14 N, 02.35 W	79.16 N, 01.17 W	320
FB	RL AIR 122	20.08.04 22:05	field blank	81.42 N, 07.14 W		
GP	RL AIR 123	21.08.04 18:45	21.08.04 19:00	78.50 N, 02.01 W	78.50 N, 00.31 W	391
GP	RL AIR 124	21.08.04 19:20	22.08.04 5:20	78.50 N, 00.31 W	78.52 N, 00.13 E	271

**Tab. 5.3:** Sampling times and air volumes for determination of TSP concentrations (to be analysed by Bremen University)

sample N°	start date	stop date	V (m <sup>3</sup> )
TSP 100	20.07.04 11:45	21.07.04 20:05	868
TSP 101 FB	21.07.04 22:30	field blank	
TSP 102	21.07.04 22:30	23.07.04 8:50	635
TSP 103	23.07.04 10:00	24.07.04 14:00	387
TSP 104	24.07.04 18:05	25.07.04 19:30	987
TSP 105	25.07.04 20:20	28.07.04 5:30	837
TSP 106 FB	28.07.04 8:30	field blank	
TSP 107	25.07.04 12:50	31.07.04 20:30	1185
TSP 108	31.07.04 22:00	01.08.04 17:25	841
TSP 109	01.08.04 18:05	02.08.04 8:15	615
TSP 110	02.08.04 10:30	03.08.04 15:00	857
TSP 111	03.08.04 15:35	08.08.04 0:35	1014
TSP 112	08.08.04 1:10	10.08.04 10:30	945
TSP 113	10.08.04 17:10	15.08.04 15:10	854

sample N°	start date	stop date	V (m <sup>3</sup> )
TSP 114	10.08.04 22:35	13.08.04 20:25	1135
TSP 115	13.8.04 20:55	14.08.04 10:20	343
TSP 116	15.08.04 24:25	15.08.04 11:25	459
TSP 117	15.08.04 15:45	16.08.04 14:05	410
TSP 118	16.08.04 14:05	17.08.04 9:10	440
TSP 119	17.08.04 23:20	19.08.04 12:00	351
TSP 120	19.08.04 16:10	19.08.04 12:00	339
TSP 121	19.08.04 14:10	20.08.04 22:05	457
TSP 116 FB	21.08.04 10:05	field blank	
TSP 122	21.08.04 18:45	21.08.04 19:00	701
TSP 124	21.08.04 19:20	22.08.04 5:20	407

Table 5.4 and 5.5 show sampling volumes and locations for the samples taken with the GKSS High-Volume air sampler in order to determine PFCs and NP in air.

**Tab. 5.4:** Sampling times, locations and air volumes for determination of perfluorinated compounds (to be analysed by GKSS, Geesthacht)

sample N°	start date	stop date	start location	stop location	volume (m <sup>3</sup> )
ARK-XX/2 -1	11.07.04 23:56				49057
ARK-XX/2 -2					
ARK-XX/2 -3	02.08.04 12:45	15.08.04 9:15	82.12 N, 09.25 W	82.10 N, 04.51 W	1022
ARK-XX/2-LB	14.08.04 15:00	15.08.04 22:00	field blank for 24 hours		
ARK-XX/2 -4	15.08.04 10:45	22.08.04 9:25	82.10 N, 04.05 W	78.50 N 00.20 E	924
ARK-XX/2-FB	15.08.04 10:45	22.08.04 9:25	field blank for 1 week		

**Tab. 5.5:** Sampling times, locations and air volumes for determination of nonylphenols (to be analysed by GKSS, Geesthacht)

sample N°	start date	stop date	start location	stop location	V (m <sup>3</sup> )
ARK-XX/2 -1	15.07.04 12:00	13.08.04 22:35	78.35 N, 08.31 E	82.43 N, 03.58 W	2201
ARK-XX/2 -2	13.08.04 23:15		82.43 N, 03.58 W		

Water samples were collected from the direct seawater inlet pipe from the keel at 11 m depth. They were separated by filtration through a 0.7 µm glass fibre filter (for particulate-bound POPs). The dissolved POPs were then retained on polymer beads in glass columns. Due to the low dissolved concentrations present in Arctic seawater, large sample volumes (ca. 1000 litres) were collected (Table 5.6). Sampling large volumes of seawater can potentially lead to 'break-through' of POPs, i.e. the loss of compounds from the filter or polymer beads. Hence we performed break-through tests on 2 occasions, in which 2 filters were used, and 2 columns were installed in series.

**Tab. 5.6:** Sampling times, locations and volumes of water samples for determination of various POPs (PAHs, PCBS, OC-pesticides and PCDD/Fs) (to be analysed by Bremen University& Lancaster University)

code N°	start date	stop date	start location	stop location	volume (L)
RLW-20	17.07.04 10:30	18.07.04 18:15	78. 50 N, 05.04 E	78.50 N, 05.59 E	1399.5 L
RLW-21	18.07.04 19:00	break-through test			
RLW-22	21.07.04 16:35	22.07.04 18:30	78. 50 N, 02.44 E	78.50 N, 03.29 E	987 L
RLW-23	21.07.04 16:35	22.07.04 18:30	78. 50 N, 02.44 E	78.50 N, 03.29 E	987 L
RLW-24	23.07.04 11:30	24.07.04 14:10	80. 15 N, 10.13 E	82.07 N, 06.48 E	1226 L
RLW-25	26.07.04 19:25	27.07.04 19:40	82. 58 N, 03.28 E	83.00 N, 00.05 E	1435 L
RLW-26	27.07.04 19:50	field blank			
RLW-27	30.07.04 20:15	01.08.04 7:40	82.53 N, 06.11 W	82.35 N, 06.38W	1500 L
RLW-28	01.08.04 18:45	02.08.04 14:50	82.30 N, 08.10 W	82.23 N, 08.12 W	1210 L
RLW-29	03.08.04 19:00	field blank			
RLW-30	03.08.04 19:30	04.08.04 20:05	83.11 N, 04.02 W	84.22 N, 02.52 E	1269 L
RLW-31	05.08.04 10:00	06.08.04 18:15	84.37 N, 02.36 E	84.39 N, 04.12 E	1201 L
RLW-32	19.08.04 14:35	20.08.04 19:30	81.12 N, 02.30 W	79.50 N, 01.45 W	1246 L

## References

- Slemr, F.; Schuster, G.; Seiler, W. J. *Atmos. Chem.* 1985, 3, 407-434.
- Lu, J. Y.; Schroeder, W. H.; Barrie, L. A.; Steffen, A.; Welch, H. E.; Martin, K.; Lockhart, L.; Hunt, R. V.; Boila, G.; Richter, A. *Geophys. Res. Lett.* 2001, 28(17), 3219-3222.
- Wheatley, B.; Paradis, S. *Water Air Soil Pollut.* 1995, 80(1), 3-11.
- Girard, M.; Dumont, C. *Water Air Soil Pollut.* 1995, 80(1), 13-19.
- Schroeder, W. H.; Anlauf, K. G.; Barrie, L. A.; Lu, J. Y.; Steffen, A.; Schneeberger, D. R.; Berg, T. *Nature* 1998, 394, 331-332.
- Poissant, L.; Northern Contaminants Programme, Synopsis of Research 2000-2001, Indian and Northern Affairs Canada, 2001.
- Lindberg, S. E.; Brooks, S.; Lin, C.-J.; Scott, K.; Meyers, T.; Chambers, L.; Landis, M.; Stevens, R. *Water Air and Soil Pollut.: Focus* 2001, 1 (5-6), 295-302.
- Berg, T.; Sekkeseter, S.; Steinnes, E.; Valdal, A.; Wibetoe, G. Presented at the 6th International Conference on Mercury as a Global Pollutant, Minamatta, Japan, October 2001.
- Skov, H.; Goodsite, M. E.; Christensen, J.; Geernaert, G.; Heidam, N. Z.; Jensen, B.; Wåhlin, P.; Feilberg, A. Presented at the Arctic Atmospheric Mercury Research Workshop, Toronto, Canada, 2002.
- Ebinghaus, R.; Kock, H. H.; Temme, C.; Einax, J. W.; Löwe, A. G.; Richter, A.; Burrows, J. P.; Schroeder, W. H. *Environ. Sci. Technol.* 2002, 36(6), 1238 -1244.
- Berg, T.; Sekkesaeter, S.; Steinnes, E.; Valdal, A-K.; Wibetoe, G. *Sci. Tot. Environ.* 2003, 304, 43-51.
- Lindberg, S. E.; Brooks, S.; Lin, C.-J.; Scott, K. J.; Landis, M. S.; Stevens, R. K.; Goodsite, M.; Richter, A. *Environ. Sci. Technol.* 2002, 36 (6), 1245-1256.
- Dommergue, A.; Ferrari, C.P.; Poissant, L.; and Boutron, C.F. *Environ. Sci. Technol.* 2003a, 37, 3289-3297.
- Dommergue A.; Ferrari C.P.; Gauchard P.A.; Boutron C.F.; Poissant L.; Pilote M.; Jitaru P.; and Adams F. *Geophys. Res. Lett.* 2003b, 30, 1621, doi: 10.1029/2003GL017308.
- Ferrari, C.P.; Dommergue, A.; Boutron, C.F.; Skov, H.; and Jensen, B. *Atmos. Environ.* 2004, 38, 2727-2735.

---

## 6. BATHYMETRY

Steffen Gauger<sup>1)</sup>, Tanja Kohls<sup>2)</sup>,  
Sebastian Röber<sup>2)</sup>

<sup>1)</sup>FIELAX GmbH, Bremerhaven

<sup>2)</sup>Alfred Wegener Institute, Bremerhaven

The main task of the bathymetric working group on this cruise was to expand the area in Fram Strait already surveyed by RV *Polarstern* during former expeditions further to the north, with special emphasis to register the geologically and oceanographically important transition from the Svalbard Deep over Lena Trough to the Gakkel Ridge. The systematic survey was done by using the multibeam sonar system Hydrosweep DS2.

The main characteristic of the Hydrosweep deep-water sounding system on RV *Polarstern* is the 90°/120° coverage angle in which the seafloor is depicted with 59 specific values for water depths (hard beams) perpendicular to the ship's long axis. The accuracy of the measurement is ~ 1 % of water depth. The refraction of the sonar beams was corrected by automatic crossfan calibration. By regular transmission and measurement of a sweep profile in the ship's longitudinal direction and comparison of the slant beams with the vertical beam, the mean sound velocity over the vertical water column is determined and is used for the depth computation.

At the beginning of the cruise, on the profile along the 78°50'N across Fram Strait, which was already surveyed by RV *Polarstern* in former years, the new HDBE Mode, (HDBE = High Definition Bearing Estimation) with 240 soft beams instead of 59 hard beams was tested. Because the resolution of the measurement in the ship's across axis is four times higher than before, the seafloor covering is more homogeneous. The calculated DTM's along that test profiles are reflecting the better system resolution by showing a more detailed seabed morphology. Unfortunately the systematic errors of the central beams became more pronounced as well.

The main part of the work was the operation of the sonar system (43 days survey, 19 of them in thick ice) and the data cleaning. Because of the ice operation the mostly automatically working multibeam sonar system had to be observed continuously in order to intervene in case of faulty or abnormal functioning. Erroneous measurements were caused by hydroacoustic disturbances and the changing of the ship's speed and direction because of ice breaking. Ice conditions made post-processing difficult, it was mandatory to check the positions, depths and the ship's attitude data for outliers or blunders, and to correct them. During the data cleaning, about 30 % of the bathymetry data in thick ice regions were rejected in comparison with 5 % in open water. This part of data processing was done by using the software CARIS HIPS and SIPS v.5.3.

In addition to the sonar operation and the data editing, the analysis of multibeam data, the preparation of quick-look track plots and the creation of preliminary bathymetric charts was carried out. For further presentations of the sea bottom topography grids were calculated out of the edited data, using the Generic Mapping Tool (GMT) software. Based on the grids, contour line maps (contour interval 100 m, scales up to 1:150000) with colour coded depth ranges were produced, which gave a vivid display of the oceanic ridge topography. Because the localization of petrologic sampling stations was accomplished based on the bathymetric maps, bathymetry has been proven as being important for geological investigations, as for the oceanographic analysis, e.g. CTD measurement (see Fig. 6.1).

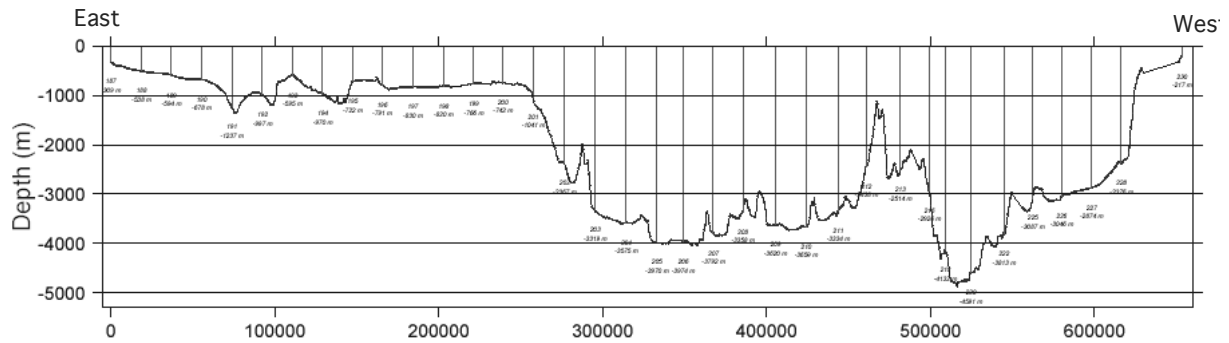


Fig. 6.1: Bathymetry of a line of CTD measurements between Svalbard, Aurora Field and Greenland (geographic position see Fig. 6.4)

For the background bathymetry in the contour maps the IBCAO Vol. 1 (grid spacing 2500 m) data set was used. But since the IBCAO in that region is based on sporadic single beam sonar tracks and predicted bathymetry from satellite data, there were substantial differences between the systematically surveyed area (of this cruise) and the IBCAO. Especially in the area of the Lena Trough and along the Gakkel Ridge there were many outstanding morphological features discovered. Fig. 6.2 shows the difference of the IBCAO and the Hydrosweep data set in a bathymetric profile over a length of ca. 45 km. The predicted basin is non existent and the maximum height difference is 2000 m on the ridge flank (Cagni Sea Mount, 82°50'N/ 4°10'W).

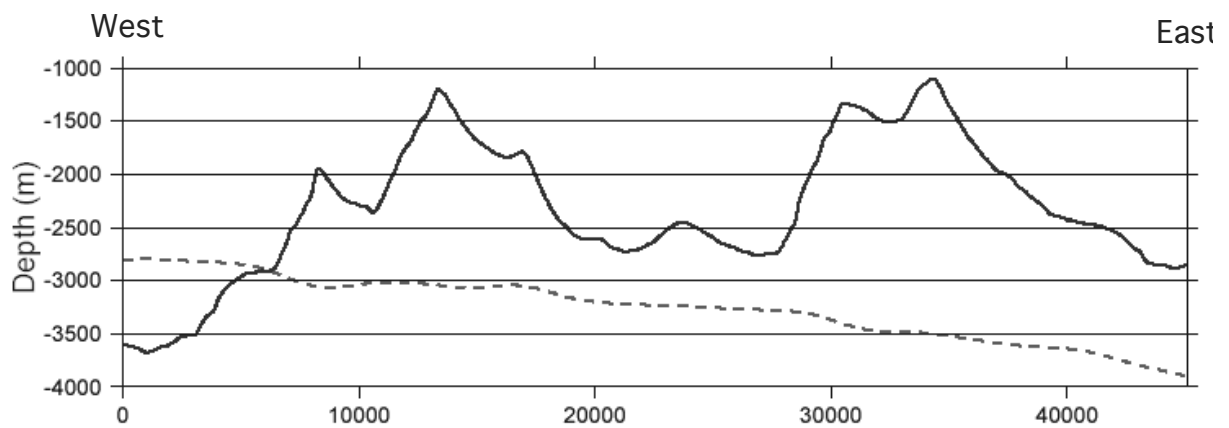
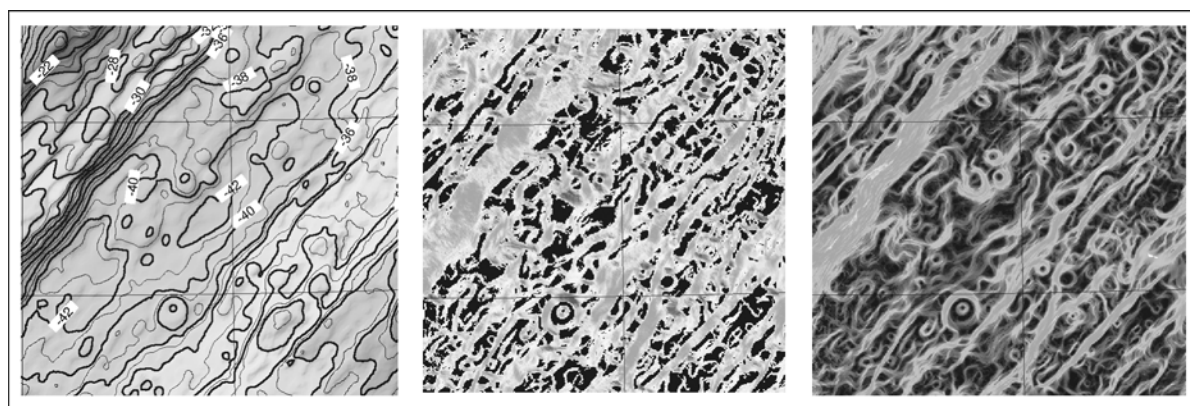


Fig 6.2: Comparison of IBCAO (dashed line) and multibeam bathymetry in Nansen Basin (geographic position see Fig. 6.5, solid line)

During this cruise, the Lena Trough was surveyed systematically for the first time by a multibeam sonar system (Fig. 6.4). The recorded area has an expanse of ca. 10000 km<sup>2</sup> and connects previously mapped areas of the Eurasian-North-American plate boundaries between Fram Strait and Gakkel Ridge. The region of Western Gakkel Ridge, mapped in 2001 by RV *Polarstern* and USCGC Healy (USA), was extended by two more profiles (each 220 km long) along the ridge.

For further morphological interpretation of Lena Trough and Gakkel Ridge slope magnitude and slope direction maps were produced (see Fig. 6.3). They show clearly the predominant slope direction (Fig. 6.3, B) and are helpful in distinction between sediment basins, small volcanos and ridge flanks, based on the slope magnitude (Fig. 6.3, C). Especially the slope magnitude map shows lots of small volcanic features, which are hard to discover in the contour line map (Fig. 6. A).



A

B

C

*Fig. 6.3: Details of the bathymetry  
(A) the slope direction  
(B) and the slope magnitude  
(C) maps in the area of Western Gakkel Ridge  
(geographic position see Fig. 6.4, black square)*

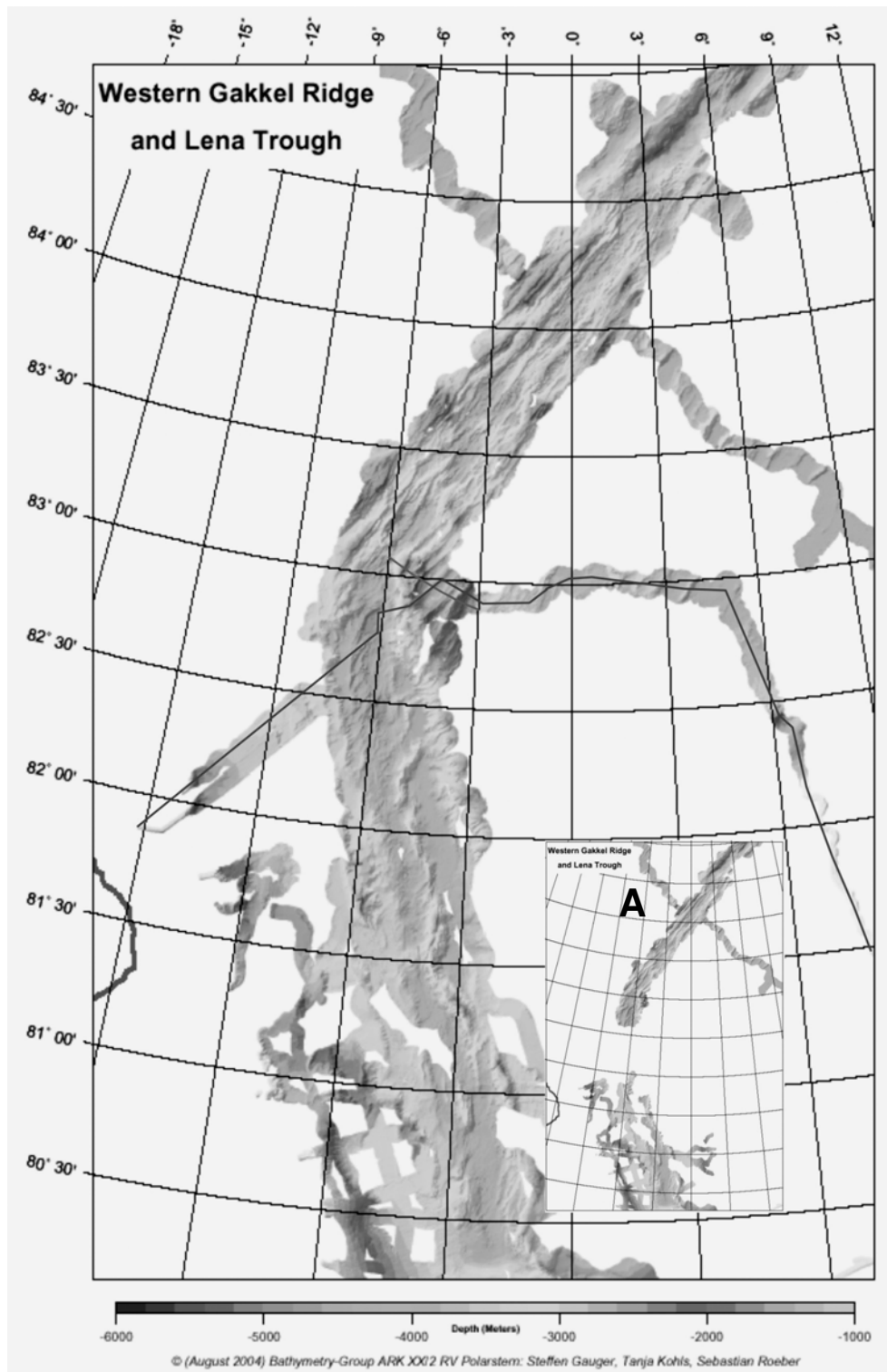


Fig 6.4: Overview of the surveyed area, in comparison to the previous mapped region (A); the lines represent the profile of depth comparison (see Fig. 6.2) and the CTD profile (see Fig. 6.1). The square represents the geographic position of the map example in Fig 6.3.

---

## 7. PETROLOGIC AND TECTONIC EVOLUTION OF THE LENA TROUGH AND WESTERN GAKKEL RIDGE

Jonathan Snow<sup>1</sup>, Schmitt<sup>2</sup> (was not on board), Biegler (was not on board), Heinrich Feldmann<sup>1</sup>, Anette v.d. Handt<sup>1</sup>, Eric Hellebrand<sup>1</sup>, Francois Nauret<sup>1</sup>, Yongjun Gao<sup>3</sup>, Sandrin Feig<sup>4</sup>, Regina Eckardt<sup>5</sup>, Timo Liesenfeld<sup>5</sup>, Simona Turini<sup>5</sup>, Zoran Janovic<sup>6</sup>, Joseph Morgan<sup>7</sup>, Kai Wiegler<sup>5</sup>

<sup>1</sup>Max-Planck-Institut für Chemie, Mainz

<sup>2</sup>Department f. Geo- und Umweltwissenschaften, München

<sup>3</sup>University of Göttingen, Göttingen

<sup>4</sup>University of Hannover, Hannover

<sup>5</sup>University of Mainz, Mainz

<sup>6</sup>University of Salzburg, Salzburg

<sup>7</sup>CITL Cambridge, Cambridge

### 7.1 Summary

The Arctic mid-ocean ridge spreading system, including Lena Trough and Gakkel Ridge, is one of the key regions of the world's mid-ocean ridge system and occupies a unique place in the tectonics of the Northern Hemisphere. ARK-XX/2 studied the petrologic, tectonic and hydrothermal development of Lena Trough and the western part of Gakkel Ridge. By taking rock samples from the sea floor, bathymetry, water samples, gravity and parasound data, the opening history of Lena Trough and its unique role as an ultraslow spreading ridge, nascent oceanic basin and gateway for the flow of deep water currents from the Arctic into the North Atlantic basin has been brought into better focus. Sampling operations were quite successful, owing to good ice conditions and improved sampling techniques since the previous cruise in 2001.

Mapping and sampling extended to complete coverage of the Lena Trough, expanding the bathymetric coverage of the western Gakkel Ridge and detailed mapping and sampling in the special region at 3°E on Gakkel Ridge. The rocks recovered correspond generally with a low degree of mantle partial melting and the attendant exposure of mantle rock types in the Lena basin. An overview of the mapping and sampling is given in figure 7.1. A (before) and 7.1 B (after).

Further highlights of the petrology programme include the recovery of hydrothermal deposits and the detection of active venting at the Lucky B field in Lena Trough. The hydrothermal activity is most likely based on a substrate of mantle rock without significant basaltic eruption nearby. Also, significant amounts of very fresh mantle peridotite were recovered from the Gakkel Ridge. Mid-ocean ridge mantle is notoriously difficult to study because of its alteration. Fresh samples are extremely rare and extremely valuable in order to solve questions about the formation of the Earth's crust and mantle. The samples from this cruise extend the world's supply of fresh abyssal peridotite by about factor four.

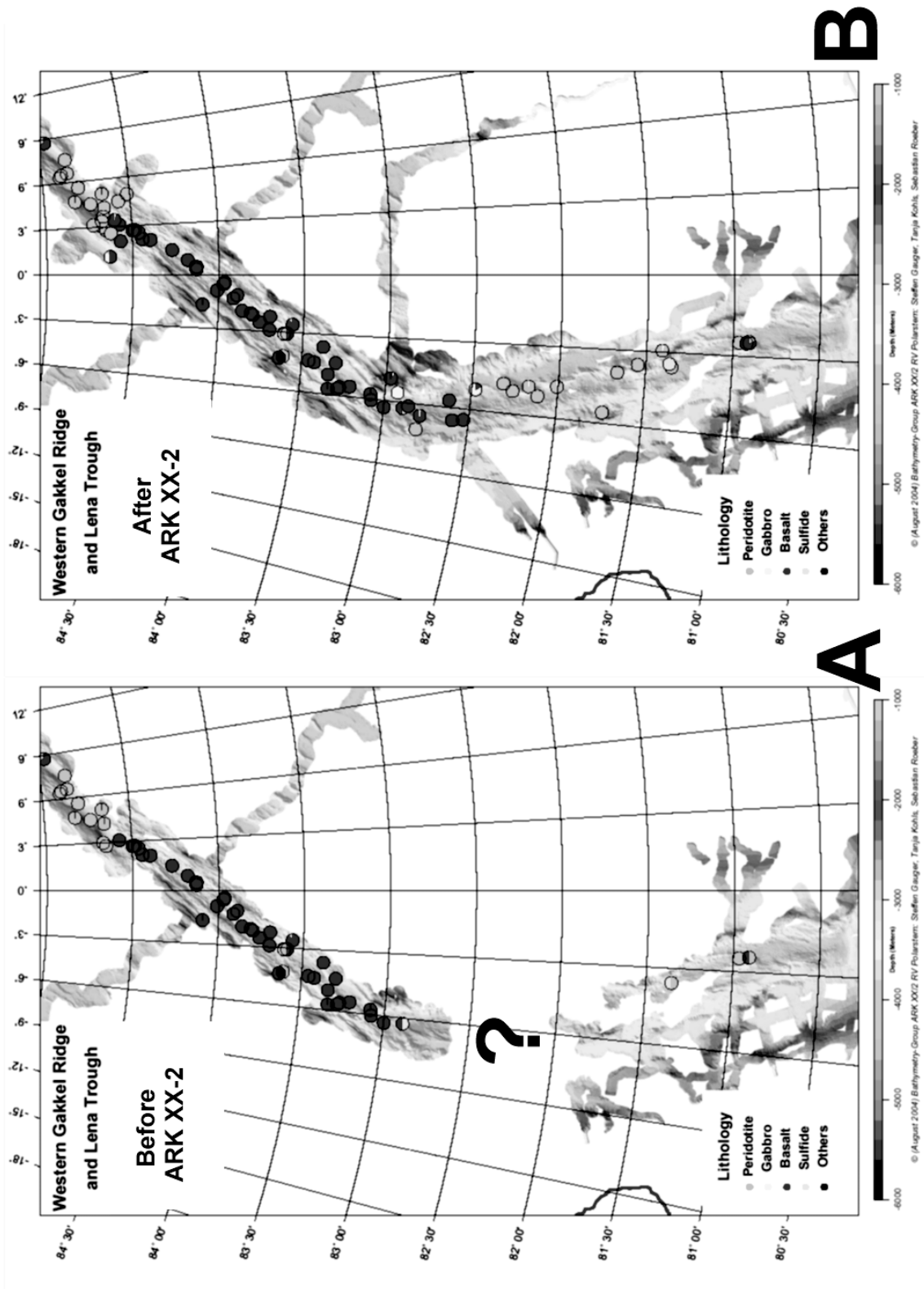


Fig. 7.1: Overview of mapping and sampling in Lena Trough and Gakkel Ridge

## 7.2 Introduction

Jonathan Snow  
Max-Planck-Institut für Chemie, Mainz

Lena Trough is an enigmatic linear deep in the Arctic Ocean that is a key region for many aspects of Arctic geography, morphology, tectonics, petrology, mantle geochemistry and ocean circulation. Gakkel Ridge is the northeastern continuation of Lena Trough through the Arctic Ocean, dividing it into the Nansen and Amundsen Basins. Lena Trough forms part of the floor of Fram Strait and the western part of the Nansen Basin. Most of Lena Trough is northward of an imaginary line crossing the narrowest part of Fram Strait, and thus can truly be said to belong to the Arctic Ocean.

The morphology of the floor of Lena Trough until now has been extremely poorly constrained because of persistent ice cover and press conditions in this region. The southern part of Lena Trough has been mapped partly on several RV *Polarstern* cruises (principally ARK-XIII/2, ARK-XV/2, and ARK-XVIII/2). The northern juncture with Gakkel Ridge was mapped on the AMORE Expedition which also mapped the Gakkel Ridge rift valley out to a longitude of 85°E. Otherwise the only constraints on the morphology of Lena Trough are several submarine crossings from the early 1960's (IBCAO, 2000). Figure 7.2 illustrates this situation, showing the traverse of ARK-XX/2 across the Nansen Basin in comparison to the preexisting data in the IBCAO data set. The long straight lines in the study from the IBCAO data are submarine tracks with standard 3.5 KHz echo sounders from before 1963, when such data became classified.

Lena Trough is 350 km long, from its junction with the Spitsbergen Fracture Zone at 80°25'N, 1°W to its junction with Gakkel Ridge at 83°N, 6°W (Fig. 7.1. B). It is a deep linear trough, flanked on either side by the continental margins of Greenland and Europe. Because of the paucity of data through the years, many different theories of the formation and significance of Lena Trough have been postulated. The first bathymetric compilation of the Arctic Ocean (Fig. 7.3) shows a narrow sill of continental shelf linking the North American and European continental margins. This feature became known as the Nansen sill, and its non-existence (and thus the existence of Lena Trough) was not shown definitively until the 1960's. Except for a few isolated basement highs in the southern portion of Lena Trough little was known otherwise about the morphology of the floor of Lena Trough until this cruise. It is shown as having depths of 4000-4200 meters and its deeper basins are filled with a massive sedimentary cover. North of Lena Trough, the rift valley mapped in 2001 becomes shallower by about 500 m and turns to the NE as Gakkel Ridge. At the bend, significant highs are produced on the inside corner, producing a volcanic ridge that extends off-axis for many kilometres. Gakkel Ridge remains straight and relatively shallow for about 200 km before deepening at the far eastern end of the present study area in the 3°E region of Gakkel Ridge.

Gakkel Ridge and Lena Trough are part of the global mid-ocean ridge spreading system, and form the boundary between the North American and European plates. Gakkel Ridge is a normal mid-ocean ridge, of a special ultraslow –spreading variety

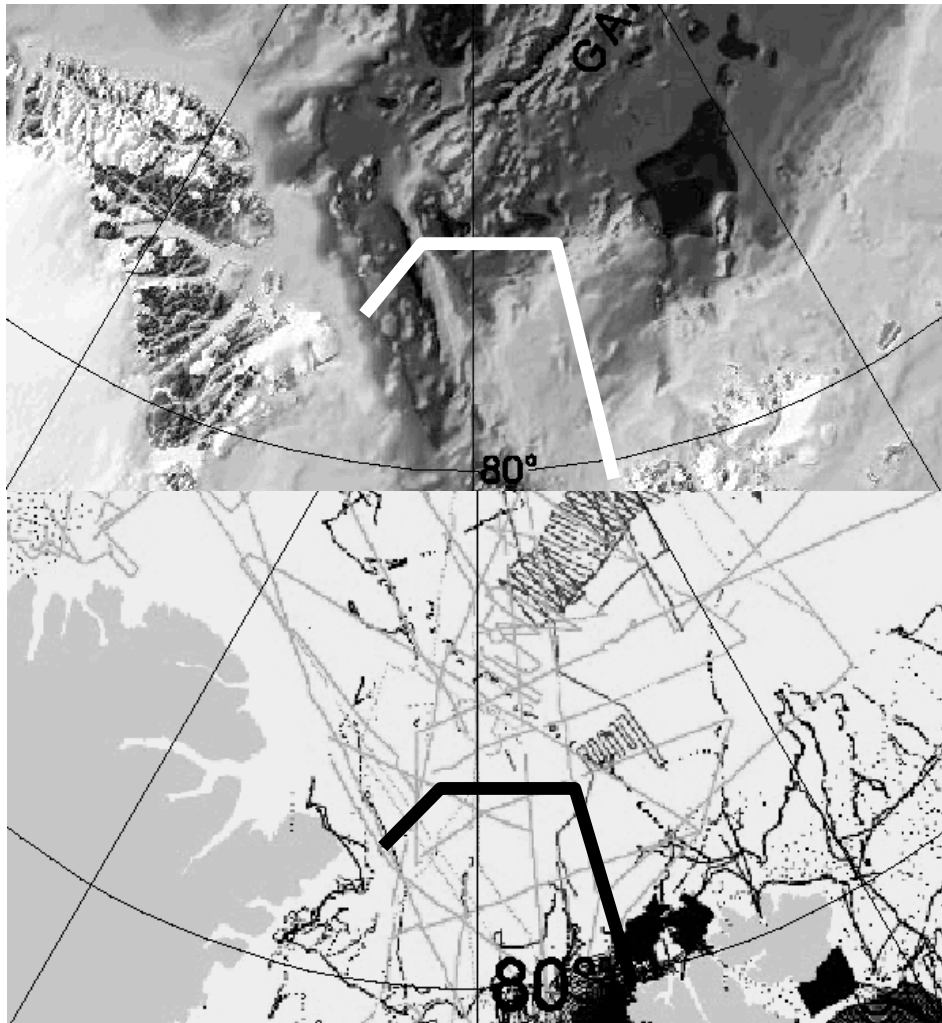


*Fig. 7.2.: Annotated IBCAO bathymetry (2a) (with data sources, 2b). The study area of ARK-XX/2 includes very few pre-existing data.*

In Lena Trough, the two continental margins are very close to one another, and so Lena Trough can be considered an Ocean-to-Continent transition (OCT), and is the only modern OCT in the world. It is thus the only modern example for several OCT's known in the geologic record, including the Iberian Margin (130 Ma) and Western alpine ophiolites (150 Ma).

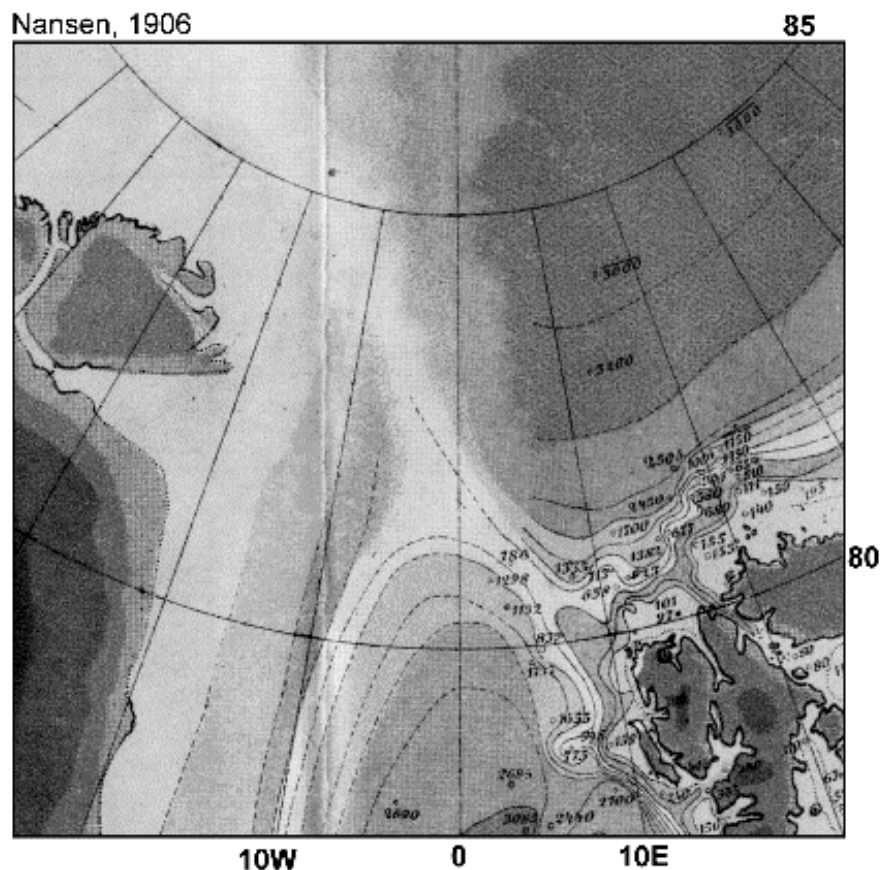
Sampling on Lena Trough and Gakkel Ridge has revealed a magmatically robust rift system in the Western Gakkel flanked by deeps in Lena Trough and the 3°E region of Gakkel Ridge which contain little or no basaltic cover. Basaltic rocks in all regions show a very low degree of partial melting, while peridotites are highly variable but

also suggest an overall low degree of partial melting. Because Gakkel Ridge/Lena Trough are the slowest spreading mid ocean ridge in the world, their basalt and peridotite compositions are expected to provide key information about the process of formation of basaltic magmas (by far the most common on Earth) in general.

Lena Trough was the last of the major oceanic gateways to open. In comparison to other gateways for oceanic circulation, the history of Lena Trough's opening has been relatively poorly studied. Except for a handful of tectonic studies, most of the history of the Lena Trough opening has been constrained indirectly through coring operations in the Greenland Sea, which attempt to reconstruct the former flow of deep water through the opening.

The petrology component of this cruise was carried out in order to place better constraints on the tectonic and petrologic history of Lena Trough and Gakkel Ridge. Here we report the results of the petrologic operations and their immediate significance for the study of the western Arctic.

Fig. 7.3:  
Nansen (1906)  
Western Arctic  
Bathymetry



## 7.3 Data and Sample Collection Methods

### 7.3.1 Dredging Methods

Jonathan Snow  
Max-Planck-Institut für Chemie, Mainz

#### Introduction

Dredging is an age-old and time-tested means of taking ocean-floor samples. It may not have the cachet of more modern and advanced techniques, and the inability to do real geology with dredged samples may make its use frustrating to the land geologist, but dredging has a lot of advantages too. For one it is simple and robust. Most operators can routinely get over 70 % success rates with dredging. It is inexpensive: dredges cost in the thousands, and even though they are sometimes lost, that makes them cheaper than more modern sampling techniques (Remotely Operated Vehicles, for example) which cost in the millions. Dredging also requires little technical support, and most ships equipped with a winch and GPS are capable of doing it.

The object of the dredge is to drag the tool across the ocean floor in a means calculated to maximize useful sample return and minimize losses.

### 7.3.2 The Equipment

#### The Dredge

Dredges come in two basic varieties, barrel dredges and frame dredges. Barrel dredges consist of a reinforced pipe with eyelets on either side and back for the support chains, steel teeth around the leading edge, and a steel grill on the bottom to let the mud out and keep the rock samples in. Figure 7.4 shows such a dredge made by Eisen- und Stahlbau Kiel. Frame dredges are more complex and consequently more expensive. Figure 7.4 also shows a frame or chain bag dredge (Kawohl GmbH, Hannover) the heart of which consists of a rectangular galvanized steel frame. On this frame are attached teeth on one side, a chain bag on the other, and on the sides a hinged massive bridle that provides the attachment to the ship's cable. The chain bag is usually so constructed that there is an attachment point on the back for a safety chain, which is a part of the system of weak links, about which more later. The chain bag is made of hardened stainless steel links and is by far the most expensive part of the dredge.

#### The Wire

Dredging is one of the most demanding applications for a deep sea cable. Done correctly, it does not result in damage to the cable. In order to understand how this is possible, some theory is necessary. Dredging wires vary strongly from ship to ship. American and Japanese ships use UNOLS standard 9/16" deep sea trawling wire. This is a load balanced multistrand wire rope, and was the first load balanced cable invented in the early 1950's precisely for use in the US research fleet. Load balancing means that the three individual bundles that make up the UNOLS wire are wound internally in the opposite direction to the direction they are wound around

each other. This balances out the loads exerted on the wire when under tension, and lessens the tendency of the wire to unwind when placed under load. In the meantime a variety of different cables are in use worldwide, on RV *Polarstern* the standard cable is Casar Starlift, an 18 mm load balanced, internally lubricated wire that is state of the art in deep sea cables.

Wire ropes can be thought of as machines. They are highly specialized devices, with a high tensile strength, but nonetheless quite flexible, and capable of being riven over a sheave (whose minimum diameter is characteristic of each wire) without damage. They require regular servicing, inspection and protection.

The strength of a cable is determined by the sum of the cross sectional areas of *continuous* strands in the cable, multiplied by the tensile strength of the steel used. A thick cable with many strands is obviously a stronger cable than a thin cable with few strands.

When placed under stress, most materials (cables included) will at first deform elastically. That means that when the stress is removed, the test object returns to its original shape. Stress in the elastic regime can be repeated over and over again without damage or loss of strength of the test piece. Beyond the elastic range, cables and other materials tend to soften, reaching a maximum stress beyond which they either fail catastrophically or deform internally, resulting in strain softening. In a cable, an unambiguous sign of this is a negative rope length at the end of a deployment. This means that the cable is longer after use than it was originally and consequently is damaged and cannot be re-used.

In practice, it is only the continuous strands that count. A break in any of the strands, anywhere in the cable, weakens the cable. For this reason cables are rated by their MBL or maximum breaking load. In the case of Starlift this is 25 metric tons. However, this load is a theoretical value for new cable. The strength of the cable is some undefined value less than the maximum breaking strength. Ordinary wear and tear, and actual damage to the cable both reduce the actual strength. The object of good dredging is to protect the wire in such a way that a maximum of its elastic range (the “working load”) can be used without putting the wire in danger of damage.

There is no defined working load for any wire. The OSHA defined “safe working load” is defined as one-sixth of the maximum breaking strength, and is intended for protecting humans whose lives depend on the wire’s strength (in elevators or cranes,



Fig. 7.4: Frame and barrel dredges used on ARK-XX/2

for example). It is much too conservative for use in dredging. Generally, 65 % of MBL is considered safe as a transient static load for most cables.

It is not wise to use a wire for dredging that is in any way damaged or old. Using old cable for dredging is a false saving, as it can result in the loss of the cable, the loss of ship time, the loss of the dredge and scientific samples and potentially damage to the winch or injury to the ship's crew.

### Rigging

Figure 7.5 shows a simple dredging arrangement. The dredge is attached to a bridle made of material far stronger than the maximum pull. Since the OSHA 6-fold rule applies here as well, shackles and chains should be chosen accordingly. For Casar Starlift (MBL 25T), 3/4" shackles (SWL 6T, breaking strength 56T) are more than adequate. If wire is used for bridle or other parts, it should be the same as the dredging cable. The rule of thumb should be that the total cross section of steel in the tackle used should be about the same as that in the dredging cable.

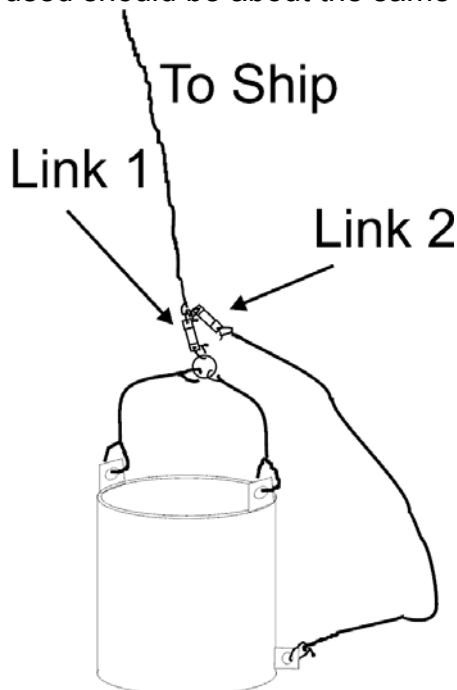


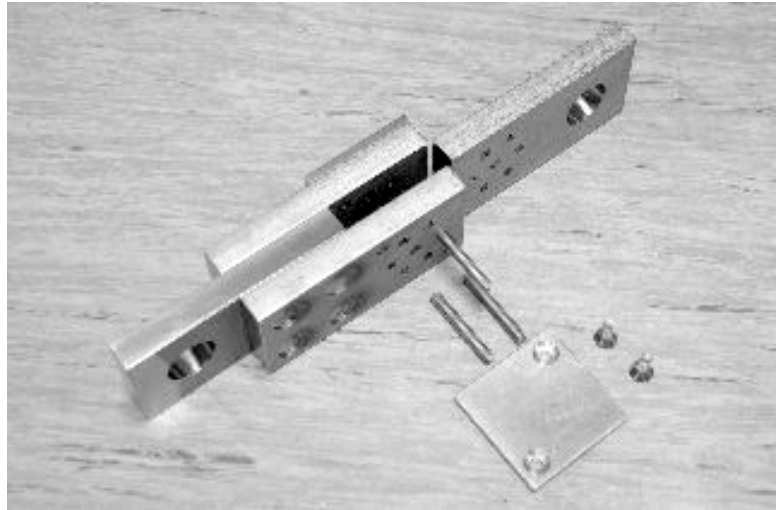
Fig. 7.5: Rigging a dredge

Wire rope has proven to be a poor material for rigging dredges. As soon as the dredge touches bottom, wire rope dredge rigging begins to deteriorate, and rapidly loses strength. Wire rope rigging often has to be replaced after only one or two uses. Chain, though more expensive, is much more durable.

### Weak Links

Modern weak links (Fig. 7.6) are constructed following a practice initiated in the US in the 1950's out of plates of precipitation-hardened stainless steel. They use pins of different compositions with predefined shear strengths to connect the plates and assure that the weak link breaks with exactly the desired load. The weak links used here are described in a previous cruise report (ARK-XVII/2) and so only the weak link table (Table 7.1) is reproduced here. The weak links are set so that they break with a predefined load on deck, 14.5 t and 15 t were used for the first and second weak links in this case.

Fig. 7.6: MPI weak link with shear pins



Tab. 7.1: MPI weak link settings for CASAR Starlift 18 mm, 1.18 kg/m in water

Dept h m.	Wire:			Breaking strength on deck Kg	Breaking strength															
	Steel	Brass	Alu99		Depths:															
1000	3	2	0	13917	1000		500													
	3	1	2	13300	15103	14510														
1500	3	1	2	13300	Depths: 1500			1000			500									
					15079	14486	13893													
	3	1	0	12473	14252	13659	13066													
					Depths: 2000						1500		1000		500					
2000	3	1	0	12473	14845	14252	13659	13066												
	3	0	2	11856	14228	13635	13042	12449												
2500	3	0	2	11856	Depths: 2500				2000		1500		500							
					14821	14228	13635	13042	12449											
	3	0	1	11442	14407	13814	13221	12628	12035											
					Depths: 3000						2500		2000		1500		1000		500	
3000	3	0	1	11442	15000	14407	13814	13221	12628	12035										
	3	0	0	11028	14586	13993	13400	12807	12214	11621										
3500	2	2	1	10655	Depths: 3500						3000		2500		2000		1500		1000	
					14806	14213	13620	13027	12434	11841										
	2	2	0	10241	14392	13799	13206	12613	12020	11427										
					Depths: 4000						3500		3000		2500		2000		1500	
4000	2	2	0	10241	14985	14392	13799	13206	12613	12020										
	2	1	2	9624	14368	13775	13182	12589	11996	11403										
4500	2	1	2	9624	Depths: 4500						4000		3500		3000		2500		2000	
					14961	14368	13775	13182	12589	11996										
	2	1	1	9210	14547	13954	13361	12768	12175	11582										
					Depths: 5000						4500		4000		3500		3000		2500	
5000	2	1	1	9210	15140	14547	13954	13361	12768	12175										
	2	1	0	8797	14727	14134	13541	12948	12355	11762										
5500	2	0	2	8180	Depths: 5500						5000		4500		4000		3500		3000	
					14703	14110	13517	12924	12331	11738										
	2	0	1	7766	14289	13696	13103	12510	11917	11324										
					Depths: 6000						5500		5000		4500		4000		3500	
6000	2	0	1	7766	14882	14289	13696	13103	12510	11917										
	2	0	0	7352	14468	13875	13282	12689	12096	11503										

### 7.3.5 The 5 Phases of Dredging

#### Positioning

Dredging is not a matter of breaking rocks off a specific outcrop. Dredging always samples loose talus from a whole slope, and thus the best dredging targets are talus piles. Unsedimented basalt pillow fields are also attractive dredging targets for the same reason. In the open ocean, positioning is simple: you drive to the base of the slope. If there is wind, and there is a choice, it is better to dredge against the wind, because it is then easier to control the ship. In ice, the problem is more complex because of the limited mobility. Ice confers some advantages, however, because of the lack of waves. It is best to dredge in a nice smooth polynya. Of course this is not always possible, but it is important to always be on the lookout for dredge sites of opportunity, and to research secondary sites carefully, so that good dredging situations can be taken advantage of.

If a polynya is not available, then a lead is needed that goes across the slope to be dredged. If this is not possible, the last option is to break a lead free. In relatively loose ice, the slope can be approached from the top, the lead broken free on the first pass, then turn and dredge up the slope. If the slope is approached from the bottom, an odd number of passes is required.

A special problem occurs when the bathymetry is approximate or unknown. In this case, the slope has to be mapped while breaking the passage. However, the multibeam mapping systems do not map ahead of the ship, so it is difficult to tell where the slope is. A good technique here is to turn the ship 360° in a clear patch, so that the side beams of the multibeam system illuminate the slope ahead. The 360° rotation allows both sets of side beams to sweep the slope.

Slopes with about 400 m of elevation change in 2 km have been shown by experience to be the optimum dredging slopes. Gentler slopes can be dredged in relatively unsedimented areas, such as young ocean crust, but steeper slopes should be avoided, as they tend to hang up the dredge.

#### Lowering

The dredge is assembled and the weak links set to just below the current depth. Dredge-in-water is recorded in the dredging log. The dredge is then lowered with 1.0 m/s for the first 100 m. After the first 100 m the lowering speed is increased to the maximum winch speed until the bottom is only 50 m below the dredge. The winch speed is reduced to 0.5 m/s and the vessel starts moving up the slope with 1 kn. A bump on the chart recorder (a pressure release of ~0.2 t !) tells when the dredge is on bottom. After the time and location are logged the paying out phase starts. It has been said that chain bag dredges should not be lowered faster than 1.5 m/s, as the chain bag might be forced up into the dredge opening by water resistance. I have no evidence to support this idea, and prefer to lower with maximum speed (usually 2 m/s) if permissible. It is important to lower as fast as possible in ice, as the ship is otherwise apt to drift off position otherwise.

It is important to keep station during the lowering phase. If this is not possible, keeping in a position to dredge the target slope is paramount. If the leads available for dredging drift into a position such that the steep part of the slope is no longer reachable, an empty bucket or a mud bucket are the likely result.

### **Paying out underway**

The object of this step is to lay out a length of cable on the ocean floor without knotting it or moving the dredge. It is not good practice to lay out cable on the ocean floor without moving. This is because without moving, the cable will lay out in loops on the ocean floor that may kink or snag when pulled straight.

The proper wire speed should be just enough to keep the wire straight on the ocean floor. If the wire is considered to be a straight line, then the Pythagorean Theorem  $A^2=B^2 + C^2$  would predict the correct wire speed to be the root of the squared water depth and distance 1 kn = 1800 m/h = 30 m/min = 0.5 m/s. In general, it is thus permissible and desirable to make at least 1 kn over ground while paying out at 0.5 m/s.

Wire should be paid out so that about 1 km of wire is on the bottom at the end of the dredging run. So for example, in water of 4000 m depth, with a lead of 1.8 km and an elevation change of 500 m, another 500 m is deployed, resulting in a 3500 m water depth at the end of the run, and 4500 m of total wire out.

### **Towing**

If the previous step has been done correctly, the tension meter will often show bottom working immediately upon stopping the winch. Usually, however, bottom working during towing is either not seen or is ineffective. This is because the resistance of the water on the wire as it is towed makes the wire angle on the bottom nearly vertical even if a relatively large amount of wire is paid out. Attention should be paid to the tension meter to avoid hang-ups, and react promptly if they occur. However, hang-ups in this stage are relatively rare. 1 kn is the usual speed for towing (=0.5 m/s wire-in), but momentary speeds of 2-3 kn are acceptable if needed for light icebreaking.

### **Reeling in**

Reeling in is the most nerve-wracking part of the dredging operation, since the operator can do relatively little to influence the process at this point. If the slope is good, the wire properly laid out, and towed straight, bottom working (small bites up to 1 ton) are the result, followed by larger bites of a few tons, followed by off-bottom. 1000 m at 0.5 m/s takes 2000 seconds, or about 40 minutes. The subsequent reeling-in time can be calculated from the water depth. If the previous steps haven't been done correctly, or if the operator is unlucky, the reward could be either a mud dredge, an empty dredge, or worse, no dredge at all.

## Hang-ups

A hang-up is defined as a bite that goes to a tension close to the breaking strength of the first weak link. At this point the tension should be monitored and not allowed to exceed more than 90 % of the weak link's strength. Often, after simply waiting for a time, the dredge comes free of its own accord. If not, the first manoeuvre to perform is backing down the wire. This is done by backing the ship (with the cable unloaded) and pulling in wire until the wire angle behind the ship is zero and the wire is vertical. Then pull to the maximum comfortable load and wait again.

The next technique to try is to unload the cable, and pay a few meters more out (~20 m), then pulling the cable tight. This is risky, as cable on the ocean floor can wrap around things at this point. If this is not successful, the ship must be turned in the opposite direction and a pull made from downslope. Again, the cable is first unloaded, then reloaded.

Finally if these techniques have been tried over and over, the next step is to go nearly to the weak link strength and try again. If that fails, pull until the weak link breaks. Usually, the dredge is free, but sometimes, the whole process has to be repeated with the second weak link and the dredge is lost.

## 7.4 Dredging Results

Eric Hellebrand, Annette von der Handt  
Max-Planck-Institut für Chemie, Mainz

On ARK-XX/2, dredging operations were carried out exclusively from the bridge. This simplified communications with the winch operator and bridge crew and made it possible to evaluate ice conditions and slope configuration simultaneously. This should be the preferred method of dredging on RV *Polarstern* from now on.

38 dredging operations were carried out. The dredging operations took on average about 4 hours to complete, but this does not include positioning and breaking free a dredging lead, which in pack ice conditions can consume considerable time. It was found that breaking a path was generally not useful, as the broken paths were often abandoned, either because of ice drift or simply by losing them in heavy fog. Light ice breaking during dredging operations, including gentle (2-3 kn) backing and ramming was found to be feasible. The low rate of hang-ups contributed to this situation, as there was thus rarely a need to back down on the wire.

Table 7.3 shows the dredging stations. 32 out of the 38 were successful, defined as containing igneous rock, there were no material losses. Thus the dredging success rate was 82 %, about on a par with the results from 2001. 4 of the last 6 dredges were unsuccessful, due to the heavy sedimentation in Lena Trough.

**Rock curation**

During ARK-XX/2 to the Lena Trough almost 3.7 tons of rocks were brought aboard in 38 dredge operations. Among these were 1451 kg of peridotites, 18 kg gabbros, 58 kg diabase as well as 1600 kg basalt. One single dredge haul PS66-258 brought 62 kg of hydrothermal deposits. The range in weight of a single sample was from a few grams up to approximately 100 kg (a large peridotite block from station 238). All samples brought on board were catalogued and described.

Once on board, the rocks were washed, cut and allowed to dry. They were then sorted into different lithologies and their subtypes. The samples were given numbers in the following way: Ship name - Cruise number – station number – sample number, for example: PS 66 – 201 – 1. The weight of each sample was noted to determine the weight distribution of the different lithologies. Additional notes were made on the dimensions, modal content, degree of alteration and deformation and the further processing. Each sample was photographed, these images are available to identify samples for further study. If available, basaltic glass was chipped from the working samples and microprobe mounts were produced. Representative samples were chosen for thin section production and thin section blocks from most samples were produced. Altogether 303 thin sections were made. The samples were then packed in sealed numbered bags.

All RV *Polarstern* samples are the property of the Alfred-Wegener-Institut für Polar- und Meeresforschung in Bremerhaven. The destination for all peridotites, gabbros and hydrothermal deposits is Mainz. Of the basalts, samples with good glass and/or typical or interesting features were defined as working samples and will be sent to Mainz whereas anything else, together with the gravel will be stored in the AWI sample repository in Bremerhaven.

The samples for the most part are stored in 10 litre plastic buckets and strapped on wooden pallets. Samples too large for the buckets are stored as loose samples on wooden pallets. Nearly all of these oversized samples are to be kept in Mainz.

**Rock description**

This cruise strictly follows the IUGS naming system for mafic plutonic rocks. Figure 7.7 shows the IUGS naming system for mafic plutonic rocks. The triangle shown represents the mineral content of mafic plutonic rocks as a folded out tetrahedron, with vertices for each of the four major minerals olivine orthopyroxene, clinopyroxene and olivine. For example, a rock containing only olivine would plot at the olivine vertex of the tetrahedron, which is at the midpoint of the lower edge of the triangle. Major oceanic rock types are marked as shaded areas in figure 7.7: Peridotites are labelled A, troctolites B and gabbros C.

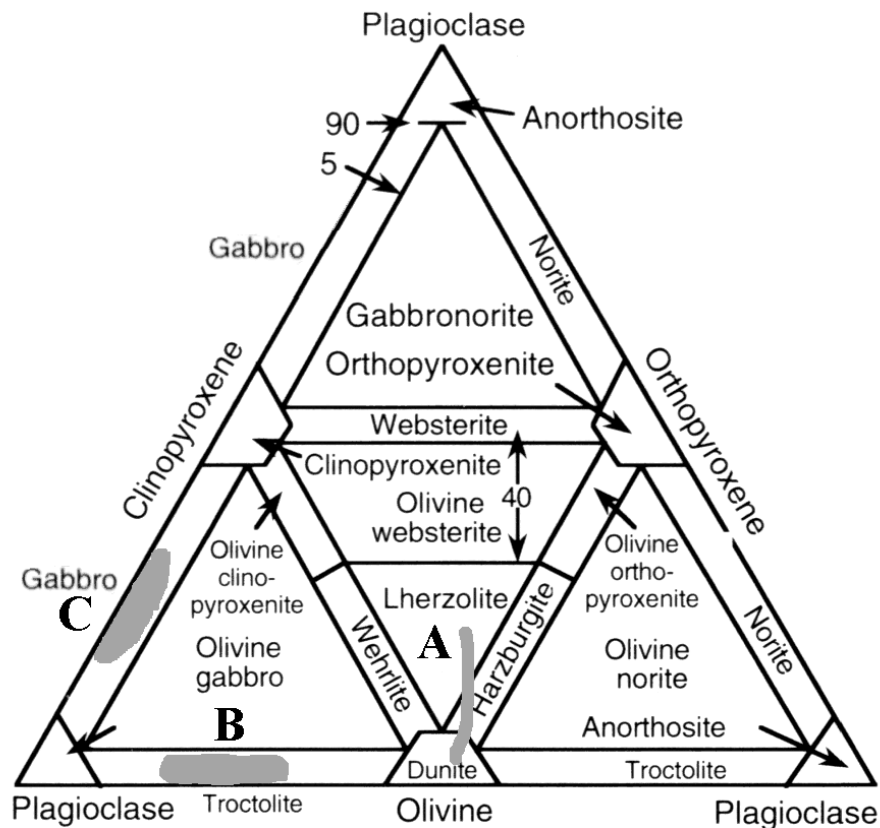


Fig. 7.7: IUGS Classification for mafic rocks.

The most common oceanic rock types are shown as shaded areas:  
 A) Residual mantle rocks B) troctolites and C) Crustal gabbroic rocks.

Most of the rocks encountered fell into a small subset of rock types: Basalts occurred with recognizable plagioclase and olivine phenocrysts and were named by their phenocryst content. It was not attempted to identify pyroxenes in volcanic rocks in hand sample, as these are generally very difficult to reliably distinguish from olivine, much less from each other. Even in thin section, the identification of pyroxenes can be difficult, as the cleavages are often poorly developed making both the distinction from olivine and the determination of the extinction angle quite difficult. The gabbros seen were mostly oxide gabbros, gabbros *sensu stricto*, olivine gabbros and troctolites (Shaded fields B and C in Figure 7.7). Once again, no attempt was made to distinguish clinopyroxene from orthopyroxene in hand sample. In any event no orthopyroxene was observed in thin section (see section on plutonic rocks), so no norites or gabbronorites were observed.

Among the ultramafic rocks, lherzolites, harzburgites and dunites were observed (Shaded field A in Figure 7.7). The IUGS nomenclature specifies 5 % cpx as the dividing line between harzburgite and lherzolite, however many petrologists consider any amount of cpx to indicate a lherzolite. Typically harzburgites can also be recognized on the basis that they are also generally poor in pyroxenes and in spinel. Though it is possible to distinguish clinopyroxene from orthopyroxene in hand

sample, it is difficult to do consistently. Dunites are generally easy to spot because of their complete lack of pyroxenes. Where thin sections were cut, the rock type descriptions determined in thin section were applied to the hand sample description. Finally, true orthopyroxene-free dunites were distinguished from opx-bearing dunites, as geochemical studies have shown that they are genetically different.

The textural features of the rocks were quantified using the criteria in table 7.2, which is adapted from standard ODP and AMORE rock description tables.

**Tab. 7.2:** Rock description terms

### **Basalts**

With glass: Pillow Basalt or sheet flow (tabular), No glass: basalt

Phenocrysts or microphenocrysts: marked with abbreviations in front of the rock name in order of abundance, e.g. pl-ol-phyric basalt.

### **Igneous Texture**

Aphyric: no phenocrysts or microphenocrysts

Phyric: phenocrysts or microphenocrysts

### **Abyssal peridotite deformation**

1: Undeformed

2: Lineation

3: Mylonite

### **Alteration of volcanics**

1: fresh, no visible alteration

2: most of the primary mineralogy is preserved

3: moderate- a majority of the primary mineralogy is preserved

### **Alteration of plutonics**

Percentage of altered minerals in hand specimen

## **Overview of dredging statistics**

In the course of ARK-XX/2, the petrology group managed to recover 3.66 tons of hard rock by 38 dredging stations at Lena Trough, westernmost Gakkel Ridge, and the amagmatic region near 3°E at Gakkel Ridge. The locations, depths and results of these stations are listed in Table 7.3. These hard rocks mainly consisted of outcropping basement rocks, typical of slow spreading ridges. One dredge returned empty, six contained solely sediments, but all other dredges yielded significant amounts of mid-ocean ridge lithologies. Considering the thick sedimentary cover and the limited access to the 'ideal' dredging target because of large and drifting ice floes, we consider this success rate of 82 % high. The average dredging statistics are listed in Table 7.3. Below, the general results of the dredging operations are described by region, as shown in the bathymetric overview map (Fig. 7.1B).

**(1) Northern Lena Trough / Westernmost Gakkel Ridge**

In the first part of the cruise, eight dredges were deployed in the area where the oblique-spreading Lena Trough continues into the orthogonal Gakkel Ridge. As known from the AMORE 2001 expedition, there is a drastic change in the ridge morphology, as well as an unusual off-axis high on the southern flank of the westernmost Gakkel Ridge. This previously unsampled high, with a top at 1600 m water depth, was named *Cagni* Seamount. Dredging results from this region are illustrated in figure 7.8. The first dredge haul of this cruise, station 214, yielded nearly

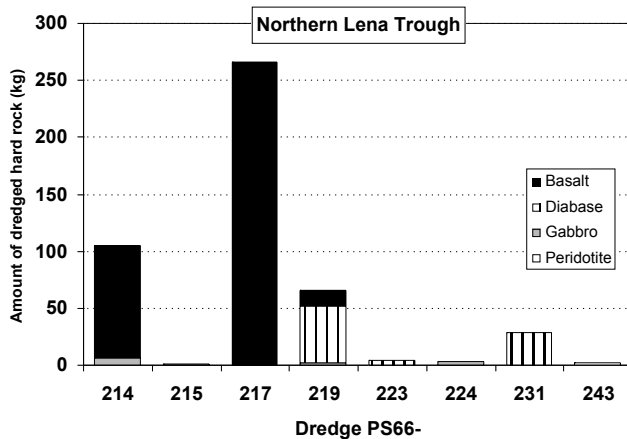


Fig. 7.8: Dredging Statistics, N. Lena Trough

100 kg of glass-bearing basalt, and subordinate amounts of microgabbro at a steep SE-facing slope of Mt. Cagni. Station 215, located at the western flank of this seamount, lies exactly at the intersection of both spreading centers. This exceptionally steep slope was target of a dredging attempt by USCGC Healy during the AMORE expedition, but unfortunately their dredge was lost, along with several km of dredging wire.

Dredge 215 yielded less than one kg of altered gabbro. The next target was the S-facing slope of the Aurora Hydrothermal Field, which was also discovered during the AMORE expedition. Here, nearly four hundred kg of glassy pillow basalt were collected during station 217.

The next four dredges (219, 221, 223, 224) were located at the western flank of the northern Lena inner valley wall, with a spacing of roughly 8 km between the dredging locations.

The first of these four dredge hauls collected 66 kg of upper crustal magmatic rocks. The empty dredge 221 was then followed by two nearly identical dredge hauls, which collected large amounts of shales and minor amounts of diabase. After a short CTD transect to the Greenland margin, dredging continued at the eastern wall of northernmost Lena Trough. Station 231, the last sampling location at Lena Trough before steaming to the amagmatic section of Gakkel Ridge near 3°E, yielded nearly 30 kg of altered basalts.

Tab. 7.3: Dredging Statistics, ARK-XX/2

Station	Date	Lat. (°N)	Long. (° = E)	Location Description	WD (m)	Lithologies (kg)	Basalt	Diabase	Gabbro	Peridotite	Hydrothermal	IRD
214	29.7.04	82 58.38	-4 55.44	W-most Gakkel, SE-slope Cagni Smt	2269	basalt	99.2		6.0			4.5
215	30.7.04	82 55.62	-5 33.70	W-most Gakkel, NW-slope @lost Healy dredge	3597	gabbro			0.6			
217	31.7.04	82 51.39	-6 8.80	S' Aurora slope	4792	basalt	266.0					7.0
219	31.7.04	82 47.11	-6 32.45	N' LT, W-flank, E-facing slope (A10)	4890	basalt, diabase	13.1	50.6	1.6			
221	31.7.04	82 42.08	-6 21.52	N' LT, axial volcano (A12)	4732	empty						
223	1.8.04	82 35.63	-6 34.69	N' LT, W-flank, E-facing slope (A17, Caiji Bank)	4562	shales, diabase	45.2	4.1				300.0
224	1.8.04	82 31.80	-6 29.80	N' LT, W-flank, E-facing slope (A19, Caiji Bank)	4242	shales, gabbro		0.1	2.8			156.0
231	2.8.04	82 37.40	-5 41.00	A18 E Wall Lena Trough	4270	basalt	28.5					7.6
232	5.8.04	82 34.06	2 4.28	Gakkel Ridge 3E G17 N wall	4262	glassy basalt	102.6					0.2
233	5.8.04	84 37.40	2 35.60	Gakkel Ridge 3E N. Wall E. of G14	4626	peridotite				1.8		
234	5.8.04	84 43.47	3 9.24	Gakkel Ridge 3E N. Wall G1	4200	peridotite				61.4		
235	5.8.04	84 40.37	3 22.08	Gakkel Ridge 3E N. Wall S G1 Bonus	5175	peridotite breccia				53.1		
236	6.8.04	84 39.75	3 39.07	Gakkel Ridge 3E S. Wall G11	5268	peridotite, breccias				150.2		
237	6.8.04	84 35.92	3 24.24	Gakkel Ridge 3E S. Wall G2	4104	basalt pillows	49.7			0.1		
238	6.8.09	84 39.23	4 12.64	Gakkel Ridge 3E S. G6 = PS59-235	3274	peridotite				274.6		
239	7.8.04	84 34.18	4 31.90	Gakkel Ridge 3E S. Off-axis	2882	peridotite				12.5		
240	7.8.04	84 30.94	4 56.65	Gakkel Ridge 3E S. farther off-axis	3274	peridotite				41.7		
241	8.8.04	83 37.90	1 7.88	Gakkel Ridge 3E N. Outer wall G16	3520	peridotite, basalt, gabbro	2.3	0.1	3.2	0.9		
243	10.8.04	82 47.90	-7 11.00	Lena Trough W. Wall A11	3886	peridotite				1.6		
244	11.8.04	82 39.98	-7 20.92	Lena Trough W. Wall A14	3713	mud						
246	13.8.04	82 36.74	-4 29.32	Lena Trough E. Wall	3199	mud						
248	14.8.04	82 28.62	-5 5.30	Lena Trough E. Wall	3881	gabbro		0.5	2.1			9.5
249	14.8.04	82 19.05	-4 44.10	Lena Trough E. Wall	3531	peridotite		2.6	44.1	144.4		7.8
250	15.8.04	82 15.70	-5 0.69	Lena Trough Central Ridge -> NOSS	3490	peridotite, gabbro			8.1	35.3		
251	15.8.04	82 10.20	-4 45.80	Lena Trough Central Ridge LR1	3983	peridotite, gabbro			0.1	93.0		
252	15.8.04	82 6.91	-5 9.15	Lena Trough Central Ridge	3849	peridotite, gabbro			0.7	44.8		
253	15.8.04	82 0.42	-4 40.7700	Lena Trough W. Wall	3624	peridotite, basalt, gabbro	3.1	0.8	1.1	117.5		
254	16.8.04	81 43.97	-5 34.0060	Lena Trough W. Wall S2	2912	peridotite, gabbro			2.5	80.9		
255	16.8.04	81 39.81	-3 54.6000	Lucky ridge S3	3250	peridotite				66.2		
256	16.8.04	81 32.82	-3 33.0710	Lucky Ridge S4 -> S5	3529	peridotite, gabbro			2.2	139.3		
257	17.8.04	81 24.58	-2 56.7900	Lucky Ridge across Lucky B Field S6	3831	peridotite, gabbro			1.0	24.0		
258	17.8.04	81 21.86	-3 27.1600	Lucky B -> Ericl S7	3524	hydrothermal precipitates				1.1	61.2	
259	19.8.04	81 7.50	-2 39.7000	Axial Volcano Lena Tr. S.	3791	mud						
260	19.8.04	81 8.18	-2 38.7000	Axial Volcano Lena Tr. S.	3526	mud						
261	19.8.04	80 55.46	-2 31.5200	Lucky Basalt Dredge	3570	basalt, peridotite	611.0			13.8		
262	20.8.04	80 54.39	-2 30.4400	1 NM south of Lucky Basalt Dredge	3545	basalt, peridotite	278.7			84.8		
263	20.8.04	80 35.88	-2 16.3000	S15	3877	carbonate						
264	20.8.04	80 32.13	-2 17.3700	S16	3715	mud						0.6

## (2) Gakkel Ridge 3°E

One of the most intriguing features of Gakkel Ridge discovered during the AMORE expedition is the abrupt change from a robust magmatic accretion in the western part of Gakkel Ridge, to an apparently magma-free extensional domain where exclusively mantle rocks are exposed. Here, at 3°E, the average water depth in the ridge axis increases from roughly 3500 m in the volcanic region to over 5000 m and is accompanied by a 10 km left-stepping offset in the location of the axis. The AMORE post-cruise petrology programme further revealed that this transition may not be entirely abrupt, but may be more related to the physical melt extraction mechanism. Gradual changes in the basalt composition west of this 'boundary' suggest that the degree of melting drops gradually, rather than abruptly. Some of the peridotites exposed in the 'amagmatic' region are exceptionally fresh, and allowed an unprecedented look into the textures and subgrain-scale compositional variations of the upper oceanic mantle. The main result of this study is that the so-called amagmatic region is not entirely amagmatic after all, since many of the mantle peridotites are infiltrated with variable amounts of stagnating melt that reacted with the peridotites, rather than producing a layer of erupted basalt on the seafloor. For these reasons, it was important to obtain a more detailed view of the crustal structure of this transition zone, by defining a closely spaced dredging programme.

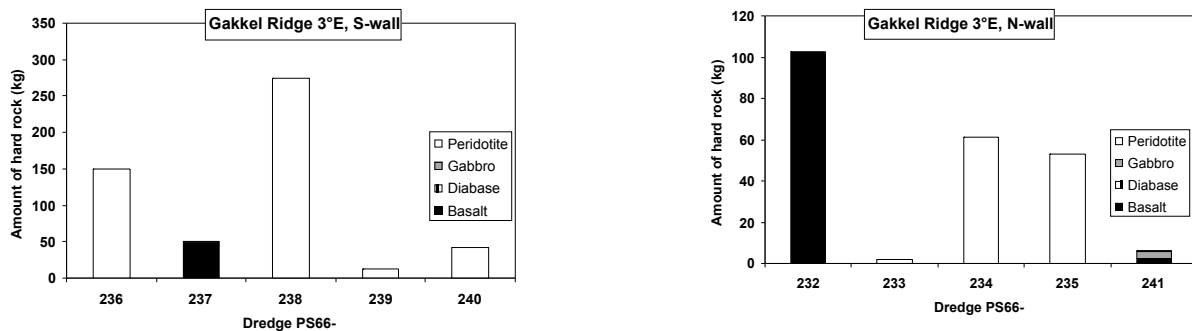


Fig. 7.9: Dredging statistics for Gakkel Ridge 3°E

Ten dredge hauls were deployed in the 3°E region, all of which were successful, yielding a total amount of 750 kg basement rocks. The distribution of rock types is given in figure 7.9. The westernmost dredge, 232, was located at the exact transition between both domains, at the bottom of a southeast-facing slope along the north flank of the ridge. This dredge haul contained one hundred kg of glassy basalt. The next station 233 on the other hand was located only 5 km to the northeast, and at this slope, 2 kg of serpentinized peridotites were recovered. Stations 234 and 235 were located at the shallow and deep part of the same slope along the northern valley wall (i.e. North American plate), respectively. Both yielded around 60 kg of serpentinites and serpentinite breccias. Station 236 was started at the exact same position as the previous station -at the deepest point along Gakkel Ridge- but instead the southern deep valley wall on the Eurasian plate was successfully sampled (150 kg serpentinized peridotite). Station 237 was deployed towards the inferred position of

the magmatic-amagmatic transition, and brought 50 kg of pillow basalts on deck, along with three fingernail sized serpentinite fragments.

One of the very special dredge hauls of this expedition was station 238, following the same dredging track as station PS59-235 of the AMORE 2001 expedition. It was even more successful, because this dredge haul contained 268 kg of completely unaltered peridotites, which is totally unprecedented. A special section in the sample description section is devoted to these unique samples.

Dredge hauls 239 and 240 were deployed off-axis, at 12 and 20 km away from the ridge axis, respectively. The former contained 12 kg, and the latter 43 kg of variably serpentinitized peridotites. After a parasound and bathymetry profile back to the northern flank of Gakkel Ridge, a northwest facing slope of the abyssal hill near station 232 was dredged. This dredge haul 241, which was the last petrology station at Gakkel Ridge, turned out to be quite heterogeneous and contained 8 kg of basalt, diabase, gabbro and serpentinitized peridotite.

### **(3) Central and Southern Lena Trough: Lucky Ridge**

With the exception of three dredge haul during ARK-XV/2 in 1999, little was known about the nature of the central and southern Lena Trough basement. In addition, very limited bathymetric data were available. However, it was already well known that the sedimentation rate is high and that the Lena Trough axis is covered by a thick sediment pile that may locally exceed one km. Therefore, in order to dredge this region successfully, precise bathymetric data had to be obtained first, before picking steep –sediment-free– slopes as dredging targets. Some of these targets were identified after a long bathymetric profile, and could therefore be rated as priority sampling stations in advance. Others slopes were sampled immediately after discovery. As this joint bathymetry/petrology programme went along, an irregularly shaped ~130 km long N-S trending ridge appeared, along which thirteen dredging stations were deployed. This narrow ridge was termed ‘Lucky Ridge’, after the Lucky B field at which hydrothermal deposits were unexpectedly dredged in 1999. In addition to these sampling stations on Lucky Ridge five stations were carried out on the western flank of Lena Trough, including the last four dredges in the southern part the Lena Trough.

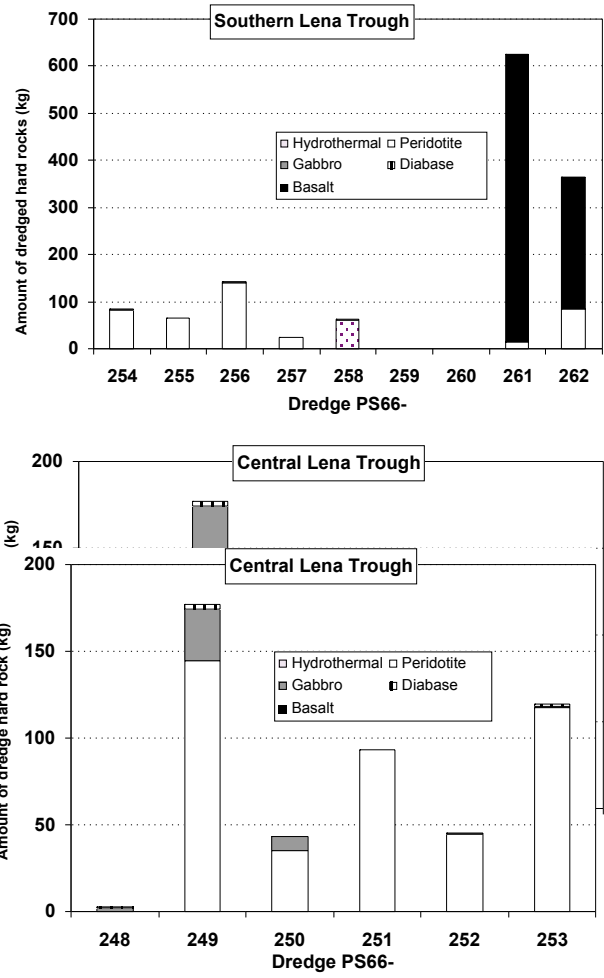


Fig. 7.10: Dredging statistics, Central and southern Lena Trough

The distribution of rock types for this region is shown in figure 7.10. Station 248, 14 km to the north of Lucky Ridge, contained 2.6 kg of diabase and gabbro. The five next closely spaced (<10 km) dredge hauls along the northern part of Lucky Ridge, yielded between 45 and 180 kg of serpentinized peridotite. Station 254 was located on the western flank at a broad irregular ridge, and contained 150 kg of strongly serpentinized peridotite.

The next six station were again on Lucky Ridge. As already found in the northern part of this ridge, the central part exclusively consists of exposed mantle rocks, as stations 255, 256 and 257 all collected exclusively serpentinized mantle peridotites (66, 139 and 24 kg, respectively).

Station 258 was yet another highlight of the petrology programme. At the Lucky B field, where massive sulfide hydrothermal precipitates were collected without any preceding obligatory hydrothermal exploration, a successful dredge haul brought

61 kg of hydrothermal precipitates and related products on board, along with three hand specimens (1.1 kg) of serpentinized peridotites. The significance of the unique association is further evaluated in a special section of this report.

At the southernmost part of Lucky Ridge, two dredge hauls (259 and 260) retrieved unconsolidated mud, confirming the intense sedimentation rate in the southern part of Lena Trough. Stations 261 and 262 were two very closely spaced dredge hauls, at the east-facing slope a 20 km long isolated ridge. Both yielded large amounts of fresh glassy pillow basalts (611 and 279 kg, respectively), as well as considerable amounts of serpentinized mantle peridotites (14 and 85 kg, respectively). At the southernmost end of Lena Trough, two stations (263 and 264) tried to recover basement rocks, but unfortunately contained solely sediments.

## 7.5 Sample preparation and data collection

Francois Nauret<sup>1)</sup>, Yongjun Gao<sup>2)</sup>,  
Zoran Janovic<sup>3)</sup>, Sandrin Feig<sup>4)</sup>,

<sup>1)</sup>Max-Planck-Institut für Chemie, Mainz

<sup>2)</sup>University of Göttingen, Göttingen

<sup>3)</sup>University of Salzburg, Salzburg

<sup>4)</sup>University of Hannover, Hannover

### Thin section preparation

The rock samples are cut into chips of 40x20x11 mm. The side of the chip, of which the thin-section will be made, is ground on an abrasive grinding machine until the side is one flat surface. This side is then ground successively with coarse to fine grinding-powder and cleaned in an ultrasonic bath to remove the grinding powder. The glass-slides (27x46 mm) on which the chips will be glued are ground a little bit, to give them a rough surface. After grinding, the slides are labelled and their thickness measured with a micrometer. The chip and the glass slides are then cleaned with Ethanol and glued together using UV glue or two-component epoxy resin. This has to be done carefully, in order not to leave any air-bubbles between glass and chip.

In the case that UV glue was used, resin hardening is quite fast - 12 minutes compared to epoxy glue which needs 6 hours to solidify. Accordingly this UV glue was used more frequently.

After this mounting procedure the bulk of the chip is cut from the glass slide so that only a 0.5 mm layer of rock remains on the glass-slide. This is done with a Struers-Discoplan-TS cut-off-machine, which integrates a saw and a grinding wheel. The thin section is then ground down with the grinding wheel to a thickness of 0.08 mm. Using the grinding-powder from coarse (320) to fine (1000), the thin-section is then ground down by hand to a thickness of 0.025 mm. The thickness can be measured approximately during grinding by using the micrometer-screw. A more precise thickness determination can be made using a microscope. The interference colour of known minerals under crossed polarized light indicates the correct thickness.

## Microscopy

Overall 303 thin sections were fabricated and subjected to microscopic investigation. Microscopic work was done with a Zeiss microscope and transmitted light was used. In order to allow an overview of the thin section, 2.5x objectives resulting in ca. 25 times magnification were used. For detailed study of minerals and textures 12x, 25x and 40x objectives gave magnifications of ca. 120, 250 and 400 times the original size. Thin section photography was accomplished using a Sony (ExwaveHad) Digital camera.

Thin sections were numbered L1-L303. Working sample numbers are listed in a thin section log file (Appendix). Where the origin of samples or thin slide numbers were unclear question marks have been added to this log. Two thin sections of the same working sample are discriminated by 'a' and 'b' following the working sample number. Most of the thin sections have been described in details, except for the number of peridotites for which there were no enough time to check for plagioclase occurrence and abundance of clinopyroxene so no further subdivision for number of peridotites is not given in thin section log file.

## Thin section overview

301 thin sections were examined by transmitted light microscopy. An overview can be seen in the Appendix. Five main rock types were found in the sample set, including basalt, diabase, gabbro, peridotite and dropstones (Table 7.4). The breccias seen were assigned to those rock types depending on composition of the clasts. The majority of the thin sections (251) consist of peridotites in all stages of alteration, from fresh to completely altered.

## Glass processing

First of all, glass chips were removed from each basalt with large amount of glass, black (fresh?) as possible, using a hammer and a fine chisel. The glass chips were put into properly labelled plastic jar. Samples selected for chip glass are listed in Table 7.5. Each glass split was crushed, sieved (0.122 to 0.466 mm), and washed in fresh water to remove clay. Samples have been rinsed with ethanol and dry down on the hot plate. Two to three grain of each sample have been hand picked and mounted into a mineral mount, for major and trace element analysis, by electron-microprobe and LA-ICPMS respectively. All glass samples go to the MPI ( F. Nauret) for further processing.

**Table 7.4:** Numbers of thin sections discriminated by rock type

Basalt*	Diabase	Gabbros	Peridotite**	Dropstones
11	15	20	251	9

\*including breccias

\*\*including veined, serpentinitised and mylonitic peridotites

Tab. 7.5: Glass samples

Dredge	Sample	Dredge	Sample	Dredge	Sample	Dredge	Sample
<b>PS66-214</b>	1	<b>PS66-219</b>	1	<b>PS66-261</b>	1	<b>PS66-262</b>	5
	2		2		3		21
	3	<b>PS66-232</b>	1		5		22
	4		2		6		32
	5		3		9		34
	6		4		10		35
	7		5		12		37
<b>PS66-217</b>	1		6		17		61
	2		7		20		78
	3		8		37		80
	4		9		38		81
	5		10		43		82
	6		11		45		83
	7				47		84
	8	<b>PS66-237</b>	1		48		85
	9				50		86
	10				54		88
	11				63		89
	12				64		90
	13				71		91
	14				72		92
<b>Total</b>							
<b>Samples: 77</b>							

### Electron beam analysis

On this cruise an electron microprobe (Microscope equipped with a electron beam energy-dispersive X-ray spectrometer) is used for the first time ever. This provides the ability to chemically identify the minerals while still on board that are impossible for polarizing microscopy (such as opaque minerals).

## Instrumentation

The Miniprobe system used on this cruise is composed of hardware and software components. The hardware part is a Carl Zeiss microscope equipped with a standard cold cathode CITL MK4 CL (manufactured by CITL – Cambridge Image Technology Ltd.) with analytical top plate and Ketek SiLi X-ray detector and a Sony Exwave-HAD video camera to get a real-time image of the analyzed thin section (Fig. 7.11). The software part is an EDS computer with EMRA 10.4 installed for hardware controlling and data analysis. The sensitivity of the EDS system corresponds to that of a SEM. An important advantage of the PIN-detector (Peltier-cooled) compared with a standard SiLi detector is that it does not need liquid nitrogen but still has an acceptable resolution of ~200 eV for daily analysis and a maximum resolution of 160 eV can be available (Vortisch et al., 2003).



Fig. 7.11: CITL MK5 Electron Mini-Probe

## Optimization and Calibration

In order to get the optimum working condition, the Miniprobe was set to run at different combinations of current and voltage for gun as well as different shooting times for the analysis of pure Ge standard. As shown in figure 7.12, the reproducibility measured by the relative standard deviation of the obtained total content (should be 100 %) is getting better with increasing the gross count. There are three possibilities to increase the gross count, increase the beam size, current or voltage of the electron beam or increase the shooting time. All these possibilities were tested for different standard materials, and it was found the optimum condition is 100  $\mu$ A+20 kV+100 $\mu$ m+100 seconds for a new gun, and 150  $\mu$ A+20 kV+100 $\mu$ m+100/200 seconds for an older gun. A minimum gross count of ~10,000 gross count is required to maintain a good analysis.

A complete set of spinels representing nearly the whole variation range of Cr # (Molar Cr/[Cr+Al]) in mantle peridotites were analyzed with Miniprobe. This is done to calibrate the Cr number obtained by the Miniprobe, as they have been analyzed with electron microprobe in MPI of Mainz.

As shown in figure 7.13, there is a very good linear correlation between the analyzed values and reference values. Based on this linear correlation, the obtained Cr numbers were corrected as  $Cr\# = 0.9594 * Cr\#(Miniprobe) - 12.833$ .

The obtained Mg# (100 mg/(Mg+Fe)) in clinopyroxene and olivine were not corrected, as there were not enough standards on board to get the correction line. However, the analysis of San Carlos olivine showed a reasonable reproducibility of the Mg# obtained by the Miniprobe (Fig. 7.14).

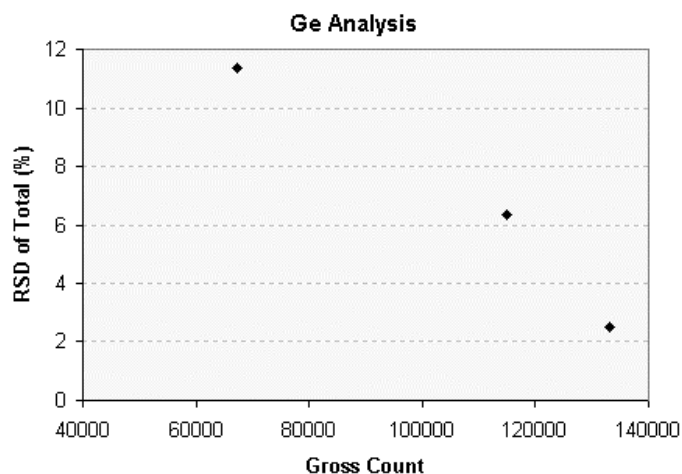


Fig. 7.12: Counting statistics for Ge

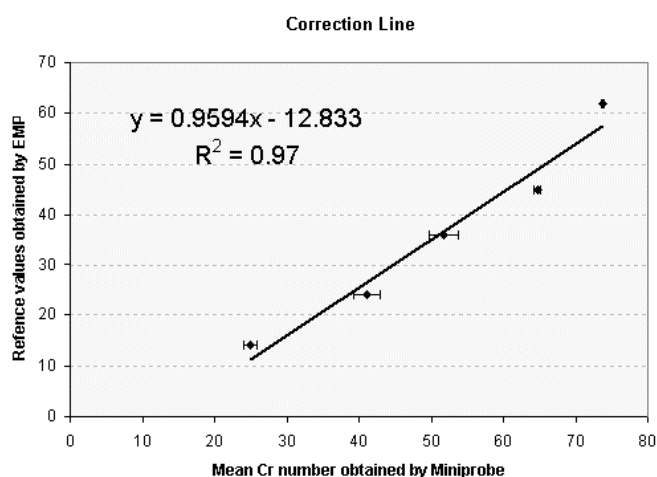


Fig. 7.13: Correlation of spinel Cr# (Molar Cr/[Cr+Al]) with the electron miniprobe

### Daily Analytical Procedures

For daily analysis, the Ge standard and scintillating glasses, as well as a MPI standard mount which contains San Carlos olivine are always in the sample holder. Before going to any analysis, the system need run about 1-2 hours to stabilize the beam condition. As long as the vacuum is better than 0.012 mbar, the daily analysis can be started.

First, the beam position was checked by locating the beam on the scintillator glass. And then Ge standard was analyzed to check the calibration to make sure both  $K\alpha$  and  $L\alpha$  lines of Ge are exactly on the middle position of their peaks, otherwise a new calibration would be done. Here after, the Ge standard was analyzed 5-6 times after adjusting the GF (General Factor) to get a 100 % content of Ge. Afterward, the San Carlos olivine are analyzed, if the obtained Mg# are in the range of  $87 \pm 1.3$  then we went to the analysis of the samples.

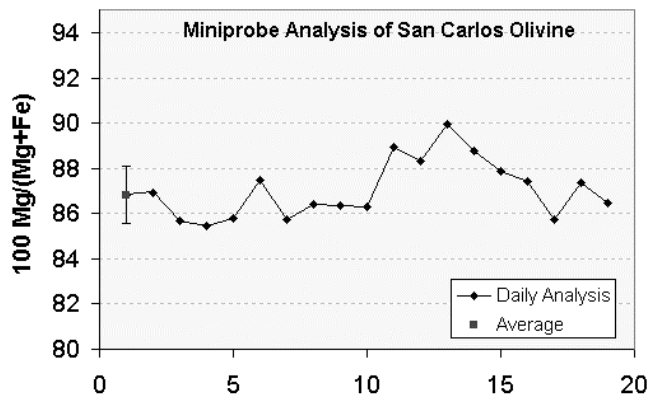


Fig. 7.14: Miniprobe analysis of San Carlos Olivine

As the thin sections made on board usually have different thickness, so it is necessary to paint a small silver dot on the blank area of the thin section to check the beam position before going to shooting on any minerals. It has been found that the beam position could change a lot with different thin sections.

**Results**

During this cruise, unpolished thin sections made on board of basalt, peridotite, and gabbros, as well as mounted basalt glass and hydrothermal product were analyzed. The obtained data are listed in an appendix. The Miniprobe is currently not good enough to make good analysis of basalt glass and plagioclase due to the low resolution. However, the results show that there is no problem to get good analysis of spinel, olivine, oxide, as well as the Mg/Fe ratio of pyroxenes. The typical spectra obtained by the Miniprobe for different minerals and basalt glass are shown below (Fig. 7.15).

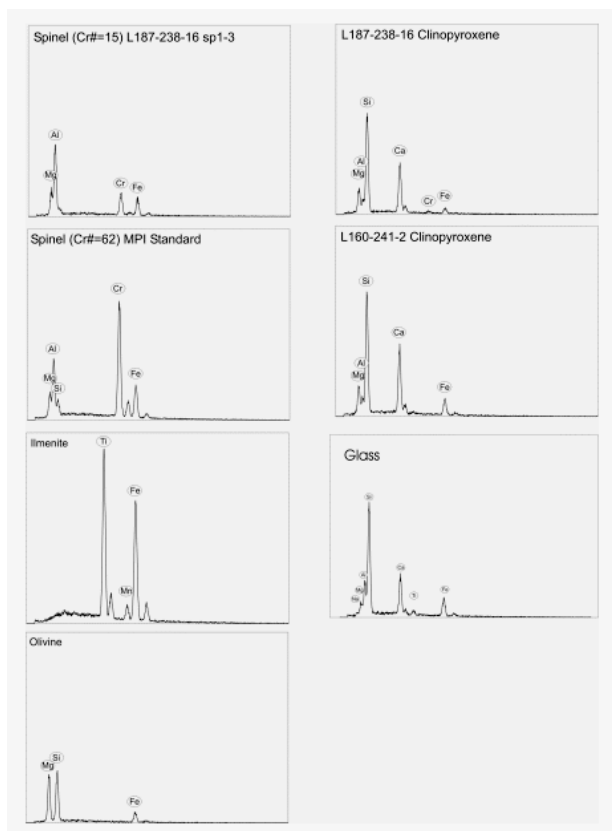


Fig. 7.15: Typical spectra for different materials obtained by Miniprobe

### Reference:

Vortisch W, Harding D, and Morgan J (2003), Petrographic analysis using cathodoluminescence microscopy with simultaneous energy-dispersive X-ray spectroscopy. *Mineralogy and Petrology*, 79, 193-202.

## Parasound

### Introduction

Bottom and sub-bottom reflection patterns can be obtained by PARASOUND, which characterizes the uppermost sediments in terms of their acoustic behaviour and also to evaluate the thickness of the sedimentary layer. This last parameter is extremely helpful to validate (or not) a potential dredge location. In other words, dredges are planned to collect solid rocks. Thus, a good PARASOUND profile, showing no sediment layer, is a strong validation for a dredge location.

A new software, Parastore 3, have been recently installed on the RV *Polarstern*. For the first time, this new software has been run, during the main part of the Leg. The Petrology group, without experience on this domain, has been in charge of the data acquisition. The PARASOUND sediment echo-sounder was in 24 hour operation by Kai, Zoran, Steffen, Regina, Timo, Simona and myself. The work on PARASOUND consisted essentially to adapt the scale of NBS and PAR Echograms to the signal.

### Parameters

Advice parameters from the technical staff are:

Frequency: 18 kHz and 4 KHz for NBS and Parametric respectively.

Filter: 16-20 kHz and 2-6 kHz filter band pass for NBS and for Parametric respectively.

### Results

Although PARASOUND system has been run as possible, acquisition time has been often stopped during several periods due to a thick ice, CTD, mooring recovering, and dredges. During those periods, either the received signal was too noisy and not enough efficient, or the ship was stopped. Although we spent a lot of time to look for good data, only 2 short good quality profiles have been obtained. Profiles 1 and 2 are reported figures 1 and 2.

As observed clearly on the profile 1 (Fig. 7.16), we observe a smooth bathymetry and a high reflectance layer with a maximum thickness of 25 meters. Such thick layer has been interpreted as a sediment layer. Concerning the second profile (Fig. 7.17), a rough bathymetry is observed and the high reflectance layer is less than 5 meters, suggesting a thin sedimentary layer.

### Limitations

The PARASOUND results are did not live up to expectations. First of all, during most of the Leg, we decided to stop the PARASOUND system due to the absence of Parametric signal. Although the NBS signal was nearly continuously received, the parametric data were too noisy to obtain a profile. Two main reasons have been suggested by the technical staff: 1) presence of the sea-ice, 2) rough bathymetry.

Although we can discuss the first reasons, the second one is more problematic. By comparison, during AMORE 2001 Expedition, PARASOUND system have been run in the same kind of rough topography, along and across Gakkel Ridge (pers. comm. J. Snow). We are not qualified enough to discuss the properties and the quality of the PARASOUND system and this new software, however we are strongly disappointed by the absence of useable PARASOUND profile in the study area.

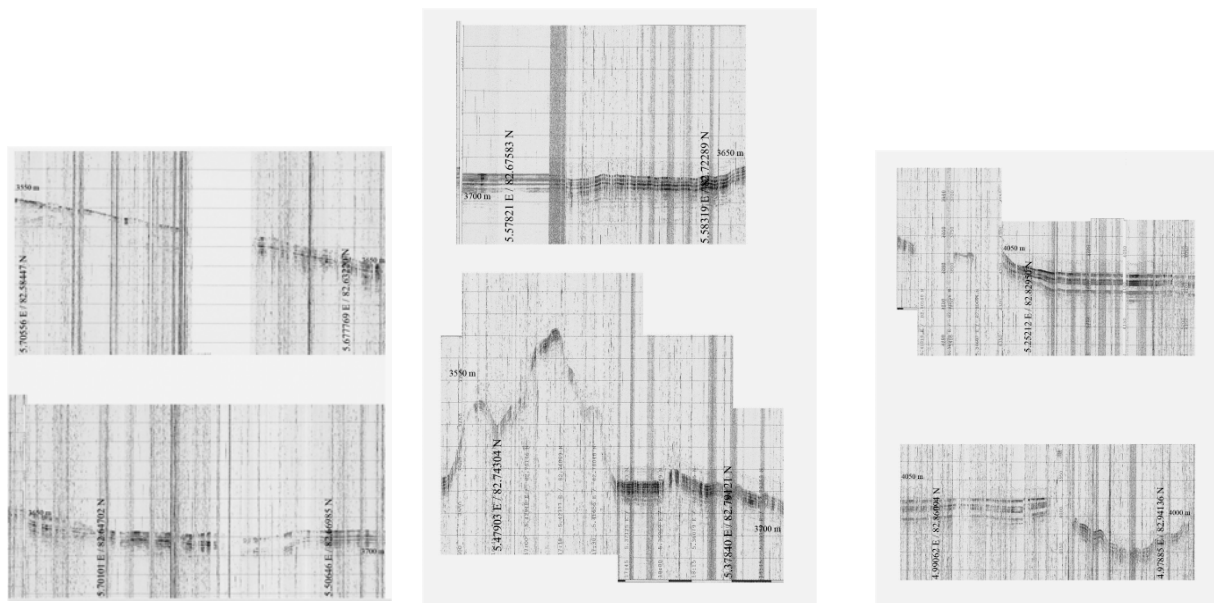


Fig. 7.16: PARASOUND profile obtained the 25.07.2004, from 10h50 to 23h05, between 5,70556 E/82,58447 N and 5,00388E/ 82,95393 N

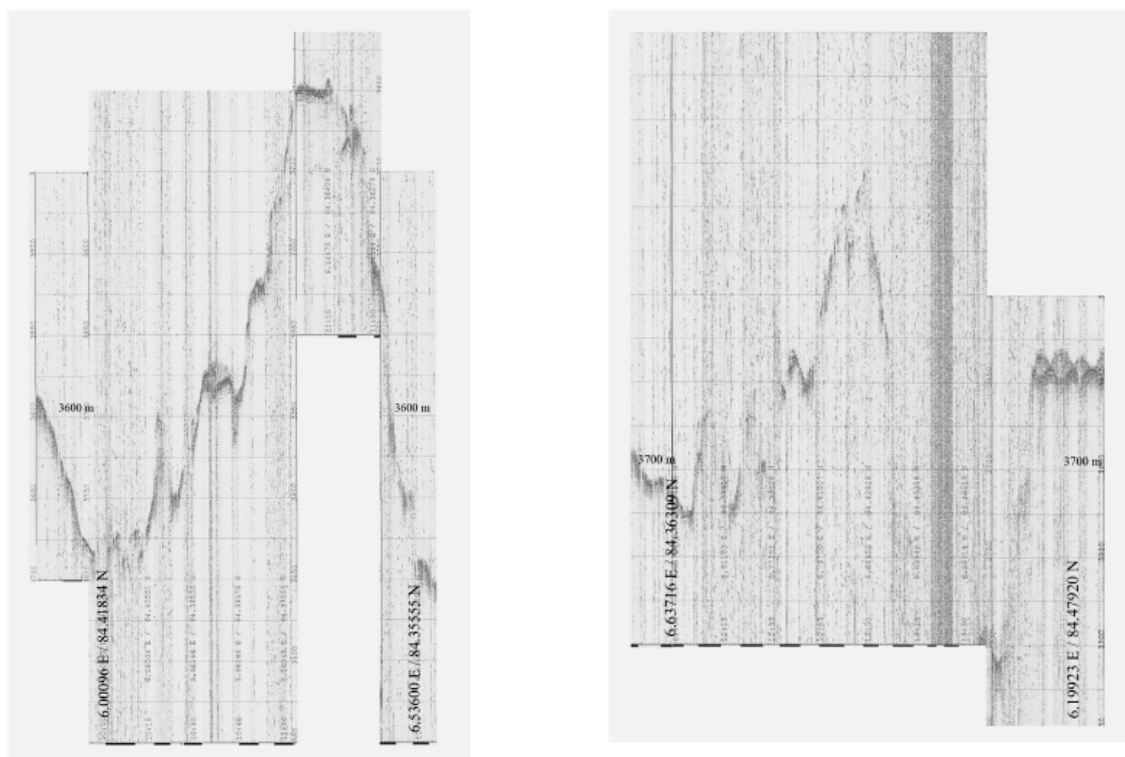


Fig. 7.17: PARASOUND profile obtain during an across Gakkel ridge axis profile. Data acquisition started the 7.08.2004 from 9h37 to 11h58, corresponding to 6.00096E/ 84,41834E and 6.19923E/84,47920N

## Education

Regina Eckardt, Timo Liesenfeld, Steffen Schmidt, Simona Turini, Kai Wiegler  
University of Mainz, Mainz

The five undergraduate students on the cruise played an active role in the scientific life of the group. We were once again the only group that included undergraduates. In addition to their duties supporting the dredging rock curation and other operations, the undergrads had a number of special activities.

**1) Polar University.** This was a lecture series initiated by the Chief Scientist, lectures were generally held every morning after breakfast and were geared to a general scientific audience. The lectures were generally held by group leaders and graduate students, and attendance among the undergraduates was high, at least among those on the day shift. The petrology undergraduate students each held 15-20 minute geology/petrology lectures in the lecture series for the benefit of the other groups. The topics were: RE and KW: Introduction to the mineralogy of the ocean basement; TL: Petrology midcruise status report 10.8.2004; SS: Volcanoes on land and in the ocean; ST: Hydrothermal activity in the ocean crust.

**2) Petrographic training.** The students were asked to completely describe a thin section of their choosing, with the help of the older scientists. The purpose was to train quantitative description in advance of the rock curation work. Another assigned task was to, as a group describe a rock provided by one of the crew. The students used all the analytical methods on board to characterize the sample (a fossiliferous arkosic sandstone from Spitsbergen, probably Devonian, and probably tailings from a coal mine). The crewman got his sample back cut and polished with a 10-page report on its composition. Finally, one student was able to take a Mineralogy final exam proctored by the group scientific staff on board.

**3) Onboard analyses.** The students found these particularly useful and interesting. Both the thin section lab and the electron mini-probe provided the students with immediate feedback about the compositions of the rocks we were collecting. All the students got to run the miniprobe and see how it works.

**4) Rock Curation.** All the students took an active interest in the scientific part of the rock curation work and were able to undertake some of the descriptive work themselves. They volunteered as well to help make thin sections, which turned out to be a very useful skill to have on hand.

**5) Planning.** Many of the students had the chance to participate in the planning of the petrology operations, helping pick dredging points and helping the nautical officers to keep on an optimal course in the ice for the bathymetric coverage.

**6) Work with other groups:** All the students took the opportunity to visit the other groups on the ship and to learn what they do and how. A particular highlight was work on the ice with the ice physics group. Some of the group were flown out to the ice by helicopter.

## Discussion

### Morphology and tectonics of Lena Trough

Jonathan Snow  
Max-Planck-Institut für Chemie, Mainz

In the westernmost Nansen basin, the accretionary plate boundary between the North American and Eurasian plates changes direction and acquires a new name. The Lena Trough is the southern extension of the Gakkel Ridge into Fram Strait. It shares some characteristics with Gakkel Ridge, particularly the ultraslow base spreading rate, but is in many respects far different from the Gakkel Ridge. The bathymetric and petrologic results of this cruise do much to clarify the history of sea floor spreading in this basin. The mapping of Lena Trough was completed sufficiently to allow a tectonic interpretation. The existing survey of the Western Gakkel robustly volcanic region was extended by two bathymetric profiles, so that more of the rift mountains have now been illuminated, and the 3°E region was resampled in order to more clearly define its tectonic and petrologic evolution.

Lena Trough is an enigmatic linear deep in the Arctic Ocean. It is also one of the least well-mapped regions of the Earth. Perfect examples of this can be found where the bathymetric data from this cruise contradicts completely the information found in compilations such as the IBCAO chart of the Arctic Ocean. Consequently, the mapping done on this cruise significantly extends the knowledge of the morphology of Lena Trough. The very existence of Lena Trough was in doubt throughout most of the 20th century. Figure 7.3 (in the introductions section) shows one of the first compilations of bathymetric data (Nansen, 1906), and shows a narrow isthmus linking the two continents. This error of extrapolation of more than 4000 meters is one of the few errors in that map.

Little more was actually known about Lena Trough before this cruise than that the Nansen sill does not exist, and that there is in fact a deep trough linking the Arctic and Atlantic oceans. Current thinking about Lena Trough before this cruise was that it is a site of normal sea-floor spreading albeit of the newly recognized class of ultraslow spreading ridges. To at least some degree, orthogonal structures were expected to be present, such as accretionary faults parallel to the Gakkel Ridge strike and fracture zones normal to it. In most published maps showing different types of data relevant to Lena Trough, it is shown as being offset by several small fracture zones. The plate boundary data set distributed with the popular mapping software GMT (used on this cruise) shows four such fracture zones, as do any maps of this area generated using this data set.

Figure 7.18 summarizes the new results of mapping and sampling in Lena Trough. Even in this relatively low-resolution figure, the gross morphology of Lena Trough is recognizable. Lena Trough is a steeply-sided sediment-filled basin. The southern and eastern regions of Lena Trough are heavily sedimented. The southwestern slope of the trough is inundated by sediments originating from the Greenland continental margin. The eastern valley wall is even more heavily sedimented. Evidence for this is shown by the highly embayed eastern wall, where mass-wasting gullies lead down to extensive sediment infilling of the basement grabens on the valley floor. However there is no continent to provide such a massive sediment influx. It is very likely that much of the sedimentary influx comes from ice-rafted continental clastic and riverine sediments carried by ice into this region from Siberia. Basement outcrops are common rising through the sediment in the southern Lena Trough, and the sediment cover thins toward the north and the intersection with Gakkel Ridge.

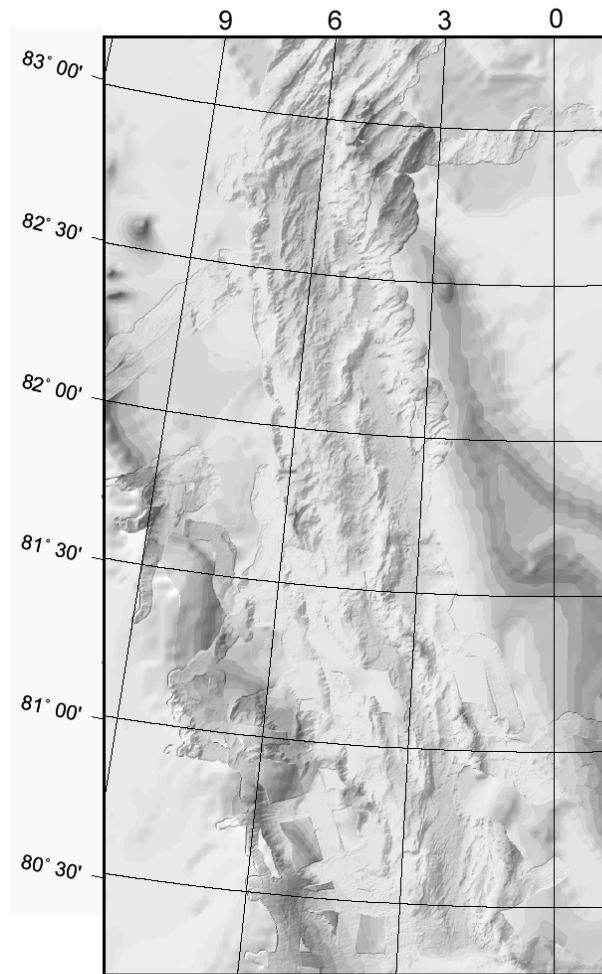


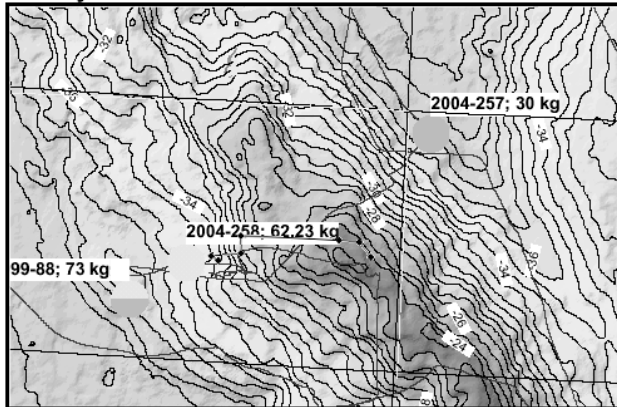
Fig. 7.18: Lena Trough bathymetry

Lena Trough consists of a single first-order segment and has no further segmentation. The rift valley walls are not offset by fracture zones. The shape of the rift valley walls is not straight, however. It appears to be dominated by the competition between master faults parallel to the plate boundary and secondary faults that branch into a direction parallel to the Gakkel plate boundary. This is particularly true in the north of Lena Trough. This gives the Lena Trough valley walls a unique jagged appearance that is unusual for any mid-ocean ridge, and a stark contrast to the long linear walls of the western Gakkel Ridge just a few miles further north.

Basement outcrops in Lena Trough (e.g. Fig. 7.19) are like nothing ever observed previously on a mid-ocean ridge. These appear to be steep-sided blocks of basement material thrown up on faults that range in strike from parallel to Gakkel Ridge to perpendicular to it. They often have flat tops and exhibit no particular vergence or tilting to one side or the other. Sampling of these basement outcrops returned predominantly.

Volcanic morphology is not apparent in Lena Trough. All of the morphologic features of the valley floor and walls are controlled by tectonism and sedimentation. No basalts were recovered between 82°30' and 81°N. The basalts that were sampled were either near to the junction with Gakkel Ridge or were erupted on peridotite, which was also found in the dredge. This reverses the normal outcrop pattern of mid-ocean ridges, where the most abundant volcanic activity occurs in the centre of first-order and second-order segments.

Lucky B Area



Lena Trough has formed the plate boundary between North America and Eurasia since about the early Miocene, when the northward drift of Greenland ceased and sea floor spreading began to propagate up the Greenland Sea. This halted the underthrusting in the transpressional plate boundary north of Greenland, possibly before true subduction could begin.

Fig. 7.19: Basement outcrop in Lena Trough, Lucky B area

The new plate boundary remained a continental strike slip shear zone until transtensional seafloor spreading began about 9 million years ago. The shapes of the plate boundaries produced by this breakup were strongly controlled by the orientations of pre-existing continental structures. Lena Trough as a basin is thus relatively young. It represents a transitional stage between a continental rift and a mid-ocean ridge, and may be analogous to a more developed version of the Red Sea Rift or possibly the Iberia Margin and Western Alpine ophiolites.

It is exceedingly difficult to match up tectonic features on opposite sides of Lena Trough. This is partly a function of the extreme obliquity of Lena Trough, and partly because many of the features on the western wall may match up with features on the eastern wall that are inundated by sediments and thus now invisible. However, where matchups are possible, it appears that the midpoints of the tie lines between them fall far to the west of the Lena Trough valley wall. This would suggest that the spreading in Lena Trough has been quite asymmetrical. There is a case to be made for considerable asymmetry in the spreading of the Knipovitch ridge further south. It is possible that the reactivation of the earlier subduction plate boundary beneath Svalbard is responsible for this

## Petrologic segmentation of Lena Trough and W. Gakkel Ridge

Eric Hellebrand, Jonathan Snow, Anette von der Handt  
Max-Planck-Institut für Chemie, Mainz

Magmatic and tectonic segmentation is one of the common characteristics of all mid-ocean ridges, and is recognized in the morphology and petrology of the ridge. This segmentation can be observed in a number of scales. First order segments, for instance, are generally bounded by large-offset transform faults, which produce fracture zones with significant strike-slip tectonics and an obvious off-axis expression. The generation of fracture zones appear to be largely independent of spreading rate, as they are present at the fast spreading East Pacific Rise (EPR), at the slow-spreading Mid-Atlantic Ridge (MAR), as well as at the ultraslow-spreading Southwest Indian Ridge (SWIR). The length of first-order segments is quite variable, and can range from several tens to several hundreds of km.

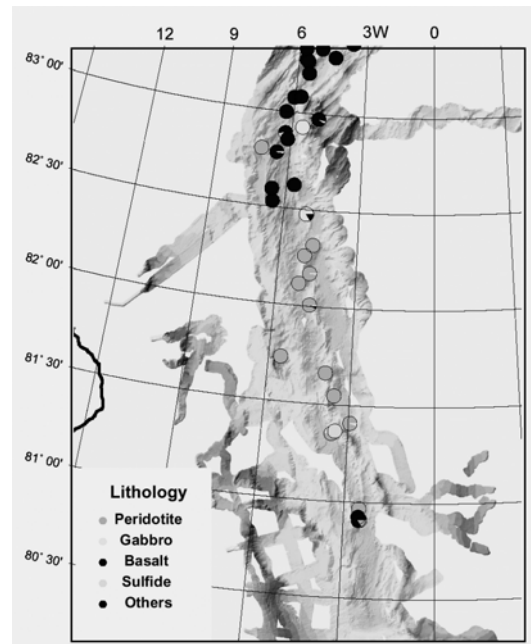


Fig. 7.20: Distribution of rock types along Lena Trough

Individual ridge segments can be further subdivided into second-order segments and their length is on the order of a few to several tens of km. Second-order discontinuities can include so-called overlapping spreading centers, most common at fast spreading ridges, or gradual changes in axial water depth. At several locations along the Mid-Atlantic Ridge, these last forms of non-transform discontinuities have been shown to correlate with the rock types exposed at the ocean floor. A single ridge segment has a shallow centre, where dominantly basaltic rocks are found. At the segment ends, water depth can increase dramatically, and predominantly serpentinized mantle peridotite, occasionally injected by gabbroic lower crustal lithologies, are observed. The driving force for such segmentation is the feedback relation of mantle upwelling and magma production rates.

At an ultraslow orthogonally spreading ridge such as Gakkel Ridge, the segmentation is less apparent. Particularly in the sparsely magmatic central zone, where dominantly mantle rocks are exposed, variations in peridotite mineral compositions can be used to define segments. Correlating this mantle compositional segmentation with morphological features of the Gakkel Ridge has not been successful yet.

As discussed in the previous section, the tectonic segmentation of Lena Trough is quite different than that of Gakkell Ridge. There is a single first order segment, and the second-order segmentation is of a wholly new type.

**Magmatically-controlled segmentation**

The most straightforward approach to identify a petrological segmentation is to check for systematic along-axis variation in the relative abundance of rock types, their constituents or even other features such as extent of deformation, or alteration, which were systematically recorded for every hand specimen collected. Figure 7.20 shows the distribution of rock types dredged along Lena Trough in relation to the morphology. Generally, basaltic rock types were sampled in the northern and southern portions of Lena Trough and not in the central part.

As shown in figure 7.21, the weight fraction of basalt per dredge suggests that there may be three clearly defined segments. A northern basalt-dominated segment, a central basalt-free segment, and a southern basalt-bearing segment.

In northern Lena Trough, there appears to be a robust volcanism, since the four northernmost axial dredge hauls yielded more than 98 % basalt or diabase. The sudden change in spreading geometry from magmatically robust orthogonal spreading at the Western Gakkell Volcanic Province to oblique near-continental spreading at Lena Trough, did not lead to an abrupt cessation in partial melting underneath the northernmost part of Lena Trough. However, this eruptive magmatism in northern Lena Trough may not have been active for a long time, since the off-axis dredge haul on the western flank at 82.8°N contained only peridotites.

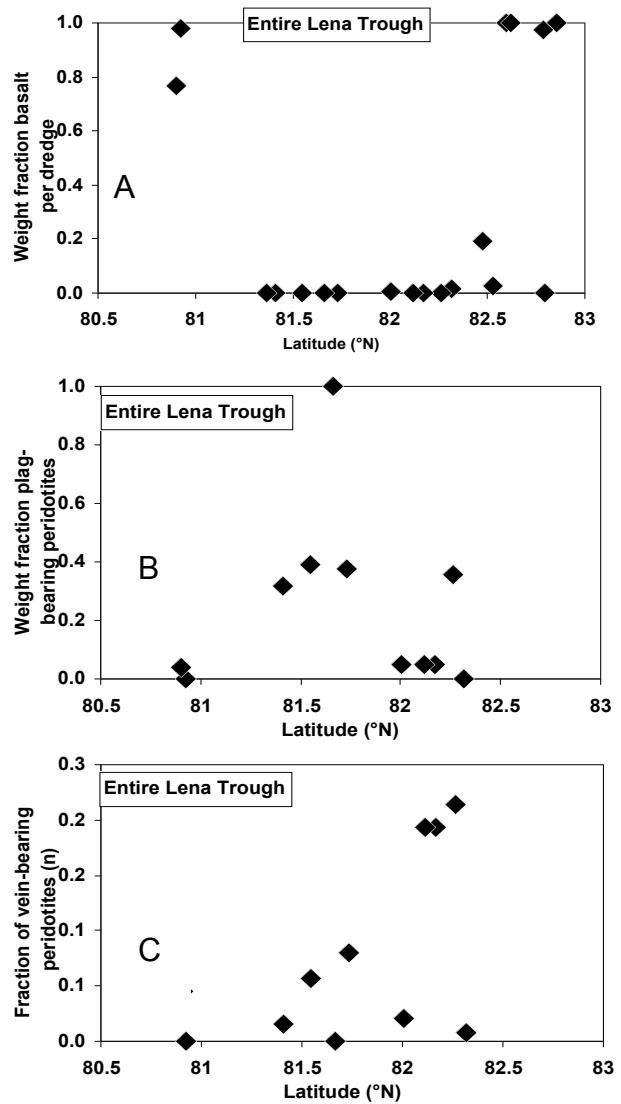


Fig. 7.21: Distribution of magma-influenced rock types in Lena Trough dredges

The central part of Lena Trough, i.e. entire Lucky Ridge, is completely devoid of basalts, and is therefore the longest (conventionally defined) amagmatic section along the global mid-ocean ridge system. Morphologically, this irregular ridge can be subdivided into 10-20 km long sigmoidal tectonic segments. With the current spacing between the dredging location, however, nothing can be said about the 10 km-scale compositional variations within these tectonic massifs and their possible controls.

In the southern 'segment' of Lena Trough, petrological information is confined to just one 20 km long segment at which two successful dredge hauls were deployed during this cruise, and two more during ARK-XV/2 in 1999. Three of these dredge hauls brought vast amounts of basalt, and serpentinized peridotites were present in all of them. It has to be noted that the presence of eruptive magmatism is not at all suggested by the morphological features of this ridge, which is in all aspects similar to the similar-scale segments of Lucky Ridge. It may therefore be possible that the non-extrusive nature of Lucky Ridge is due to 'unfortunate' sampling, although we rate this chance as quite low.

### **Amagmatic extension versus melt stagnation**

It is tempting to refer to amagmatic extension with regard to the central Lena Trough. In the conventional sense, the lack of basalt and the exclusive presence of mantle rocks exposed on the ocean floor directly translates to amagmatic extension. This is not exactly true however, because it is likely that some partial melting occurred underneath Lucky Ridge, but the melt may not have been extracted from the mantle, and is still present in the form of disseminated plagioclase and veins. Our studies on mantle rocks from Gakkel Ridge, the Southwest Indian and Central Indian Ridge, suggest that a significant fraction (10-30 %) of all abyssal peridotites there are not only the product of partial melting alone. Instead, their mineral chemistry is dominated by a late-stage melt stagnation event. In most cases, such mantle rocks contain plagioclase, a mineral that is only stable at low pressures. The mineral composition of plagioclase peridotites as well as their textures can only be explained by significant melt entrapment. Furthermore, the extreme chemical disequilibrium between the minerals in almost all plagioclase-bearing abyssal peridotites worldwide suggests rapid cooling rates, supporting a very low-pressure origin of the melt injection.

For this reason, the distribution of plagioclase-bearing peridotites along Lucky Ridge may provide additional information about melt generation and stagnation. As shown in figure 7.21, the weight fraction of plagioclase-bearing peridotites per total amount of peridotite recovered per dredge appears to behave systematically. Plagioclase is virtually absent in the southernmost and northernmost dredge hauls and gradually increases towards the centre of Lena Trough. In dredge haul 254, all collected peridotites contained plagioclase. However, a note of caution must be added to this observation. At face value the along ridge systematics suggests a systematic central peak. Dredge 254 is not located at Lucky Ridge, but is located on the western flank of the ridge and thus represents an isolated sampling location on that portion of the ridge. Still, even leaving out this dredge haul, it still seems that plagioclase is more abundant in the central Lena Trough mantle rocks.

One preliminary conclusion may therefore be that melt generation occurred along the entire length of Lena Trough. In the northernmost part, these melts were extracted from the mantle and formed a basaltic layer, possibly a very thin one. In the central part of Lena Trough, melts were formed in the mantle, but never managed to focus, pool and erupt. The reason for this may be caused by an increase in lithospheric thickness from the Gakkel Ridge/Lena Trough intersection towards the south. In the central part of Lena Trough, the lithosphere may be exceptionally thick resulting from the conductively cooling influences of the extreme obliquity, the ultraslow spreading and the vicinity to the continental margin of Greenland and Svalbard.

### **Petrology and tectonics of the Gakkel 3°E 'amagmatic' segment**

Anette von der Handt, Eric Hellebrand, Jonathan Snow  
Max-Planck-Institut für Chemie, Mainz

Between 3°E and 8°E, the ultraslow spreading Gakkel Ridge consists of an 'amagmatic' segment. There, the axial valley plunges 2000 m deeper from a magmatically robust area at 3000 m depth by an oblique crossing high. This area was investigated twice by dredging operations, during the AMORE expedition in 2001 and during ARK-XX/2. While the AMORE expedition had the whole western portion of Gakkel Ridge as target of their investigations, the return to Gakkel Ridge during ARK-XX/2 focused on the transition from the magmatic to amagmatic segment at 3°E. Here, a more detailed dredging programme and a more intensive bathymetry were the main objectives.

#### **Dredging results**

Overall, ten dredge hauls were carried out in the 3°E amagmatic area of Gakkel Ridge in the course of ARK-XX/2 (Fig. 7.22), which adds to the information obtained during AMORE 2001. Dredging of the axial high brought, both in 2001 (PS66-232) and 2004 (PS59-234), altered basalts which suggest that this high was not magmatically active for some time.

Further north along the rift, no other evidence for the creation of a magmatic crust can be found except in dredge haul PS66-241 off-axis of the western valley that recovered 3.4 kg gabbro and 2.3 kg basalts. Despite the absence of a magmatic crust this segment shows evidence of intense melt infiltration and reaction with the residual peridotites. Seven out of ten dredge hauls contain plagioclase-bearing peridotites, ranging from plagioclase lherzolites to plagioclase-enstatite-dunites.

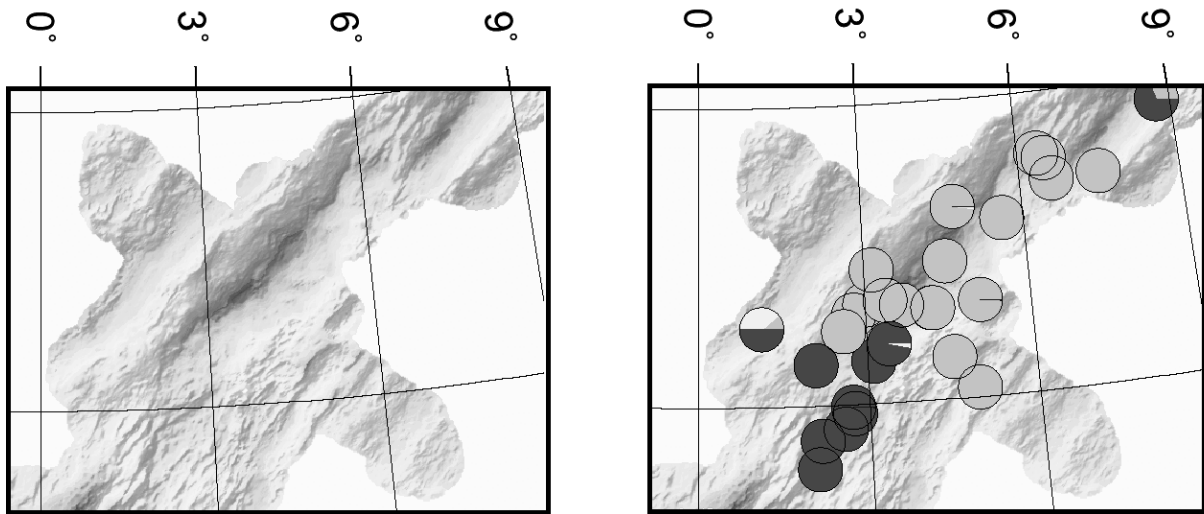


Fig. 7.22: Bathymetry and rock type distributions in the Gakkel 3°E region

The modal content of plagioclase and distribution seems to be correlated with the stratigraphic level; The peridotite samples with less plagioclase occur in the deeper parts of the valley and higher modal contents are found in most samples in the higher structural levels (PS234 and PS238). Additionally to the plagioclase-bearing lithologies, some dredge hauls contain vein-bearing peridotites with both gabbro (PS66-234) and pyroxenite (PS66-236) veins.

For the interpretation of the tectonic history of this area the degree of deformation was noted for each sample. Peridotites recovered from the bottom of the flanks show signs of intense deformation on both sides of the flank. The two dredge hauls of the western flank both show deformation where PS66-233 consists only of low-temperature brittle cataclasites, two also with a high modal content of plagioclase, whereas PS66-235 mainly consists of breccias whose clasts show intense deformation. On the opposite side of the rift valley, dredge haul PS236 consists of mylonites and other deformed samples. Unfortunately, most of them also show a high degree of alteration.

The two dredge hauls that lie at a higher level on either side of the wall show some deformation but considerably weaker than the ones previously mentioned. Samples from dredge haul PS66-234 at the western wall have aligned minerals and even some protomylonitic samples. The dredge haul on the other side of the rift (PS66-238) also showed the same order of deformation. Dredging on off-axis highs on the western side of the ridge valley recovered only peridotites as well. There the peridotites of dredge haul PS 239 also showed abundant mylonitic features.

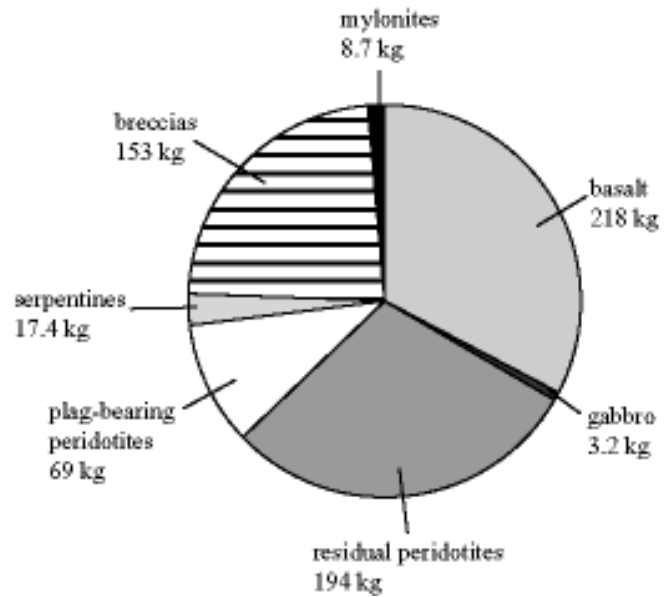
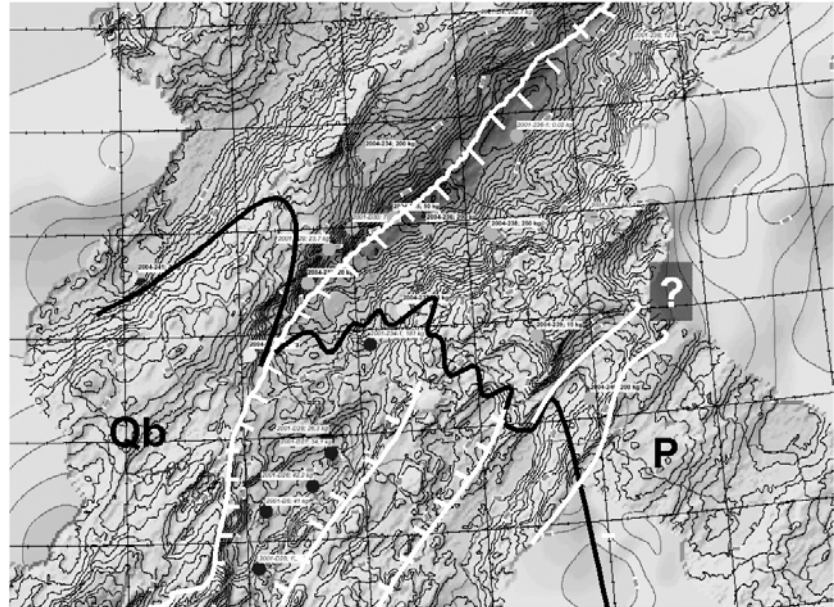


Fig. 7.23: Overview of lithologies recovered by dredging at 3°E at Gakkel Ridge during ARK-XX/2

### Dredge haul PS66-238

The strong alteration of abyssal peridotites inhibits often the intensive study that is crucial to answer important questions of mantle petrology. In 2001, the AMORE expedition recovered with dredge haul PS59-235 some very fresh mantle peridotite but unfortunately not many and of small sizes. Therefore, an attempt to repeat the dredging track was made during ARK-XX/2 that ended successfully and brought 275 kg of the freshest abyssal peridotites known on board. Among those are two big boulders whose bigger one weighs at about 100 kg and will give unlimited analyses opportunities. Furthermore, samples from this dredge haul do not only show in general a degree of alteration of less than 10 % but also all major peridotite types are present except for real dunites. Besides the residual lithologies almost half of the peridotite (Fig. 7.23) consists of plagioclase-bearing peridotites whose subgroups mirror the residual ones in matching proportions. The modal content of plagioclase in the samples covers a wide range from a few interstitial grains up to at about 15 %. This plagioclase is most likely be derived by reaction between the residual host-rock and an impregnating basaltic melt. Those plagioclase-bearing samples show abundant textures of this interaction and due to the freshness and the overall low degree of deformation even fragile textures like symplectites did survive.

*Fig. 7.24: Preliminary geologic interpretation of the 3°E region based on AMORE 2001 and ARK-XX/2 bathymetric and petrologic data*



Apart from the obvious melt impregnation recorded in the plagioclase-bearing samples other signs of later modifications of the residual samples can be seen also. Among others are distinct modal changes of pyroxene contents in hand specimens as well as pyroxene textures believed to originate by melt interaction. Diffuse cpx-veins or layering could be observed several times but also two pyroxenite samples were found.

Taken together, the tremendous range in lithologies and textures and the simple size of the dredge haul and its individual samples, will open up new possibilities of investigation and push mantle petrology into a new dimension of quantitative study of mid-ocean ridge mantle processes.

### **Summary**

Using the dredging results, the bathymetric map and the gravity and magnetics data for this area it is now possible to draw a geologic map for the 3°E region (Fig. 7.24). The large throw on most of the faults makes it clear that the northern SE-dipping master fault from the WVZ curves northward to join the main fault of the amagmatic section. The southern rift faults however do not have any continuity, truncating against the highs (which are also gravity highs) on the south side of the amagmatic zone. The faults on the southern limb of the amagmatic zone also appear to dip to the SE, and thus do not appear to face inward to the valley walls. This pattern of faulting is generally unusual for mid-ocean ridges. It is also unclear why the north wall of the magmatic zone has no clearly defined mullion structure, even though it appears to be the surface of a major detachment.

## Mineralogy and microstructures of peridotites

Jovanovic Zoran  
University of Salzburg

Ultraslow spreading ridges have recently been recognised as a new class of mid-ocean spreading environments. The joint cruise of RV *Polarstern* and Healy – AMORE 2001 (Gakkel Ridge) made an important contribution to the discovery of the unique characteristics of ultraslow spreading ridges. One of these is their segmentation into magmatic and amagmatic regions. In amagmatic regions, mantle peridotites crop out at the ocean floor. This represents an excellent opportunity to study mantle processes. One of the main goals of this cruise was to return to a selected part of Gakkel Ridge (3°E

East) and complete the data sets, as well as to sample larger amount of samples for extended geochemical investigations. The second set of peridotites was collected at Lena Trough. Lena Trough is mostly an amagmatic region but its tectonic setting is not well understood, since it is complicated by proximity of the Greenland and Spitsbergen continental margins. Besides that it has slowest effective full spreading rate on earth (7.5 mm per year) and it could represent modern analogue of amagmatic continental rift recently described at Iberia margin. Peridotites dredged at Lena Trough will be studied in order to test these possibilities.

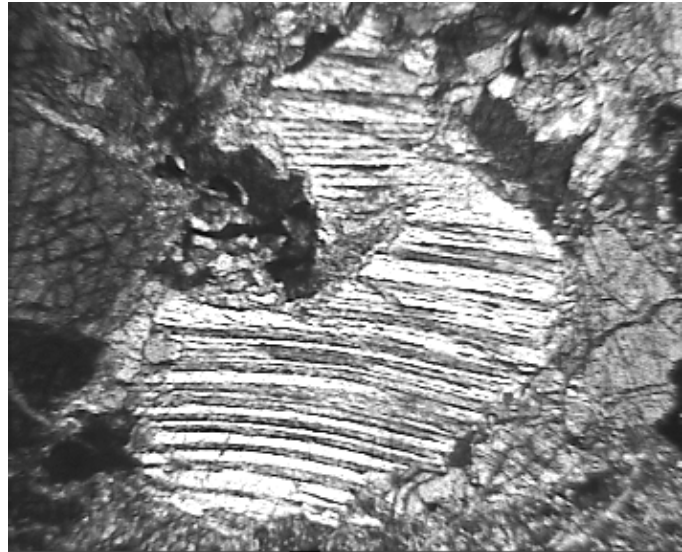


*Fig. 7.25: Clinopyroxene porphyroblast with highly irregular –reacted grain boundaries.  
Field of view is 2.3 mm.*

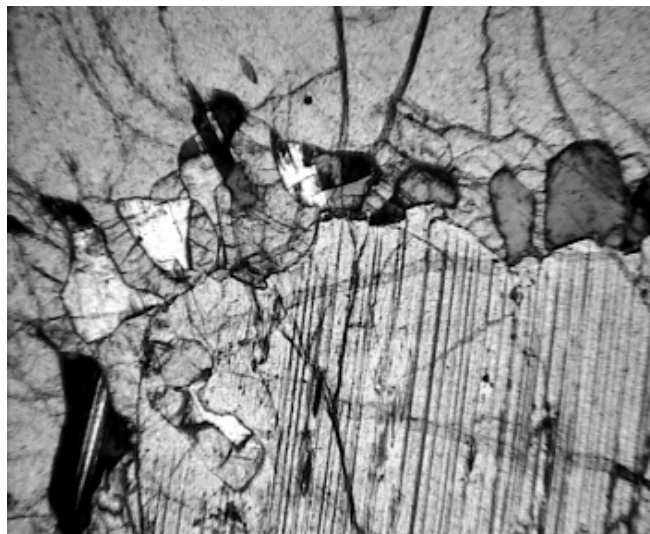


*Fig. 7.26: Plagioclase blebs in orthopyroxene porphyroblast*

During this cruise hundreds of hand specimens were examined and representative ones were selected for petrographic investigations in order to better constrain their mineralogical composition. Most of peridotites are altered 70-90 % but many have preserved sufficient relict mineral phases for further geochemical investigations on shore. Nevertheless, some of peridotites are extremely fresh and show no signs of alteration. Fresh abyssal peridotites are a rare phenomenon, and in that respect dredge 238, where almost all the samples are completely fresh without any serpentinization is particularly unique and valuable.

One of the main observations in both the Gakkel and Lena Trough areas is the high variability of lithologies present. They vary from dunites, enstatite-dunites and harzburgites to plagioclase and spinel lherzolites. Mylonites are also present in both regions. Residual spinel mineralogy varies from highly depleted to fertile. This is further supported by miniprobe analysis where the Cr# ( $\text{Cr}/[\text{Cr}+\text{Al}]$ ) of spinels varies from 10 to 40 in residual spinel peridotites (see geochemical variations chapter for details). However only a very limited number of the samples recovered have a purely residual nature. Most of the samples have opx and cpx porphyroclasts with highly irregular, deeply embayed grain boundaries (Fig. 7.25), which is an indication of presence of percolating melt.

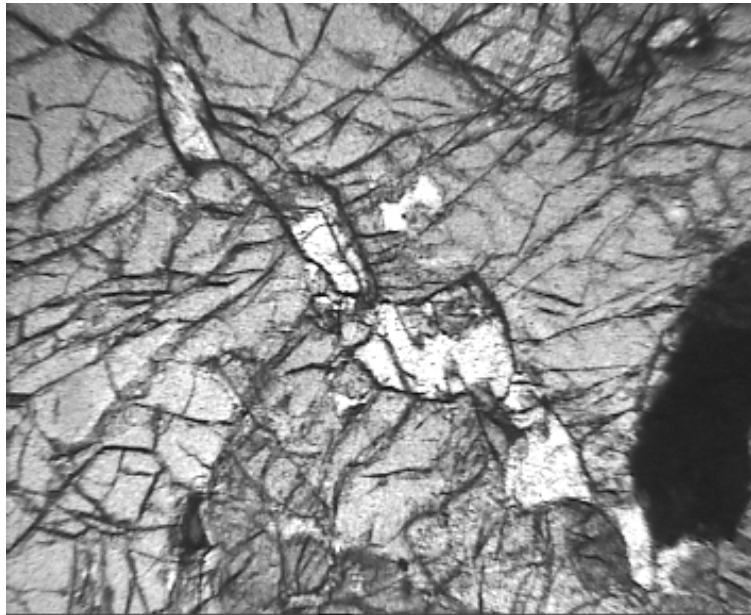


Fig. 7.27: Plagioclase trail in orthopyroxene

Additionally many samples are plagioclase bearing. The origin of such plagioclase is still a matter of debate. However, textures present in plag-bearing samples as plag-opx symplectites, blebs of plagioclase in opx (Fig. 7.26) and trails of plag in opx (Fig. 7.27) are in agreement with an origin of the plagioclase through melt-peridotite reaction.

**Geochemical variations of peridotite -- Miniprobe data**

Yongjun Gao<sup>1)</sup>, Jonathan Snow<sup>2)</sup>

<sup>1)</sup>University of Göttingen, Göttingen

<sup>2)</sup>Max-Planck-Institut für Chemie, Mainz

The Lena Trough and the 3°E area of Gakkel Ridge were intensively investigated by dredging together with a detailed bathymetric mapping during the ARK-XX/2 expedition. Although most of peridotites are highly altered (70-90 %), many of them have preserved fresh spinels and pyroxenes that are sufficient for further geochemical investigations. While on board, 18 peridotite thin sections which contain large (>0.5 mm) and fresh spinels (checked with polarized microscopy) were investigated with the Miniprobe (Electron beam energy-dispersive X-ray spectroscopy) for the chemical composition of spinels as well as clinopyroxenes. The analyzed results are listed in the Appendix (Miniprobe analysis result). Due to the large beam size of the miniprobe (100 and 200 μm), it is often not possible to avoid shooting on an area which contain some alteration product for the daily analysis of spinels. So according to the spectra, those mixed analysis with large Si peaks were filtered out.

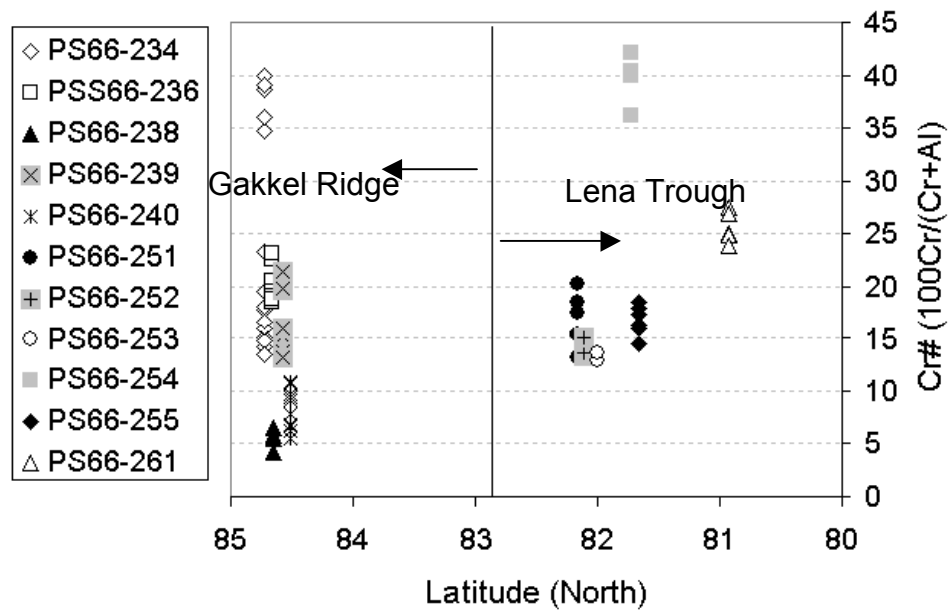


Fig. 7.28: Cr/(Cr+Al) for Gakkel Ridge and Lena Trough peridotite spinels

As shown in figure 7.28, the peridotites from Gakkel Ridge (3°E area) and Lena Trough are both characterized by low degree partial melting suggested by the broad existence of low Cr-number spinels. Generally, the analyzed spinels have Cr number of about 14 to 25, although both higher and lower Cr numbers were also observed. However, in Lena Trough, the analyzed peridotite from dredge PS66-253 is directly contacted with a gabbro dyke, the peridotite from dredge PS66-261 was recovered together with huge amount of basalt (~98 % by weight), while a small amount of

gabbros were also recovered together with peridotite in dredge PS66-251, PS66-252, and PS66-253. So it is most likely that the mantle beneath Lena Trough has a uniform fertile nature, and even more fertile than those beneath Gakkel Ridge. However, more analysis of the peridotite from Lena Trough especially those from pure peridotite dredges are required to draw any definite conclusions

Among these 18 peridotites, 5 contain fresh clinopyroxene that were analyzed with the Miniprobe (the data are listed in the Appendix). Due to the low resolution of the Miniprobe, the Al and Cr content in clinopyroxene can not be obtained precisely. So only the Mg# (100 mg/(Mg+Fe)) are plotted in figure 7.29. As can be seen, clinopyroxenes in Gakkel Ridge appear to have a large variation from ~80 to ~92, which is unlikely to reflect real variations in mineral chemistry.

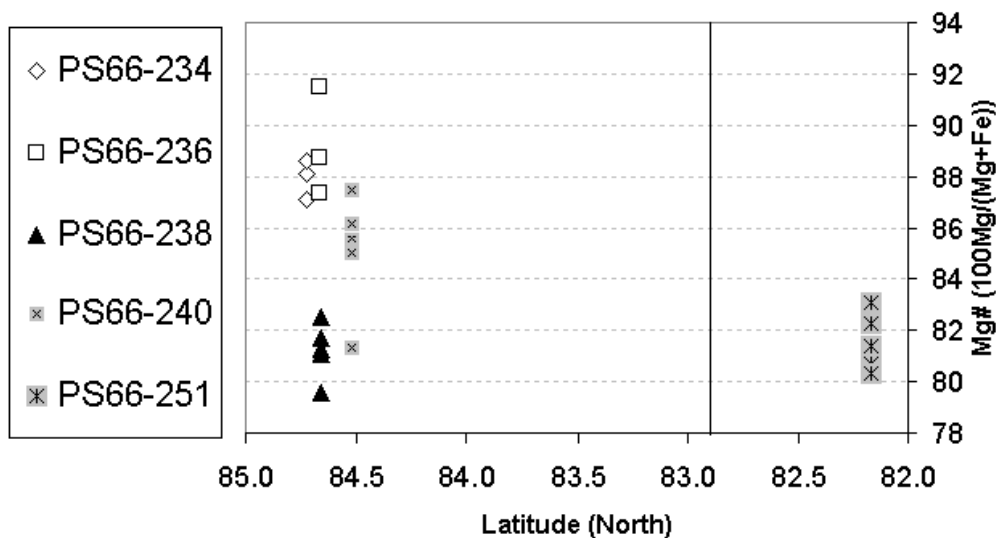


Fig. 7.29: Mg/(Mg+Fe<sup>2+</sup>) in Clinopyroxenes from Gakkel Ridge and Lena Trough

### Petrography of Gabbros and Dykes

Yongjun Gao<sup>1)</sup>, Sandrin Feig<sup>2)</sup>

<sup>1)</sup>University of Göttingen, Göttingen

<sup>2)</sup>University of Hannover, Hannover

Gabbros and dykes are plutonic rocks that have cooled more slowly than basalts, under greater pressure and in the more protracted presence of volatiles. At fast spreading ridges, the oceanic crust is characterized by a general 'layer-cake' structure with gabbros making up most of the lower crust overlying mantle peridotites while underlying pillow basalts and sheeted dykes. A thick gabbroic layer together with dykes is generally a sign for the presence of a magma chamber beneath ocean ridge. However, mid-ocean ridges with slow spreading rates (<40 mm/yr of full spreading rate) are characterized by lithologic complexity and lack a well organized vertical structure. Gakkel Ridge and Lena trough represent the end member of slow spreading ridges (<14 mm/yr of full spreading rate), thus the lithology of gabbros and dykes in this area provide a means to investigate the crust structure as well as the magma supply at extremely slow spreading ridges.

In contrast to the relatively greater recovery of basalt and peridotite, gabbros and dykes were only recovered from 8 stations which are less than 3 % by weight of the recovered rocks. It is interesting to point out that 5 out of 8 of these plutonic rock (gabbros and dykes) stations are located at the kink area between Gakkel Ridge and Lena Trough. This has been found to be a volcanic region that extended northward into the western volcano part of Gakkel Ridge. The other 3 gabbro stations are at about 82°N area of Lena trough. In the kink volcano region gabbros were recovered either together with basalts or dykes or both, while in the 82°N region of Lena trough, gabbros were recovered always together with peridotite and very often appeared as dykes in peridotite. All of this suggests that the gabbros of the northern Lena region occur as a layer, while those from the central Lena trough region do not. They more likely form distinct bodies and small intrusions in the peridotites, which suggests that the melt has been dyking directly through the mantle peridotites to form a basaltic layer on top. Magma chambers that form a gabbro layer thus apparently do not exist in this region. But, on its way to the surface, the melt forms gabbroic- sills and dykes or

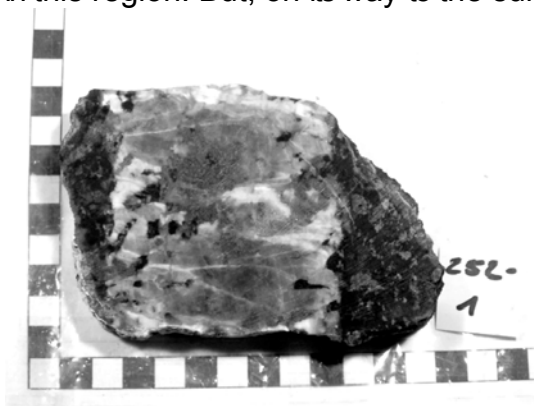


Fig. 7.30: Photo of sample PS66-252-1 showing a gabbroic dyke intruding peridotite

even intrusive bodies in the mantle section, that we dredge together with the peridotites. This is further supported by the relatively high ratio of dykes to gabbros of about 4 by weight.

The gabbros recovered are classified based on the primary mineralogy estimated by in thin-section, following the standard IUGS nomenclature and the general marine usage established at Hole 735B. The recovered gabbros are mainly olivine-bearing gabbro (with 0-5 % olivine), micro-gabbro and oxide gabbro, while olivine gabbro (olivine >5 %), troctolite and troctolitic gabbro were not recovered. Figure 31 shows typical textures in olivine bearing gabbro and diabase.

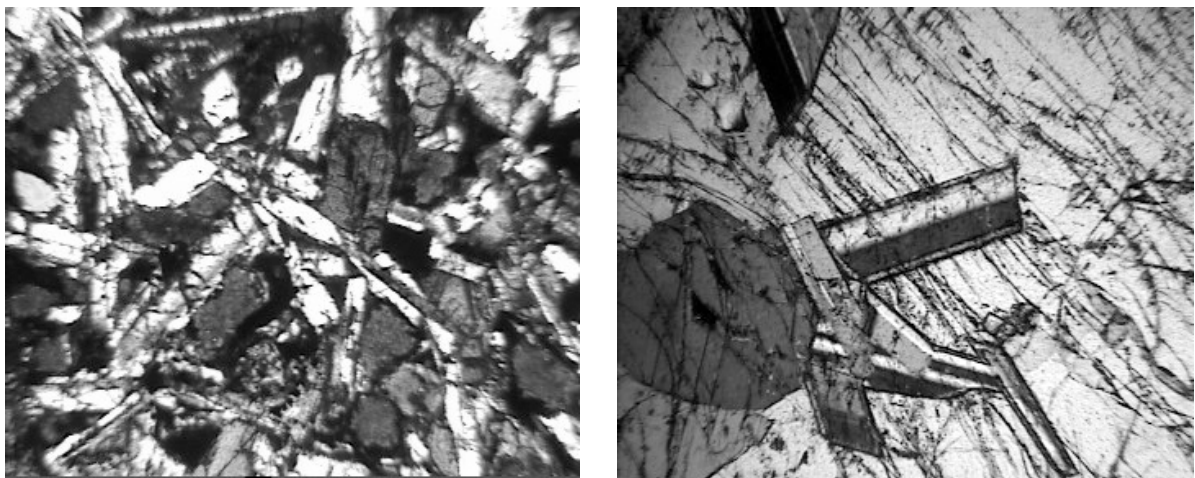


Fig. 7.31: Two photos to show the texture of gabbro and dyke. The field of view is 3 mm across on these micrographs. A) A typical diabase showing ophitic plagioclase laths. B) Gabbro showing poikilitic clinopyroxene enclosing plagioclase.

The primary textures of recovered gabbros are characterized by poikilitic clinopyroxenes that enclose or partially enclose euhedral plagioclase and sometimes olivine. This indicates that olivine and plagioclase crystallized together prior to the crystallization of clinopyroxene. Some plagioclases have obviously continuous zoning patterns with relatively high-Ca cores to high-Na rims. Clinopyroxene usually has (001) exsolution lamellae or exsolution patches. While the dykes are characterized by typical diabase texture with olivine and /or clinopyroxene enclosed by the framework of interlocking tabular plagioclase.

The recovered gabbros and dykes are generally altered, among them 6 relatively fresh gabbros were analyzed on board by miniprobe. The clinopyroxenes in these analyzed gabbros generally have magnesium number (100 mg/(Mg+Fe)) of 60-70, which suggest these gabbros were formed from relatively evolved melt. This is also suggested by the presence of primary ilmenite in the gabbros (Fig. 7.15).

### Geochemical variation of gabbros

Yongjun Gao<sup>1)</sup>, Sandrin Feig<sup>2)</sup>

<sup>1)</sup>University of Göttingen, Göttingen

<sup>2)</sup>University of Hannover, Hannover

We have analyzed 6 gabbros, one is from the kink volcanic region, the transition zone between Gakkel ridge and Lena Trough, and the other 5 are from the western volcano region of Gakkel ridge at ~3°E, which were recovered together with peridotites. As described before, it was not possible to analyze the plagioclase of the samples due to inadequate beam conditions for getting reliable sodium contents. In our measurements we focused on the clinopyroxenes and oxides of the samples.

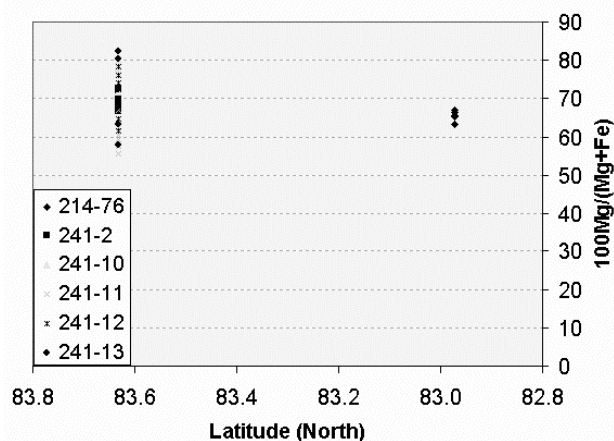


Fig. 7.32: Mg/(Mg+Fe) in gabbroic clinopyroxenes

In the clinopyroxenes of the analyzed samples, large variations in the Mg# of the gabbros from Gakkel ridge were observed, reflecting melt/rock interaction or melt fractionation. In Lena Trough region only one sample is measured so we can not make any detailed discussion, but however it is in the range of the Mg# variations of Gakkel ridge gabbros (Fig. 7.32).

Beside clinopyroxene also oxides were analyzed at least in one sample. The oxides of the other samples are too small to identify them with the "electron mini-probe". The analysis shows that the oxide is ilmenite, which means that this oxide is a primary phase crystallized from evolved melt.

## Hydrothermal Activity

Jonathan Snow<sup>1)</sup>, Yongjun Gao<sup>2)</sup>,  
Sandrin Feig<sup>3)</sup>

<sup>1)</sup>Max-Planck Institut für Chemie  
<sup>2)</sup>University of Göttingen, Göttingen  
<sup>3)</sup>University of Hannover, Hannover

Lena Trough and Gakkel Ridge both show evidence of active hydrothermal systems. On this cruise we have investigated two of these hydrothermal occurrences further. CTD work and dredging was carried out in the vicinity of both the Aurora and Lucky B hydrothermal sites. The Aurora site showed video evidence of active venting in 2001, and fresh sulfides were dredged there. Dredging there on this cruise returned additional glassy basalts from a low bench immediately beneath the Aurora site. CTD's performed in the area show signs of distant hydrothermal activity, but we were not able to localize the Aurora plume. At the Lucky B site we conducted a tow-yo operation, which again detected large thermal signals probably related to active venting. Dredging nearby produced abundant mantle peridotites, massive carbonates and fresh sulfides.

### Aurora

The Aurora Field was discovered in 2001 as a part of the AMORE Expedition when the USCGC Healy dredged fresh hydrothermal sulfides from a small seamount in the intersection of Lena Trough with Gakkel Ridge. RV *Polarstern* then conducted an OFOS investigation, which produced a videotape showing evidence for active venting. Both OFOS and dredge deployments used MAPR hydrothermal recorders, which recorded large signals.

At station 218, we conducted CTD operations at one site directly above the Aurora field and several more in the rift valley near Aurora. In each case, tow-yo operations were not possible because there was no provision to run the CTD from the rear A-frame in pack ice. However, it is important to note that this capability had not been requested in advance. In future investigations, this will be done.

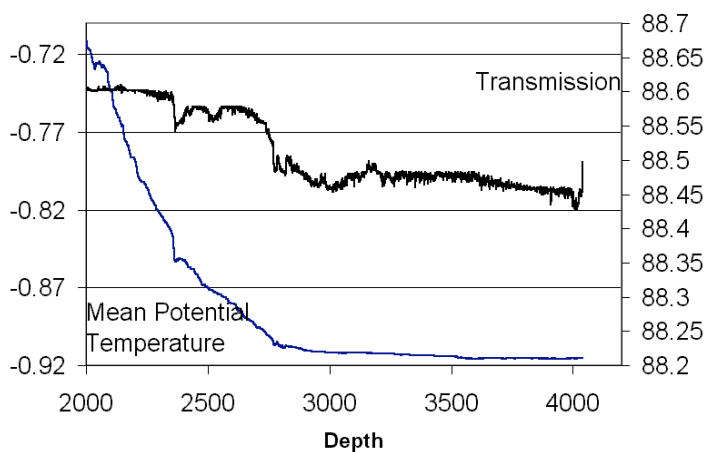


Fig. 7.33: Aurora Field Hydrothermal signals, Station 222 (Lena Rift near Aurora)

At the Aurora site, the CTD signals were weak and diffuse, but were present in nearly all the CTD casts performed in the rift valley. Figure 7.33 shows a typical hydrothermal anomaly from the Aurora site. Light transmission and thermal anomalies are not always coincident, this may be due to diffusion and particle settling

in the plume, and points to a distal portion of the plume. It is possible that the signal recorded is not the Aurora plume at all. Water samples were collected at several locations in the lower 100 meters of the water column, and will be analyzed for Mn and other trace metals at the Southampton Oceanography Center.

### Lucky B

The Lucky B site was discovered in 1999 on the ARK-XV/2 cruise of PFS RV *Polarstern*. As was the case with the Aurora Field, the discovery was more a matter of luck than design. Massive hydrothermal sulfides and hydrothermal mud were recovered from a basement slope in Lena Trough. However, since the surrounding topography could not be mapped or sampled due to the ice conditions, the substrate of the hydrothermal sulfides remained somewhat in doubt. Pieces of serpentine recovered with the hydrothermal rocks suggested an ultramafic substrate, however such deposits are very rare, and thus it was difficult to say definitively at the time whether in fact ultramafic rocks were the substrate of the hydrothermal field.

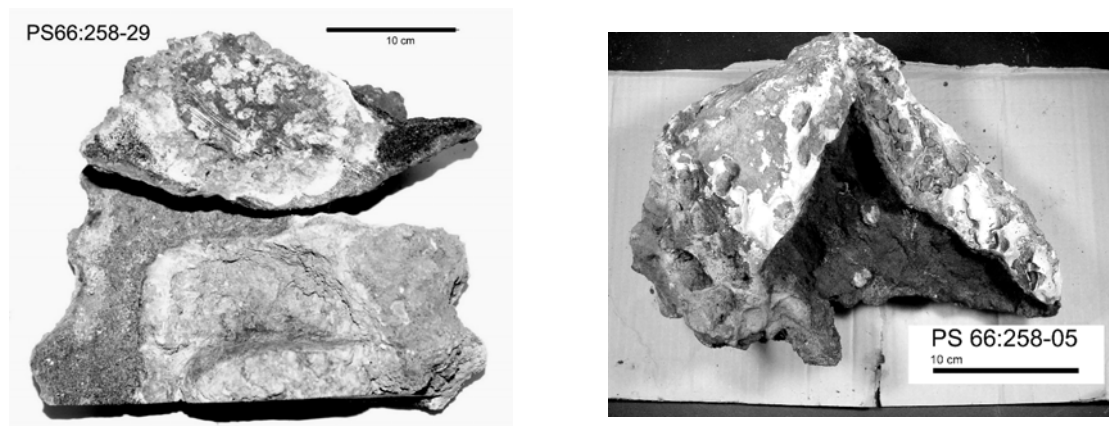


Fig. 7.34: Samples of hydrothermal sulfide from Lucky B. 34a: Sample 258-28. UM shows the location of serpentinized peridotite clast. 34b: Sample 258-05, Massive carbonate chimney piece

During ARK-XX/2, we mapped the area of the Lucky B site thoroughly. The site was found to reside on a prominent basement ridge jutting out from the floor of Lena Trough. 7 dredge hauls from this ridge returned 97 % mantle peridotite. One dredge haul from the side of the ridge opposite to Lucky B returned 24 kg of mantle peridotite, which tends to confirm the ultramafic nature of the Lucky B hydrothermal site.

Further dredging was conducted at the Lucky B site at station 258. This dredge haul returned 62 kg of massive hydrothermal sulfide and carbonate, including travertine. These rock types, particularly the carbonates, are typical of ultramafic hydrothermal occurrences: Basalt-hosted hydrothermal deposits rarely if ever contain deep sea carbonate, being instead based on anhydrite and sulfide. Figure 7.34 shows some of the samples from Station 258, including a carbonate-cemented sulfide chimney piece and a block of ultramafic rock in a massive-sulfide breccia.

CTD Station 258-2 was run just at the end of the dredge run of station 258. The idea was to determine whether active venting is occurring at Lucky B by locating and sampling the hydrothermal plume, and to try to localize the active venting site if possible. Figure 7.35 shows the CTD results of two traverses of the hydrothermal plume, showing a clear signal in both transmission and potential temperature. However, the signals were not as strong as expected and thus a localization of the hydrothermal venting site was not possible. The plume was sampled in three locations, and the samples will be analyzed for trace metals at the Southampton Oceanography Center.

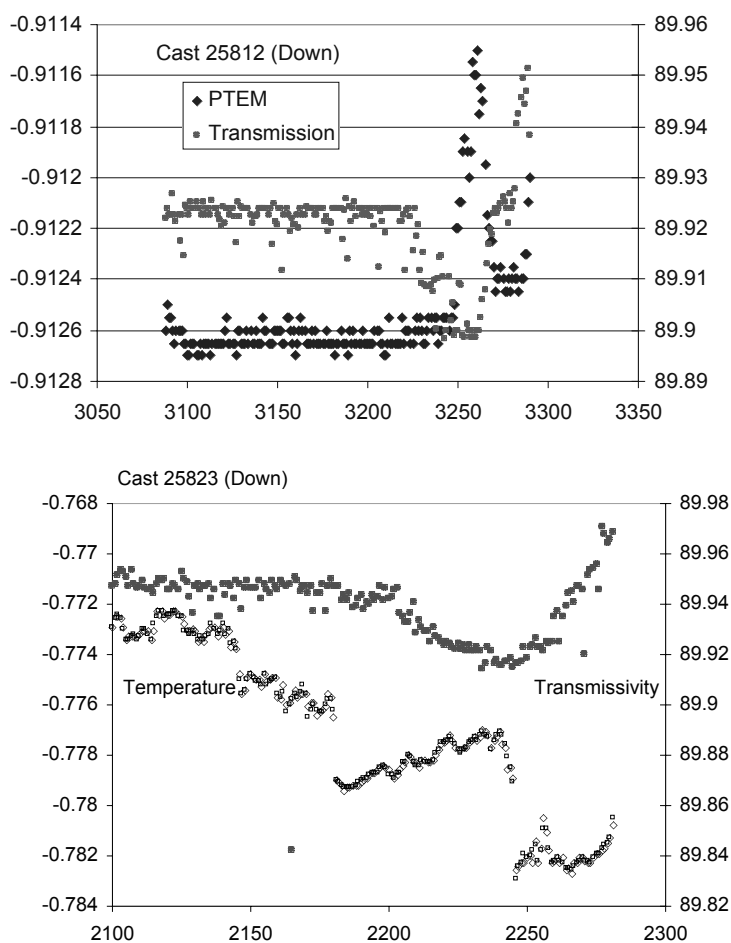


Fig. 7.35: CTD Traverses of the Lucky B hydrothermal plume

### Mineralogy and geochemistry of "Lucky B" hydrothermal rocks (PS66-258)

Dredge 258 at the Lucky B field provided a huge variety of hydrothermal rocks. A total of 62.2 kg of massive hydrothermal sulfides, low-temperature Fe-oxides/hydroxides and carbonates were collected. The hydrothermal rocks often contain a black crust.

The massive carbonates have a light grey colour and form crusts on the iron-oxides/hydroxides and sulfides. On the surface of some carbonates structures of “vent-life-forms” are visible. Furthermore the carbonate crust is dissolved at some places. This can be explained by changing pH of the hydrothermal solution.

Beside the carbonates, pyrite is common in the dredge. The mineral has a dark grey colour and forms crystals with a size of up to 1 mm. In the hydrothermal rocks we find specimens consisting of pyrite-aggregate and samples where the pyrite is mixed with a black fine crystalline material and some carbonate in between. At some places fluid veins cross-cutting the rock are visible.

Finally there is a huge variety of different Fe-oxides/hydroxides with colours ranging from yellow to dark red.

Due to the loose structure of the hydrothermal rocks no thin sections were prepared and only a few specimens were cut. A few grains of the different rocks were mounted in an epoxy-disc and analyses with mini-probe (see below). A detailed study of the rocks and their microstructure will be done later on at the MPI in Mainz.

### **Miniprobe results**

The hydrothermal rocks of Lucky B (PS66-258; 81°20'N and 3°20'W) have been analysed with the “electron mini-probe” to determine the modal composition. For the measurement we used the “100 µm” beam size, an acceleration voltage of 20 kV, a beam current of 100 mA and a counting time of 100s. The prevailing vacuum is controlled by the beam current (usually between 0.020 and 0.004 mbar).

For the analyses fragments of the hydrothermal rocks with different colour and porosity structure were chosen and mounted into two epoxy-discs. At that time the rocks were not labelled. It is not possible to relate the analyses to a certain rock. But the rock types are easy to distinguish from each other. And when we collected the different peaces, we tried to have the whole variety of hydrothermal deposits in our epoxy-discs.

The analysed rocks can be separated into three groups: carbonates, iron-oxides/hydroxides and sulfides. The carbonates are on the outside of the chimney fragments and are generated as travertine or from “vent-life-forms”. The “electron mini-probe” analyses show that there is no dolomite occurring in the deposits (Fig. 7.36a). The crusts are made of pure calcium carbonate. The peaks of sulphur and iron represent a small modal fraction of pyrite and maybe some calcium sulfide in the crust. The iron-oxides/hydroxides of the dredge were identified by an iron-peak in the spectra that is higher than one could explain with a silicate or sulfide structure (Fig. 7.36b-f). With the electron mini-probe it is not possible to distinguish between magnetite, hematite, goethite or other iron structures. First, the electron mini-probe does not measure the amount of oxygen nor hydrogen in the mineral structure. Second the uncertainties in the totals are too large to use the totals of the analyses to distinguish between minerals with iron in a reduced state and iron in an oxidized state (for example hematite and magnetite). This could be done with an electron microprobe with wavelength dispersive spectrometers.

And finally we found two different sulfides in the hydrothermal deposits, pyrite ( $\text{FeS}_2$ ) and chalcopyrite  $\text{CuFeS}_2$  (Fig. 7.36c). Pyrite forms small euhedral gray crystals, while the chalcopyrite occurs as a black fine crystalline material. Macroscopic, the minerals form aggregates which are separated by a distinct boundary from each other, but normally there is always a certain amount of pyrite in chalcopyrite and the other way around. The resolution of the beam of the electron mini-probe is not good enough to measure individual crystals. Typically also Ca-bearing phases are in between (Fig. 7.36d-f). Due to the presence of sulfur, the Ca-phase cannot be identified exactly, but it should be a mixture of carbonate and calcium-sulfate.

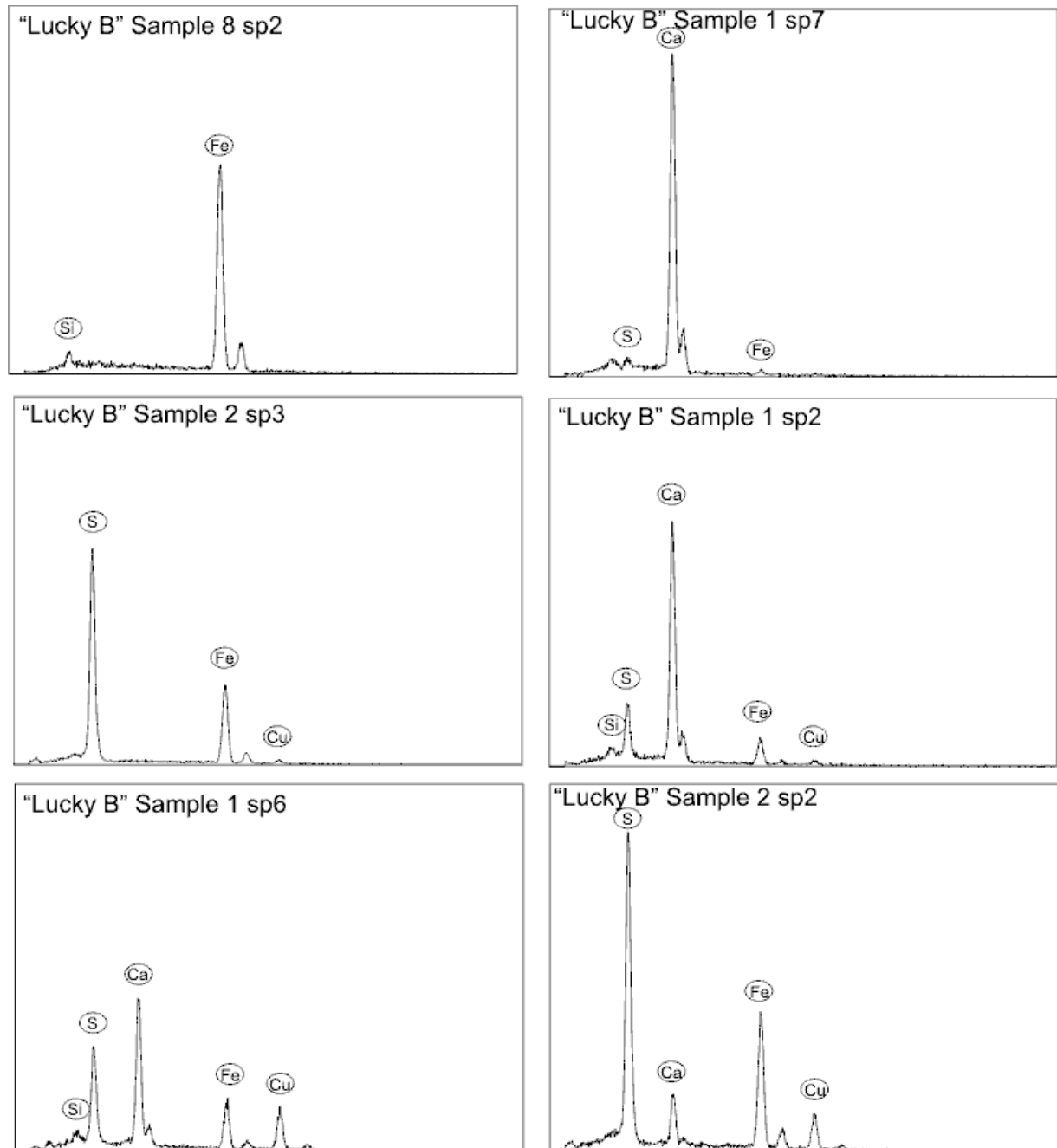


Fig. 7.36 a-f: Miniprobe spectra of hydrothermal minerals

## Mineralogy and microstructures of basalts

Francois Nauret  
Max-Planck Institut für Chemie

### Introduction

Basalts from Lena Trough are believed to be the products of the smallest degree of mantle partial melting ever studied. As a likely consequence of this small degree of partial melting, basalt seems to cover only a limited surface along Lena Trough. Only very few basalts have been collected, compare to what we expected. Thus, Lena Trough basalts are rare and thus Lena Trough can be considered as an amagmatic segment. Only 7 dredges containing basalt have been recovered during cruise ARK-XX/2. Most of the basalt samples were collected during the last day of dredging. As a consequence, due to the peridotite-saturation of the thin-section lab, only 10 thin sections of early dredged basalts have been realized. Thin sections for PS66-261 and 262 will be done at the MPI.

### Basalt types

Four different locations are distinguished, from the North to the South: Gakkel ridge, Aurora field (hydrothermal field), Lena Trough (region between Aurora and Lucky B fields), and Lucky B field (hydrothermal field in the south part of Lena Trough). The Aurora and lucky fields frame Lena Trough (see map). Basalt-type, discriminated based on the mineralogy, are reported in figure 7.37. However, the main difference between these rocks is the percent of vesicle. A comparison between the percent of vesicle for MORB collected during ARK-XX/2 and those collected along Gakkel ridge during XVII/2 is reported in figure 7.38. First, we observe that Lena Trough MORB display only a low percent of vesicles (<1 %) (Fig. 7.38B). Second, the distribution between Gakkel Ridge and Aurora field basalt is relatively similar (Fig. 7.38B), suggesting that both region are part of the same unit. In comparison with Gakkel Ridge MORB, collected during AMORE Expedition (ARK-XVII/2, 2001), ARK-XX/2 MORB are less vesicular (Fig. 7.38A and B). However, it appears that the distribution presents the same shape but shifted toward less percent of vesicle. Such

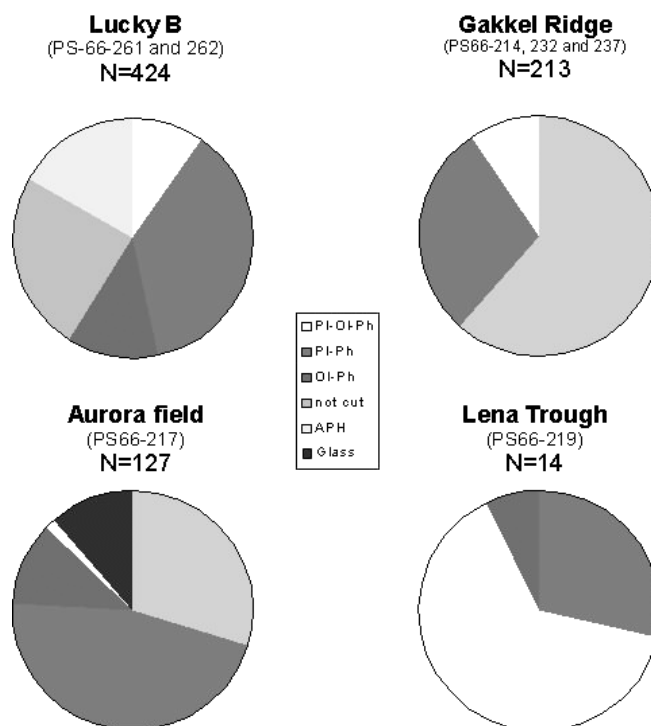


Fig. 7.37: Basalt types discriminated by the mineral phenocryst phase, from four different locations. "Not cut" samples are either too small or were saved because they have a thick glassy rim. Ol.: olivine, Pl: plagioclase, Ph.: phyrice

shift can be real but can also reflected a “human” error factor during the visual estimation of the percent of vesicles. As a consequence, Aurora field is interpreted as the boundary between Gakkel Ridge and Lena Trough. Third, basalt collected in the southern part of Lena Trough (PS 66-261 and 262) are vesicular (>10 %) (Fig. 38C). It is the first main characteristic of these basalts. This characteristic feature is either due to higher volatile content or to a shallow depth eruption. To discriminate between these two possibilities, further chemical analyses will be done at the MPI to investigate this important difference.

## **Mineralogy**

### **Phenocrysts**

7 thin sections have been studied by means of transmitted light microscopy. They all display a porphyric texture with olivine and/or plagioclase as phenocryst phases (Figs. 7.39, 7.40, 7.41).

Olivine, as phenocryst, is present in 6 different thin sections, and plagioclase phenocryst in 5. Observed olivine phenocryst are 1 to 5 mm large and make up 10 % of the thin section. Most of the olivine are euhedral shape. Forsterite content (%Fo) of Olivine have been analyzed by the miniprobe in the thin section L4 and L129, corresponding to sample PS66 214-4 and 237-1 respectively. The %Fo=  $87\pm 1$  and  $83\pm 2$  for L4 and L129. As a consequence those olivine can be considered to be relatively primitive, suggesting a relatively high MgO content of the host lava.

Plagioclase phenocrysts are generally large (10 mm). Generally, plagioclase and olivine are associated as phenocryst, except in the sample PS66-219-14 where only plagioclase as phenocryst has been identified. A particular interest have been given to sample PS-66-237-2. This sample displays very large plagioclase (20 %, 10 mm) with extremely high number of melt inclusions (Fig. 7.39). This particular feature shows that phenocryst of this sample have grown extremely rapidly.

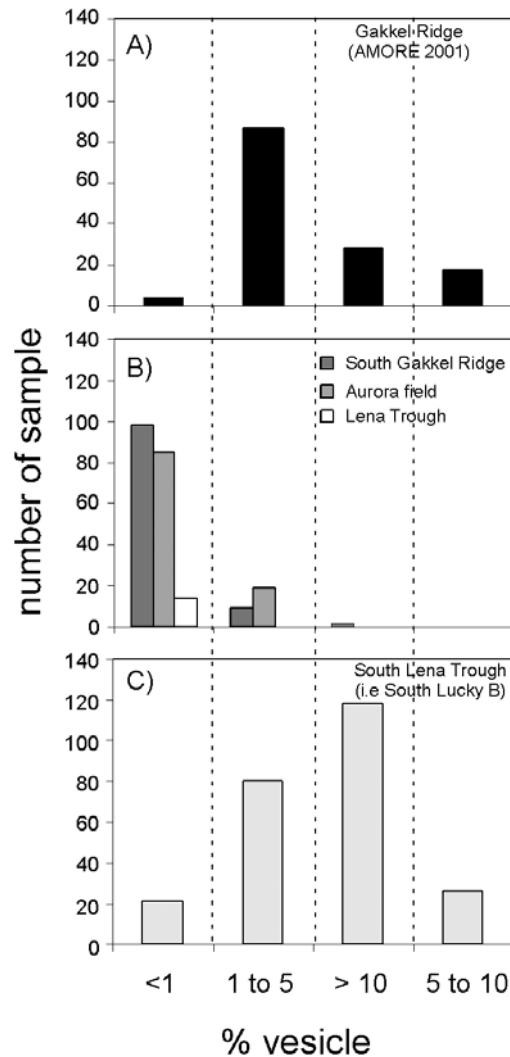
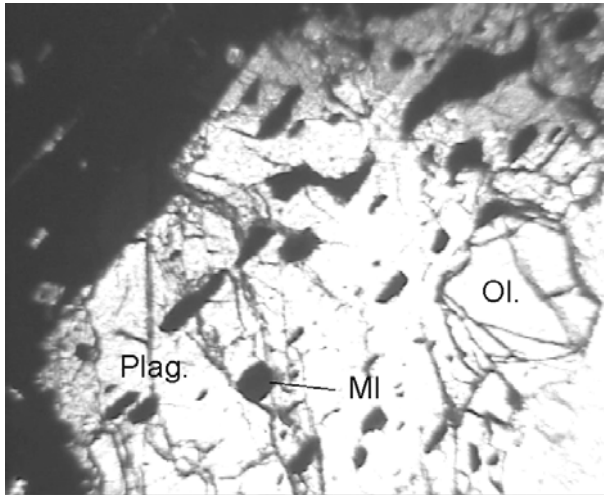


Fig. 7.38: Comparison between the percentage of vesicles of ARK-XX/2 MORB and ARK-XVII/2 MORB. Inside ARK-XX/2 MORB, we define 4 different regions: Gakkel ridge, Aurora hydrothermal field, Lena Trough proper between Aurora and Lucky B hydrothermal fields, and finally the part of Lena Trough South Lucky B.

### Groundmass

The groundmass of the samples are mainly composed of plagioclase and clinopyroxene microlites and glass. Oxides are relatively rare. Microlites do not show a particular orientation. The glass, observed in thin section is still relatively fresh, and has a dark-brown to light-brown colors. Based on the relationship between mineral phase, the crystallization sequence for the all thin section set is the following: olivine (when present), plagioclase and glass.



*Fig. 7.39: Plagioclase phenocryst hosting a olivine (PS66-237-1). Forsterite composition of this olivine have been analyzed (%Fo=83) using the miniprobe. We observe large glassy melt inclusion hosted by the plagioclase. Ol.: Olivine, Plag.: Plagioclase, MI: melt inclusion*



*Fig. 7.40: Typical texture of the ARK-XX/2 MORB, with olivine and plagioclase phenocrysts surrounded by a matrix composed by fresh glass, olivine and plagioclase*



*Fig.7.41: Euhedral olivine phenocryst surrounded by glass-plagioclase microlite matrix*

## Conclusions

ARK-XX/2 had the petrologic objective of mapping and sample Lena Trough and the 3°E portion of Gakkel Ridge. The sampling programme enjoyed great operational success, and was able to sample more quickly than was originally assumed, more efficiently even than in 2001. 9/10ths pack ice is truly no hindrance to a petrologic sampling programme in a good year.

The goal of sampling all of the tectonic features of Lena Trough was not achieved, but as this was an initial exploration of Lena Trough, it would have been

unreasonable to expect complete coverage. On Gakkel Ridge we were able to complete the survey begun in 2001 for a limited but highly interesting area of the ridge. In the western part of the 3°E area, we have probably exhausted the possibilities of the sampling tools used here. Further investigation at the western part of 3°E will require more precise mapping and sampling tools in order to understand the geological evolution of this region.

The mapping programme was also a success. Due to unexpectedly good ice conditions, much time was won and far more bathymetric survey could be carried out than was originally planned. In fact, the mapping programme probably benefited more from the additional time due to good ice than did the petrology programme. The result is a nearly complete map of Lena Trough, where before there was little north of 81°N and nothing between 81°30'N and about 83°N. This is particularly important in the area we surveyed, because even though the existing SCICEX data set from the SCAMP mapping instrument is of somewhat poorer quality than Hydrosweep, even those data are only available further east on Gakkel Ridge. The Western Nansen basin is truly one of the most poorly studied regions of the Earth's surface. A good example for this is the discovery of a new seamount, reaching thousands of meters above the previously recognized topography. Even on Mars there are no such discoveries left to be made, as the inner planets are all better mapped than the Western Nansen Basin.

It was expected that the exploration of Lena Trough would be scientifically very fruitful, and this has turned out to be the case. The highlights of the cruise include defining the tectonics of the only modern young ocean basin, sampling mantle rocks in a region where there is nearly no melting, and the confirmation of active ultramafic hydrothermal venting at the Lucky B hydrothermal field. Further work in this area is almost guaranteed, as there are very few known ultramafic hydrothermal fields. None of them are in the Arctic basin, where it is postulated that vent fauna have been cut off from contact with the rest of the world's oceans during geologic time, and thus may represent species that are at present completely unknown.

An additional bonus was the retrieval of a set of mid-ocean ridge mantle samples from 3°E that contains unaltered peridotite in large quantities. It is hard to overstate the importance of this find: The mid-ocean ridge mantle is the most important chemical reservoir on Earth for the production of the crust we stand on, the water we drink, the air we breathe. Direct studies of mid-ocean ridge mantle have always been hampered by their seafloor alteration, which plays havoc with volatile contents, sensitive trace element indicators of mantle processes, and generally contaminates everything. These samples will allow us to answer several key problems in the evolution of the Earth's crust definitively for the first time. The AMORE expedition in 2001 caused a minor sensation by finding a few kg of rocks such as these. Entire papers are being published on just a few thin sections at a time of the 2001 material. We have found several hundred kg of even better and fresher mantle material. It remains a mystery why this very fresh mantle material is exposed on Gakkel Ridge, but its existence here (and non-existence elsewhere) is a fact. These samples could be compared to the first samples from the Moon in their significance for the study of the Earth.

The future of petrologic research in the high Arctic is by no means a finished story. The Eastern Gakkel Ridge remains completely unexplored. In the West, only the most superficial work has been done (on a mean sampling interval of 20 km!). Understanding this particular mid-ocean ridge system in detail is worth the additional cost and expense of launching expeditions up here, because fundamental problems in Earth Science can be addressed here that can not be addressed on other mid-ocean ridges.

Beyond the mid-ocean ridge system, the pre-Pangean history of the arctic basin is nearly entirely unconstrained, despite the enormous significance of the arctic for the tectonic and climatic evolution of the Earth. Such structures as the Morris Jessup Rise, Lomonosov Ridge, Alpha Ridge, and Mendeleev Rise represent a large part of the remaining geological mysteries on the planet. No ocean crust older than the Jurassic is known outside of ophiolite complexes, and these are known to be non-representative of ocean crust. But the Arctic basin is clearly pre-Pangean, (i.e., older than the Jurassic). What can we learn about the evolution of the Earth from being able to study true fossil ocean crust from that time? We haven't even begun to think of the questions to ask of that ancient ocean basin, much less what answers might await us.

---

## **APPENDIX**

**A.1 Participants**

**A.2 Participating Institutions**

**A.3 Ship's Crew**

**A.4 Station List**

## A.1 PARTICIPANTS

<b>Name</b>	<b>Vorname/ First Name</b>	<b>Institut/ Institute</b>	<b>Beruf / Profession</b>
Aspmo	Katrine	NIAR Kjeller	Student
Beszczyńska-Möller	Agnieszka	AWI	Oceanographer
Biegler	Maik	MPI Mainz	Taxidermist
Bishop	John	Uni Tasmanien	Geophysicist
Busche	Thomas	AWI	Geographer
Doppler	Judith	epo-Film	Assistant cameraman
Eckardt	Regina	Uni Mainz	Student
Fain	Xavier	LGGE, St. Martin	Student
Feig	Sandrin T.	Uni Hannover	Scientist
Feldmann	Heinrich	MPI Mainz	Technician
Ferrari	Christophe	LGGE, St. Martin	Scientist
Fieg	Kerstin	AWI	Scientist
Flechtenhar	Kurt	DWD	Meteorologist
Flinspach	David	AWI	Student
Gao	Yongjun	Uni Göttingen	Ph.D. Student
Gauchard	Pierre-Alexis	LGGE, St. Martin	Student
Gauger	Steffen	Fielax	Engineer
Goldstein	Steven	Columbia Uni	Professor
Handt, v.d.	Anette	MPI Mainz	Student
Hayek	Wolfgang	AWI	Student
Hellebrand	Eric	MPI Mainz	Geologist
Kohls	Tanja	AWI	Student
Lahrman	Uwe	HeliTransair	Pilot
Lemke	Peter	AWI	Chief Scientist
Liesenfeld	Timo	Uni Mainz	Student
Lieser	Jan	AWI	Meteorologist

<b>Name</b>	<b>Vorname/ First Name</b>	<b>Institut/ Institute</b>	<b>Beruf / Profession</b>
Lohmann	Rainer	Uni Bremen	Scientist
Marnela	Marika	FIMR Helsinki	Scientist.
Martin	Torge	AWI	Meteorologist
Mayer	Kurt	epo-Film	Producer
Monsees	Matthias	Optimare	Technician
Mussil	Stephan	epo-Film	Cinematographer
Nauret	Francois	MPI Mainz	Scientist
Nizzetto	Luca	Uni Varese	Student
Pfaffling	Andreas	AWI	Geophysicist
Röber	Sebastian	AWI	Student
Rohr	Harald	Optimare	Physicist
Rudolf	Anton	HeliTransair	Pilot
Saldern, von	Carola	AWI	Physicist
Schmidt	Steffen	Uni Mainz	Student
Schmitt	Wolfgang	LMU München	Scientist
Schütt	Ekkehard	AWI	Technician
Schwegler	Helmut	Uni Bremen	Professor
Snow	Jonathan	MPI Mainz	Scientist
Sonnabend	Hartmut	DWD	Meteorologist
Spreen	Gunnar	Uni Bremen	Scientist
Stimac	Mihael	HeliTransair	Technician
Turini	Simona	Uni Mainz	Student
Will	Jan Martin	HeliTransair	Technician
Wisotzki	Andreas	AWI	Oceanographer
Zenk	Oliver	Optimare	Engineer

---

## A.2 PARTICIPATING INSTITUTES

### Address

---

AWI	Stiftung Alfred-Wegener-Institut für Polar- und Meeresforschung in der Helmholtz-Gemeinschaft Postfach 12 01 61 27515 Bremerhaven / Germany
NIAR	Norwegian Institute for Air Research P.O. Box 100 NO-2027 Kjeller / Norway
University Hannover	Institut für Mineralogie Universität Hannover Callinstr. 3 30167 Hannover / Germany
University Göttingen	Geochemie Institut University Göttingen Goldschmidt Str. 1 37077 Göttingen / Germany
LMU München	Department f. Geo- und Umweltwissenschaften LMU München Sektion Mineralogie, Petrologie und Geochemie Theresienstr. 41/III 80333 München / Germany
LDEO	Columbia University Lamont-Doherty Earth Observatory 61 Rt. 9W Palisades, NY 10964 / USA
DWD	Deutscher Wetterdienst Bernhard-Nocht-Str. 76 20359 Hamburg / Germany
epo	epo-film Edelsinnstr. 58 1120 Wien / Austria

---

**Address**


---

FIELAX	FIELAX GmbH Schifferstr. 10-14 27568 Bremerhaven / Germany
FIMR	Finnish Institute of Marine Research P.O. Box 33 00931 Helsinki / Finland
Heli Transair	Heli Transair GmbH Am Flugplatz 63329 Egelsbach / Germany
LGGE	Laboratoire de Glaciologie et Geophysique de L'environnement LGGE 54 rue Molière BP 96 38402 Saint Martin d'Herès / France
MPI Mainz	Max-Planck-Institut für Chemie Johann-J. Becherweg 27 55128 Mainz / Germany
Optimare	Optimare Sensorsysteme AG Am Luneort 15 27572 Bremerhaven / Germany
RCOM	RCOM P.O. Box 330440 University of Bremen 28334 Bremen / Germany
University Bremen	Universität Bremen Fachbereich 1 (Physik) Postfach 330440 28334 Bremen / Germany
University TAS	Mitre Geophysics P/L University of Tasmania P.O. Box 974 Sandy Bay 700 b / Australia



## A.4 STATION LIST ARK-XX/2

Station	Date	Time	PositionLat	PositionLon	Depth [m]	Gear (Abbrev.)	Action
PS66/141-1	17.07.04	05:20	78° 50.13' N	5° 1.15' E	2702.0	MOR	Hydroph. into water
PS66/141-1	17.07.04	05:44	78° 50.07' N	5° 0.83' E	2702.0	MOR	action
PS66/141-1	17.07.04	06:25	78° 50.30' N	4° 57.35' E	0.0	MOR	action
PS66/142-1	17.07.04	06:57	78° 49.93' N	5° 0.50' E	2698.3	MOR	Hydroph. into water
PS66/141-2	17.07.04	06:57	78° 49.93' N	5° 0.50' E	2698.3	MOR	Hydroph. into water
PS66/142-1	17.07.04	07:05	78° 50.03' N	5° 0.39' E	2699.6	MOR	Hydroph. into water
PS66/141-2	17.07.04	07:05	78° 50.03' N	5° 0.39' E	2699.6	MOR	Hydroph. into water
PS66/142-1	17.07.04	07:09	78° 50.07' N	5° 0.21' E	166.5	MOR	released
PS66/142-1	17.07.04	07:20	78° 50.26' N	4° 59.76' E	2716.0	MOR	Hydrophone on Deck
PS66/142-1	17.07.04	07:24	78° 50.33' N	4° 59.57' E	2719.0	MOR	Hydroph. into water
PS66/142-1	17.07.04	07:30	78° 50.40' N	4° 59.25' E	2725.0	MOR	Hydrophone on deck
PS66/142-1	17.07.04	07:51	78° 49.95' N	5° 1.51' E	0.0	MOR	Hydroph. into water
PS66/142-1	17.07.04	07:52	78° 49.94' N	5° 1.39' E	0.0	MOR	released
PS66/142-1	17.07.04	08:16	78° 50.29' N	5° 1.19' E	0.0	MOR	Hydrophone on deck
PS66/142-1	17.07.04	08:26	78° 49.99' N	5° 1.18' E	0.0	MOR	Hydroph. into water
PS66/142-1	17.07.04	08:35	78° 50.07' N	5° 0.81' E	0.0	MOR	Hydrophone on deck
PS66/142-1	17.07.04	09:10	78° 49.92' N	5° 0.69' E	0.0	MOR	action
PS66/142-1	17.07.04	09:26	78° 49.81' N	5° 1.39' E	0.0	MOR	Hydroph. into water
PS66/142-1	17.07.04	09:33	78° 49.91' N	5° 1.17' E	0.0	MOR	action
PS66/142-1	17.07.04	09:44	78° 49.67' N	5° 2.56' E	2690.0	MOR	on the surface
PS66/142-1	17.07.04	10:10	78° 49.50' N	5° 4.84' E	2668.0	MOR	action
PS66/142-1	17.07.04	10:15	78° 49.47' N	5° 4.95' E	2669.0	MOR	action
PS66/142-1	17.07.04	10:20	78° 49.51' N	5° 4.91' E	2668.0	MOR	on deck
PS66/142-1	17.07.04	10:55	78° 49.72' N	5° 2.92' E	2688.0	MOR	on deck
PS66/142-1	17.07.04	11:03	78° 49.83' N	5° 3.55' E	2690.0	MOR	on deck
PS66/142-1	17.07.04	11:12	78° 49.92' N	5° 3.38' E	2691.0	MOR	mooring on deck
PS66/143-1	17.07.04	12:38	78° 49.95' N	5° 59.07' E	2486.0	MOR	released
PS66/143-1	17.07.04	16:09	78° 50.44' N	5° 59.11' E	2488.0	MOR	action
PS66/143-1	17.07.04	16:54	78° 50.46' N	5° 59.14' E	2487.0	MOR	action
PS66/143-1	17.07.04	18:03	78° 50.45' N	5° 58.15' E	2494.0	MOR	action

Station	Date	Time	PositionLat	PositionLon	Depth [m]	Gear (Abbrev.)	Action
PS66/143-1	17.07.04	19:08	78° 50.59' N	5° 59.42' E	2487.0	MOR	action
PS66/143-1	17.07.04	19:32	78° 50.35' N	5° 59.16' E	2487.0	MOR	action
PS66/143-1	17.07.04	19:43	78° 50.35' N	5° 59.23' E	2486.0	MOR	action
PS66/143-1	17.07.04	19:59	78° 50.35' N	5° 59.22' E	2489.0	MOR	action
PS66/143-1	17.07.04	20:10	78° 50.40' N	5° 59.33' E	2486.0	MOR	action
PS66/143-1	17.07.04	20:31	78° 50.29' N	5° 59.47' E	2486.0	MOR	action
PS66/143-1	17.07.04	20:36	78° 50.35' N	5° 59.36' E	2487.0	MOR	action
PS66/143-1	17.07.04	21:38	78° 49.97' N	5° 59.30' E	2484.0	MOR	action
PS66/144-1	17.07.04	23:08	78° 50.02' N	5° 4.89' E	2685.0	CTD/RO	surface
PS66/144-1	17.07.04	23:59	78° 50.04' N	5° 5.51' E	2681.0	CTD/RO	at depth
PS66/144-1	18.07.04	00:48	78° 50.19' N	5° 6.06' E	2679.0	CTD/RO	on deck
PS66/145-1	18.07.04	01:21	78° 50.01' N	5° 19.97' E	2637.0	CTD/RO	surface
PS66/145-1	18.07.04	02:18	78° 49.91' N	5° 21.20' E	2631.0	CTD/RO	at depth
PS66/145-1	18.07.04	03:02	78° 49.74' N	5° 22.44' E	2626.0	CTD/RO	on deck
PS66/146-1	18.07.04	03:33	78° 50.04' N	5° 39.69' E	2585.0	CTD/RO	surface
PS66/146-1	18.07.04	04:26	78° 49.84' N	5° 38.82' E	2587.0	CTD/RO	at depth
PS66/146-1	18.07.04	05:13	78° 49.59' N	5° 36.87' E	2592.0	CTD/RO	on deck
PS66/147-1	18.07.04	05:47	78° 49.77' N	5° 55.22' E	2509.0	CTD/RO	surface
PS66/147-1	18.07.04	06:35	78° 49.65' N	5° 53.27' E	2522.0	CTD/RO	at depth
PS66/147-1	18.07.04	07:10	78° 49.78' N	5° 53.45' E	2521.0	CTD/RO	on deck
PS66/148-1	18.07.04	08:52	78° 49.85' N	6° 59.02' E	1490.0	MOR	Hydroph. into water
PS66/148-1	18.07.04	09:01	78° 49.77' N	6° 58.57' E	1497.0	MOR	released
PS66/148-1	18.07.04	09:02	78° 49.76' N	6° 58.60' E	1496.0	MOR	on the surface
PS66/148-1	18.07.04	09:03	78° 49.76' N	6° 58.64' E	1495.0	MOR	Hydrophone on deck
PS66/148-1	18.07.04	09:36	78° 50.41' N	6° 59.01' E	1470.0	MOR	action
PS66/148-1	18.07.04	09:37	78° 50.41' N	6° 59.00' E	1469.0	MOR	on deck
PS66/148-1	18.07.04	09:42	78° 50.47' N	6° 58.74' E	1474.0	MOR	on deck
PS66/148-1	18.07.04	09:44	78° 50.49' N	6° 58.63' E	1474.0	MOR	on deck
PS66/148-1	18.07.04	09:56	78° 50.48' N	6° 58.20' E	1486.0	MOR	on deck
PS66/148-1	18.07.04	10:04	78° 50.44' N	6° 58.16' E	1489.0	MOR	on deck
PS66/148-1	18.07.04	10:09	78° 50.44' N	6° 58.01' E	1493.0	MOR	releaser on deck
PS66/148-2	18.07.04	10:55	78° 50.00' N	6° 59.94' E	1471.0	MOR	surface

Station	Date	Time	PositionLat	PositionLon	Depth [m]	Gear (Abbrev.)	Action
PS66/148-2	18.07.04	11:08	78° 50.04' N	7° 0.07' E	1469.0	MOR	surface
PS66/148-2	18.07.04	11:25	78° 50.08' N	7° 0.21' E	1466.0	MOR	surface
PS66/148-2	18.07.04	11:38	78° 50.07' N	7° 0.12' E	1468.0	MOR	surface
PS66/148-2	18.07.04	11:49	78° 50.02' N	7° 0.06' E	1469.0	MOR	surface
PS66/148-2	18.07.04	11:55	78° 50.08' N	7° 0.05' E	1468.0	MOR	surface
PS66/148-2	18.07.04	11:58	78° 50.11' N	7° 0.10' E	1466.0	MOR	surface
PS66/148-2	18.07.04	12:01	78° 50.15' N	7° 0.04' E	1454.0	MOR	surface
PS66/148-2	18.07.04	12:03	78° 50.17' N	7° 0.01' E	1454.1	MOR	on the ground
PS66/148-2	18.07.04	12:04	78° 50.17' N	7° 0.00' E	1454.2	MOR	slipped
PS66/148-2	18.07.04	12:05	78° 50.18' N	7° 0.01' E	1453.4	MOR	Hydrophone on deck
PS66/149-1	18.07.04	15:00	78° 50.48' N	5° 58.58' E	2493.0	MOR	action
PS66/149-1	18.07.04	15:15	78° 50.47' N	5° 58.33' E	2493.0	MOR	action
PS66/149-1	18.07.04	15:30	78° 50.47' N	5° 58.31' E	2732.0	MOR	action
PS66/149-1	18.07.04	17:30	78° 50.47' N	5° 57.66' E	2497.0	MOR	action
PS66/149-1	18.07.04	18:11	78° 50.18' N	5° 58.55' E	2492.0	MOR	action
PS66/149-1	18.07.04	18:44	78° 49.95' N	5° 59.46' E	2483.0	MOR	action
PS66/149-1	18.07.04	19:35	78° 49.86' N	5° 58.82' E	2479.2	MOR	action
PS66/149-1	18.07.04	19:48	78° 49.77' N	5° 58.62' E	2490.0	MOR	action
PS66/150-1	18.07.04	20:38	78° 49.96' N	6° 10.03' E	2371.0	CTD/RO	surface
PS66/150-1	18.07.04	21:22	78° 49.99' N	6° 9.62' E	2374.0	CTD/RO	at depth
PS66/150-1	18.07.04	21:54	78° 50.06' N	6° 9.69' E	2376.0	CTD/RO	on deck
PS66/151-1	18.07.04	22:33	78° 50.04' N	6° 30.14' E	1985.0	CTD/RO	surface
PS66/151-1	18.07.04	23:11	78° 50.05' N	6° 29.84' E	1990.0	CTD/RO	at depth
PS66/151-1	18.07.04	23:40	78° 50.07' N	6° 29.88' E	1988.0	CTD/RO	on deck
PS66/152-1	19.07.04	00:18	78° 50.05' N	6° 54.62' E	1596.0	CTD/RO	surface
PS66/152-1	19.07.04	00:49	78° 50.00' N	6° 55.09' E	1563.0	CTD/RO	at depth
PS66/152-1	19.07.04	01:18	78° 50.06' N	6° 55.03' E	1564.0	CTD/RO	on deck
PS66/153-1	19.07.04	02:24	78° 50.05' N	7° 10.01' E	1360.0	CTD/RO	surface
PS66/153-1	19.07.04	02:52	78° 49.98' N	7° 10.23' E	1356.0	CTD/RO	at depth
PS66/153-1	19.07.04	03:14	78° 50.02' N	7° 10.25' E	1353.0	CTD/RO	on deck
PS66/154-1	19.07.04	03:44	78° 49.99' N	7° 29.49' E	1177.0	CTD/RO	surface
PS66/154-1	19.07.04	04:08	78° 49.98' N	7° 30.02' E	1173.0	CTD/RO	at depth

Station	Date	Time	PositionLat	PositionLon	Depth [m]	Gear (Abbrev.)	Action
PS66/154-1	19.07.04	04:29	78° 50.00' N	7° 30.11' E	1171.0	CTD/RO	on deck
PS66/155-1	19.07.04	05:10	78° 49.99' N	7° 54.96' E	1064.0	CTD/RO	surface
PS66/155-1	19.07.04	05:47	78° 49.94' N	7° 54.26' E	1069.0	CTD/RO	at depth
PS66/155-1	19.07.04	05:56	78° 49.86' N	7° 54.11' E	1066.0	CTD/RO	on deck
PS66/156-1	19.07.04	08:23	78° 49.93' N	6° 0.61' E	2473.0	MOR	surface
PS66/156-1	19.07.04	08:25	78° 49.92' N	6° 0.65' E	2474.0	MOR	surface
PS66/156-1	19.07.04	08:55	78° 49.93' N	6° 0.32' E	2475.0	MOR	surface
PS66/156-1	19.07.04	09:13	78° 49.97' N	6° 0.14' E	2477.0	MOR	surface
PS66/156-1	19.07.04	09:29	78° 49.95' N	6° 0.08' E	2476.0	MOR	surface
PS66/156-1	19.07.04	09:38	78° 49.95' N	6° 0.34' E	2477.0	MOR	surface
PS66/156-1	19.07.04	09:42	78° 49.94' N	6° 0.19' E	2474.0	MOR	surface
PS66/156-1	19.07.04	09:46	78° 49.93' N	6° 0.10' E	2477.0	MOR	on the ground
PS66/156-1	19.07.04	09:47	78° 49.94' N	6° 0.08' E	2476.0	MOR	slipped
PS66/157-1	19.07.04	11:13	78° 49.88' N	5° 2.77' E	2698.0	MOR	surface
PS66/157-1	19.07.04	11:16	78° 49.87' N	5° 2.58' E	2699.0	MOR	surface
PS66/157-1	19.07.04	11:39	78° 49.81' N	5° 1.90' E	2699.0	MOR	surface
PS66/157-1	19.07.04	12:02	78° 49.80' N	5° 1.49' E	2702.0	MOR	surface
PS66/157-1	19.07.04	12:17	78° 49.78' N	5° 1.34' E	2700.0	MOR	surface
PS66/157-1	19.07.04	12:27	78° 49.79' N	5° 1.33' E	2700.0	MOR	surface
PS66/157-1	19.07.04	12:29	78° 49.80' N	5° 1.30' E	2701.0	MOR	surface
PS66/157-1	19.07.04	12:32	78° 49.80' N	5° 1.31' E	2702.0	MOR	surface
PS66/157-1	19.07.04	12:35	78° 49.80' N	5° 1.34' E	2701.0	MOR	on the ground
PS66/157-1	19.07.04	12:36	78° 49.80' N	5° 1.33' E	2701.0	MOR	releaser on deck
PS66/157-1	19.07.04	12:36	78° 49.80' N	5° 1.33' E	2701.0	MOR	slipped
PS66/158-1	19.07.04	16:02	78° 50.08' N	7° 58.43' E	1045.0	MOR	Hydroph.intowater
PS66/158-1	19.07.04	16:14	78° 50.16' N	7° 58.45' E	1047.0	MOR	released
PS66/158-1	19.07.04	16:16	78° 50.18' N	7° 58.46' E	1048.0	MOR	on the surface
PS66/158-1	19.07.04	16:42	78° 50.03' N	7° 59.44' E	1038.0	MOR	action
PS66/158-1	19.07.04	17:04	78° 50.06' N	7° 59.01' E	1043.0	MOR	on deck
PS66/159-1	19.07.04	17:36	78° 50.23' N	8° 19.32' E	799.8	MOR	released
PS66/159-1	19.07.04	17:37	78° 50.25' N	8° 19.31' E	799.1	MOR	on the surface
PS66/159-1	19.07.04	18:07	78° 50.01' N	8° 19.83' E	792.7	MOR	action

Station	Date	Time	PositionLat	PositionLon	Depth [m]	Gear (Abbrev.)	Action
PS66/159-1	19.07.04	18:33	78° 49.98' N	8° 20.05' E	786.5	MOR	on deck
PS66/160-1	19.07.04	19:04	78° 49.88' N	8° 39.06' E	286.1	MOR	Hydroph.into water
PS66/160-1	19.07.04	19:05	78° 49.88' N	8° 39.08' E	282.2	MOR	released
PS66/160-1	19.07.04	19:24	78° 49.89' N	8° 39.93' E	249.0	MOR	action
PS66/160-1	19.07.04	19:31	78° 49.90' N	8° 39.64' E	257.0	MOR	on deck
PS66/161-1	19.07.04	20:07	78° 49.98' N	9° 0.25' E	219.9	CTD	surface
PS66/161-1	19.07.04	20:15	78° 49.98' N	9° 0.22' E	218.8	CTD	at depth
PS66/161-1	19.07.04	20:20	78° 49.99' N	9° 0.20' E	219.2	CTD	on deck
PS66/162-1	19.07.04	20:41	78° 50.00' N	8° 49.62' E	227.2	CTD/RO	surface
PS66/162-1	19.07.04	20:49	78° 50.02' N	8° 49.43' E	233.9	CTD/RO	at depth
PS66/162-1	19.07.04	20:56	78° 50.04' N	8° 49.35' E	238.7	CTD/RO	on deck
PS66/163-1	19.07.04	21:21	78° 50.02' N	8° 42.87' E	255.7	CTD/RO	surface
PS66/163-1	19.07.04	21:29	78° 50.07' N	8° 42.94' E	259.9	CTD/RO	at depth
PS66/163-1	19.07.04	21:34	78° 50.07' N	8° 42.91' E	260.6	CTD/RO	on deck
PS66/164-1	19.07.04	21:51	78° 50.04' N	8° 36.30' E	394.3	CTD/RO	surface
PS66/164-1	19.07.04	22:01	78° 50.04' N	8° 36.33' E	392.1	CTD/RO	at depth
PS66/164-1	19.07.04	22:08	78° 50.01' N	8° 36.20' E	400.6	CTD/RO	on deck
PS66/165-1	19.07.04	22:31	78° 50.03' N	8° 29.63' E	592.0	CTD/RO	surface
PS66/165-1	19.07.04	22:45	78° 50.02' N	8° 29.80' E	587.4	CTD/RO	at depth
PS66/165-1	19.07.04	22:55	78° 50.04' N	8° 29.95' E	584.2	CTD/RO	on deck
PS66/166-1	19.07.04	23:12	78° 49.98' N	8° 22.05' E	753.6	CTD/RO	surface
PS66/166-1	19.07.04	23:28	78° 49.98' N	8° 22.21' E	750.4	CTD/RO	at depth
PS66/166-1	19.07.04	23:39	78° 49.98' N	8° 22.32' E	749.0	CTD/RO	on deck
PS66/167-1	20.07.04	00:01	78° 50.00' N	8° 11.73' E	918.0	CTD/RO	surface
PS66/167-1	20.07.04	00:21	78° 50.01' N	8° 12.00' E	915.0	CTD/RO	at depth
PS66/167-1	20.07.04	00:41	78° 50.00' N	8° 12.20' E	912.0	CTD/RO	on deck
PS66/168-1	20.07.04	04:30	78° 50.51' N	8° 20.10' E	781.8	MOR	Hydroph.into water
PS66/168-1	20.07.04	05:08	78° 50.42' N	8° 21.57' E	759.7	MOR	Hydrophone on deck
PS66/168-1	20.07.04	06:28	78° 50.14' N	8° 20.34' E	785.0	MOR	Hydroph.into water
PS66/168-1	20.07.04	06:53	78° 50.21' N	8° 19.16' E	802.0	MOR	action
PS66/169-1	20.07.04	07:31	78° 49.95' N	8° 39.51' E	257.7	MOR	action
PS66/169-1	20.07.04	07:33	78° 49.95' N	8° 39.60' E	255.0	MOR	action

Station	Date	Time	PositionLat	PositionLon	Depth [m]	Gear (Abbrev.)	Action
PS66/169-1	20.07.04	07:37	78° 49.95' N	8° 39.70' E	252.6	MOR	action
PS66/169-1	20.07.04	07:46	78° 49.96' N	8° 39.69' E	252.2	MOR	action
PS66/169-1	20.07.04	07:49	78° 49.95' N	8° 39.78' E	249.0	MOR	action
PS66/169-1	20.07.04	07:51	78° 49.94' N	8° 39.83' E	248.4	MOR	action
PS66/169-1	20.07.04	07:53	78° 49.94' N	8° 39.84' E	248.9	MOR	on the ground
PS66/169-1	20.07.04	07:55	78° 49.95' N	8° 39.84' E	247.9	MOR	releaser on deck
PS66/170-1	20.07.04	08:55	78° 50.13' N	8° 19.12' E	805.7	MOR	surface
PS66/170-1	20.07.04	08:57	78° 50.14' N	8° 19.11' E	806.1	MOR	surface
PS66/170-1	20.07.04	09:13	78° 50.14' N	8° 19.51' E	799.2	MOR	surface
PS66/170-1	20.07.04	09:26	78° 50.15' N	8° 19.54' E	799.0	MOR	surface
PS66/170-1	20.07.04	09:29	78° 50.14' N	8° 19.70' E	798.0	MOR	surface
PS66/170-1	20.07.04	09:37	78° 50.14' N	8° 19.64' E	798.0	MOR	slipped
PS66/170-1	20.07.04	09:37	78° 50.14' N	8° 19.64' E	798.0	MOR	on the ground
PS66/170-1	20.07.04	09:39	78° 50.14' N	8° 19.64' E	798.2	MOR	Hydrophone on deck
PS66/171-1	20.07.04	10:18	78° 50.32' N	7° 59.28' E	1043.0	MOR	surface
PS66/171-1	20.07.04	10:20	78° 50.34' N	7° 59.25' E	1043.0	MOR	surface
PS66/171-1	20.07.04	10:30	78° 50.31' N	7° 59.17' E	1044.0	MOR	surface
PS66/171-1	20.07.04	10:46	78° 50.33' N	7° 59.44' E	1042.0	MOR	surface
PS66/171-1	20.07.04	10:57	78° 50.31' N	7° 59.59' E	1041.0	MOR	surface
PS66/171-1	20.07.04	11:01	78° 50.31' N	7° 59.60' E	1041.0	MOR	surface
PS66/171-1	20.07.04	11:02	78° 50.31' N	7° 59.59' E	1040.0	MOR	surface
PS66/171-1	20.07.04	11:07	78° 50.30' N	7° 59.55' E	1042.0	MOR	on the ground
PS66/171-1	20.07.04	11:09	78° 50.32' N	7° 59.51' E	1042.0	MOR	Hydrophone on deck
PS66/168-1	20.07.04	11:40	78° 50.35' N	8° 19.82' E	787.8	MOR	Hydroph. into water
PS66/168-1	20.07.04	11:58	78° 50.35' N	8° 20.61' E	0.0	MOR	released
PS66/168-1	20.07.04	12:06	78° 50.17' N	8° 20.47' E	783.0	MOR	Hydrophone on deck
PS66/168-1	20.07.04	13:08	78° 50.36' N	8° 19.74' E	0.0	MOR	Hydroph. into water
PS66/168-1	20.07.04	13:17	78° 50.42' N	8° 19.95' E	0.0	MOR	released
PS66/168-1	20.07.04	13:35	78° 50.20' N	8° 20.85' E	0.0	MOR	Hydrophone on deck
PS66/168-1	20.07.04	14:00	78° 50.42' N	8° 20.60' E	775.5	MOR	Hydroph. into water
PS66/168-1	20.07.04	14:09	78° 50.32' N	8° 21.28' E	0.0	MOR	released
PS66/168-1	20.07.04	14:12	78° 50.29' N	8° 21.33' E	0.0	MOR	Hydrophone on deck

Station	Date	Time	PositionLat	PositionLon	Depth [m]	Gear (Abbrev.)	Action
PS66/168-1	20.07.04	15:48	78° 50.42' N	8° 19.96' E	785.5	MOR	action
PS66/172-1	20.07.04	17:45	78° 50.18' N	9° 1.78' E	217.5	ADCP	Start Profile
PS66/172-2	20.07.04	17:45	78° 50.18' N	9° 1.78' E	217.5	HS_PS	start track
PS66/172-1	21.07.04	02:50	78° 50.02' N	2° 51.62' E	2489.0	ADCP	Finish profile
PS66/172-2	21.07.04	02:51	78° 50.01' N	2° 51.13' E	2491.0	HS_PS	profile end
PS66/173-1	21.07.04	03:06	78° 49.96' N	2° 49.54' E	2494.0	CTD/RO	surface
PS66/173-1	21.07.04	03:54	78° 50.02' N	2° 49.66' E	2485.9	CTD/RO	at depth
PS66/173-1	21.07.04	04:32	78° 49.99' N	2° 49.27' E	2486.4	CTD/RO	on deck
PS66/174-1	21.07.04	06:29	78° 50.05' N	3° 58.71' E	2332.0	MOR	Hydroph. into water
PS66/174-1	21.07.04	06:32	78° 50.05' N	3° 58.67' E	2330.0	MOR	action
PS66/174-1	21.07.04	06:37	78° 50.10' N	3° 58.26' E	2330.0	MOR	action
PS66/174-1	21.07.04	06:44	78° 50.08' N	3° 57.57' E	2328.0	MOR	released
PS66/174-1	21.07.04	06:46	78° 50.06' N	3° 57.44' E	2329.0	MOR	action
PS66/174-1	21.07.04	06:56	78° 49.99' N	3° 57.10' E	2330.0	MOR	Hydroph. into water
PS66/174-1	21.07.04	06:57	78° 49.99' N	3° 57.03' E	2331.0	MOR	action
PS66/174-1	21.07.04	07:02	78° 49.97' N	3° 56.62' E	2332.0	MOR	Hydrophone on deck
PS66/174-1	21.07.04	08:02	78° 50.03' N	3° 59.79' E	2342.0	MOR	action
PS66/174-1	21.07.04	08:04	78° 50.03' N	3° 59.65' E	2341.0	MOR	Hydroph. into water
PS66/174-1	21.07.04	08:08	78° 50.08' N	3° 59.42' E	2339.0	MOR	Hydrophone on deck
PS66/174-1	21.07.04	08:12	78° 50.14' N	3° 59.43' E	2342.0	MOR	Hydroph. into water
PS66/174-1	21.07.04	08:13	78° 50.15' N	3° 59.47' E	2342.0	MOR	action
PS66/174-1	21.07.04	08:15	78° 50.17' N	3° 59.55' E	2343.0	MOR	action
PS66/174-1	21.07.04	08:17	78° 50.17' N	3° 59.65' E	2344.0	MOR	Hydrophone on deck
PS66/174-1	21.07.04	08:24	78° 50.37' N	3° 57.02' E	2329.0	MOR	action
PS66/174-1	21.07.04	09:00	78° 51.01' N	3° 52.95' E	2338.0	MOR	action
PS66/174-1	21.07.04	09:02	78° 51.03' N	3° 52.79' E	2337.0	MOR	on deck
PS66/174-1	21.07.04	09:09	78° 51.11' N	3° 52.36' E	2336.0	MOR	on deck
PS66/174-1	21.07.04	09:19	78° 51.26' N	3° 51.97' E	2336.0	MOR	on deck
PS66/174-1	21.07.04	09:46	78° 51.56' N	3° 49.74' E	2345.0	MOR	on deck
PS66/175-1	21.07.04	11:12	78° 50.30' N	2° 47.95' E	2498.0	MOR	surface
PS66/175-1	21.07.04	11:16	78° 50.13' N	2° 47.27' E	2503.0	MOR	released
PS66/175-1	21.07.04	11:19	78° 50.12' N	2° 47.10' E	2504.0	MOR	on the surface

Station	Date	Time	PositionLat	PositionLon	Depth [m]	Gear (Abbrev.)	Action
PS66/175-1	21.07.04	12:19	78° 49.55' N	2° 45.09' E	2510.0	MOR	action
PS66/175-1	21.07.04	12:20	78° 49.55' N	2° 45.02' E	2509.0	MOR	on deck
PS66/175-1	21.07.04	12:28	78° 49.53' N	2° 44.62' E	2512.0	MOR	on deck
PS66/175-1	21.07.04	12:39	78° 49.50' N	2° 44.08' E	2510.0	MOR	on deck
PS66/175-1	21.07.04	12:55	78° 49.33' N	2° 43.28' E	2518.0	MOR	on deck
PS66/175-1	21.07.04	13:13	78° 49.17' N	2° 43.23' E	2522.0	MOR	mooring on deck
PS66/176-1	21.07.04	13:36	78° 49.85' N	2° 47.17' E	0.0	MOR	Hydroph. into water
PS66/176-1	21.07.04	13:46	78° 49.81' N	2° 46.27' E	0.0	MOR	Hydrophone on deck
PS66/176-1	21.07.04	13:55	78° 49.84' N	2° 47.49' E	0.0	MOR	Hydroph. into water
PS66/176-1	21.07.04	14:56	78° 50.22' N	2° 44.22' E	0.0	MOR	released
PS66/176-1	21.07.04	15:00	78° 50.26' N	2° 44.06' E	0.0	MOR	Hydrophone on deck
PS66/176-1	21.07.04	16:11	78° 49.38' N	2° 43.14' E	2519.0	MOR	on the surface
PS66/176-1	21.07.04	16:38	78° 49.80' N	2° 44.37' E	2509.0	MOR	on deck
PS66/177-1	21.07.04	17:28	78° 50.00' N	3° 9.66' E	2443.0	CTD/RO	surface
PS66/177-1	21.07.04	18:12	78° 50.12' N	3° 9.63' E	2441.0	CTD/RO	at depth
PS66/177-1	21.07.04	18:53	78° 50.35' N	3° 9.80' E	2438.0	CTD/RO	on deck
PS66/178-1	21.07.04	19:27	78° 50.05' N	3° 24.16' E	2376.0	CTD/RO	surface
PS66/178-1	21.07.04	20:11	78° 50.16' N	3° 24.42' E	2375.0	CTD/RO	at depth
PS66/178-1	21.07.04	20:45	0° 0.00' N	0° 0.00' E	0.0	CTD/RO	on deck
PS66/179-1	21.07.04	21:25	78° 49.95' N	3° 44.85' E	2275.0	CTD/RO	surface
PS66/179-1	21.07.04	22:07	78° 50.06' N	3° 44.30' E	2278.0	CTD/RO	at depth
PS66/179-1	21.07.04	22:39	78° 50.13' N	3° 44.32' E	2280.0	CTD/RO	on deck
PS66/180-1	21.07.04	23:07	78° 50.01' N	4° 0.19' E	2339.4	CTD/RO	surface
PS66/180-1	21.07.04	23:31	78° 50.04' N	3° 59.31' E	2330.3	CTD/RO	at depth
PS66/180-1	22.07.04	00:24	78° 50.05' N	3° 59.20' E	2329.5	CTD/RO	on deck
PS66/181-1	22.07.04	01:04	78° 49.99' N	4° 24.71' E	2411.9	CTD/RO	surface
PS66/181-1	22.07.04	01:49	78° 49.97' N	4° 24.98' E	2412.8	CTD/RO	at depth
PS66/181-1	22.07.04	02:22	78° 50.02' N	4° 24.79' E	2413.1	CTD/RO	on deck
PS66/182-1	22.07.04	03:20	78° 50.01' N	4° 45.02' E	2652.4	CTD/RO	surface
PS66/182-1	22.07.04	04:13	78° 49.93' N	4° 45.45' E	2628.5	CTD/RO	at depth
PS66/182-1	22.07.04	04:58	78° 49.56' N	4° 45.57' E	2523.1	CTD/RO	on deck
PS66/183-1	22.07.04	06:07	78° 50.01' N	3° 59.71' E	2334.8	MOR	action

Station	Date	Time	PositionLat	PositionLon	Depth [m]	Gear (Abbrev.)	Action
PS66/183-1	22.07.04	06:10	78° 50.01' N	3° 59.77' E	2336.0	MOR	action
PS66/183-1	22.07.04	06:30	78° 50.01' N	3° 59.85' E	2336.7	MOR	action
PS66/183-1	22.07.04	06:52	78° 50.01' N	3° 59.95' E	2338.1	MOR	action
PS66/183-1	22.07.04	07:06	78° 50.01' N	4° 0.01' E	2338.8	MOR	action
PS66/183-1	22.07.04	07:17	78° 50.00' N	4° 0.05' E	2339.7	MOR	action
PS66/183-1	22.07.04	07:18	78° 50.00' N	4° 0.05' E	2339.2	MOR	action
PS66/183-1	22.07.04	07:25	78° 49.99' N	4° 0.03' E	2338.7	MOR	slipped
PS66/183-1	22.07.04	07:27	78° 49.99' N	4° 0.04' E	2334.8	MOR	releaser on deck
PS66/184-1	22.07.04	09:17	78° 50.14' N	2° 47.67' E	2502.0	MOR	surface
PS66/184-1	22.07.04	09:20	78° 50.15' N	2° 47.61' E	2501.0	MOR	surface
PS66/184-1	22.07.04	09:42	78° 50.07' N	2° 47.93' E	2501.0	MOR	surface
PS66/184-1	22.07.04	09:57	78° 50.06' N	2° 48.11' E	2502.0	MOR	surface
PS66/184-1	22.07.04	10:10	78° 50.05' N	2° 47.99' E	2501.0	MOR	surface
PS66/184-1	22.07.04	10:20	78° 50.04' N	2° 48.08' E	2501.0	MOR	surface
PS66/184-1	22.07.04	10:21	78° 50.05' N	2° 48.08' E	2499.0	MOR	surface
PS66/184-1	22.07.04	10:26	78° 50.05' N	2° 48.09' E	2491.2	MOR	slipped
PS66/184-1	22.07.04	10:26	78° 50.05' N	2° 48.09' E	2491.2	MOR	on the ground
PS66/184-1	22.07.04	10:27	78° 50.05' N	2° 48.10' E	2490.7	MOR	releaser on deck
PS66/185-1	22.07.04	13:43	78° 49.89' N	5° 1.02' E	0.0	MOR	Hydroph.into water
PS66/185-1	22.07.04	14:03	78° 50.07' N	5° 0.88' E	0.0	MOR	action
PS66/185-1	22.07.04	14:22	78° 50.27' N	5° 2.21' E	2711.0	MOR	released
PS66/185-1	22.07.04	15:00	78° 50.55' N	5° 6.09' E	0.0	MOR	Hydrophone on deck
PS66/185-1	22.07.04	15:02	78° 50.57' N	5° 6.26' E	0.0	MOR	action
PS66/185-1	22.07.04	15:15	78° 50.50' N	5° 7.52' E	2677.0	MOR	on the surface
PS66/185-1	22.07.04	15:44	78° 49.75' N	5° 1.41' E	2704.0	MOR	mooring on deck
PS66/186-1	22.07.04	21:00	78° 50.36' N	8° 20.24' E	780.8	MOR	Hydroph.into water
PS66/186-1	22.07.04	21:03	78° 50.39' N	8° 20.33' E	777.1	MOR	action
PS66/186-1	22.07.04	21:38	78° 50.86' N	8° 23.80' E	0.0	MOR	Hydrophone on deck
PS66/186-1	22.07.04	22:03	78° 50.21' N	8° 19.61' E	0.0	MOR	action
PS66/186-1	22.07.04	22:04	78° 50.19' N	8° 19.61' E	0.0	MOR	Hydroph.into water
PS66/186-1	22.07.04	22:13	78° 50.31' N	8° 19.88' E	0.0	MOR	released
PS66/186-1	22.07.04	22:32	78° 50.63' N	8° 21.65' E	0.0	MOR	action

Station	Date	Time	PositionLat	PositionLon	Depth [m]	Gear (Abbrev.)	Action
PS66/186-1	22.07.04	22:47	78° 50.85' N	8° 23.15' E	0.0	MOR	Hydrophone on deck
PS66/186-1	22.07.04	23:05	78° 50.74' N	8° 21.33' E	759.7	MOR	action
PS66/187-1	23.07.04	08:22	79° 56.85' N	10° 42.83' E	314.7	CTD/RO	surface
PS66/187-1	23.07.04	08:31	79° 56.87' N	10° 42.68' E	321.5	CTD/RO	at depth
PS66/187-1	23.07.04	08:40	79° 56.90' N	10° 42.42' E	326.5	CTD/RO	on deck
PS66/188-1	23.07.04	10:05	80° 6.55' N	10° 25.84' E	517.0	CTD/RO	surface
PS66/188-1	23.07.04	10:17	80° 6.59' N	10° 25.33' E	518.8	CTD/RO	at depth
PS66/188-1	23.07.04	10:25	80° 6.56' N	10° 25.27' E	518.4	CTD/RO	on deck
PS66/189-1	23.07.04	12:00	80° 16.04' N	10° 10.29' E	606.9	CTD/RO	surface
PS66/189-1	23.07.04	12:13	80° 16.02' N	10° 10.12' E	608.1	CTD/RO	at depth
PS66/189-1	23.07.04	12:29	80° 16.01' N	10° 9.88' E	608.7	CTD/RO	on deck
PS66/190-1	23.07.04	13:56	80° 25.75' N	9° 53.97' E	695.6	CTD/RO	surface
PS66/190-1	23.07.04	14:12	80° 25.72' N	9° 54.09' E	694.1	CTD/RO	at depth
PS66/190-1	23.07.04	14:27	80° 25.71' N	9° 53.98' E	695.1	CTD/RO	on deck
PS66/191-1	23.07.04	15:49	80° 35.33' N	9° 37.68' E	1272.0	CTD/RO	surface
PS66/191-1	23.07.04	16:14	80° 35.30' N	9° 37.71' E	1271.0	CTD/RO	at depth
PS66/191-1	23.07.04	16:39	80° 35.28' N	9° 38.17' E	1261.0	CTD/RO	on deck
PS66/192-1	23.07.04	18:01	80° 45.09' N	9° 21.05' E	1025.0	CTD/RO	surface
PS66/192-1	23.07.04	18:21	80° 44.93' N	9° 21.14' E	1007.0	CTD/RO	at depth
PS66/192-1	23.07.04	18:40	80° 44.88' N	9° 21.35' E	1002.0	CTD/RO	on deck
PS66/193-1	23.07.04	19:51	80° 54.73' N	9° 4.35' E	609.8	CTD/RO	surface
PS66/193-1	23.07.04	20:05	80° 54.69' N	9° 4.44' E	610.5	CTD/RO	surface
PS66/193-1	23.07.04	20:19	80° 54.64' N	9° 4.39' E	610.4	CTD/RO	on deck
PS66/194-1	23.07.04	21:36	81° 4.36' N	8° 47.00' E	995.8	CTD/RO	surface
PS66/194-1	23.07.04	21:57	81° 4.35' N	8° 46.60' E	995.4	CTD/RO	at depth
PS66/194-1	23.07.04	22:12	81° 4.31' N	8° 46.36' E	994.5	CTD/RO	on deck
PS66/195-1	23.07.04	23:31	81° 13.94' N	8° 29.56' E	746.4	CTD/RO	surface
PS66/195-1	23.07.04	23:47	81° 13.89' N	8° 29.01' E	739.1	CTD/RO	at depth
PS66/195-1	23.07.04	23:57	81° 13.91' N	8° 28.73' E	731.1	CTD/RO	on deck
PS66/196-1	24.07.04	01:40	81° 23.40' N	8° 11.91' E	811.1	CTD/RO	surface
PS66/196-1	24.07.04	01:57	81° 23.46' N	8° 12.24' E	819.2	CTD/RO	at depth
PS66/196-1	24.07.04	02:09	81° 23.52' N	8° 12.22' E	824.2	CTD/RO	on deck

Station	Date	Time	PositionLat	PositionLon	Depth [m]	Gear (Abbrev.)	Action
PS66/197-1	24.07.04	03:33	81° 33.11' N	7° 53.67' E	852.7	CTD/RO	surface
PS66/197-1	24.07.04	03:52	81° 33.14' N	7° 54.37' E	856.0	CTD/RO	at depth
PS66/197-1	24.07.04	04:06	81° 33.11' N	7° 55.03' E	856.7	CTD/RO	on deck
PS66/198-1	24.07.04	06:02	81° 42.86' N	7° 32.67' E	844.8	CTD/RO	surface
PS66/198-1	24.07.04	06:21	81° 42.94' N	7° 34.34' E	849.1	CTD/RO	at depth
PS66/198-1	24.07.04	06:35	81° 42.99' N	7° 35.20' E	852.0	CTD/RO	on deck
PS66/199-1	24.07.04	08:11	81° 52.54' N	7° 14.56' E	789.0	CTD/RO	surface
PS66/199-1	24.07.04	08:31	81° 52.63' N	7° 15.38' E	793.7	CTD/RO	at depth
PS66/199-1	24.07.04	08:42	81° 52.63' N	7° 15.93' E	785.0	CTD/RO	on deck
PS66/200-1	24.07.04	10:29	82° 1.87' N	6° 57.20' E	767.3	CTD/RO	surface
PS66/200-1	24.07.04	10:46	82° 1.92' N	6° 57.55' E	764.1	CTD/RO	at depth
PS66/200-1	24.07.04	10:58	82° 1.95' N	6° 57.55' E	765.4	CTD/RO	on deck
PS66/201-1	24.07.04	16:07	82° 11.67' N	6° 39.94' E	1076.0	CTD/RO	surface
PS66/201-1	24.07.04	16:31	82° 11.75' N	6° 39.83' E	1120.0	CTD/RO	at depth
PS66/201-1	24.07.04	16:48	82° 11.82' N	6° 39.74' E	1138.0	CTD/RO	on deck
PS66/202-1	25.07.04	02:01	82° 22.13' N	6° 39.06' E	2435.0	CTD/RO	surface
PS66/202-1	25.07.04	02:45	82° 22.19' N	6° 42.01' E	2350.0	CTD/RO	at depth
PS66/202-1	25.07.04	03:17	82° 22.23' N	6° 44.20' E	2285.0	CTD/RO	on deck
PS66/203-1	25.07.04	06:39	82° 30.63' N	5° 57.72' E	3425.0	CTD/RO	surface
PS66/203-1	25.07.04	07:43	82° 30.70' N	6° 2.18' E	3388.0	CTD/RO	at depth
PS66/203-1	25.07.04	08:35	82° 30.72' N	6° 4.33' E	3375.0	CTD/RO	on deck
PS66/204-1	25.07.04	13:03	82° 40.56' N	5° 34.69' E	3688.0	CTD/RO	surface
PS66/204-1	25.07.04	14:13	82° 40.92' N	5° 35.67' E	3671.6	CTD/RO	at depth
PS66/204-1	25.07.04	14:59	82° 41.16' N	5° 36.83' E	3695.0	CTD/RO	on deck
PS66/205-1	25.07.04	20:15	82° 50.39' N	5° 14.46' E	4095.0	CTD/RO	surface
PS66/205-1	25.07.04	21:32	82° 50.56' N	5° 15.07' E	4093.0	CTD/RO	at depth
PS66/205-1	25.07.04	22:25	82° 50.64' N	5° 16.05' E	4100.0	CTD/RO	on deck
PS66/206-1	26.07.04	05:39	82° 58.70' N	4° 54.76' E	4091.0	CTD/RO	surface
PS66/206-1	26.07.04	07:03	82° 58.67' N	4° 55.66' E	4093.0	CTD/RO	at depth
PS66/206-1	26.07.04	08:00	82° 58.70' N	4° 56.05' E	4095.0	CTD/RO	on deck
PS66/207-1	26.07.04	13:34	82° 59.71' N	3° 32.85' E	3907.0	CTD/RO	surface
PS66/207-1	26.07.04	14:46	82° 59.77' N	3° 32.77' E	3910.0	CTD/RO	at depth

Station	Date	Time	PositionLat	PositionLon	Depth [m]	Gear (Abbrev.)	Action
PS66/207-1	26.07.04	15:37	82° 59.82' N	3° 32.97' E	3910.0	CTD/RO	on deck
PS66/208-1	27.07.04	01:12	82° 59.80' N	2° 12.39' E	3454.0	CTD/RO	surface
PS66/208-1	27.07.04	02:18	82° 59.78' N	2° 12.51' E	3458.0	CTD/RO	at depth
PS66/208-1	27.07.04	03:03	82° 59.76' N	2° 12.62' E	3466.0	CTD/RO	on deck
PS66/209-1	27.07.04	09:00	83° 1.85' N	0° 46.13' E	3732.0	ICE	Alongside Floe
PS66/209-1	27.07.04	09:42	83° 1.84' N	0° 46.02' E	3730.0	ICE	Ice Gangway on the ice
PS66/209-1	27.07.04	09:50	83° 1.85' N	0° 46.03' E	3732.0	ICE	Scientists on the ice
PS66/209-1	27.07.04	09:59	83° 1.85' N	0° 46.05' E	3730.0	ICE	Scientists on the ice
PS66/209-1	27.07.04	11:58	83° 1.97' N	0° 46.15' E	3730.0	ICE	Scientists on board
PS66/209-1	27.07.04	12:00	83° 1.98' N	0° 46.23' E	3728.0	ICE	Ice Gangway on board
PS66/209-2	27.07.04	12:11	83° 2.00' N	0° 46.37' E	3731.0	CTD/RO	surface
PS66/209-2	27.07.04	12:58	83° 2.08' N	0° 46.56' E	3731.0	CTD/RO	Information
PS66/209-2	27.07.04	13:12	83° 2.14' N	0° 45.83' E	3726.0	CTD/RO	surface
PS66/209-2	27.07.04	14:19	83° 2.28' N	0° 46.04' E	3723.0	CTD/RO	at depth
PS66/209-2	27.07.04	15:16	83° 2.40' N	0° 46.36' E	3721.0	CTD/RO	on deck
PS66/210-1	28.07.04	16:50	83° 0.96' N	0° 37.03' W	3763.0	CTD/RO	surface
PS66/210-1	28.07.04	18:01	83° 1.06' N	0° 38.65' W	3764.0	CTD/RO	at depth
PS66/210-1	28.07.04	18:56	83° 1.09' N	0° 39.79' W	3760.0	CTD/RO	on deck
PS66/211-1	29.07.04	00:18	82° 57.83' N	2° 1.40' W	3440.0	CTD/RO	surface
PS66/211-1	29.07.04	01:21	82° 57.85' N	2° 2.24' W	3410.0	CTD/RO	at depth
PS66/211-1	29.07.04	02:12	82° 57.87' N	2° 2.97' W	3406.0	CTD/RO	on deck
PS66/212-1	29.07.04	06:58	82° 55.67' N	3° 15.09' W	2505.0	CTD/RO	surface
PS66/212-1	29.07.04	07:46	82° 55.66' N	3° 14.48' W	2511.0	CTD/RO	at depth
PS66/212-1	29.07.04	08:29	82° 55.65' N	3° 13.83' W	2521.0	CTD/RO	on deck
PS66/213-1	29.07.04	12:55	82° 59.84' N	4° 41.13' W	2583.0	CTD/RO	surface
PS66/213-1	29.07.04	13:43	82° 59.90' N	4° 40.67' W	2585.0	CTD/RO	at depth
PS66/213-1	29.07.04	14:27	82° 60.00' N	4° 39.73' W	2584.0	CTD/RO	on deck
PS66/214-1	29.07.04	18:36	82° 58.38' N	4° 55.44' W	2264.0	DRG	surface
PS66/214-1	29.07.04	19:06	82° 58.41' N	4° 55.56' W	2270.0	DRG	Information
PS66/214-1	29.07.04	19:45	82° 58.87' N	4° 58.51' W	2035.0	DRG	start dredging
PS66/214-1	29.07.04	20:47	82° 59.08' N	5° 2.84' W	1437.0	DRG	Information

Station	Date	Time	PositionLat	PositionLon	Depth [m]	Gear (Abbrev.)	Action
PS66/214-1	29.07.04	22:04	82° 58.99' N	5° 3.33' W	1465.0	DRG	stop dredging
PS66/214-1	29.07.04	22:25	82° 58.99' N	5° 3.85' W	1502.0	DRG	on deck
PS66/215-1	30.07.04	01:20	82° 55.49' N	5° 33.36' W	3604.0	DRG	surface
PS66/215-1	30.07.04	02:16	82° 55.63' N	5° 33.06' W	3603.0	DRG	Information
PS66/215-1	30.07.04	02:47	82° 55.44' N	5° 30.68' W	3322.0	DRG	start dredging
PS66/215-1	30.07.04	03:17	82° 55.34' N	5° 28.29' W	2921.0	DRG	Information
PS66/215-1	30.07.04	03:46	82° 55.59' N	5° 29.11' W	2994.0	DRG	Information
PS66/215-1	30.07.04	05:02	82° 55.71' N	5° 28.88' W	2889.0	DRG	Information
PS66/215-1	30.07.04	05:44	82° 55.67' N	5° 26.73' W	2551.0	DRG	on deck
PS66/216-1	30.07.04	06:45	82° 52.35' N	5° 30.33' W	3011.0	CTD/RO	surface
PS66/216-1	30.07.04	07:41	82° 52.23' N	5° 28.46' W	2946.0	CTD/RO	at depth
PS66/216-1	30.07.04	08:29	82° 52.19' N	5° 27.21' W	2812.0	CTD/RO	on deck
PS66/217-1	30.07.04	13:21	82° 51.38' N	6° 8.77' W	4824.0	DRG	surface
PS66/217-1	30.07.04	14:23	82° 51.54' N	6° 9.14' W	4795.0	DRG	Information
PS66/217-1	30.07.04	15:03	82° 51.75' N	6° 11.96' W	4734.0	DRG	start dredging
PS66/217-1	30.07.04	17:10	82° 52.90' N	6° 14.81' W	4268.0	DRG	Information
PS66/217-1	30.07.04	18:22	82° 52.95' N	6° 12.96' W	4283.0	DRG	Information
PS66/217-1	30.07.04	19:35	82° 53.03' N	6° 11.26' W	4274.0	DRG	on deck
PS66/218-1	30.07.04	20:02	82° 53.13' N	6° 11.94' W	4241.0	CTD/RO	surface
PS66/218-1	30.07.04	21:21	82° 53.03' N	6° 11.27' W	4275.0	CTD/RO	at depth
PS66/218-1	30.07.04	22:34	82° 53.04' N	6° 10.29' W	4283.0	CTD/RO	on deck
PS66/219-1	31.07.04	02:54	82° 47.16' N	6° 32.39' W	4849.0	DRG	surface
PS66/219-1	31.07.04	04:05	82° 47.28' N	6° 30.89' W	4884.0	DRG	Information
PS66/219-1	31.07.04	04:44	82° 47.37' N	6° 35.94' W	4595.0	DRG	start dredging
PS66/219-1	31.07.04	06:11	82° 47.54' N	6° 41.00' W	4374.0	DRG	Information
PS66/219-1	31.07.04	07:03	82° 47.73' N	6° 39.13' W	4391.0	DRG	Information
PS66/219-1	31.07.04	08:00	82° 47.90' N	6° 37.09' W	4547.0	DRG	on deck
PS66/220-1	31.07.04	09:44	82° 44.79' N	6° 24.27' W	4713.0	CTD/RO	surface
PS66/220-1	31.07.04	11:09	82° 44.93' N	6° 21.00' W	4732.0	CTD/RO	at depth
PS66/220-1	31.07.04	12:19	82° 45.15' N	6° 17.83' W	4789.0	CTD/RO	on deck
PS66/221-1	31.07.04	14:06	82° 42.06' N	6° 24.46' W	4784.0	DRG	surface
PS66/221-1	31.07.04	15:17	82° 42.08' N	6° 21.56' W	4776.0	DRG	Information

Station	Date	Time	PositionLat	PositionLon	Depth [m]	Gear (Abbrev.)	Action
PS66/221-1	31.07.04	16:01	82° 42.36' N	6° 21.95' W	4771.0	DRG	start dredging
PS66/221-1	31.07.04	17:17	82° 42.47' N	6° 30.00' W	4400.0	DRG	Information
PS66/221-1	31.07.04	17:59	82° 42.53' N	6° 28.98' W	4397.0	DRG	Information
PS66/221-1	31.07.04	18:49	82° 42.51' N	6° 26.51' W	4650.0	DRG	on deck
PS66/222-1	01.08.04	00:00	82° 36.48' N	7° 21.65' W	3894.0	ICE	Alongside Floe
PS66/222-1	01.08.04	00:04	82° 36.50' N	7° 21.45' W	3895.0	ICE	Ice Gangway on the ice
PS66/222-1	01.08.04	00:05	82° 36.50' N	7° 21.40' W	3905.0	ICE	Scientists on the ice
PS66/222-2	01.08.04	00:19	82° 36.56' N	7° 20.73' W	3904.0	CTD/RO	surface
PS66/222-1	01.08.04	01:23	82° 36.85' N	7° 17.49' W	4062.0	ICE	Scientists on board
PS66/222-2	01.08.04	01:33	82° 36.90' N	7° 17.02' W	4067.0	CTD/RO	at depth
PS66/222-2	01.08.04	02:32	82° 37.20' N	7° 13.97' W	4053.0	CTD/RO	on deck
PS66/222-1	01.08.04	02:42	82° 37.25' N	7° 13.56' W	4059.0	ICE	Ice Gangway on board
PS66/222-1	01.08.04	02:43	82° 37.25' N	7° 13.57' W	4058.0	ICE	Departure from floe
PS66/223-1	01.08.04	04:39	82° 35.61' N	6° 34.98' W	4503.0	DRG_C	surface
PS66/223-1	01.08.04	06:22	82° 35.38' N	6° 30.95' W	4567.0	DRG_C	start dredging
PS66/223-1	01.08.04	08:27	82° 34.53' N	6° 42.39' W	4144.0	DRG_C	Information
PS66/223-1	01.08.04	09:06	82° 34.36' N	6° 44.76' W	3886.0	DRG_C	Information
PS66/223-1	01.08.04	09:29	82° 34.12' N	6° 44.62' W	3924.0	DRG_C	Information
PS66/223-1	01.08.04	09:53	82° 34.13' N	6° 43.64' W	4109.0	DRG_C	stop dredging
PS66/223-1	01.08.04	10:10	82° 34.15' N	6° 42.87' W	4242.0	DRG_C	Information
PS66/223-1	01.08.04	10:50	82° 34.25' N	6° 41.10' W	4402.0	DRG_C	on deck
PS66/224-1	01.08.04	12:17	82° 31.03' N	6° 24.99' W	4263.0	DRG	surface
PS66/224-1	01.08.04	13:10	82° 30.98' N	6° 23.76' W	4282.0	DRG	Information
PS66/224-1	01.08.04	13:33	82° 30.77' N	6° 26.59' W	4234.0	DRG	start dredging
PS66/224-1	01.08.04	14:37	82° 29.97' N	6° 39.04' W	3677.0	DRG	Information
PS66/224-1	01.08.04	15:31	82° 29.98' N	6° 39.46' W	3693.0	DRG	stop dredging
PS66/224-1	01.08.04	16:23	82° 29.85' N	6° 37.63' W	3648.0	DRG	on deck
PS66/225-1	01.08.04	18:02	82° 29.70' N	8° 13.11' W	3123.0	CTD/RO	surface
PS66/225-1	01.08.04	19:05	82° 29.65' N	8° 7.96' W	3254.0	CTD/RO	at depth
PS66/225-1	01.08.04	19:56	82° 29.31' N	8° 6.04' W	3245.0	CTD/RO	on deck
PS66/226-1	01.08.04	21:25	82° 22.18' N	8° 58.38' W	3104.0	CTD/RO	surface

Station	Date	Time	PositionLat	PositionLon	Depth [m]	Gear (Abbrev.)	Action
PS66/226-1	01.08.04	22:21	82° 22.20' N	8° 58.67' W	3106.0	CTD/RO	at depth
PS66/226-1	01.08.04	23:11	82° 22.36' N	8° 58.70' W	3129.0	CTD/RO	on deck
PS66/227-1	02.08.04	00:30	82° 14.73' N	9° 47.07' W	2938.0	CTD/RO	surface
PS66/227-1	02.08.04	01:23	82° 14.77' N	9° 47.65' W	2940.0	CTD/RO	at depth
PS66/227-1	02.08.04	02:11	82° 14.82' N	9° 47.61' W	2940.0	CTD/RO	on deck
PS66/228-1	02.08.04	03:40	82° 7.22' N	10° 34.90' W	2435.0	CTD/RO	surface
PS66/228-1	02.08.04	04:26	82° 7.35' N	10° 33.95' W	2416.0	CTD/RO	at depth
PS66/228-1	02.08.04	05:09	82° 7.44' N	10° 34.75' W	2399.0	CTD/RO	on deck
PS66/229-1	02.08.04	06:22	81° 59.54' N	11° 22.32' W	238.3	CTD/RO	surface
PS66/229-1	02.08.04	06:35	81° 59.58' N	11° 23.04' W	233.2	CTD/RO	at depth
PS66/229-1	02.08.04	06:45	81° 59.59' N	11° 23.31' W	232.2	CTD/RO	on deck
PS66/230-1	02.08.04	08:04	81° 51.98' N	12° 9.44' W	225.6	CTD/RO	surface
PS66/230-1	02.08.04	08:10	81° 51.92' N	12° 9.42' W	228.4	CTD/RO	at depth
PS66/230-1	02.08.04	08:22	81° 51.87' N	12° 9.67' W	232.7	CTD/RO	on deck
PS66/231-1	02.08.04	22:30	82° 37.73' N	5° 42.69' W	4305.0	DRG	surface
PS66/231-1	02.08.04	23:07	82° 37.50' N	5° 41.64' W	4215.0	DRG	Information
PS66/231-1	02.08.04	23:23	82° 37.42' N	5° 41.11' W	4150.0	DRG	Information
PS66/231-1	03.08.04	00:01	82° 37.32' N	5° 36.50' W	3911.0	DRG	start dredging
PS66/231-1	03.08.04	02:28	82° 37.52' N	5° 30.68' W	3604.0	DRG	stop dredging
PS66/231-1	03.08.04	03:13	82° 37.45' N	5° 29.53' W	3654.0	DRG	on deck
PS66/232-1	05.08.04	01:53	84° 34.04' N	2° 20.23' E	4347.0	DRG	surface
PS66/232-1	05.08.04	02:51	84° 34.00' N	2° 20.67' E	4337.0	DRG	Information
PS66/232-1	05.08.04	03:13	84° 33.99' N	2° 18.34' E	4276.0	DRG	start dredging
PS66/232-1	05.08.04	04:48	84° 33.79' N	2° 5.56' E	3718.0	DRG	Information
PS66/232-1	05.08.04	05:37	84° 33.70' N	2° 4.30' E	3631.0	DRG	Information
PS66/232-1	05.08.04	06:24	84° 33.63' N	2° 0.99' E	3579.0	DRG	on deck
PS66/233-1	05.08.04	09:11	84° 37.40' N	2° 36.83' E	4736.0	DRG	surface
PS66/233-1	05.08.04	10:18	84° 37.42' N	2° 35.78' E	4638.0	DRG	Information
PS66/233-1	05.08.04	10:41	84° 37.40' N	2° 33.38' E	4464.0	DRG	start dredging
PS66/233-1	05.08.04	11:53	84° 37.81' N	2° 29.48' E	3774.0	DRG	Information
PS66/233-1	05.08.04	12:56	84° 37.78' N	2° 30.38' E	3879.0	DRG	stop dredging
PS66/233-1	05.08.04	13:54	84° 37.79' N	2° 30.86' E	3964.0	DRG	on deck

Station	Date	Time	PositionLat	PositionLon	Depth [m]	Gear (Abbrev.)	Action
PS66/234-1	05.08.04	15:47	84° 43.48' N	3° 9.24' E	4204.0	DRG	surface
PS66/234-1	05.08.04	16:38	84° 43.39' N	3° 8.12' E	4191.0	DRG	Information
PS66/234-1	05.08.04	16:45	84° 43.41' N	3° 6.31' E	4206.0	DRG	start dredging
PS66/234-1	05.08.04	17:59	84° 42.95' N	2° 56.34' E	3764.0	DRG	Information
PS66/234-1	05.08.04	18:40	84° 42.91' N	2° 55.72' E	3760.0	DRG	Information
PS66/234-1	05.08.04	19:30	84° 42.85' N	2° 54.13' E	3734.0	DRG	on deck
PS66/235-1	05.08.04	20:55	84° 40.27' N	3° 24.11' E	5347.0	DRG	surface
PS66/235-1	05.08.04	22:05	84° 40.38' N	3° 22.72' E	5260.0	DRG	Information
PS66/235-1	05.08.04	22:22	84° 40.59' N	3° 21.94' E	5211.0	DRG	start dredging
PS66/235-1	05.08.04	23:49	84° 41.06' N	3° 14.43' E	4724.0	DRG	Information
PS66/235-1	05.08.04	23:53	84° 41.08' N	3° 14.13' E	4711.0	DRG	Information
PS66/235-1	06.08.04	00:34	84° 41.09' N	3° 14.15' E	4714.0	DRG	stop dredging
PS66/235-1	06.08.04	01:36	84° 41.07' N	3° 14.43' E	4709.0	DRG	on deck
PS66/236-1	06.08.04	03:08	84° 39.85' N	3° 39.16' E	5322.0	DRG	surface
PS66/236-1	06.08.04	04:20	84° 39.76' N	3° 39.09' E	5276.0	DRG	Information
PS66/236-1	06.08.04	04:34	84° 39.54' N	3° 39.45' E	5098.0	DRG	start dredging
PS66/236-1	06.08.04	05:47	84° 38.79' N	3° 41.22' E	4660.0	DRG	stop dredging
PS66/236-1	06.08.04	06:38	84° 38.53' N	3° 40.04' E	4561.0	DRG	Information
PS66/236-1	06.08.04	07:37	84° 38.32' N	3° 38.11' E	4502.0	DRG	on deck
PS66/237-1	06.08.04	09:22	84° 36.30' N	3° 23.59' E	4109.0	DRG	surface
PS66/237-1	06.08.04	10:18	84° 36.15' N	3° 22.95' E	4080.0	DRG	Information
PS66/237-1	06.08.04	10:36	84° 35.93' N	3° 24.24' E	3971.0	DRG	start dredging
PS66/237-1	06.08.04	13:11	84° 34.58' N	3° 27.17' E	3512.0	DRG	stop dredging
PS66/237-1	06.08.04	13:59	84° 34.28' N	3° 29.70' E	3399.0	DRG	on deck
PS66/238-1	06.08.04	16:51	84° 39.23' N	4° 13.79' E	4154.0	DRG	surface
PS66/238-1	06.08.04	17:43	84° 38.90' N	4° 12.15' E	4160.0	DRG	Information
PS66/238-1	06.08.04	17:59	84° 38.75' N	4° 11.57' E	4117.0	DRG	start dredging
PS66/238-1	06.08.04	18:59	84° 38.13' N	4° 12.19' E	3783.0	DRG	Information
PS66/238-1	06.08.04	19:50	84° 37.73' N	4° 12.64' E	3717.0	DRG	stop dredging
PS66/238-1	06.08.04	20:44	84° 37.34' N	4° 11.98' E	3502.0	DRG	on deck
PS66/239-1	07.08.04	00:13	84° 34.37' N	4° 31.92' E	2968.0	DRG	surface
PS66/239-1	07.08.04	00:56	84° 34.18' N	4° 31.85' E	2881.0	DRG	Information

Station	Date	Time	PositionLat	PositionLon	Depth [m]	Gear (Abbrev.)	Action
PS66/239-1	07.08.04	01:10	84° 34.03' N	4° 33.02' E	2769.0	DRG	start dredging
PS66/239-1	07.08.04	03:00	84° 33.33' N	4° 40.49' E	2420.0	DRG	stop dredging
PS66/239-1	07.08.04	03:33	84° 33.03' N	4° 42.64' E	2876.0	DRG	on deck
PS66/240-1	07.08.04	04:44	84° 31.41' N	4° 55.15' E	3436.0	DRG	surface
PS66/240-1	07.08.04	05:31	84° 31.15' N	4° 55.34' E	3362.0	DRG	Information
PS66/240-1	07.08.04	05:46	84° 30.94' N	4° 56.65' E	3274.0	DRG	start dredging
PS66/240-1	07.08.04	06:54	84° 30.15' N	4° 59.67' E	2953.0	DRG	stop dredging
PS66/240-1	07.08.04	07:29	84° 29.99' N	4° 59.32' E	2915.0	DRG	Information
PS66/240-1	07.08.04	08:07	84° 29.69' N	5° 0.66' E	2758.0	DRG	on deck
PS66/241-1	08.08.04	08:29	84° 38.00' N	1° 8.69' E	4283.0	DRG	surface
PS66/241-1	08.08.04	09:33	84° 37.91' N	1° 7.74' E	4283.0	DRG	Information
PS66/241-1	08.08.04	09:52	84° 37.66' N	1° 9.30' E	4144.0	DRG	start dredging
PS66/241-1	08.08.04	11:19	84° 37.13' N	1° 15.62' E	3595.0	DRG	Information
PS66/241-1	08.08.04	12:05	84° 37.09' N	1° 16.47' E	3586.0	DRG	stop dredging
PS66/241-1	08.08.04	12:51	84° 37.01' N	1° 17.13' E	3548.0	DRG	on deck
PS66/242-1	08.08.04	14:08	84° 38.03' N	1° 10.33' E	4249.0	ICE	Alongside Floe
PS66/242-1	08.08.04	14:10	84° 38.02' N	1° 10.34' E	4242.0	ICE	Ice Gangway on the ice
PS66/242-1	08.08.04	14:19	84° 37.99' N	1° 10.41' E	4234.0	ICE	Scientists on the ice
PS66/242-2	08.08.04	14:22	84° 37.98' N	1° 10.44' E	4233.0	CTD/RO	surface
PS66/242-2	08.08.04	15:40	84° 37.67' N	1° 10.81' E	4081.0	CTD/RO	at depth
PS66/242-2	08.08.04	16:41	84° 37.43' N	1° 10.55' E	3935.0	CTD/RO	on deck
PS66/242-1	08.08.04	22:27	84° 37.18' N	1° 3.15' E	4109.0	ICE	Scientists on board
PS66/242-1	08.08.04	22:33	84° 37.19' N	1° 3.10' E	4117.0	ICE	Ice Gangway on board
PS66/242-1	08.08.04	22:37	84° 37.18' N	1° 3.05' E	4119.0	ICE	Departure from floe
PS66/243-1	10.08.04	21:12	82° 47.90' N	7° 11.25' W	3942.0	DRG	surface
PS66/243-1	10.08.04	22:24	82° 47.77' N	7° 12.01' W	3882.0	DRG	Information
PS66/243-1	10.08.04	22:44	82° 47.78' N	7° 14.48' W	3664.0	DRG	start dredging
PS66/243-1	10.08.04	23:08	82° 47.80' N	7° 16.02' W	3501.0	DRG	Information
PS66/243-1	10.08.04	23:43	82° 47.70' N	7° 16.06' W	3468.0	DRG	stop dredging
PS66/243-1	11.08.04	00:30	82° 47.49' N	7° 15.60' W	3507.0	DRG	on deck
PS66/244-1	11.08.04	07:21	82° 40.11' N	7° 20.91' W	3740.0	DRG	surface

Station	Date	Time	PositionLat	PositionLon	Depth [m]	Gear (Abbrev.)	Action
PS66/244-1	11.08.04	08:09	82° 39.99' N	7° 20.85' W	3716.0	DRG	Information
PS66/244-1	11.08.04	08:22	82° 39.82' N	7° 22.13' W	3555.0	DRG	start dredging
PS66/244-1	11.08.04	09:34	82° 39.27' N	7° 24.40' W	3169.0	DRG	Information
PS66/244-1	11.08.04	10:01	82° 39.22' N	7° 24.01' W	3158.0	DRG	stop dredging
PS66/244-1	11.08.04	10:44	82° 39.10' N	7° 23.30' W	3123.0	DRG	on deck
PS66/245-1	12.08.04	14:04	82° 6.95' N	2° 42.69' W	2586.0	ICE	Alongside Floe
PS66/245-1	12.08.04	14:11	82° 6.94' N	2° 42.85' W	2589.0	ICE	Ice Gangway on the ice
PS66/245-1	12.08.04	14:21	82° 6.92' N	2° 43.06' W	2605.0	ICE	Scientists on the ice
PS66/245-2	12.08.04	14:29	82° 6.91' N	2° 43.23' W	2616.0	CTD/RO	surface
PS66/245-2	12.08.04	15:19	82° 6.84' N	2° 44.19' W	2673.0	CTD/RO	at depth
PS66/245-2	12.08.04	16:03	82° 6.75' N	2° 44.95' W	2708.0	CTD/RO	on deck
PS66/245-1	12.08.04	17:00	82° 6.65' N	2° 45.64' W	2736.0	ICE	Scientists on board
PS66/245-1	12.08.04	17:05	82° 6.63' N	2° 45.71' W	2740.0	ICE	Departure from floe
PS66/246-1	13.08.04	07:24	82° 36.71' N	4° 29.33' W	3190.0	DRG	surface
PS66/246-1	13.08.04	08:09	82° 36.74' N	4° 29.38' W	3193.0	DRG	Information
PS66/246-1	13.08.04	08:27	82° 36.83' N	4° 27.26' W	3136.0	DRG	start dredging
PS66/246-1	13.08.04	10:01	82° 37.14' N	4° 21.90' W	2855.0	DRG	Information
PS66/246-1	13.08.04	10:26	82° 37.18' N	4° 21.95' W	2857.0	DRG	stop dredging
PS66/246-1	13.08.04	11:07	82° 37.35' N	4° 20.37' W	2828.0	DRG	on deck
PS66/247-1	13.08.04	12:40	82° 42.96' N	4° 10.38' W	2151.0	ICE	Alongside Floe
PS66/247-1	13.08.04	12:57	82° 42.96' N	4° 9.89' W	2152.0	ICE	Ice Gangway on the ice
PS66/247-1	13.08.04	13:01	82° 42.97' N	4° 9.80' W	2154.0	ICE	Scientists on the ice
PS66/247-2	13.08.04	13:06	82° 42.97' N	4° 9.69' W	2152.0	CTD/RO	surface
PS66/247-2	13.08.04	13:46	82° 42.97' N	4° 8.68' W	2161.0	CTD/RO	at depth
PS66/247-2	13.08.04	14:22	82° 42.98' N	4° 7.85' W	2163.0	CTD/RO	on deck
PS66/247-1	13.08.04	23:07	82° 42.90' N	3° 55.08' W	1863.0	ICE	Scientists on board
PS66/247-1	13.08.04	23:12	82° 42.90' N	3° 55.01' W	1861.0	ICE	Ice Gangway on board
PS66/247-1	13.08.04	23:14	82° 42.90' N	3° 54.99' W	1862.0	ICE	Departure from floe
PS66/248-1	14.08.04	10:27	82° 28.74' N	5° 5.41' W	3839.0	DRG	surface
PS66/248-1	14.08.04	11:22	82° 28.62' N	5° 5.32' W	3880.0	DRG	Information
PS66/248-1	14.08.04	11:32	82° 28.59' N	5° 4.36' W	3743.0	DRG	start dredging

Station	Date	Time	PositionLat	PositionLon	Depth [m]	Gear (Abbrev.)	Action
PS66/248-1	14.08.04	12:07	82° 28.50' N	5° 1.93' W	3347.0	DRG	Information
PS66/248-1	14.08.04	12:44	82° 28.43' N	5° 2.87' W	3462.0	DRG	stop dredging
PS66/248-1	14.08.04	13:45	82° 28.30' N	5° 2.69' W	3490.0	DRG	on deck
PS66/249-1	14.08.04	17:35	82° 18.85' N	4° 46.38' W	3780.0	DRG	surface
PS66/249-1	14.08.04	18:25	82° 19.05' N	4° 44.21' W	3635.0	DRG	Information
PS66/249-1	14.08.04	18:39	82° 19.14' N	4° 42.73' W	3456.0	DRG	start dredging
PS66/249-1	14.08.04	19:41	82° 19.41' N	4° 37.29' W	3030.0	DRG	stop dredging
PS66/249-1	14.08.04	20:28	82° 19.42' N	4° 36.71' W	3046.0	DRG	stop dredging
PS66/249-1	14.08.04	21:08	82° 19.54' N	4° 35.63' W	3077.0	DRG	on deck
PS66/250-1	15.08.04	02:41	82° 15.72' N	5° 0.71' W	3503.0	DRG	surface
PS66/250-1	15.08.04	03:30	82° 15.60' N	5° 0.89' W	3462.0	DRG	Information
PS66/250-1	15.08.04	03:48	82° 15.58' N	4° 59.54' W	3268.0	DRG	start dredging
PS66/250-1	15.08.04	04:20	82° 15.46' N	4° 56.86' W	3006.0	DRG	stop dredging
PS66/250-1	15.08.04	04:52	82° 15.52' N	4° 56.62' W	3014.0	DRG	Information
PS66/250-1	15.08.04	05:31	82° 15.34' N	4° 53.41' W	2879.0	DRG	on deck
PS66/251-1	15.08.04	06:28	82° 10.19' N	4° 45.16' W	4102.0	DRG	surface
PS66/251-1	15.08.04	07:19	82° 10.25' N	4° 45.65' W	4094.0	DRG	Information
PS66/251-1	15.08.04	07:30	82° 10.19' N	4° 47.03' W	3951.0	DRG	Information
PS66/251-1	15.08.04	08:22	82° 9.86' N	4° 50.74' W	3509.0	DRG	Information
PS66/251-1	15.08.04	08:51	82° 9.86' N	4° 50.97' W	3504.0	DRG	stop dredging
PS66/251-1	15.08.04	09:36	82° 9.86' N	4° 50.40' W	3510.0	DRG	on deck
PS66/252-1	15.08.04	10:37	82° 6.85' N	5° 10.43' W	3903.0	DRG	surface
PS66/252-1	15.08.04	11:27	82° 6.90' N	5° 9.26' W	3849.0	DRG	Information
PS66/252-1	15.08.04	11:44	82° 6.99' N	5° 7.48' W	3730.0	DRG	start dredging
PS66/252-1	15.08.04	12:59	82° 7.32' N	5° 3.48' W	3327.0	DRG	stop dredging
PS66/252-1	15.08.04	13:43	82° 7.41' N	5° 3.16' W	3354.0	DRG	on deck
PS66/253-1	15.08.04	16:04	82° 0.43' N	4° 40.86' W	3624.0	DRG	surface
PS66/253-1	15.08.04	16:57	82° 0.42' N	4° 40.77' W	3624.0	DRG	Information
PS66/253-1	15.08.04	17:13	82° 0.63' N	4° 39.07' W	3396.0	DRG	start dredging
PS66/253-1	15.08.04	18:14	82° 0.87' N	4° 37.50' W	3114.0	DRG	stop dredging
PS66/253-1	15.08.04	18:55	82° 0.94' N	4° 35.87' W	2899.0	DRG	on deck
PS66/254-1	16.08.04	10:23	81° 43.92' N	5° 34.47' W	2906.0	DRG	surface

Station	Date	Time	PositionLat	PositionLon	Depth [m]	Gear (Abbrev.)	Action
PS66/254-1	16.08.04	11:03	81° 43.96' N	5° 34.78' W	2914.0	DRG	Information
PS66/254-1	16.08.04	11:18	81° 44.02' N	5° 36.43' W	2765.0	DRG	start dredging
PS66/254-1	16.08.04	13:01	81° 44.64' N	5° 41.85' W	2380.0	DRG	stop dredging
PS66/254-1	16.08.04	13:30	81° 44.85' N	5° 41.13' W	2432.0	DRG	on deck
PS66/255-1	16.08.04	15:33	81° 39.95' N	3° 54.88' W	3327.0	DRG	surface
PS66/255-1	16.08.04	16:16	81° 39.81' N	3° 54.60' W	3320.0	DRG	Information
PS66/255-1	16.08.04	16:30	81° 39.85' N	3° 52.76' W	3189.0	DRG	start dredging
PS66/255-1	16.08.04	17:09	81° 39.87' N	3° 49.20' W	2802.0	DRG	stop dredging
PS66/255-1	16.08.04	17:41	81° 39.84' N	3° 48.75' W	2777.0	DRG	Information
PS66/255-1	16.08.04	18:15	81° 39.67' N	3° 47.30' W	2721.0	DRG	on deck
PS66/256-1	16.08.04	20:00	81° 32.82' N	3° 32.37' W	3530.0	DRG	surface
PS66/256-1	16.08.04	20:46	81° 32.81' N	3° 33.05' W	3530.0	DRG	Information
PS66/256-1	16.08.04	21:03	81° 32.98' N	3° 34.39' W	3374.0	DRG	start dredging
PS66/256-1	16.08.04	21:42	81° 33.16' N	3° 38.18' W	3021.0	DRG	Information
PS66/256-1	16.08.04	22:17	81° 32.98' N	3° 39.42' W	3017.0	DRG	stop dredging
PS66/256-1	16.08.04	22:57	81° 32.77' N	3° 41.65' W	2852.0	DRG	on deck
PS66/257-1	17.08.04	00:35	81° 24.62' N	2° 56.46' W	3906.0	DRG	surface
PS66/257-1	17.08.04	01:26	81° 24.58' N	2° 56.74' W	3885.0	DRG	Information
PS66/257-1	17.08.04	01:41	81° 24.46' N	2° 57.53' W	3842.0	DRG	start dredging
PS66/257-1	17.08.04	03:00	81° 23.75' N	3° 1.93' W	3338.0	DRG	Information
PS66/257-1	17.08.04	03:39	81° 23.67' N	3° 1.34' W	3337.0	DRG	stop dredging
PS66/257-1	17.08.04	04:20	81° 23.54' N	3° 1.64' W	3257.0	DRG	on deck
PS66/258-1	17.08.04	05:25	81° 21.75' N	3° 28.61' W	3558.0	DRG	surface
PS66/258-1	17.08.04	06:15	81° 21.86' N	3° 27.27' W	3555.0	DRG	Information
PS66/258-1	17.08.04	06:28	81° 21.87' N	3° 25.64' W	3438.0	DRG	start dredging
PS66/258-1	17.08.04	08:05	81° 21.73' N	3° 18.10' W	2898.0	DRG	Information
PS66/258-1	17.08.04	08:15	81° 21.73' N	3° 18.08' W	2892.0	DRG	Information
PS66/258-1	17.08.04	09:11	81° 21.77' N	3° 20.69' W	3081.0	DRG	Information
PS66/258-1	17.08.04	09:53	81° 21.71' N	3° 23.05' W	3266.0	DRG	Information
PS66/258-1	17.08.04	09:54	81° 21.71' N	3° 23.07' W	3265.0	DRG	stop dredging
PS66/258-1	17.08.04	10:37	81° 21.68' N	3° 23.46' W	3289.0	DRG	on deck
PS66/258-2	17.08.04	10:52	81° 21.67' N	3° 23.22' W	3272.0	CTD/RO	surface

Station	Date	Time	PositionLat	PositionLon	Depth [m]	Gear (Abbrev.)	Action
PS66/258-2	17.08.04	11:54	81° 21.65' N	3° 23.37' W	3279.0	CTD/RO	at depth
PS66/258-2	17.08.04	16:46	81° 22.01' N	3° 6.50' W	2279.0	CTD/RO	Information
PS66/258-2	17.08.04	17:10	81° 22.01' N	3° 6.06' W	2301.0	CTD/RO	Information
PS66/258-2	17.08.04	18:12	81° 21.79' N	3° 3.63' W	2344.0	CTD/RO	at depth
PS66/258-2	17.08.04	19:02	81° 21.84' N	3° 2.49' W	2376.0	CTD/RO	on deck
PS66/259-1	19.08.04	15:29	81° 7.51' N	2° 40.00' W	3882.0	DRG	surface
PS66/259-1	19.08.04	16:17	81° 7.61' N	2° 39.95' W	3840.0	DRG	Information
PS66/259-1	19.08.04	16:28	81° 7.81' N	2° 39.00' W	3661.0	DRG	start dredging
PS66/259-1	19.08.04	17:20	81° 8.46' N	2° 37.11' W	3225.0	DRG	stop dredging
PS66/259-1	19.08.04	17:51	81° 8.45' N	2° 37.34' W	3240.0	DRG	Information
PS66/259-1	19.08.04	18:32	81° 8.49' N	2° 37.26' W	3217.0	DRG	on deck
PS66/260-1	19.08.04	18:48	81° 8.20' N	2° 39.92' W	3561.0	DRG	surface
PS66/260-1	19.08.04	19:34	81° 8.18' N	2° 38.77' W	3528.0	DRG	Information
PS66/260-1	19.08.04	19:44	81° 8.31' N	2° 38.07' W	3393.0	DRG	start dredging
PS66/260-1	19.08.04	19:59	81° 8.52' N	2° 37.27' W	3214.0	DRG	Information
PS66/260-1	19.08.04	20:17	81° 8.50' N	2° 36.88' W	3219.0	DRG	stop dredging
PS66/260-1	19.08.04	20:58	81° 8.51' N	2° 36.03' W	3229.0	DRG	on deck
PS66/261-1	19.08.04	22:56	80° 55.45' N	2° 29.44' W	3944.0	DRG_C	surface
PS66/261-1	19.08.04	23:44	80° 55.45' N	2° 29.86' W	3856.0	DRG_C	Information
PS66/261-1	20.08.04	00:15	80° 55.46' N	2° 31.38' W	3579.0	DRG_C	start dredging
PS66/261-1	20.08.04	01:16	80° 55.29' N	2° 34.60' W	3334.0	DRG_C	stop dredging
PS66/261-1	20.08.04	02:05	80° 55.10' N	2° 36.10' W	3097.0	DRG_C	on deck
PS66/262-1	20.08.04	02:36	80° 54.44' N	2° 29.02' W	3817.0	DRG_C	surface
PS66/262-1	20.08.04	03:24	80° 54.39' N	2° 30.43' W	3613.0	DRG_C	Information
PS66/262-1	20.08.04	03:39	80° 54.32' N	2° 31.97' W	3458.0	DRG_C	start dredging
PS66/262-1	20.08.04	04:18	80° 54.14' N	2° 35.60' W	3075.0	DRG_C	stop dredging
PS66/262-1	20.08.04	04:54	80° 54.48' N	2° 35.74' W	3111.0	DRG_C	Information
PS66/262-1	20.08.04	05:32	80° 54.68' N	2° 36.53' W	3057.0	DRG_C	on deck
PS66/263-1	20.08.04	08:15	80° 36.13' N	2° 15.68' W	3973.0	DRG_C	surface
PS66/263-1	20.08.04	09:11	80° 35.88' N	2° 16.23' W	3946.0	DRG_C	Information
PS66/263-1	20.08.04	09:21	80° 35.87' N	2° 17.15' W	3914.0	DRG_C	start dredging
PS66/263-1	20.08.04	10:32	80° 35.82' N	2° 23.92' W	3491.0	DRG_C	Information

Station	Date	Time	PositionLat	PositionLon	Depth [m]	Gear (Abbrev.)	Action
PS66/263-1	20.08.04	11:07	80° 35.60' N	2° 24.79' W	3415.0	DRG_C	stop dredging
PS66/263-1	20.08.04	11:46	80° 35.56' N	2° 27.43' W	3270.0	DRG_C	on deck
PS66/264-1	20.08.04	12:48	80° 32.11' N	2° 16.61' W	3862.0	DRG_C	surface
PS66/264-1	20.08.04	13:40	80° 32.17' N	2° 17.27' W	3811.0	DRG_C	Information
PS66/264-1	20.08.04	13:53	80° 32.17' N	2° 18.62' W	3752.0	DRG_C	start dredging
PS66/264-1	20.08.04	14:33	80° 32.18' N	2° 22.83' W	3556.0	DRG_C	Information
PS66/264-1	20.08.04	14:52	80° 32.26' N	2° 23.35' W	3543.0	DRG_C	stop dredging
PS66/264-1	20.08.04	15:40	80° 32.16' N	2° 25.38' W	3401.0	DRG_C	on deck
PS66/265-1	21.08.04	00:55	78° 50.07' N	1° 7.28' W	2623.0	CTD/RO	surface
PS66/265-1	21.08.04	01:44	78° 50.09' N	1° 7.18' W	2618.0	CTD/RO	at depth
PS66/265-1	21.08.04	02:28	78° 49.97' N	1° 7.22' W	2629.0	CTD/RO	on deck
PS66/266-1	21.08.04	03:16	78° 50.05' N	1° 25.38' W	2697.0	CTD/RO	surface
PS66/266-1	21.08.04	04:07	78° 50.13' N	1° 25.42' W	2696.0	CTD/RO	at depth
PS66/266-1	21.08.04	04:40	78° 50.10' N	1° 26.68' W	2699.0	CTD/RO	on deck
PS66/267-1	21.08.04	05:50	78° 49.65' N	2° 0.84' W	2722.0	MOR	Hydroph.intowater
PS66/267-1	21.08.04	06:10	78° 49.71' N	2° 0.60' W	0.0	MOR	released
PS66/267-1	21.08.04	06:11	78° 49.69' N	2° 0.67' W	0.0	MOR	on the surface
PS66/267-1	21.08.04	06:43	78° 49.69' N	2° 1.87' W	2726.0	MOR	action
PS66/267-1	21.08.04	07:44	78° 49.58' N	2° 6.31' W	2720.0	MOR	on deck
PS66/267-2	21.08.04	08:07	78° 49.99' N	1° 59.28' W	2727.0	CTD/RO	surface
PS66/267-2	21.08.04	08:57	78° 49.94' N	2° 0.04' W	2726.0	CTD/RO	at depth
PS66/267-2	21.08.04	09:42	78° 49.82' N	2° 0.51' W	2724.0	CTD/RO	on deck
PS66/268-1	21.08.04	11:28	78° 50.12' N	0° 48.74' W	0.0	MOR	Hydroph.intowater
PS66/268-1	21.08.04	11:32	78° 50.13' N	0° 49.13' W	0.0	MOR	released
PS66/268-1	21.08.04	11:33	78° 50.14' N	0° 49.27' W	0.0	MOR	on the surface
PS66/268-1	21.08.04	12:02	78° 50.35' N	0° 49.01' W	2673.0	MOR	action
PS66/268-1	21.08.04	12:04	78° 50.36' N	0° 49.21' W	2671.0	MOR	on deck
PS66/268-1	21.08.04	12:09	78° 50.36' N	0° 49.54' W	2671.0	MOR	on deck
PS66/268-1	21.08.04	12:16	78° 50.35' N	0° 49.72' W	2674.0	MOR	on deck
PS66/268-1	21.08.04	12:26	78° 50.40' N	0° 50.00' W	2676.0	MOR	on deck
PS66/268-1	21.08.04	12:39	78° 50.39' N	0° 50.65' W	2673.0	MOR	on deck
PS66/268-1	21.08.04	13:01	78° 50.39' N	0° 51.21' W	2675.0	MOR	mooring on deck

Station	Date	Time	PositionLat	PositionLon	Depth [m]	Gear (Abbrev.)	Action
PS66/268-2	21.08.04	13:21	78° 50.33' N	0° 48.31' W	2674.0	CTD/RO	surface
PS66/268-2	21.08.04	14:10	78° 50.32' N	0° 48.50' W	2674.0	CTD/RO	at depth
PS66/268-2	21.08.04	14:45	78° 50.28' N	0° 48.57' W	2671.0	CTD/RO	on deck
PS66/268-3	21.08.04	15:05	78° 50.30' N	0° 48.55' W	2672.0	MOR	surface
PS66/268-3	21.08.04	15:11	78° 50.30' N	0° 48.50' W	2671.0	MOR	surface
PS66/268-3	21.08.04	15:56	78° 50.29' N	0° 48.56' W	2672.0	MOR	surface
PS66/268-3	21.08.04	16:17	78° 50.30' N	0° 48.73' W	2674.0	MOR	surface
PS66/268-3	21.08.04	16:33	78° 50.30' N	0° 48.83' W	2672.0	MOR	surface
PS66/268-3	21.08.04	16:44	78° 50.30' N	0° 48.70' W	2674.0	MOR	surface
PS66/268-3	21.08.04	16:50	78° 50.31' N	0° 48.73' W	2673.0	MOR	surface
PS66/268-3	21.08.04	16:55	78° 50.32' N	0° 48.73' W	2673.0	MOR	action
PS66/268-3	21.08.04	17:18	78° 50.33' N	0° 48.70' W	2672.0	MOR	surface
PS66/268-3	21.08.04	17:26	78° 50.33' N	0° 48.74' W	2671.0	MOR	on the ground
PS66/268-3	21.08.04	17:27	78° 50.33' N	0° 48.73' W	2675.0	MOR	on deck
PS66/269-1	21.08.04	18:06	78° 49.92' N	0° 29.97' W	2700.0	CTD/RO	surface
PS66/269-1	21.08.04	18:58	78° 49.91' N	0° 31.34' W	2698.0	CTD/RO	at depth
PS66/269-1	21.08.04	19:35	78° 50.06' N	0° 31.94' W	2700.0	CTD/RO	on deck
PS66/270-1	21.08.04	20:14	78° 50.14' N	0° 12.49' W	2654.0	CTD/RO	surface
PS66/270-1	21.08.04	21:02	78° 50.10' N	0° 12.89' W	2653.0	CTD/RO	at depth
PS66/270-1	21.08.04	21:40	78° 50.04' N	0° 12.33' W	2652.0	CTD/RO	on deck
PS66/271-1	21.08.04	22:17	78° 49.98' N	0° 5.86' E	2635.0	CTD/RO	surface
PS66/271-1	21.08.04	23:05	78° 50.04' N	0° 5.31' E	2640.0	CTD/RO	at depth
PS66/271-1	21.08.04	23:42	78° 49.98' N	0° 5.66' E	2637.0	CTD/RO	on deck
PS66/272-1	22.08.04	00:41	78° 49.99' N	0° 41.25' E	2484.0	CTD/RO	surface
PS66/272-1	22.08.04	01:28	78° 50.09' N	0° 40.41' E	2493.0	CTD/RO	at depth
PS66/272-1	22.08.04	02:04	78° 50.25' N	0° 40.27' E	2493.0	CTD/RO	on deck
PS66/273-1	22.08.04	02:38	78° 49.99' N	1° 0.24' E	2498.0	CTD/RO	surface
PS66/273-1	22.08.04	03:27	78° 50.08' N	0° 59.74' E	2500.0	CTD/RO	at depth
PS66/273-1	22.08.04	04:00	78° 50.22' N	0° 59.71' E	2504.0	CTD/RO	on deck
PS66/274-1	22.08.04	05:56	78° 49.96' N	0° 23.65' E	0.0	MOR	Hydroph. into water
PS66/274-1	22.08.04	05:59	78° 49.98' N	0° 23.49' E	0.0	MOR	released
PS66/274-1	22.08.04	06:02	78° 49.96' N	0° 23.34' E	0.0	MOR	on the surface

Station	Date	Time	PositionLat	PositionLon	Depth [m]	Gear (Abbrev.)	Action
PS66/274-1	22.08.04	06:23	78° 50.22' N	0° 21.61' E	2594.0	MOR	action
PS66/274-1	22.08.04	07:16	78° 50.38' N	0° 18.42' E	2602.0	MOR	on deck
PS66/274-2	22.08.04	07:39	78° 50.19' N	0° 23.85' E	2588.0	CTD/RO	surface
PS66/274-2	22.08.04	08:28	78° 50.11' N	0° 23.37' E	2592.0	CTD/RO	at depth
PS66/274-2	22.08.04	09:02	78° 50.07' N	0° 23.58' E	2591.0	CTD/RO	on deck
PS66/274-3	22.08.04	09:08	78° 50.05' N	0° 24.06' E	2587.0	MOR	surface
PS66/274-3	22.08.04	09:10	78° 50.05' N	0° 24.01' E	2591.0	MOR	surface
PS66/274-3	22.08.04	09:38	78° 50.07' N	0° 24.01' E	2581.0	MOR	surface
PS66/274-3	22.08.04	09:58	78° 50.10' N	0° 24.16' E	2580.7	MOR	surface
PS66/274-3	22.08.04	10:11	78° 50.11' N	0° 23.37' E	2583.0	MOR	surface
PS66/274-3	22.08.04	10:26	78° 50.07' N	0° 23.73' E	2589.0	MOR	surface
PS66/274-3	22.08.04	10:31	78° 50.07' N	0° 23.79' E	2589.0	MOR	surface
PS66/274-3	22.08.04	10:36	78° 50.07' N	0° 23.77' E	2590.0	MOR	on deck
PS66/274-3	22.08.04	10:54	78° 50.05' N	0° 23.81' E	2588.0	MOR	surface
PS66/274-3	22.08.04	10:58	78° 50.05' N	0° 23.81' E	2588.0	MOR	on the ground
PS66/274-3	22.08.04	10:59	78° 50.05' N	0° 23.81' E	2588.0	MOR	slipped
PS66/274-3	22.08.04	11:00	78° 50.05' N	0° 23.81' E	2589.0	MOR	releaser on deck
PS66/275-1	22.08.04	12:42	78° 49.95' N	1° 17.79' E	2532.0	CTD/RO	surface
PS66/275-1	22.08.04	13:29	78° 49.93' N	1° 17.98' E	2538.0	CTD/RO	at depth
PS66/275-1	22.08.04	14:05	78° 49.97' N	1° 18.01' E	2532.0	CTD/RO	on deck
PS66/276-1	22.08.04	14:35	78° 50.01' N	1° 34.87' E	2556.0	MOR	Hydroph. into water
PS66/276-1	22.08.04	14:38	78° 49.99' N	1° 34.64' E	2555.0	MOR	released
PS66/276-1	22.08.04	14:48	78° 49.82' N	1° 33.52' E	2555.0	MOR	Hydrophone on deck
PS66/276-1	22.08.04	15:16	78° 49.94' N	1° 34.75' E	2557.0	MOR	action
PS66/276-1	22.08.04	15:32	78° 49.94' N	1° 36.36' E	2558.0	MOR	Hydroph. into water
PS66/276-1	22.08.04	15:38	78° 49.94' N	1° 36.13' E	2557.0	MOR	released
PS66/276-1	22.08.04	15:44	78° 49.86' N	1° 35.83' E	2557.0	MOR	Hydrophone on deck
PS66/276-1	22.08.04	15:50	78° 49.80' N	1° 36.15' E	2559.0	MOR	Hydroph. into water
PS66/276-1	22.08.04	15:55	78° 49.74' N	1° 35.87' E	2558.0	MOR	Hydrophone on deck
PS66/276-1	22.08.04	16:04	78° 50.04' N	1° 36.93' E	0.0	MOR	Hydroph. into water
PS66/276-1	22.08.04	16:05	78° 50.04' N	1° 36.87' E	0.0	MOR	action
PS66/276-1	22.08.04	16:10	78° 49.98' N	1° 36.62' E	0.0	MOR	action

Station	Date	Time	PositionLat	PositionLon	Depth [m]	Gear (Abbrev.)	Action
PS66/276-1	22.08.04	16:15	78° 49.94' N	1° 36.27' E	0.0	MOR	action
PS66/276-1	22.08.04	16:20	78° 49.89' N	1° 35.79' E	0.0	MOR	action
PS66/276-1	22.08.04	16:22	78° 49.87' N	1° 35.58' E	0.0	MOR	action
PS66/276-1	22.08.04	16:26	78° 49.84' N	1° 35.14' E	2560.0	MOR	action
PS66/276-1	22.08.04	17:31	78° 49.81' N	1° 35.71' E	0.0	MOR	Hydroph. into water
PS66/276-1	22.08.04	17:43	78° 49.95' N	1° 34.82' E	0.0	MOR	Hydroph. into water
PS66/276-1	22.08.04	17:49	78° 49.97' N	1° 35.45' E	0.0	MOR	Hydroph. into water
PS66/276-1	22.08.04	18:12	78° 50.01' N	1° 33.59' E	0.0	MOR	action
PS66/277-1	22.08.04	18:25	78° 49.91' N	1° 33.60' E	2554.0	CTD/RO	surface
PS66/277-1	22.08.04	19:10	78° 49.82' N	1° 32.74' E	2555.0	CTD/RO	at depth
PS66/277-1	22.08.04	19:45	78° 49.70' N	1° 33.19' E	2556.0	CTD/RO	on deck
PS66/278-1	22.08.04	20:19	78° 50.00' N	1° 55.29' E	2568.0	CTD/RO	surface
PS66/278-1	22.08.04	21:06	78° 49.98' N	1° 54.69' E	2569.0	CTD/RO	at depth
PS66/278-1	22.08.04	21:43	78° 49.96' N	1° 54.28' E	2568.0	CTD/RO	on deck
PS66/279-1	22.08.04	22:16	78° 50.06' N	2° 15.47' E	2551.0	CTD/RO	surface
PS66/279-1	22.08.04	23:04	78° 49.99' N	2° 14.96' E	2553.0	CTD/RO	at depth
PS66/279-1	22.08.04	23:36	78° 49.95' N	2° 14.67' E	2551.0	CTD/RO	on deck
PS66/280-1	23.08.04	00:17	78° 50.08' N	2° 35.03' E	2530.0	CTD/RO	surface
PS66/280-1	23.08.04	01:06	78° 50.04' N	2° 35.69' E	2529.0	CTD/RO	at depth
PS66/280-1	23.08.04	01:42	78° 49.95' N	2° 35.59' E	2529.0	CTD/RO	on deck
PS66/281-1	23.08.04	05:39	78° 49.86' N	1° 35.76' E	2556.0	MOR	Hydroph. into water
PS66/281-1	23.08.04	05:44	78° 49.85' N	1° 35.45' E	0.0	MOR	action
PS66/281-1	23.08.04	05:53	78° 49.81' N	1° 34.51' E	0.0	MOR	Hydrophone on deck
PS66/281-1	23.08.04	08:20	78° 49.80' N	1° 35.68' E	2556.0	MOR	Hydroph. into water
PS66/281-1	23.08.04	08:22	78° 49.78' N	1° 35.67' E	0.0	MOR	action
PS66/281-1	23.08.04	08:26	78° 49.72' N	1° 35.69' E	0.0	MOR	Hydrophone on deck
PS66/281-1	23.08.04	08:36	78° 50.02' N	1° 35.32' E	0.0	MOR	Hydroph. into water
PS66/281-1	23.08.04	08:48	78° 49.83' N	1° 35.28' E	0.0	MOR	action
PS66/281-1	23.08.04	08:58	78° 50.04' N	1° 35.65' E	0.0	MOR	Hydroph. into water
PS66/281-1	23.08.04	09:11	78° 49.85' N	1° 35.67' E	0.0	MOR	action
PS66/281-1	23.08.04	09:14	78° 49.79' N	1° 35.60' E	0.0	MOR	Hydrophone on deck
PS66/281-1	23.08.04	09:42	78° 49.88' N	1° 33.64' E	2544.5	MOR	action

Station	Date	Time	PositionLat	PositionLon	Depth [m]	Gear (Abbrev.)	Action
PS66/281-1	23.08.04	09:43	78° 49.88' N	1° 33.64' E	2544.5	MOR	action
PS66/281-1	23.08.04	09:58	78° 49.90' N	1° 34.23' E	2544.4	MOR	action
PS66/281-1	23.08.04	10:10	78° 49.90' N	1° 34.14' E	2544.4	MOR	action
PS66/281-1	23.08.04	10:23	78° 49.89' N	1° 33.80' E	2544.5	MOR	action
PS66/281-1	23.08.04	10:29	78° 49.89' N	1° 33.86' E	2544.9	MOR	action
PS66/281-1	23.08.04	10:34	78° 49.90' N	1° 34.15' E	2542.8	MOR	action
PS66/281-1	23.08.04	11:10	78° 50.00' N	1° 35.07' E	2545.2	MOR	surface
PS66/281-1	23.08.04	14:06	78° 49.43' N	1° 34.95' E	2548.0	MOR	action
PS66/281-1	23.08.04	14:17	78° 49.39' N	1° 34.82' E	2548.1	MOR	action
PS66/281-1	23.08.04	14:28	78° 49.29' N	1° 34.67' E	2548.5	MOR	on deck
PS66/281-1	23.08.04	14:58	78° 48.99' N	1° 34.20' E	2563.0	MOR	on deck
PS66/281-1	23.08.04	15:20	78° 48.63' N	1° 33.48' E	2559.0	MOR	on deck
PS66/281-1	23.08.04	15:54	78° 48.23' N	1° 32.15' E	2558.0	MOR	on deck
PS66/281-1	23.08.04	16:25	78° 47.94' N	1° 28.93' E	2539.0	MOR	on deck
PS66/281-2	23.08.04	17:06	78° 49.95' N	1° 36.35' E	2557.0	MOR	surface
PS66/281-2	23.08.04	17:30	78° 49.98' N	1° 36.43' E	2558.0	MOR	surface
PS66/281-2	23.08.04	17:44	78° 50.00' N	1° 36.62' E	2557.0	MOR	surface
PS66/281-2	23.08.04	17:56	78° 49.99' N	1° 36.57' E	2555.0	MOR	surface
PS66/281-2	23.08.04	18:09	78° 50.00' N	1° 36.59' E	2556.0	MOR	surface
PS66/281-2	23.08.04	18:12	78° 50.00' N	1° 36.60' E	2558.0	MOR	surface
PS66/281-2	23.08.04	18:13	78° 50.00' N	1° 36.60' E	2559.0	MOR	surface
PS66/281-2	23.08.04	18:14	78° 50.00' N	1° 36.59' E	2558.0	MOR	slipped
PS66/282-1	23.08.04	21:41	78° 50.02' N	1° 44.97' W	2724.0	CTD/RO	surface
PS66/282-1	23.08.04	22:31	78° 49.98' N	1° 45.34' W	2723.0	CTD/RO	at depth
PS66/282-1	23.08.04	23:12	78° 49.92' N	1° 45.60' W	2723.0	CTD/RO	on deck
PS66/283-1	24.08.04	00:14	78° 49.88' N	2° 23.54' W	2672.0	CTD/RO	surface
PS66/283-1	24.08.04	01:04	78° 49.44' N	2° 22.64' W	2675.0	CTD/RO	at depth
PS66/283-1	24.08.04	01:48	78° 49.07' N	2° 22.73' W	2678.0	CTD/RO	on deck
PS66/284-1	24.08.04	02:37	78° 49.97' N	2° 51.52' W	2585.0	CTD/RO	surface
PS66/284-1	24.08.04	03:24	78° 49.69' N	2° 50.82' W	2588.0	CTD/RO	at depth
PS66/284-1	24.08.04	04:08	78° 49.28' N	2° 51.49' W	2591.0	CTD/RO	on deck
PS66/285-1	24.08.04	06:24	78° 49.90' N	2° 0.01' W	2728.0	MOR	surface

Station	Date	Time	PositionLat	PositionLon	Depth [m]	Gear (Abbrev.)	Action
PS66/285-1	24.08.04	06:48	78° 49.90' N	1° 59.86' W	2728.0	MOR	surface
PS66/285-1	24.08.04	07:03	78° 49.89' N	1° 59.92' W	2725.0	MOR	surface
PS66/285-1	24.08.04	07:16	78° 49.89' N	2° 0.02' W	2726.0	MOR	surface
PS66/285-1	24.08.04	07:21	78° 49.89' N	2° 0.03' W	2730.0	MOR	surface
PS66/285-1	24.08.04	07:31	78° 49.88' N	2° 0.05' W	2728.0	MOR	surface
PS66/285-1	24.08.04	07:35	78° 49.88' N	2° 0.07' W	2725.0	MOR	surface
PS66/285-1	24.08.04	07:37	78° 49.88' N	2° 0.06' W	2727.0	MOR	on the ground
PS66/285-1	24.08.04	07:38	78° 49.88' N	2° 0.06' W	2727.0	MOR	releaser on deck
PS66/286-1	24.08.04	09:19	78° 49.98' N	3° 20.39' W	2394.0	CTD/RO	surface
PS66/286-1	24.08.04	10:04	78° 50.00' N	3° 20.22' W	2398.0	CTD/RO	at depth
PS66/286-1	24.08.04	10:42	78° 50.00' N	3° 20.52' W	2392.0	CTD/RO	on deck
PS66/287-1	24.08.04	12:17	78° 49.90' N	3° 43.09' W	2150.0	CTD/RO	surface
PS66/287-1	24.08.04	12:58	78° 49.65' N	3° 43.53' W	2141.0	CTD/RO	surface
PS66/287-1	24.08.04	13:39	78° 49.38' N	3° 43.76' W	2135.0	CTD/RO	on deck
PS66/288-1	24.08.04	14:19	78° 49.94' N	4° 8.89' W	1814.0	CTD/RO	surface
PS66/288-1	24.08.04	14:57	78° 49.52' N	4° 8.75' W	1802.0	CTD/RO	at depth
PS66/288-1	24.08.04	15:35	78° 49.13' N	4° 9.76' W	1782.0	CTD/RO	on deck
PS66/289-1	24.08.04	16:15	78° 50.09' N	4° 34.77' W	1446.0	CTD/RO	surface
PS66/289-1	24.08.04	16:43	78° 49.93' N	4° 35.76' W	1428.0	CTD/RO	at depth
PS66/289-1	24.08.04	17:14	78° 49.83' N	4° 35.39' W	1429.0	CTD/RO	on deck
PS66/290-1	24.08.04	17:56	78° 50.09' N	5° 0.05' W	1051.0	CTD/RO	surface
PS66/290-1	24.08.04	18:18	78° 50.16' N	5° 0.18' W	1052.0	CTD/RO	at depth
PS66/290-1	24.08.04	18:42	78° 50.25' N	5° 0.28' W	1054.0	CTD/RO	on deck
PS66/291-1	24.08.04	19:27	78° 49.95' N	5° 26.33' W	621.0	CTD/RO	surface
PS66/291-1	24.08.04	19:41	78° 49.94' N	5° 26.20' W	622.8	CTD/RO	at depth
PS66/291-1	24.08.04	19:58	78° 49.93' N	5° 26.29' W	620.0	CTD/RO	on deck
PS66/292-1	24.08.04	21:24	78° 50.03' N	6° 18.27' W	309.0	CTD/RO	surface
PS66/292-1	24.08.04	21:30	78° 50.03' N	6° 18.35' W	309.0	CTD/RO	at depth
PS66/292-1	24.08.04	21:44	78° 50.00' N	6° 18.37' W	309.6	CTD/RO	on deck
PS66/293-1	24.08.04	23:05	78° 50.04' N	7° 9.67' W	236.7	CTD/RO	surface
PS66/293-1	24.08.04	23:13	78° 50.03' N	7° 9.50' W	237.8	CTD/RO	at depth
PS66/293-1	24.08.04	23:23	78° 50.03' N	7° 9.40' W	237.5	CTD/RO	on deck

Station	Date	Time	PositionLat	PositionLon	Depth [m]	Gear (Abbrev.)	Action
PS66/294-1	25.08.04	00:49	78° 49.95' N	8° 0.71' W	188.6	CTD/RO	surface
PS66/294-1	25.08.04	00:57	78° 49.90' N	8° 0.82' W	188.2	CTD/RO	at depth
PS66/294-1	25.08.04	01:08	78° 49.83' N	8° 0.78' W	190.3	CTD/RO	on deck
PS66/295-1	25.08.04	02:28	78° 49.85' N	8° 52.41' W	253.8	CTD/RO	surface
PS66/295-1	25.08.04	02:36	78° 49.76' N	8° 52.40' W	248.7	CTD/RO	at depth
PS66/295-1	25.08.04	02:46	78° 49.64' N	8° 52.09' W	245.1	CTD/RO	on deck
PS66/296-1	25.08.04	12:33	79° 19.87' N	13° 49.62' W	139.0	ICE	Alongside Floe
PS66/296-1	25.08.04	12:56	79° 19.87' N	13° 49.59' W	138.8	ICE	Ice Gangway on the ice
PS66/296-1	25.08.04	13:33	79° 19.88' N	13° 49.60' W	138.7	ICE	Scientists on the ice
PS66/296-1	25.08.04	13:45	79° 19.88' N	13° 49.59' W	138.5	ICE	Scientists on board
PS66/296-1	25.08.04	15:08	79° 19.87' N	13° 49.61' W	138.8	ICE	Scientists on the ice
PS66/296-1	25.08.04	22:15	79° 19.88' N	13° 49.54' W	138.0	ICE	Scientists on board
PS66/296-1	25.08.04	22:30	79° 19.89' N	13° 49.61' W	138.0	ICE	Ice Gangway on board
PS66/296-1	25.08.04	22:35	79° 19.94' N	13° 49.86' W	135.6	ICE	Departure from floe
PS66/297-1	26.08.04	11:21	78° 50.14' N	11° 28.24' W	256.8	CTD/RO	surface
PS66/297-1	26.08.04	11:29	78° 50.12' N	11° 27.92' W	260.3	CTD/RO	at depth
PS66/297-1	26.08.04	11:38	78° 50.10' N	11° 27.57' W	263.9	CTD/RO	on deck
PS66/298-1	26.08.04	13:06	78° 50.01' N	10° 36.16' W	393.7	CTD/RO	surface
PS66/298-1	26.08.04	13:21	78° 49.95' N	10° 36.26' W	394.8	CTD/RO	at depth
PS66/298-1	26.08.04	13:38	78° 50.03' N	10° 36.10' W	392.4	CTD/RO	on deck
PS66/299-1	26.08.04	15:04	78° 49.96' N	9° 44.17' W	226.0	CTD/RO	surface
PS66/299-1	26.08.04	15:15	78° 49.87' N	9° 43.88' W	225.5	CTD/RO	at depth
PS66/299-1	26.08.04	15:23	78° 49.82' N	9° 43.48' W	225.7	CTD/RO	on deck